Regulation of the spatial distribution of the actomyosin network in developing *Drosophila* epithelia by the cell adhesion molecule Echinoid

Arsida Noçka
Department of Biology
McGill University
Montreal, Quebec, Canada

Doctor of Philosophy

January, 2015

A thesis submitted to McGill University in partial fulfillment of the requirement of the degree of Doctor of Philosophy

Acknowledgements

No thesis is the product of only one person's work. During my doctoral work, I have been help by many people, whom I would like to acknowledge.

I would like to express my immense gratitude to my supervisor Laura for her support and guidance during the course of my Ph.D. I am greatly indebted to Laura for permitting considerable independence during my doctoral work and thus allowing me the opportunity to succeed in my own terms and in my own time. I would also like to thank Laura for being very generous with her time, particularly during the writing phase of the thesis, and for giving me the chance and encouraging me to present my work at different scientific conferences.

I thank members of my supervisory committee, Francois Fagotto and Frieder Schöck, for their input and discussion on my project during the meetings.

I am grateful to the past and present lab colleagues: to J-F for his sharing his fly-pushing expertise, his helpful advice on my project, and the non-work related conversations; to Phoenix for keeping the lab running smoothly; to Josée for being a great colleague, for her great help with some of the experiments, for our conversations about cooking and teaching me how to ski, making the Montreal winters less depressing and snowfall even more exciting; to Mariana, Rahul, Danny, Dragana, Scott and Fiona for their interest and their discussions on my project; to my undergraduate student, Cheryl, for her keen interest in the project and her superior record keeping, which provided very useful as I was writing. I thank Jenny Long for her patience and thoughtful critique of less than well-written drafts of the chapters. Lydianne for translating my abstract into French. And, both girls for the encouraging words and listening ears, especially during our short-lived time in the student office.

I would like to thank the CIAN staff, especially Elke Küster-Schöck for keeping the microscopy facility running smoothly. I am very grateful to Dr. Chiara Gamberi for patiently teaching me biochemical techniques. I thank Eric Bonneil at the IRIC Proteomic facility for assistance with the mass spectrometry. I thank members of the Lasko, Moon, and Schöck labs for their feedback at the fly lab meetings. I am deeply thankful to Beili Hu for the numerous and successful injections of my DNA constructs, and to Mr. Lee for making the fly food. I would like to thank the McGill University Alma Howard Alumni and the Department of Biology for providing travel awards for attendance at conferences. My work greatly benefited from the reagents kindly provided by the laboratories of Andreas Wodarz, David Hipfner, Celeste Berg, Henry Krause, and Hugo Bellen.

I would like to express my sincere gratitude to my undergraduate thesis mentor, Dr. Mitchell (who would very much appreciate that I address her simply as Beth, but I can't), who very kindly allowed me to join her lab when I didn't know how to even hold a pipetman. Under her tutelage, I learned how to think scientifically. Her emphasis and insistence on good writing taught me how to craft a good sentence, a paragraph, and ultimately a story. In the early stages of my scientific career, she supported my curiosity and encouraged me to present my work at different conferences.

I would like to thank my parents, Klara and Mikel, for allowing me to realize my own potential by morally and financially supporting my decision to move and study abroad at a young age. Quite simply, I could not be where I am today without their unconditional love and encouragement, for all three of their children, to become independent. To my sister, Doris, for our frequent conversation, our laughs, and for setting a great example of personal accomplishment. And, my brother Dhimitri, for his young spirit and constant entertainment.

Lastly, I would like to express my immense gratitude to Levin for all his support and friendship, for the laughs, and for bringing Poppy into our lives.

Table of Contents

List of Figures

List of Abbreviations

ABPs	Actin binding proteins
ADP	Adenosine diphosphate
AJ	Adherens junctions
ANC	Actin nucleating centers
Arp2/3	Actin related protein complex
AS	Amnioserosa
Arm	Armadillo (*Drosophila* homologue of β-catenin)
ATP	Adenosine triphosphate
aPKC	Atypical protein kinase C
Baz	Bazooka (*Drosophila* homologue of Par-3)
CBP	Calmodulin binding peptide
Cno	Canoe
CAM	Cell adhesion molecule
DE-Cad	*Drosophila* E-cadherin
Dlg	Discs large
Dia	Diaphanous formin
DME	Dorsal most epidermal cells
D/V boundary	Dorsal/ventral boundary
ECL	Essential light chain of myosin
Ed	Echinoid
EdΔC	Echinoid protein lacking the intracellular domain
EdΔP	Echinoid protein lacking the PDZ-binding motif
EJC	Exon junction complex
F-actin	Filamentous actin
Fas III	Fascilin III
FH1/2	Formin homology domain 1 or 2
FSH	FLAG-Strep-His tag
FRAP	Fluorescence recovery after photobleaching
F-actin	Filamentous actin

Fred	Friend-of-Echinoid
Fog	Folded Gastrulation
G-actin	Globular monomeric actin
GAP	GTPase activation protein
GBE	Germband extension
GDI	Guanine nucleotide dissociation inhibitors
GFP	Green fluorescence protein
GEF	Guanine nucleotide exchange factor
HECT	Homologous to the E6-AP Carboxyl Terminus
Hpo	Hippo
Hrs	Hepatocyte growth factor-regulated tyrosine kinase substrate
ISH	Non-isotopic *in situ* hybridization
IQ motif	Isoleucine and glutamine sequence motif
Jar	Jaguar
LE	Leading edge
Lgl	Lethal giant larvae
MARK	Microtubule affinity regulating kinases
MAP	Microtubule-associated proteins
MARCM	Mosaic analysis with a repressible cell marker
MBS	Myosin binding subunit of myosin phosphatase
Mlc-c	Myosin ligh chain cytoplasmic
MRLC	Myosin regulatory light chain
pMRLC	Phosphorylated (active) form of myosin regulatory light chain
MLCP	Myosin phosphatase
Myo V	Myosin V/Didum
NFA	Nucleotide-free actin
NMJ	Neuromuscular junctions
NPF	Nucleation promoting factor
Nrg	Neuroglian
Par-1	Partition-defective-1

PDZ	Post synaptic density protein (PSD95), Drosophila disc large tumor suppressor (DLG1), zonula occludens-1 protein (ZO-1)
PH	Pleckstrin homology domain
Pi	Inorganic phosphate
PIP2	Phosphatidylinositol 4, 5-bis-phosphate
PIP3	Phosphatidylinositol 3, 4, 5-triphosphate
PIP5K	Phosphatidylinositol-4-phosphate 5-kinase
PTEN	Phosphatase and tensin homologue
Sav	Salvador
Sqh	*spaghetti squash*
TAP	Tandem affinity purification
UAS	Upstream activating sequence
YFP	Yellow fluorescence protein
WASP	Wiskott-Aldrich syndrome protein

Contributions of authors

My Ph.D. work is presented as three manuscript-based chapters.

Chapter 2:

I performed all the experiments described in this chapter. I collected and analyzed the data. I wrote the manuscript and prepared all the figures. Laura Nilson provided guidance and revisions to the written work.

Chapter 3 is a manuscript in preparation:

I performed all the experiments described in this chapter. I collected and analyzed the data. I wrote the manuscript and prepared all the figures with guidance and revisions from Laura Nilson.

Chapter 4:

I performed all the experiments described in this chapter. I collected and analyzed the data. I wrote the manuscript and prepared all the figures with guidance and revisions from Laura Nilson.

Abstract

Epithelial morphogenesis underlies many biological processes that are essential to the development of an organism. Global epithelial tissue remodeling often arises as a consequence of shape changes at the level of the individual cells, and a driving force for such cell shape changes is the spatially localized contractile activity of the actomyosin network. Upstream mechanisms generate cellular signals that act as spatial cues that position this localized contractility, but how this spatial information is conveyed into cytoskeletal changes is unclear.

The homophilic binding cell adhesion molecule (CAM) Echinoid (Ed) has been previously demonstrated to act as a cellular signal in shaping the cells in an epithelium by modulating the organization the actomyosin cytoskeleton. During development, Ed disappears from defined populations of cells generating interfaces where cells expressing Ed abut cells lacking Ed (Ed/no Ed interfaces). Such interfaces exhibit a smooth contour, display a contractile actomyosin cable, and are essential for proper morphogenesis. A similar phenotype is observed at ectopically induced Ed/no Ed interfaces generated within the same type of cells, indicating that loss of Ed is sufficient to provoke this effect. The homophilic binding property of Ed is essential to stabilize Ed at the membrane, and therefore at Ed/no Ed interfaces the absence of Ed from one cell results in the loss of Ed from the apposing face of the neighboring Ed-expressing cell, thus generating a planar polarized distribution of Ed in the Ed-expressing cell. Such distribution is essential for promoting localized actomyosin contractility.

In this work, we investigated the mechanisms by which Ed communicates with the cytoskeleton to regulate actomyosin remodeling. While Ed utilizes the extracellular domain for homophilic binding, we found that it uses the intracellular domain to drive cytoskeletal changes. Through analysis of Ed transgenes and chimeric proteins, we found that the planar polarized distribution of the Ed intracellular domain is necessary and sufficient for this function of Ed, and we identified two regions within this domain that mediate cable formation. To identify Ed effector proteins that directly interact with Ed, we took a biochemical approach and found several putative candidates. We also took a candidate gene approach and investigated the polarity protein Bazooka/Par-3 (Baz) as an Ed effector. Baz localization appears disrupted at Ed/no Ed interfaces, thus generating a planar polarized distribution of Baz in the Ed-expressing cell. This effect appears to be indirect, since loss of Ed is not sufficient to disrupt the localization

of Baz. We found that in the absence of Baz, Ed/ no Ed interfaces are not smooth. These findings suggest that asymmetric distribution of Ed promotes a polarized distribution of Baz, which in turn mediates actomyosin organization.

Since generation of endogenous Ed/no Ed interfaces relies on loss of Ed from certain cell populations, we also investigated the upstream mechanisms responsible for the downregulation of Ed levels. We found that in the embryo, the disappearance of Ed protein from the amnioserosa coincides with the loss of e*d* mRNA, suggesting the presence of a negative regulation at the transcriptional level in this tissue. In the follicular epithelium, this relationship is more complex. Unlike the protein, *ed* mRNA appears to be present, suggesting that Ed expression is regulated at the post-transcriptional level in this tissue. This conclusion is further supported by the observation that ectopic expression of Ed under a heterologous promoter does not induce high expression levels of Ed.

In this work, we have investigated the upstream mechanisms that contribute to loss of Ed from epithelia generating populations of cells expressing or lacking Ed during development. We have also examined how this differentially expressed CAM mediates localized actomyosin network reorganization. Collectively, our findings define a paradigm where a difference in gene expression between two cell populations becomes translated into a localized effect on cell shape.

Résumé

La morphogénèse épithéliale est à la base de nombreux procédés biologiques essentiels au développement d'un organisme. Le remodelage global du tissue épithélial est souvent la conséquence d'un changement de forme au niveau des cellules individuelles. Une des forces qui joue un rôle moteur dans un tel changement est localisée dans l'activité contractile du réseau d'actomyosine. Des mécanismes en amont génèrent des réponses cellulaires qui agissent comme signaux permettant le positionnement de cette contractilité localisée. Cependant, comment cette information spatiale est transmise en changement dans le cytosquelette reste obscure.

La molécule d'adhésion cellulaire à liaison homophile (CAM) Echinoid (Ed) a été démontrée d'agir en signal dans les cellules épithéliales en modulant l'organisation du cytosquelette d'actomyosine. Plus tard dans le développement, Ed disparait des populations de cellules définies, ce qui génère une interface entre les cellules qui expérimente Ed et celles qui l'expriment pas (interface Ed/no Ed). De telles interfaces exhibent un contour lisse, un câble d'actomyosine contractile et sont aussi essentielles pour une bonne morphogénèse. Un phénotype similaire est observé aux interfaces exprimé ectopiquement Ed/no Ed générées dans le même type de cellules, indiquant que la perte d'Ed est suffisante pour provoquer cet effet.

Dans ce travail, nous investiguons les mécanismes que Ed utilise pour communiquer avec le cytosquelette afin de réguler la remodulation de l'actomyosin. Alors qu'Ed utilise son domaine extracellulaire pour la liaison homophile, nous avons trouvé que la protéine utilise le domaine intracellulaire pour mener les changements du cytosquelette. Par l'analyse de transgènes d'Ed et de protéines chimères, nous avons trouvé que la distribution en plan polarisé du domaine intracellulaire d'Ed est nécessaire et suffisante pour la fonction d'Ed. Nous avons ainsi deux régions à l'intérieur de ce domaine qui facilite la formation du câble d'actomyosine. Afin d'identifier les protéines effectrices de Ed, nous avons utilisé une approche biochimique et identifié plusieurs candidates. Nous avons aussi utilisé une approche de gène candidat et étudié la protéine de polarité Bazooka/Par-3 (Baz) comme effecteur d'Ed. La localisation de Baz apparait anormale à l'interface Ed/no Ed, ce qui génère une distribution en plan polarisé de Baz dans les cellules exprimant Ed. Cette conséquence apparait indirecte, puisque la perte d'Ed n'est pas suffisante pour déranger la localisation de Baz. Nous avons trouvé qu'en absence de Baz, les interfaces Ed/no Ed ne sont pas lisses. Ces résultats suggèrent que la distribution asymétrique d'Ed

promeut la distribution polarisée de Baz, ce qui en retour sert de médiateur pour l'organisation de l'actomyosine.

Puisque la génération des interfaces Ed/no Ed dépend de la perte d'Ed dans certaines populations cellulaires, nous avons exploré les mécanismes en responsable pour la régulation négative des niveaux d'Ed. Nous avons découvert que dans l'embryon, la disparition de la protéine Ed de l'amnioserosa coïncide avec la perte de l'ARN messager *ed*. Ceci suggère la présence d'une régulation négative au niveau transcriptionnel dans ce tissue. Dans l'épithélium folliculaire, cette relation apparait plus complexe. Contrairement à la protéine, l'ARN messager de Ed est présent, suggérant que l'expression de Ed est régale au niveau post-transcriptionnel dans ce tissue. Cette conclusion est supportée par l'observation que l'expression ectopique d'Ed sous un promoteur hétérologue n'induit pas de fort taux d'expression d'Ed.

Dans ce travail, nous avons exploré les mécanismes en amont qui contribuent à la perte d'Ed de l'épithélium générant des populations de cellules exprimant ou laquant Ed durant le développement. Nous avons aussi examiné comment l'expression différentielle de CAM affecte la localisation de la réorganisation du réseau d'actomyosine. En conclusion, nos découvertes définissent un paradigme ou la différence dans l'expression d'un gène entre deux populations cellulaires mène à un effet localisé sur la forme cellulaire.

Chapter 1: Literature Review

1.1 Introduction

Epithelial tissues undergo extensive remodeling often generating complex structures during development. These remodeling events are driven by shape changes occurring at the cellular level. In recent years, advances in imaging have led to a better characterization and understanding of cell shape changes and movements during different morphogenetic events (Labouesse, 2011). As a result, morphogenesis is becoming to be appreciated not simply as a biochemical event governed by signaling pathways, but rather as a biomechanical process driven by the mechanical properties of the individual cells (Lecuit and Lenne, 2007; Paluch and Heisenberg, 2009). Therefore uncovering how the biochemical pathways regulate a cell's mechanical properties is important to understanding how cell shape changes are regulated during development.

Mechanical forces, generated by subcellular signaling events, regulate fundamental aspects of cell shape. One important component of the main force-producing machinery inside the cell is the actin cytoskeleton. Subcellular actomyosin contractility generates a tensile force that contributes to changes in cell shape (Rauzi and Lenne, 2011). In epithelial cells, the contractile activity of the actin cytoskeleton is driven by nonmucle myosin II (Quintin et al., 2008; Rauzi and Lenne, 2011). Through tight association mediated by adhesion molecules, these individual cell shape deformations are transmitted and coordinated at the tissue level to induce global tissue morphogenesis.

Various upstream subcellular signals that directly regulate the activity of the actomyosin network have been identified. For example, the RhoGTPase family regulate formation of actin

filaments and the activity of myosin motors that modulate contractility. On the other hand, other proteins act as positional cues that affect the spatial distribution of the actomyosin network. However, how this spatial information is translated into the reorganization of the cytoskeleton within a cell is unclear. The work presented in this thesis explores this concept focusing on how one particular cell adhesion molecule, Echinoid (Ed), mediates the localized contractility of the actomyosin network.

1.2 The actomyosin cytoskeleton

1.2.1 Actin filaments form the architecture of the cytoskeleton

Actin filaments are involved in various cellular processes, such as cellular motility, intracellular transport, cell adhesion, and maintenance of cell shape (Pollard and Cooper, 2009). To engage in these various processes, actin filaments are frequently remodeled into different structures via regulatory actin binding proteins (ABPs). Together, the actin filaments and ABPs form the actin cytoskeleton.

Actin filaments are polymerized from monomeric globular actin (G-actin). Structurally, the 375-amino-acid long actin monomer is folded into two domains, known as the outer (small) and the inner (large) domains, which are separated by a nucleotide-binding cleft (ATP or ADP) (Kabsch et al., 1985) and a ABP-binding hydrophobic cleft (Oda et al., 2009). Due to a difference in molecular mass between the domains, G-actin imparts a distinct structural polarity. The large domain is also called “the barbed end” or “the plus end” and the small domain called “the pointed end” or “the minus end” (Kabsch et al., 1990). Actin filaments exhibit the same polarity, as the monomers undergoing polymerization are oriented in the same direction (Moore

et al., 1970; Woodrum et al., 1975). This structural polarity has important implications in the polymerization rate (Pollard, 1983; Wegner, 1976; Wegner and Isenberg, 1983).

Polymerization of actin into filaments occurs when G-actin monomers assemble into trimers that act as nuclei for the growing filament. Even though such nuclei are thermodynamically unstable, once formed they allow for a rapid growth of the filament (Cooper et al., 1983; Pollard and Borisy, 2003). Only G-actin bound to ATP can be added to a filament. Upon polymerization, G-actin undergoes a conformational change that increases its ATPase activity and triggers an irreversible hydrolysis of ATP, ultimately generating F-ADP-actin and inorganic phosphate (Pi) (Carlier et al., 1988; Murakami et al., 2010; Pollard and Weeds, 1984). Following the addition of a monomer into a growing filament, ATP hydrolysis occurs relatively quickly after a certain lag time (Blanchoin and Pollard, 2002; Carlier et al., 1988; Rould et al., 2006). In addition, the release of Pi, one of the byproducts of ATP hydrolysis, occurs even slower and therefore, the newly assembled filament contains an F-ADP-Pi intermediate (Carlier and Pantaloni, 1986). Under polymerizing conditions, a growing filament is a heterogeneous polymer composed of a mixture of F-ATP actin subunits at the growing ends, F-ADP-Pi actin subunits at the less distal ends, and F-ADP actin subunits, added early during polymerization, positioned deep into the filament (Carlier and Pantaloni, 1986; Pollard and Borisy, 2003).

Polymerization precedes ATP hydrolysis. The two processes can be separated since hydrolysis occurs significantly after the monomer is incorporated into the growing filament (Pardee and Spudich, 1982). Further evidence for this distinction between the two processes comes from studying the composition of the filament. Under polymerizing conditions, only a small percentage of newly incorporated monomers have their ATP hydrolyzed (Pollard and Weeds, 1984). *In vitro* studies indicate that nucleotide-free actin monomers (NFA) are able to

polymerize into filaments at high concentrations of sucrose, which is needed to structurally stabilize NFA (De La Cruz et al., 2000). These NFA filaments appear to be 1.5 times longer than the nucleotide-bound filaments, indicating that ATP hydrolysis is not strictly required for polymerization (De La Cruz et al., 2000). In addition, *in vitro* F-actin polymerization still occurred even when ATP was substituted with an ATP-analogue, adenylyl imidodiphosphate (AMP-PNP), which could bind to G-actin monomers but could not be hydrolyzed (Cooke and Murdoch, 1973). Together, these observations suggest that F-actin polymerization is not dependent on ATP hydrolysis.

Although hydrolysis of ATP does not appear to be necessary to drive polymerization, binding of ATP provides structural stability to the monomer since NFA monomers denature rapidly in the absence of a stabilizing reagent (Cooke and Murdoch, 1973; De La Cruz et al., 2000; Pardee and Spudich, 1982; Pollard and Weeds, 1984). Cryo-electron microscopy studies have shown that following polymerization, ATP hydrolysis and the subsequent release of Pi cause a conformational change in the filament, which destabilizes it (Murakami et al., 2010). ADP-bound actin is an unstable structure within the filament and preferentially dissociates from it (Carlier and Pantaloni, 1986; Fujiwara et al., 2007; Pollard, 1986). Interestingly, following ATP hydrolysis, exchange of the nucleotide, from ADP to ATP, has not been observed to occur when actin is embedded in the filament, suggesting that such an exchange occurs only in the monomer stage (Fujiwara et al., 2007). Collectively, these data indicate that the difference in the stability of the nucleotide-bound actin monomers provides an intrinsic mechanism for the disassembly of the filament.

In cells, both actin species, G-actin and F-actin, exist in a dynamic equilibrium (Asakura et al., 1960), therefore monomers are constantly added and lost from the filaments. G-actin

monomer addition occurs at both ends, the barbed end and the pointed end, of the growing polymer. However, experiments that determined the association and dissociation constants showed that the rate of addition of the monomers differs at each end (Carlier and Pantaloni, 1986; Fujiwara et al., 2002; Fujiwara et al., 2007; Pollard, 1983, 1986; Selve and Wegner, 1986; Wegner, 1976; Wegner and Isenberg, 1983). G-ATP actin monomers preferentially associate with the barbed end of the filament, whereas G-ADP actin preferentially dissociate from the pointed end. When the concentration of G-actin monomers and F-actin is in an equilibrium state there is a net polymerization at one end (the barbed end) and a net depolymerization at the other end (the pointed end) of the filament. At steady-state, this process of dynamic instability of the filament is termed treadmilling (Wegner, 1976), where the rate of ATP-actin association and ADP-actin dissociation is balanced.

Treadmilling is made possible by the fact that ATP hydrolysis in the polymer is an irreversible chemical reaction (Carlier et al., 1988). The phenomenon of treadmilling was theoretically concluded (Wegner, 1976) and observed *in vitro* (Pollard, 1986; Selve and Wegner, 1986; Wegner and Isenberg, 1983), even on single actin filaments (Fujiwara et al., 2002). However, the polymerization and depolymerization of the filaments *in vivo* occurs faster than predicted by *in vitro* treadmilling (Pollard, 2007; Pollard and Borisy, 2003; Watanabe and Mitchison, 2002), suggesting that ABPs exert an important role in actin dynamics *in vivo*.

1.2.1.1 Actin filament dynamics is regulated by ABPs

Because actin polymerization depends on the concentration of free G-actin monomers, some ABPs modulate actin dynamics *in vivo* by influencing the pool of available G-actin. Two such proteins are cofilin/ADF and profilin, which promote filament depolymerization and

polymerization respectively. Cofilin/ADF (cosediments with filamentous act*in*, encoded by *twinstar* in *Drosophila*) is a member of the Actin Depolymerizing Factors (ADF) family. When cofilin/ADF binds to the pointed end of the actin filament, it introduces a conformational twist, which destabilizes the actin-actin interaction (Bamburg, 1999; Bamburg et al., 1999; McGough et al., 1997). Thus, one way that cofilin/ADF increases the pool of G-actin monomers is by enhancing the rate of dissociation of ADP-actin from the pointed end of the filament (Bamburg, 1999; Carlier et al., 1997; Lappalainen and Drubin, 1997). Cofilin/ADF also binds actin filaments inwards. Such binding does not cause monomer dissociation but rather filament severing that generates more barbed/pointed filament ends thus allowing for a more rapid actin turnover/ treadmilling (Bamburg et al., 1999; Pollard and Borisy, 2003).

Unlike cofilin/ADF that binds to F-actin, profilin (profilamentous actin or profilactin, encoded by *chickaddee* in *Drosophila*) directly binds to monomeric G-actin in a 1:1 stochiometric ratio, which prompted an initial hypothesis that profilin inhibited actin polymerization by acting as an actin monomer sequestering protein (Carlsson et al., 1977). However, studies measuring the concentration of profilin-bound and -unbound actin in polymorphonuclear leukocytes showed that the concentration of profilin within these cells was low and therefore could not account for the higher concentration of free actin monomers (Southwick and Young, 1990). Following work reported that profilin acted as a nucleotide exchange factor: by binding to ADP-actin and converting it into ATP-actin, thus increasing the available pool of actin monomers for subsequent polymerization processes (Goldschmidt-Clermont et al., 1991; Pollard and Borisy, 2003). Profilin, via its interaction with the ABP formin dimers, increases the rate of filament elongation, thus promoting polymerization (Pollard, 2007; Romero et al., 2004). Collectively, the roles of cofilin/ADP and profilin, would predict a

simple mechanism for a more rapid actin turnover: cofilin/ADP, by destabilizing the filament, increases the pool of ADP-actin and profilin binds to such monomers and converts then into ATP-actin, favoring polymerization.

1.2.1.2 New actin filament formation is regulated by ABPs

An additional step regulated by ABPs is the *de novo* formation of actin filaments. Generally these ABPs are termed actin nucleators because they catalyze the nucleation step of filament formation. As spontaneous nucleation events by G-ATP-actin monomers are energetically unfavorable and G-ATP-actin dimers and trimers are unstable, nucleator ABPs ensure fast *de novo* actin polymerization in cells that require rapid actin remodeling (Cooper et al., 1983; Pollard, 2007; Pollard and Borisy, 2003). Two main actin nucleators are the formins and the Arp2/3 complex.

Formins are a family of related proteins that all share the conserved formin homology domain –FH1 and FH2. They are homodimers and each formin contains two FH2 domains that mediate actin binding and in turn stabilize G-actin dimers to allow for filament nucleation (Goode and Eck, 2007; Liu et al., 2010). The FH1 domain contains a proline rich region which allows for a direct interaction with profilin-G-ATP-actin structures, thus supplying the actin monomers for nucleation. In addition, once formins mediate the nucleation step, they remain connected to the growing filament at the barbed end (Pollard, 2007; Pruyne et al., 2002; Romero et al., 2004), and via their interaction with actin-bound-profilin, formins increase the rate of elongation/polymerization of the growing filament (Kovar et al., 2006). Thus formins not only assist filament nucleation but also filament elongation. Formin-meditated actin polymers are long, thin filaments that can then organize into highly-ordered structures. Examples of such

structures include filopodia and actin cables, which function in cell motility and contraction (Mattila and Lappalainen, 2008; Pollard, 2007).

Besides the highly ordered parallel structures, actin filaments also organize into branched arrangements, which are found in lamellopodia and endocytic vesicle forming at the plasma membrane (Pollard and Borisy, 2003). Formation of a branched structure would suggest that new actin filaments are assembled with one end attached to a preexisting filament and the other end free for polymerization. Indeed, the Arp2/3 complex nucleates *de novo* actin filament formation on the side of existing filaments, by attaching the pointed end of the new filament onto an existing F-actin, while leaving its barbed end free for addition of new G-actin monomers (Mullins et al., 1998; Pollard, 2007; Pollard and Cooper, 2009).

The Arp2/3 complex is composed of seven protein subunits – the Arp2 and Arp3, and ARPC1 to 5 that all interact with actin (Blanchoin et al., 2000; Pollard and Borisy, 2003). The Arp2/3 complex is intrinsically inactive, because the two Arp subunits are distant from each other, and thus cannot catalyze filament nucleation (Pollard, 2007). However, upon interaction with nucleation promoting factors (NPFs), the Arp2/3 complex undergoes a conformational change that renders it active and ready to nucleate a new filament (Pollard, 2007). Generally, unlike the long forming-nucleated actin filaments, Arp2/3 nucleated filaments are short and rigid (Pollard and Borisy, 2003).

In summary, the actin network is a highly dynamic structure composed of G-actin monomers that assemble and arrange into a multitude of structures. Each step in the formation of this network is tightly regulated by ABPs. This regulation allows not only the rapid rearrangement, such as quick nucleation, polymerization or depolymerization of filaments, in

response to extracellular or intracellular clues, but also prevents unnecessary self-assembly which could prove to be detrimental to the cell.

1.2.2 Myosin-II is the motor driving contractility

Although the actin network provides the mechanical and architectural support for the cell, it is the motor proteins, myosins that provide the driving force for the movement of the filaments. Myosins comprise a large family of mechanoenzymes that bind to and move unidirectionally along the actin filaments by using free energy released from ATP hydrolysis (Sellers, 2000). Phylogenetic analyses have categorized this superfamily into several classes, but they all share the same properties: actin binding, ATP hydrolysis, and force production. Based on their specific function and composition, myosins are further classified into the conventional and unconventional myosins (Cheney and Mooseker, 1992). Class II myosins are known as the conventional myosins (Sellers, 2000) and are the focus of this work. Specifically, non-muscle myosin II will be discussed in more detail.

Each non-muscle myosin II (myosin II hereafter) molecule is a hexamer composed of three different subunit pairs: the heavy chain subunit (encoded by *zipper* in *Drosophila*), the essential light chain subunit (ECL) (encoded by *myosin light chain cytoplasmic* (*Mlc-c*) in *Drosophila),* and the regulatory light chain subunit (MRLC) (encoded by *spaghetti squash* (*sqh*) in *Drosophila*). Myosin heavy chain subunit is a highly polarized structure and is organized into three distinct structural and functional domains. The N-terminal globular head domain contains a binding site for actin and ATP. The neck domain, which follows the head domain, is essential for the mechanical movements driven by ATP hydrolysis (Houdusse et al., 1999) and contains two IQ motifs that serve as binding sites for the light chains (Cheney and Mooseker, 1992).

Following the neck domain, the C-terminal part of the subunit contains a helical coiled-coil domain that promotes dimerization (Vicente-Manzanares et al., 2009). The two light chains are structurally similar to calmodulin and contain four helix-loop-helix motifs (EF-hand) (Nakayama et al., 1992; Rayment et al., 1993; Ushakov, 2008; Xie et al., 1994). Given that the ECL also binds the head domain of the heavy chain, it appears to function in transmitting conformational changes due to ATP hydrolysis between the head and the neck domains as well as stabilize the heavy chain subunit (Edwards et al., 1995; Ushakov, 2008; Vicente-Manzanares et al., 2009). On the other hand, the MRLC is necessary for the activation of myosin II as well as filament assembly, which is essential for the contractile function of myosin II (Craig et al., 1983; Jung et al., 2008; Vicente-Manzanares et al., 2009).

Unphosphorylated single myosin II homodimers exist in a closed/compact conformation, termed the assembly incompetent form (Jung et al., 2008). In this conformation, the two head domains interact (head-head interaction) with each other and block actin binding and ATPase activity. In addition, the coiled-coil domains assume a folded conformation and directly interact with the head domains (head-tail interaction) (Craig et al., 1983; Jung et al., 2008; Vicente-Manzanares et al., 2009). Folded myosin II molecules appear to be non-functional as they do not bind actin and cannot hydrolyze ATP (Cross et al., 1986). However, phosphorylation of the MRLC is associated with a conformation change of the homodimers that disrupts the head-head and head-tail interactions, allowing myosin II to assume an unfolded conformation (Craig et al., 1983). In this unfolded conformation, myosin II dimers associate with each other via their coiled-coil domains and assemble into highly ordered antiparallel minifilaments. Such filaments are highly processive structures that bind to antiparallel actin filaments and use ATP hydrolysis to drive contraction (Vicente-Manzanares et al., 2009). On the contrary, phosphorylation of the

C-terminal domain of the heavy-chain mediates minifilament disassembly (Vicente-Manzanares et al., 2009).

Given that assembly into minifilaments is essential for myosin II function, it is tightly regulated. To allow proper application of the contractile forces generated by these minifilaments, the phosphorylation state of MRLC is controlled by kinases and phosphatases.

1.3 RhoGTPases are upstream regulators of actomyosin contractility

The actomyosin network plays a pivotal role inside the cell by engaging in various cellular processes that are dependent on the contractile forces this network can generate. Examples of such processes include cytokinesis, cell motility via the formation of lamellipodia or filopodia, cell shape changes that contribute to tissue morphogenesis and endocytosis. The assembly and disassembly of the actomyosin network is tightly regulated within a cell to ensure proper function of the network. As discussed above, a plethora of proteins assist many aspects of the assembly of this network from actin polymerization to myosin filament assembly. Despite the diversity of such proteins and their various functions, they appear to be regulated, in one form or another, by a family of regulators that are part of the Rho family of small guanosine phosphatases (GTPases) members. Therefore, these small GTPases are responsible for regulating the activity of the actomyosin network.

1.3.1 Regulation of the small GTPases

Given the seemingly simple modulation of their activity state, RhoGTPases have been described as molecular switches that regulate the assembly and organization of the actomyosin

network (Etienne-Manneville and Hall, 2002; Hall, 1998; Van Aelst and Symons, 2002). RhoGTPases transition between a GTP-bound active state and a GDP-bound inactive state. The cycling between an active and an inactive state of the small GTPases is mediated by various upstream regulators, which fall into three distinct classes of proteins. The guanine exchange factors (GEFs) mediate the exchange between GDP and GTP. GEFs bind to GDP-bound GTPases, promote the release of GDP and allow GTP to occupy the empty space (Cherfils and Chardin, 1999; Hart et al., 1994; Schmidt and Hall, 2002). On the contrary, GTPase-activating proteins (GAPs) stimulate the intrinsic rate of GTP hydrolysis of RhoGTPases by directly interacting with the active site, and thus converting the GTPase into an inactive state (Bernards, 2003). In addition, guanine nucleotide dissociation inhibitors (GDIs) associate weakly with the GTP-bound GTPases and inhibit hydrolysis of GTP, thus blocking their activity (Chuang et al., 1993; Hart et al., 1992; Olofsson, 1999).

An additional level of regulation of RhoGTPases depends on their ability to become anchored to the membrane (Cohen et al., 2000). This membrane localization is facilitated by GEFs, GAPs, and GDIs. RhoGTPases are post-translationally modified by the addition of a C-terminal lipophilic prenyl group that allows interaction with the membrane (Cohen et al., 2000; Hori et al., 1991). GDIs interact with the C-terminal isoprenoid modification and sequester RhoGTPase to the cytoplasm, thus inhibiting its activity (Michaelson et al., 2001; Mondal et al., 2000). An alternative way that RhoGTPases are targeted to membranes with a specific composition of phospholipids is by their interaction with GEFs. In addition to the catalytic domain, GEFs also contain a pleckstrin homology (PH) domain that binds to membrane phospholipids (Rebecchi and Scarlata, 1998), thus activating the GTPase to distinct membrane sites (Buchsbaum, 2007; Schmidt and Hall, 2002). The function of the GTPases appears to

depend on their intracellular localization and the subsequent localized activation at specific membrane sites, which ultimately leads to a spatially localized regulation of actomyosin contractility.

1.3.2 RhoGTPases regulate actomyosin contractility

The best-characterized small GTPases are Rho, Rac, and Cdc42. Each of these proteins promotes the assembly of different structures of the actomyosin network. These GTPases promote F-actin polymerization and influence myosin activation, thereby regulating both components of the network.

Rac and Cdc42 influence actin polymerization by acting on the Arp2/3 complex to promote lamellipodia and filopodia formation respectively (Mattila and Lappalainen, 2008; Nobes and Hall, 1995; Pollard and Borisy, 2003). Active Rac-GTP activates the Arp2/3 complex indirectly via the Scar/WAVE proteins, which are part of the NPF family (Machesky et al., 1999; Pollard and Borisy, 2003). In cells, the intrinsically active Scar/WAVE is kept inactive by interacting with the WAVE complex, composed of four different proteins. Membrane-bound Rac-GTP dissociates the WAVE complex from Scar/WAVE (Eden et al., 2002; Miki et al., 1998). Following this dissociation, Scar/WAVE returns to an active state, and is then able to activate the Arp2/3 complex, enabling the formation of new branched actin filaments (Eden et al., 2002; Machesky et al., 1999; Miki et al., 1998). On the other hand, GTP-bound Cdc42, in concert with phosphatidylinositol 4,5-bis-phosphate (PIP2), regulates activation of Arp2/3 complex via the Wiskott-Aldrich syndrome protein (WASp) (Pollard, 2007; Symons et al., 1996). Due to autoinihibition by its N-terminal domain, WASp is in an inactive conformational state (Pollard, 2007). Binding of Cdc42 to WASp relieves this autoinhibition, and allows it to

directly interact with and activate Arp2/3 complex (Machesky et al., 1999; Pollard, 2007; Rohatgi et al., 1999). However, Cdc42 activated Arp2/3 complex has been shown to mediate filopodia formation, suggesting that this complex not only polymerizes branch actin filaments but also contributes to unbranched F-actin bundles (Mattila and Lappalainen, 2008).

The other member of the GTPase family, Rho, influences actomyosin contractility by promoting actin polymerization and myosin activity. Rho directly binds to formins at their N-terminal Rho-binding domain (RBD), relieves their autoinhibition, and renders them active (Kohno et al., 1996; Otomo et al., 2005; Pollard, 2007; Rose et al., 2005). Once activated, formins nucleate new filaments and promote actin polymerization (Pollard, 2007). To influence myosin contractility, Rho regulates the activity of its downstream effector Rho-kinase (Fujisawa et al., 1996; Leung et al., 1996; Leung et al., 1995; Riento and Ridley, 2003). A serine/threonine kinase, Rho-kinase contains an RBD and PH domain that mediate direct binding to Rho and membrane phospholipids respectively. Rho binding disrupts an intramolecular interaction between the kinase domain and the C-terminal autoinhibitory region of Rho-kinase, thereby freeing the kinase domain (Riento and Ridley, 2003).

Upon Rho activation, Rho-kinase regulates myosin activity in two ways: by promoting myosin II activity and by blocking the activity of a myosin II inhibitor. Rho-kinase directly phosphorylates MRLC at a conserved serine residue, which ultimately results in increased contractility (Amano et al., 1996; Riento and Ridley, 2003). In addition, Rho-kinase phosphorylates myosin phosphatase (MLCP), at its myosin-binding subunit (MBS), promoting its dissociation from myosin resulting in a concomitant increase of myosin II activity (Kimura et al., 1996; Velasco et al., 2002; Vicente-Manzanares et al., 2009).

Rho promotes localized actomyosin contractility by influencing the phospholipid composition in the membrane. Rho, via its effector Rho-kinase, activates phosphatidylinositol-4-phosphate 5-kinase (PIP5K), which promotes PIP2 synthesis at distinct sites in the membrane (Weernink et al., 2004; Weernink et al., 2000). Given that GEFs contain a PH domain that allows them to interact with specific phosphoinositides (Rebecchi and Scarlata, 1998), this spatially localized enrichment of PIP2 generates a microenvironment within the membrane where GEFs could target and positively regulate the activity of Rho downstream effector Rho-kinase at select membrane sites. This in turn could presumably lead to myosin activation at PIP2-rich membranes. Thus Rho might act as a positional cue that via a positive feedback loop drives localized activation of actomyosin contractility.

1.4 Actomyosin contractility directs cell shape changes that regulate tissue morphogenesis

The spatial regulation of the contractile activity of the actomyosin network within a cell induces individual cell shape changes that ultimately contribute to global tissue morphogenesis. Although constriction occurs cell autonomously, given that cells within a tissue are mechanically coupled by junctions, constriction also exerts a non-cell autonomous effect on the neighboring cells and alters their shapes. Thus, regulation of actomyosin dynamics within a cell is conveyed into the neighboring cell, which then gets propagated into the tissue.

In the following section, four morphogenetic events during *Drosophila* development will be reviewed focusing on how the local changes of actomyosin contractility induce cell shape changes that contribute to tissue deformations. Examples of such cell shape changes include apical constriction and anisotropic constriction at cell-cell interfaces (Figure 1.1). In early

embryogenesis, tissue internalization is driven by the apical constriction of the presumptive mesodermal cells in the ventral region of the embryo (Figure 1.1 A; Martin et al., 2009; Sweeton et al., 1991). Later on, embryonic tissue elongation during germband extension is directed by spatially polarized constriction (Figure 1.1 C), which promotes cell intercalation and neighbor exchange (Bertet et al., 2004; Blankenship et al., 2006; Fernandez-Gonzalez et al., 2009; Kasza et al., 2014; Zallen and Wieschaus, 2004). Tube formation in the developing egg chamber is driven by similar mechanisms, where two distinct groups of cells within the dorsal appendage primordia, the floor cells and the roof cells, display characteristic shape changes. The floor cells exhibit anisotropic contractile properties, while the roof cells undergo apical constriction (Figure 1.1 B, C). Together, coordination of these cell shape changes lead to dorsal appendage formation during oogenesis (Dorman et al., 2004; Osterfield et al., 2013; Ward and Berg, 2005). In late embryogenesis, the process of dorsal closure is driven by several cell shape changes occurring in two different tissues, the apically constricting extraembryonic amnioserosa cells and the planar polarized contracting epidermal cells (Figure 1.1 A, D; David et al., 2010; Franke et al., 2005; Gorfinkiel et al., 2009; Jacinto et al., 2002b; Kiehart et al., 2000; Solon et al., 2009). During this process, not only are the cell shape changes coordinated within each tissue, but coordination also occurs between the different tissues (Franke et al., 2005; Jacinto et al., 2002b; Kiehart et al., 2000). Collectively, these examples of different morphogenetic processes highlight that local modulations in cell shape, driven by spatially polarized actomyosin network contractility, direct tissue morphogenesis.

1.4.1 Pulsed actomyosin contractions drive apical constriction and tissue bending

Invagination of the presumptive mesoderm in the early *Drosophila* embryo is associated with several cell shape changes driven by actomyosin contractility that induces apical constriction within a defined population of cells in the ventral most region of the embryo. Following apical constriction, the ventral cells elongate along their apicobasal axis, pushing their cytoplasm and nuclei basally, and expand their basal surface (Sweeton et al., 1991). After reaching their maximum length, the cells shorten to their original length but keep their apices constricted. These shape changes result in a wedged morphology of the individual cells, which aids with the inward bending of the tissue (Sweeton et al., 1991).

Individual ventral cells that undergo characteristic morphological changes are specified by the Dorsal morphogen gradient, which reaches the highest level in the ventral region (Hong et al., 2008; Jiang and Levine, 1993; Leptin, 1999). Dorsal induces expression of two transcription factors Snail and Twist, which are the most upstream signals directing cell shape changes (Leptin and Grunewald, 1990; Sweeton et al., 1991). Although the downstream targets of Snail remain unknown, Twist induces expression of the transmembrane protein T48 and the apically secreted protein Folded Gastrulation (Fog). The spatially localized secretion of Fog activates the membrane localized Gα protein Concertina (Cta) that together with T48 lead to the apical activation and anchoring of RhoGEF2 (Dawes-Hoang et al., 2005; Kölsch et al., 2007; Nikolaidou and Barrett, 2004; Parks and Wieschaus, 1991). The spatially restricted activation of RhoGEF2 provides a positional cue for the apical activation of myosin II and F-actin localization (Barrett et al., 1997; Fox and Peifer, 2007; Nikolaidou and Barrett, 2004).

Although it was initially hypothesized that the actomyosin network localized in a circumferential belt around the apical perimeter at the level of AJ was the sole driving force inducing apical constriction (Hildebrand, 2005), visualization of myosin II staining in fixed and

live cells of the presumptive mesodermal cells revealed that myosin II assumes a more dispersed localization across the apical surface of the cells in spot-like structures (Dawes-Hoang et al., 2005; Martin et al., 2009). Quantitative analysis of these structures showed that myosin II spots increase in intensity as they move closer together towards the middle of the apical cortex. This process is termed myosin coalescence (Martin et al., 2009). Comparative analysis of the apical cell shape and myosin coalescence indicated that apical constriction correlated and was preceded by bursts of myosin accumulation, suggesting this medial apically localized myosin drives cell shape changes (Martin et al., 2009).

Analysis of cell shape indicated that the decrease in apical perimeter occurred gradually within the tissue. Interestingly, individual cells decreased their apices incrementally through cycles of contraction pulses and stabilization. Transient pulses of constriction were followed by a stabilizing period where the cells remained in a constricted state before starting a new pulse of contraction (Martin et al., 2009). Constriction pulses correlated with myosin coalescence within the individual cells. It was determined that Snail promotes contraction pulses that deform the shape of the cell, whereas Twist inhibited complete relaxation after each contraction and stabilized the cell shape (Martin et al., 2009).

During mesoderm invagination, individual cell apices are not the same length suggesting that constriction does not occur simultaneously and the same rate in all the cells (Martin et al., 2009; Sweeton et al., 1991). It is unclear what initiates apical constriction, although it has been previously reported that several ventral cells spontaneously initiate constriction prior to the global constriction of the mesodermal cell population (Kam et al., 1991; Sweeton et al., 1991).

Cells within a tissue are mechanically coupled by junctional complexes. Apical junctional complexes, more specifically the adherens junctions (AJs), are attached to this

actomyosin network and have been proposed to allow mechanical coordination between adjacent cells (Martin et al., 2010; Martin et al., 2009). Consistent with this hypothesis, diminishing the levels of AJ components caused tears within the epithelium, suggesting that AJs transmit the contractile forces generated by the actomyosin network between neighboring cells (Martin et al., 2010).

The asynchronously contracting mesodermal cells drive global tissue morphogenesis. Actomyosin contraction pulls the cell membrane inwards at discrete junctional sites, causing deformation of the constricting cell (Figure 1.1 A; Kam et al., 1991; Martin et al., 2009). As cells are interconnected, this change in cell shape is transmitted to the neighboring cells, which then stretch to accommodate the constriction. Cell stretching has been reported to induce contraction in the same cell, if stretching exceeds a certain threshold (Kam et al., 1991). Thus through a series of stretching, constriction followed by a stabilization period in a contractile state, individual cell shape changes driven by actomyosin constriction contribute to tissue deformation.

1.4.2 Anisotropic actomyosin contractility generates in tissue elongation

Following the onset of the internalization of the presumptive mesoderm, the *Drosophila* embryo undergoes another morphogenetic event, which results in the extension (elongation) of the anteroposterior axis and the convergence (narrowing) of the dorsoventral axis. This morphogenetic process is germband extension (GBE) and is driven by cells intercalating between their dorsal and ventral neighbors, promoting neighbor exchange resulting in the overall elongation of the tissue (Bertet et al., 2004; Blankenship et al., 2006; Irvine and Wieschaus, 1994; Zallen and Wieschaus, 2004). The directionality of the intercalation is dependent on the anteroposterior patterning genes (Irvine and Wieschaus, 1994; Zallen and Wieschaus, 2004).

While prior to rearrangement, the embryonic epidermal cells form a regular hexagonal array, during GBE changes in cell shape perturb the regularity of the array, thereby increasing the disorder of the *status quo* and promoting intercalation (Bertet et al., 2004; Blankenship et al., 2006; Irvine and Wieschaus, 1994; Zallen and Zallen, 2004).

Tissue elongation is driven by two modes of cell intercalation (Bertet et al., 2004; Blankenship et al., 2006). In early GBE, cell intercalation is primarily driven by individual cells shrinking their vertical interfaces (AP interfaces that run parallel to the D/V axis) to form a point-like vertex, which then resolves perpendicularly into a new interface (DV interface), ultimately resulting in neighbor exchange (Bertet et al., 2004). This type of intercalation is called T1-T2-T3 transition based on the types of cell junctions during each transitional point (Bertet et al., 2004). During later stages of GBE, cell intercalation occurs predominantly through a higher level of organization of cell rearrangements (Blankenship et al., 2006; Fernandez-Gonzalez et al., 2009). A group of 5 – 11 cells align their AP interfaces forming a multicellular rosette structure (Blankenship et al., 2006). This interface shrinks causing the individual cells to meet at a common vertex, which then resolves perpendicular to the original AP interfaces forming multiple new DV interfaces (Blankenship et al., 2006). Both modes of cell intercalation increase disorder and ultimately result in the elongation of the tissue (Bertet et al., 2004; Blankenship et al., 2006; Fernandez-Gonzalez et al., 2009).

The process of cell intercalation coincides with the polarized enrichment of F-actin and myosin II in the cell cortex at the level of AJs at the AP interfaces of individual cells (Bertet et al., 2004; Zallen and Wieschaus, 2004). In multicellular rosettes, actomyosin enrichment spans several vertically aligned AP interfaces resembling a cable-like structure (Blankenship et al., 2006). The observations that enrichment of actomyosin occurred at the same AP interfaces that

undergo a decrease in length led to a model where the planar polarized contractile activity of the actomyosin network at the cell cortex generates local anisotropic tension around the cell circumference, which in turn is responsible for the shrinking of those interfaces resulting in cell shape changes (Blankenship et al., 2006; Fernandez-Gonzalez et al., 2009; Rauzi et al., 2010; Zallen and Wieschaus, 2004). Consistent with this model, laser ablation experiments on individual AP interfaces demonstrate that such interfaces are under tension as cutting of the interface caused it to relax (Fernandez-Gonzalez et al., 2009; Rauzi et al., 2008). Also, the same experiments demonstrated that the mechanical tension at the AP interfaces is greater than at the DV ones (Fernandez-Gonzalez et al., 2009; Rauzi et al., 2008). Computational modeling revealed that this difference in tensile forces between the interfaces is sufficient to drive cell intercalation resulting in tissue elongation (Rauzi et al., 2008). Tension along the AP interfaces is a consequence of contractile activity of the actomyosin network generated by myosin II. Pharmacological experiments revealed that disrupting or uniformly increasing the activity of myosin II negatively affects tissue elongation (Bertet et al., 2004; Fernandez-Gonzalez et al., 2009; Simoes Sde et al., 2010). Thus, asymmetrical tension generated by the contractile activity of the actomyosin network induces cell intercalation which drives germband extension.

The planar polarized enrichment of the actomyosin network components leads to the asymmetric contractile actomyosin activity, which in turn generates the anisotropic tension in the intercalating cells (Figure 1.1 C). In early embryogenesis, both F-actin and myosin II are symmetrically distributed around the cell cortex. Just prior to GBE, F- actin becomes enriched at the AP interfaces, followed by and enrichment of myosin II (Blankenship et al., 2006; Zallen and Wieschaus, 2004). The molecular mechanism that triggers the spatial reorganization of F-actin and myosin II is not clear, however their planar polarized distribution appears to be dependent on

the A/P patterning (Bertet et al., 2004; Blankenship et al., 2006; Irvine and Wieschaus, 1994; Zallen and Wieschaus, 2004). Loss of function of A/P patterning genes as well as the pair-rule genes *even-skipped* and *runt* result in loss of enrichment of myosin II at the AP interfaces, ultimately leading to disruption of GBE (Bertet et al., 2004; Blankenship et al., 2006; Irvine and Wieschaus, 1994; Zallen and Wieschaus, 2004). These data suggest that A/P patterning events regulate the spatial distribution of the actomyosin network, although the molecular link between the two is not clear.

The reorganization of the actomyosin network occurs concurrently with the redistribution of other apically localized proteins in the epidermal cells. The polarity protein Bazooka (Baz/ Par-3) along with AJ components, E-cadherin and Armadillo (Arm, β-catenin), becomes enriched at the DV interfaces, thus assumes a complementary distribution to the localization of F-actin and myosin II, which are enriched at the AP interfaces (Bertet et al., 2004; Blankenship et al., 2006; Zallen and Wieschaus, 2004). The significance of the redistribution of the AJ components remains unclear, although it has been proposed that diminishing adhesive connections between the cells in a polarized manner might provide the directional cue for the intercalation process (Irvine and Wieschaus, 1994). On the other hand, redistribution of Baz localization appears to be required for the enrichment of myosin II at the AP interfaces as well as enrichment of the AJs at the DV interfaces (Simoes Sde et al., 2010). Together, these observations led to a model where Baz appears to be the positional cue that promotes the polarized distribution of cytoskeletal and junctional components during this process (Simoes Sde et al., 2010; Zallen and Wieschaus, 2004).

The asymmetric distribution of Baz within the cell appears to be dependent on the Rho-kinase, which appears enriched at the AP interfaces and thus assumes a similar distribution to

actomyosin (Simoes Sde et al., 2010; Simões et al., 2014). Rho-kinase directly binds to and phosphorylates Baz at its C-terminal coiled-coil domain and in turn destabilizes its cortical localization (Simoes Sde et al., 2010). Loss of Baz from the AP interfaces is concomitant with enrichment of myosin II at the same interfaces (Blankenship et al., 2006; Zallen and Wieschaus, 2004). Thus, the planar polarized distribution of Rho-kinase appears to have a dual function on myosin II. Not only does Rho-kinase positively regulate its activity by changing the phosphorylation state of myosin II, but also influences its spatial distribution within the cell (Simoes Sde et al., 2010). The polarized distribution and activity of Rho-kinase depends on RhoGTPase signaling (Simões et al., 2014), which in turn appears to be influenced by AP patterning genes (Irvine and Wieschaus, 1994; Zallen and Wieschaus, 2004).

In summary, while the precise molecular mechanisms that translate AP patterning signals into the planar polarized distribution of cytoskeletal and junctional components remain unknown, the phenotypic manifestations of this spatial organization are well documented. During GBE, the spatially localized actomyosin activity generates anisotropic tensile forces around the cell circumference, which induce contraction of the AP interfaces (Bertet et al., 2004; Fernandez-Gonzalez et al., 2009; Kasza et al., 2014; Simoes Sde et al., 2010; Zallen and Wieschaus, 2004). The perpendicular resolution of these interfaces into a new DV interface ultimately results in the elongation of the germband (Bertet et al., 2004; Blankenship et al., 2006; Lecuit and Lenne, 2007).

1.4.3 Actomyosin induced anisotropic contractility and apical constriction drive tube formation in the follicular epithelium

Asymmetric constriction within a defined group of cells is one of the driving forces of tissue deformation that converts a flat sheet of epithelial cells into a tubular structure (Dorman et al., 2004; Osterfield et al., 2013; Ward and Berg, 2005). This morphogenetic event occurs in the dorsal-anterior region of the follicular epithelium that envelops the developing egg and gives rise to two distinct appendages asymmetrically located at the dorsal anterior side of the eggshell. Similarly to the individual epidermal cell behaviors during germband extension (Bertet et al., 2004; Blankenship et al., 2006), appendage morphogenesis proceeds by a series of asymmetric constrictions and neighbor exchange within a defined population of cells, called the floor cells (Dorman et al., 2004; Osterfield et al., 2013). Concomitantly, another group of cells, termed the roof cells, undergo apical constriction (Dorman et al., 2004; Ward and Berg, 2005). Together, coordinated cell shape changes occurring in the floor and roof cells result in the formation of a tube from a flat epithelial sheet of cells.

These cell shape deformations are preceded by patterning events that specify the two appendage primordia. Localized secretion of a TGFα-like ligand, Gurken, from the oocyte activates the epidermal growth factor receptor (EGFR) pathway in the overlying follicle cells (Nilson and Schupbach, 1999). The spatially localized activity of this pathway then specifies the two populations of cells that are part of the dorsal appendage primordia. The floor cells form the seam of the tube and express *rhomboid-lacZR1.1* marker, whereas the roof cells form the top of the tube and expressed high levels of the transcription factor Broad (Dorman et al., 2004; Ward and Berg, 2005). Because of their gene expression patterns and their respective morphology, these cell types are easily distinguishable from each other and from the rest of the follicular cells.

The floor cells are arranged in a single row that borders the roof cells at the anterior and dorsal sides in an L-shape conformation. At the beginning of morphogenesis, these cells

straighten the interfaces where they abutt the roof cells and the anterior and more dorsal follicle cells (Dorman et al., 2004; Osterfield et al., 2013). This morphological change is followed by a shrinking of the dorsal-anterior most edge of the floor cell resulting in lateral movement of these cells, which ultimately change neighbors (Osterfield et al., 2013). These ordered cell rearrangements caused by the asymmetrically constricting floor cells to form into a rosette-like conformation, similar to the epidermal cells in germband extension, and bend underneath the roof cells (Blankenship et al., 2006; Osterfield et al., 2013), causing an out of plane deformation of the tissue. The rosette structure then resolves in a perpendicular direction to the axis of formation, generating new floor-floor cell contacts, which contribute to the closing of the tube (Osterfield et al., 2013).

The morphological changes in the floor cells coincide with accumulation of F-actin and myosin II at straightened floor cell borders (Dorman et al., 2004; Osterfield et al., 2013). Concomitantly, several proteins become cleared from these interfaces and assume a polarized distribution in the floor cells reciprocal to that of the actomyosin enrichment. These include the apically localized proteins Ed and Baz (A. Noçka, unpublished observations, Figure 1.2 A, arrow; Laplante and Nilson, 2006; Osterfield et al., 2013), as well as the basolaterally localized Fasciclin 3 (Fas3) (Ward and Berg, 2005). Visualization of myosin II staining in these cells revealed that floor cell edges at the dorsal anterior corner (the apex) display higher levels of spatially localized myosin II (Dorman et al., 2004; Osterfield et al., 2013). Consistent with this finding, computational modeling indicated that such interfaces are under greater tension than the other floor cell edges, and this disparity is necessary for the shortening and bending of the interface (Osterfield et al., 2013). Collectively, these data suggest that spatially reorganized

actomyosin cytoskeleton generates polarized tension that induces cell shape changes, which lead to tissue deformations.

Concurrent with the morphological changes in the floor cells, the roof cells also undergo shape changes. However, unlike the asymmetrically constricting floor cells, the roof cells exhibit symmetrical constriction of their apical surface (Figure 1.1 B) resulting in a wedge-like shape, similar to the presumptive mesodermal cells in the ventral region of the embryo (Dorman et al., 2004; Sweeton et al., 1991). Interestingly, apical constriction does not occur simultaneously in all roof cells. Instead, the cells near the apex constrict first and more lateral and posterior ones follow (Dorman et al., 2004). Nonetheless, this transformation in cell shape coincides with an enrichment of F-actin along the apical cortex at the level of AJs (Dorman et al., 2004), suggesting that actomyosin generated contractility might influence constriction in these cells. Once all the roof cells are apically constricted, they remain in a constricted state for the duration of the morphogenetic event and cause the flat epithelium to curve (Dorman et al., 2004).

Although the floor and roof-cell undergo characteristic morphological changes during appendage morphogenesis, they maintain their connections to each other and the rest of the epithelial cells. In both cells populations, cell shape changes initially occur in a graded fashion. The cells at the apex are the first ones to manifest the deformations, which are then spread to the rest of the cells (Dorman et al., 2004; Osterfield et al., 2013), thus highlighting the importance of proper coordination not only between like cells but also between the two different cell types.

1.4.4 Dorsal closure is orchestrated by multiple actomyosin structures occurring in two tissues.

Dorsal closure is one of the most studied developmental processes where cell shape changes, driven by local changes in actomyosin network organization, are coordinated between

two different tissues and result into global tissue morphogenesis. During this process, two lateral sheets of epidermal cells migrate dorsally over the amnioserosa (AS), an extraembryonic tissue that temporarily covers the dorsal side, and ultimately meet to close the dorsal hole. The lateral migration of the epidermal cells is highly coordinated, resulting in a well-executed closure (Blanchard et al., 2010; Jacinto et al., 2002a; Jacinto et al., 2002b). Multiple cellular processes, mostly driven by actomyosin contractility in both tissues, contribute to dorsal closure (Franke et al., 2005; Gorfinkiel et al., 2009; Jacinto et al., 2002b; Kiehart et al., 2000). The AS cells undergo apical constriction and apoptosis, while the epidermal cells spatially remodel their actomyosin network to form contractile cables and filopodia to orient cell movements (Blanchard et al., 2010; David et al., 2010; Franke et al., 2005; Jacinto et al., 2002a; Kiehart et al., 2000; Millard and Martin, 2008; Solon et al., 2009; Toyama et al., 2008; Young et al., 1993). Abrogation of one of the forces necessary for the cell shape changes does not inhibit dorsal closure, suggesting that they act redundantly and give robustness to this developmental process (Kiehart et al., 2000). However, in the absence of one force dorsal closure does not proceed normally, indicating that a contribution from each force is needed for proper morphogenesis (Franke et al., 2005; Kiehart et al., 2000; Laplante and Nilson, 2011).

Although it was previously thought that the AS was simply a passive tissue, recent studies into the contribution of forces that drive dorsal closure indicate that these extraembryonic cells not only undergo active morphological changes, but also that such changes are integral to the whole developmental process (Blanchard et al., 2010; David et al., 2010; Franke et al., 2005; Solon et al., 2009; Toyama et al., 2008). Live-image analysis of a developing embryo indicated that AS cells experience a pulsatile behavior driven by cyclical apical constriction prior to the initiation of dorsal closure (Blanchard et al., 2010; Solon et al., 2009). Individual cell

constrictions as long-lasting (Blanchard et al., 2010; Gorfinkiel et al., 2009), but do not result in global tissue contractions, as the cells fully relax into their initial shape. However, because AS is connected to the epidermis, the pulling force generated by the apical cell shape fluctuations pulls the epidermal cells dorsally and after the AS relaxation, the epidermis regresses ventrally (Solon et al., 2009). Thus, prior to dorsal closure, the epidermis displays an oscillatory behavior in the dorsal/ventral axis, but with no net dorsal movement (Solon et al., 2009). Upon initiation of dorsal closure, the AS cells undergo quicker cycles of contraction/relaxation (Blanchard et al., 2010; Gorfinkiel et al., 2009), but the first row of the AS cell that are in direct contact with the epidermis dampen their pulsing behavior and are stabilized in a contracted state (Solon et al., 2009). This cell behavior is proposed to mediate net AS tissue contraction that ultimately promotes movement of the lateral epidermis (Solon et al., 2009).

Quantitative image analysis of actin and myosin dynamics of individual AS cells revealed that apical constriction of the cell coincides with accumulation of actomyosin foci that coalesce at the medial apical surface (Blanchard et al., 2010; Franke et al., 2005; David et al., 2010). This process is similar to the apically constriction mesodermal cells (Figure 1.1 A; Martin et al., 2009). These bursts of actomyosin coalescence are functionally relevant, as demonstrated by genetic manipulation experiments (Azevedo et al., 2011; Blanchard et al., 2010; Franke et al., 2005; Homem and Peifer, 2008). Increasing actin polymerization by overexpressing a constitutively active form of Diaphanous (Dia), a formin family protein, and increasing myosin activity, through overexpression of a constitutively active form of myosin light chain kinase (MLCK), lead to premature AS cell contraction (Blanchard et al., 2010; Homem and Peifer, 2008). Conversely, reducing actomyosin activity by overexpressing a dominant-negative form of RhoGTPase inhibited apical constriction in these cells (Blanchard et al., 2010). In addition,

expression of myosin II exclusively in the AS of *zipper* mutant embryos was able to rescue apical cell constriction (Franke et al., 2005). Together these data suggest that cell shape changes in the AS are driven by the actomyosin network contractility.

During dorsal closure, the organization and dynamics of the actomyosin network are also responsible for the shape changes in the dorsal-most epidermal (DME) cells, which drive the movement of the epidermal sheets. At the onset of dorsal closure, the DME cells elongate along the dorsal-ventral axis and straighten the interface where they abutt the AS cells, termed the leading edge (LE). These cell shape changes coincide with the formation of a supracellular actomyosin cable that functions as a purse-string to generate a contractile force that increases tension and stiffens the LE (Figure 1.1 D; Kiehart et al., 2000; Young et al., 1993). One proposed function of the actomyosin cable is that it acts as a ratchet to prevent complete relaxation of the apically constricting AS cells by stabilizing the contractile state of the ventral most AS cells and thus promoting net AS tissue constriction (Solon et al., 2009). Consistent with this ratchet-like function, laser cutting experiments demonstrated that the tension generated by the cable is necessary to prevent a ventral-recoil of the epidermal cells as a consequence of the AS pulsatile behavior (Franke et al., 2005; Solon et al., 2009). However, genetic manipulation experiments that affect the formation of this cable, suggest that it rather functions as a fence to prevent premature and uncoordinated dorsal movement of the DME cells (Jacinto et al., 2002a; Laplante and Nilson, 2011). Although these two models propose a different function for the actomyosin cable, they agree that it generates a contractile force that is necessary for proper tissue movement.

Formation of the actomyosin cable coincides with the reorganization of the apical surface of the DME cells (Kaltschmidt et al., 2002). At the onset of dorsal closure, the DME cells

reorient their microtubules along the dorsal ventral axis, followed by the accumulation of F-actin in distinct foci at the tricellular junctions, termed actin nucleating centers (ANC) (Jankovics and Brunner, 2006; Kaltschmidt et al., 2002). RhoGEF2, a RhoGTPase activating protein, also becomes enriched at the ANC, suggesting that upstream signals that mediate cable formation assume a spatially polarized distribution (Harden et al., 1999; Laplante and Nilson, 2011; Magie et al., 1999). Several proteins become cleared from the LE. These include the apically localized proteins Ed, the focus of this thesis, Baz, Cno, and Fmi, which as a result of this remodeling assume a planar polarized distribution in the DME cells (Kaltschmidt et al., 2002; Laplante and Nilson, 2011; Lin et al., 2007; Pickering et al., 2013). In addition, the LE membrane accumulates higher levels of phosphatidylinositol 3,4,5-trisphosphate (PIP3), forming a distinct microenvironment that promotes the protrusive behavior of the LE (Pickering et al., 2013). Genetic manipulation experiments have place Ed as the most upstream signal for the polarized remodeling of the apical membrane of the DME cells and the formation of the actomyosin cable (Laplante and Nilson, 2011), suggesting that molecular differences between two tissues are conveyed into cytoskeletal changes.

As dorsal closure progresses, the LE extends filopodia protrusions that spread dorsally and mediate contact between opposing DME cells (Jacinto et al., 2000; Millard and Martin, 2008). Formation of these actin-based protrusions appears to depend on the small GTPase Cdc42 signaling and PIP3 accumulation at the LE (Jacinto et al., 2000; Pickering et al., 2013). Disruption of filopodia extensions cause defects in the fusion of the two epithelial sheets and misalignment between opposing epidermal segments, suggesting that these structures are necessary to mediate cell-cell contacts and might also play a sensory role to allow proper neighbor recognition (Jacinto et al., 2000; Millard and Martin, 2008).

Cooperation of the different forces generated by contractile actomyosin structures from two distinct epithelial tissues drives morphogenesis (Gorfinkiel et al., 2009; Kiehart et al., 2000). However, for dorsal closure to proceed normally, such forces are tightly coordinated (Gorfinkiel et al., 2009; Solon et al., 2009). The mechanical connections between the tissues via junctional components allows for proper transmission of forces thus contributing to the dorsal movement of the lateral epidermis in a highly coordinated fashion.

1.4.5 Adherens junctions coordinate individual cell deformations during tissue morphogenesis

Epithelial cells within a tissue are mechanically coupled by junctions, which allow cells to interact with their neighbors and thus presumably influence their shape in response to extrinsic forces. Disruption of intercellular junctions diminishes the adhesive properties between the cells, which can cause tissue tears upon force application (Martin et al., 2010; Muller, 2000). Loss of cohesiveness between cells can also fail to propagate individual cell shape changes within a tissue, leading to disruptive morphogenesis (Dawes-Hoang et al., 2005). These observations suggest that junctions are an essential component of morphogenetic events. Although there are different cell types with various types of junction, epithelial cells are the focus of this work.

In epithelia, cellular junctions span the apical and basolateral membranes of the cell. Distinct types of junctions are localized in specific domains along the lateral membrane, conferring a spatial polarity to the plasma membrane, termed apical basal polarity (Tepass et al., 2001). This polarity is actively maintained through interaction between junctional components localized at different positions along the lateral membrane that inhibit lateral diffusion and thus maintain epithelial cell polarity (Bilder and Perrimon, 2000; Klebes and Knust, 2000; Knox and

Brown, 2002; Müller and Wieschaus, 1996; Tepass et al., 1996). In invertebrates, like *Drosophila*, the lateral membrane is mainly composed of two types of junctions. The adherens junctions (AJs) are often localized in a belt-like structure, forming the zonula adherens along the apical region, while the septate junctions localize along the basolateral membrane (Bilder and Perrimon, 2000; Muller, 2000; Müller and Wieschaus, 1996). Because the abovementioned morphogenetic events are driven by local changes in cell shape occurring specifically at the apical side of the cell, coordination of such changes across the tissue spatially occurs at the level of AJs (Bertet et al., 2004; Blankenship et al., 2006; Gorfinkiel et al., 2009; Martin et al., 2009; Osterfield et al., 2013; Solon et al., 2009). Therefore, AJs and their associated proteins will be the focus of this section.

The core components of AJs are the classical cadherin proteins, with E-cadherin (E-cad or DE-cad in *Drosophila*) being the most common in epithelial cells. As a transmembrane protein, E-cad engages in homophilic interactions *in trans* via its extracellular domain, and thus facilitates cell-cell recognition (Harris and Tepass, 2010). In addition, the extracellular domain of E-cad also mediates homophilic interaction *in cis*, contributing to lateral E-cad dimerization which ultimately form dense clusters (Harris and Tepass, 2010; Troyanovsky, 2005). E-cad clusters are thought to stabilize the weak interaction between two E-cad proteins at apposing sides of neighboring cells, and thus promote stronger intercellular adhesion (Troyanovsky, 2005). On the cytoplasmic side, E-cad influences the actin cytoskeleton, by interacting with catenins. The intracellular domain of E-cad directly binds to β-catenin, which in turn binds to α-catenin. As α-catenin can directly interact with both E-cad-β-catenin complex and F-actin, it was proposed to mediate intracellular interaction between cadherins and the cytoskeleton (Harris and Tepass, 2010; Tepass et al., 2001). This hypothesis was further supported by studies of *α-catenin*

null mutant Drosophila eggchambers and embryos (Desai et al., 2013). As predicted, a transgene coding for wild-type *α-catenin* restored *α-catenin* mutant phenotypes. Interestingly, *α-catenin* transgenes that did not bind to β-catenin did not rescue the mutant phenotype, suggesting that the physical link between α-catenin and β-catenin/E-cad complex is functionally and biologically relevant (Desai et al., 2013). However, other studies have shown that α-catenin does not simultaneously bind to β-catenin and actin (Drees et al.; Yamada et al.). Monomeric α-catenin preferentially binds to the cadherin-catenin complex, whereas α-catenin homodimers bind F-actin with greater affinity (Drees et al.; Yamada et al.). These results indicated that α-catenin might not provide the physical link between the junctional proteins and the cytoskeleton (Drees et al.; Yamada et al.). These findings raise the possibility that the connection between AJs and actin might be more dynamic than previously anticipated or could be established by other intermediary proteins that interact with the cadherin-catenin complex (Gates and Peifer).

An alternative possibility is that other proteins that localize at the AJs influence the actin cytoskeleton either directly or indirectly. One example of such proteins is Afadin (Canoe, Cno in *Drosophila*), that directly binds to actin via its actin-binding domain as well as the transmembrane protein Nectin (Mandai et al., 1997; Takai et al., 2008; Takai and Nakanishi, 2003). Thus, Afadin could provide a direct link between AJs and the cytoskeleton. Two other AJ proteins that indirectly influence the distribution and thus the activity of the actomyosin cytoskeleton during *Drosophila* development are Baz and Ed. As mentioned previously, Baz assumes a reciprocal localization to the localized enrichment of actomyosin in various cell types, which is necessary for proper morphogenesis (Laplante and Nilson, 2011; Osterfield et al., 2013; Pickering et al., 2013; Simoes Sde et al., 2010; Zallen and Wieschaus, 2004). Similar to Baz, Ed

appears to influence the distribution of actomyosin indirectly. How Ed exerts this function will be in focus in the following sections of this work.

1.5 Differential expression of cell adhesion molecule Echinoid regulates actomyosin network organization during Drosophila development

Echinoid (Ed) is an AJ component that regulates the distribution of the actomyosin network, directs its localized contractility, and thereby contributes to proper morphogenesis (Ahmed et al., 2003; Laplante and Nilson, 2006, 2011; Lin et al., 2007; Wei et al., 2005). The effect on the actomyosin network is manifested at the apical interfaces between populations of cells that express and lack Ed (Ed/no Ed interfaces, or differential Ed-expression interfaces). Such interfaces are functionally relevant because disruption of differential Ed expression, either by removing Ed from the Ed-expressing cells or by introducing Ed in cells that lack Ed, abolishes the contractile actomyosin cable and results in defective morphogenesis (Laplante and Nilson, 2006, 2011; Lin et al., 2007). These observations indicated that it is not simply the loss of Ed but rather the juxtaposition of cells with and without Ed that directs the actomyosin cable formation (Laplante and Nilson, 2011).

During development, actomyosin contractility associated with endogenous Ed/no Ed interfaces generates cell shape changes that contribute to epithelial morphogenesis in the follicular epithelium (Laplante and Nilson, 2006). In this tissue, Ed/no Ed interfaces occur between the two cells types of the appendage primordia, the roof cells and the floor cells (Figure 1.2 A, arrow; Dorman et al., 2004; Ward and Berg, 2005). In a stage 11 egg chamber, Ed is expressed in the floor cells but is nearly undetectable from the roof cells (Figure 1.2 A, A", arrow, asterisk; Figure 4.1 E; Laplante and Nilson, 2006). The interfaces between the two cell

types exhibit the characteristic smooth contour of Ed/no Ed interfaces and display an enrichment of F-actin and pMRLC (Dorman et al., 2004; Laplante and Nilson, 2006; Ward and Berg, 2005). As a consequence of the contractile force of the actomyosin network, the floor cells elongate, form a trapezoid shape and ultimately meet together to close the floor of the appendage forming tube (Dorman et al., 2004; Laplante and Nilson, 2006; Osterfield et al., 2013). Loss of Ed/no Ed interfaces in appendage primordia mutant for *ed* results in actomyosin cable abolishment, which prevents proper closure of the floor cells that ultimately leads to appendages with an open floor phenotype (Laplante and Nilson, 2006).

Endogenous Ed/no Ed interfaces are also observed during dorsal closure (Laplante and Nilson, 2011; Lin et al., 2007). Loss of Ed expression from the amnioserosa prior to dorsal closure generates a differential Ed expression interface between the amnioserosa and the DME cells in the lateral epidermis (Figure 1.2 B, arrow; Laplante and Nilson, 2006; Lin et al., 2007). Generation of such interfaces spatially and temporally coincides with the contractile actomyosin cable present in the DME cells (Figure 1.2 B", arrow; Laplante and Nilson, 2006, 2011; Lin et al., 2007), which provides one of the driving forces for proper closure of the dorsal hole (Jacinto et al., 2002b; Kiehart et al., 2000). Genetic manipulation experiments have demonstrated that Ed appears to be the most upstream signal for the formation of the contractile actomyosin cable in the DME cells (Laplante and Nilson, 2011). Abolishment of Ed/no Ed interfaces abrogates actomyosin cable formation, resulting in the loss of DME cell elongation and defective dorsal closure (Laplante and Nilson, 2011; Lin et al., 2007).

Similarly to endogenous Ed/no Ed interfaces, ectopically induced clones of $ed^{-/-}$ mutant cells in the follicular epithelium and epithelial cells in the wing imaginal disc display a smooth contour and an enrichment of actomyosin components at the apical interface where they abutt the

neighboring wild-type cells (Figure 1.3 A, A', arrow; Chang et al., 2011; Laplante and Nilson, 2006; Rakic, 2013; Rawlins et al., 2003a; Wei et al., 2005; Yue et al., 2012). These observations demonstrated that differential expression of Ed alone, rather than other differences between the cell types, is responsible for organizing the actomyosin cytoskeleton at the Ed-expression interface (Laplante and Nilson, 2011).

1.5.1 Ed protein structure

Ed is a member of the immunoglobulin (Ig) domain-containing transmembrane protein superfamily. In its extracellular domain, Ed contains seven Ig-like domains and a fibronectin type-III domain. The transmembrane domain anchors Ed at the plasma membrane, while the 314 amino acid long intracellular domain does not contain any readily identifiable functional domain except a 4 amino acid long PDZ-binding motif at its very C-terminus (Bai et al., 2001; Laplante and Nilson, 2006; Wei et al., 2005). Ed sequence analysis indicates that the protein is well conserved between *Drosophila* species, with a high degree of similarity (Figure 1.4 A). Comparative protein sequence analysis revealed that Ed is also found in two mosquito species, which share a high degree of similarity in the extracellular domain, but also show that the intracellular domain contains well-conserved and non-conserved regions (Figure 1.4 B; data not shown). Although it was proposed that an Ed homologue is present in *C. elegans* (Vogel et al., 2003), sequence alignment of the two proteins from the different species showed that while the extracellular domains of the two proteins exhibit a high degree of similarity, due to the fact that they contain Ig domains, the intracellular domains differed significantly and do not show highly conserved regions, except for the last five amino acids (Figure 1.4 C; data not shown).

The domain structure of the extracellular region of Ed suggested that Ed is able to engage in homophilic and heterophilic interactions (Bai et al., 2001; Vogel et al., 2003) and such interactions have been indeed observed *in vivo* and in cultured cells (Islam et al., 2003; Laplante and Nilson, 2006; Lin et al., 2007; Wei et al., 2005). On the other hand, functional predictions of the intracellular domain are not straightforward, because it does not contain any functional domains. However it was predicted, and later demonstrated biochemically, that Ed engages in protein-protein interactions via the PDZ binding motif (Wei et al., 2005). Given the protein structure of Ed, it could be predicted that Ed utilizes the extracellular domain in cell-cell recognition, and transmits that extracellular information to the inside of the cell via its intracellular domain.

1.5.2 Homophilic binding property of Ed generates the positional cue that drives localized actomyosin organization

Homophilic interactions stabilize Ed at the plasma membrane at the level of the adherens junctions (Laplante and Nilson, 2006; Wei et al., 2005). Cell culture experiments with transfected transgenic Ed demonstrated a requirement for the extracellular domain engaging in homophilic interactions *in trans* to stably localize Ed at the interface of two cells (Islam et al., 2003; Rawlins et al., 2003a; Yue et al., 2012). A similar requirement was also demonstrated *in vivo*, where loss of Ed from a population of cells, such as in *ed* mutant clones in epithelia, affects the membrane localization of Ed at the interface in the adjacent cell (Chang et al., 2011; Laplante and Nilson, 2006, 2011; Lin et al., 2007; Rawlins et al., 2003a; Wei et al., 2005; Yue et al., 2012). These observations indicated that homophilic interactions are necessary for the subcellular localization of Ed at the membrane.

Given that Ed is dependent on homophilic interactions *in trans* to mediate the membrane localization, Ed localization is affected at Ed/no Ed interfaces (Figure 1.2 A, B, arrow; Figure 1.3 A, arrow). Absence of Ed in the *ed* mutant cell causes a non-cell autonomous disruption of Ed localization in the neighboring wild-type cell at the contact interface, where Ed is either absent or in distinct sparse puncta (Figure 1.3 A, arrow; Chang et al., 2011; Laplante and Nilson, 2006; Rawlins et al., 2003a; Wei et al., 2005). This loss of Ed from one face of the Ed-expressing cell generates a planar polarized localization of Ed in that cell (Laplante and Nilson, 2006).

The asymmetric distribution of Ed is necessary for actomyosin cable formation. Disruption of this polarized distribution in the Ed-expressing cell, either by removing Ed or by providing a binding partner in the adjacent cell to stably localize Ed at the interface, abolishes actomyosin cable formation and the smooth contour of the Ed/no Ed interface (Chang et al., 2011; Laplante and Nilson, 2011). These observations suggested that it is not simply the absence or presence of Ed that regulates the rearrangement of the cytoskeleton, because cells that lack Ed or display symmetrically localized Ed do not exhibit a localized enrichment in actomyosin structures (Chang et al., 2011; Laplante and Nilson, 2006, 2011; Wei et al., 2005). Collectively, these observations prompted the hypothesis that the planar polarized distribution of Ed generates the spatially restricted actomyosin cable formation (Laplante and Nilson, 2011).

The requirement for the asymmetric distribution of Ed in the reorganization of the cytoskeleton implies that the actomyosin cable forms in the Ed-expressing cell. Indeed the well-characterized actomyosin cable that drives dorsal closure is present at the leading edge of the DME cells, where Ed is distributed asymmetrically (Kiehart et al., 2000; Laplante and Nilson, 2011; Lin et al., 2007). Upstream regulators of actomyosin contractility appear to be enriched in

the DME cells (Jacinto et al., 2002b; Kaltschmidt et al., 2002; Laplante and Nilson, 2011). In addition, magnified images of ectopic Ed/no Ed interfaces generated by *ed* mutant clones in the imaginal wing disc, show an enrichment of phalloidin staining, which detects F-actin, in the Ed-expressing cell (Chang et al., 2011). Taken together, these data lend further support to the hypothesis that the polarized distribution of Ed in the Ed-expressing cell triggers the formation of an actomyosin cable (Laplante and Nilson, 2011). However, the molecular signals by which the planar polarized distribution of Ed promotes localized actomyosin contractility are unknown, and therefore are one of the focuses of this work.

1.5.3 Ed plays other functions during Drosophila development

In addition to its effect on the organization of the actomyosin cytoskeleton, Ed has been implicated in acting as a signaling molecule to determine cell fate and cell size. Ed has been shown to interact with the EGFR pathway in the eye imaginal disc (Bai et al., 2001; Rawlins et al., 2003b; Spencer and Cagan, 2003) and the Notch pathway in the wing disc (Ahmed et al., 2003; Chandra et al., 2003; Escudero et al., 2003; Rawlins et al., 2003a) to specify cell fate. Ed has also been shown to interact with the Hippo (Hpo) pathway to regulate cell size and proliferation (Yue et al., 2012).

Ed modulates the levels of EGFR signaling during eye development (Bai et al., 2001; Rawlins et al., 2003b; Spencer and Cagan, 2003). Loss of *ed* function causes patterning and organizational defects in the eye disc, which are associated with aberrant EGFR signaling in this tissue. Ommatidia mutant for *ed* exhibit a duplication of R8 photoreceptor cell fate that is accompanied by variations in the number of other photoreceptors and accessory cells (Bai et al., 2001; Rawlins et al., 2003b; Spencer and Cagan, 2003). On the other hand, overexpression of Ed

in these cells was associated with a decrease in the number of photoreceptors (Bai et al., 2001). Because these defects are similar to hyperactivation of EGFR signaling, it was predicted that Ed might function as a negative regulator of the pathway. Consistent with this prediction, *ed* mutant cells exhibited an increase in EGFR activity, as indicated by the elevated levels of the phosphorylated form of the EGFR effector, ERK MAP kinase (Rawlins et al., 2003b). Further characterization of the relationship between Ed and EGFR showed that *ed* genetically interacted with EGFR signaling components. Together these data indicate that Ed negatively regulates EGFR activity in the developing ommatidia (Bai et al., 2001; Rawlins et al., 2003b; Spencer and Cagan, 2003). Interestingly, Ed does not appear to interact with EGFR pathway in the follicular epithelium (Laplante and Nilson, 2006).

In mesothorax bristle patterning, Ed has been reported to function during sensory organ precursor (SOP) specification by acting synergistically with Notch signaling (Ahmed et al., 2003; Escudero et al., 2003; Rawlins et al., 2003a). During the third instar larvae and early pupal stages, one cell within a distinct group of cells, the proneural cluster, is specified and develops into an SOP, which gives rise to the adult sensory bristles, the macrochaetae and microchaetae. This specification process occurs through lateral inhibition, similar to the neural differential program, mediated by Notch signaling. Disruption of lateral inhibition results into more than one proneural cluster cells becoming specified as SOP (Hartenstein and Posakony, 1990; Heitzler and Simpson, 1991; Parks and Muskavitch, 1993). Flies mutant for *ed* exhibit additional bristles in close proximity to each other raising the hypothesis that SOP specification was not restricted to only one proneural cell (Ahmed et al., 2003; Escudero et al., 2003; Rawlins et al., 2003a). Consistent with this hypothesis, overexpression of Ed leads to loss of SOP specification from the proneural cells, suggesting that Ed promotes SOP specification from the cell cluster (Rawlins et

al., 2003a). During this process, Ed has been shown to genetically interact with components of the Notch pathway (Ahmed et al., 2003; Escudero et al., 2003; Rawlins et al., 2003a). Localization analysis demonstrated that Ed associates with Notch and preferentially with its ligand Delta at the cell membrane as well as in early endosomal vesicles (Rawlins et al., 2003a). Collectively, these observations suggested that Ed modulates Notch signaling by promoting Delta trafficking in the future SOP cell thus promoting SOP cell fate determination (Rawlins et al., 2003a).

In a genetic modifier screen, *ed* was identified as a negative regulator of the Hippo (Hpo) pathway (Yue et al., 2012). A kinase-signaling cascade, the Hpo pathway regulates organ size by modulating cell growth, cell proliferation, and cell death (Yu and Guan, 2013). Loss of *ed* in mitotically induced clones in the eye and wing imaginal discs enhanced the tissue overgrowth phenotype associated with abrogated Hpo signaling. Indeed *ed* clones associated with elevated levels of the transcription factor Yorkie (Yki), which regulates the transcription of Hpo pathway target genes (Yu and Guan, 2013; Yue et al., 2012). Through co-immunoprecipitaion of cell culture lysates, it was demonstrated that Ed directly binds to Salvador (Sav), a Hpo interacting protein. Furthermore, analysis of the localization of Ed and Sav in cultured cells and wing imaginal disc indicated that Ed mediates the membrane localization of Sav at the AJs. By stabilizing Sav at the membrane, Ed contributes to low phosphorylated/active levels of Yki, and thus less Hpo signaling (Yue et al., 2012). Collectively, the relationship between Hpo signaling and Ed indicates that Ed functions as an upstream regulator of the Hpo pathway to regulate cell growth and proliferation (Yue et al., 2012).

1.5.4 Ed functions may or may not be mediated by the same downstream effectors

During development Ed appears to have diverse functions. Ed affects the spatial distribution of the actomyosin cytoskeleton at endogenous Ed/no Ed interfaces (Laplante and Nilson, 2006, 2011; Lin et al., 2007). Ed also modulates cell face specification by interacting with the EGFR and Notch pathways in specific tissues (Ahmed et al., 2003; Escudero et al., 2003; Fetting et al., 2009; Islam et al., 2003; Rawlins et al., 2003a; Rawlins et al., 2003b; Spencer and Cagan, 2003). Lastly, Ed affects cell size and number by interacting with the Hpo pathway (Yue et al., 2012). It is not clear how these various functions of Ed relate to one another. It is possible that Ed has different functions in different tissues. It is equally possible that simply Ed has only one function that causes different phenotypes in distinct tissues. To discern between these possibilities, it is essential to have a clear understanding of the downstream Ed effectors.

Current knowledge of the downstream mediators of Ed function remains limited. It is possible that Ed employs the same downstream effectors to function in the various processes. However, it is equally possible that the different functions of Ed are mediated by different downstream effector proteins, present in the different cell types. For example, regulation of the cytoskeleton might be mediated by different downstream proteins that might either be absent or engaged in other processes in the cells where Ed functions as a cell fate determinant. As the reorganization of the cytoskeleton requires the polarized distribution of Ed, in tissues where Ed functions as a cell fate determining signal, it might not assume a clear asymmetric distribution. Therefore, identifying the downstream Ed effectors would help to elucidate the mechanisms of the different roles of Ed during development. In this thesis, we used a biochemical (Chapter 2) and a gene candidate (Chapter 3) to determine the downstream molecular signals that mediate Ed function in remodeling of the actomyosin cytoskeleton. In addition, we also examined the

upstream mechanisms that promoted formation of Ed/no Ed interfaces during development by regulating Ed expression (Chapter 4).

Figure 1.1. Mechanisms of cell shape changes that promote tissue morphogenesis.

(A – D) Diagrams of the apical surface of cells demonstrating the mechanisms by which the apically localized contractile activity of the actomyosin network induces cell shape changes. Red lines indicate actin filaments and green short segments indicate myosin II minifilame02nts. Uniform actomyosin contractility leads to incremental (A) or continuous (B) constriction of the apical surface. However, anisotropic actomyosin contractility induces contraction of a single interface (C) or stiffens the interface to resist extrinsic forces (D).

Uniform apical contractility

A

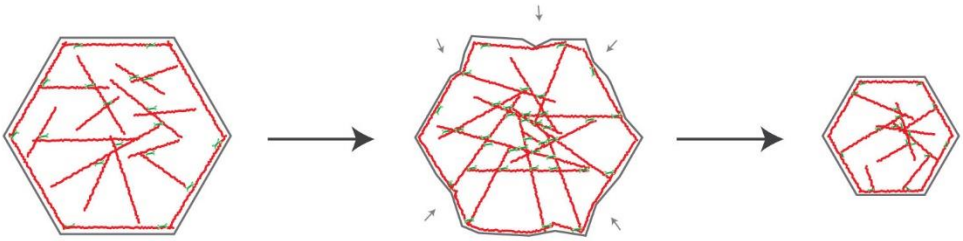

Tissue invagination: mesodermal cells
Dorsal closure: aminoserosa cells

B

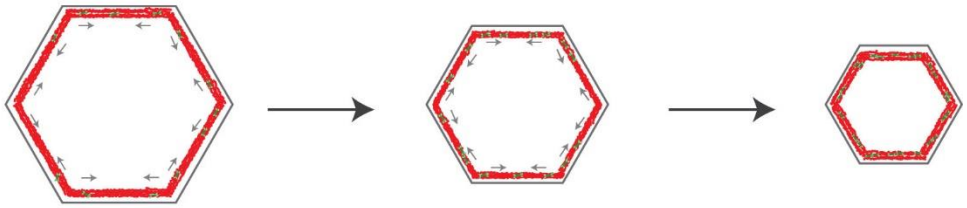

Appendage morphogenesis: roof cells

Localized apical contractility

C

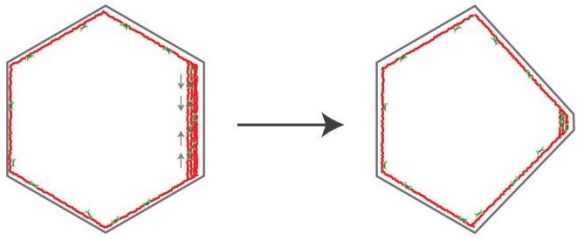

Germband extension: cell intercalation
Appendage morphogenesis: roof cells

D

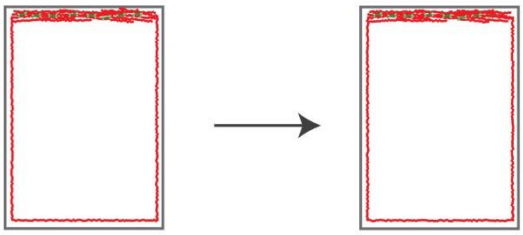

Dorsal closure: DME cells

Figure 1.2. Endogenous Ed/no Ed interfaces exhibit a smooth contour.

(A – A') Follicular epithelial cells stained for Ed, highlighting the membranes of the floor cells (FC) and Broad, marking the nuclei of roof cells (RC, asterisk). (A") Due to a difference in the plane of localization between these two populations of cells, some of the roof cell nuclei marked with Broad appear inside the floor cells in the merge image. (B – B") Dorsal closure stage embryo stained for Ed (B), Arm (B'), and F-actin (B"). AS indicates the amnioserosa tissue, whereas DME indicates the dorsal-most epidermal cells. (A, B) Arrows indicate the endogenous Ed/no Ed interfaces, as well as the loss of Ed staining from that interface. (B") Arrow indicates enrichment of F-actin and the arrowhead indicates the filopodia structures at the AS/DME interface.

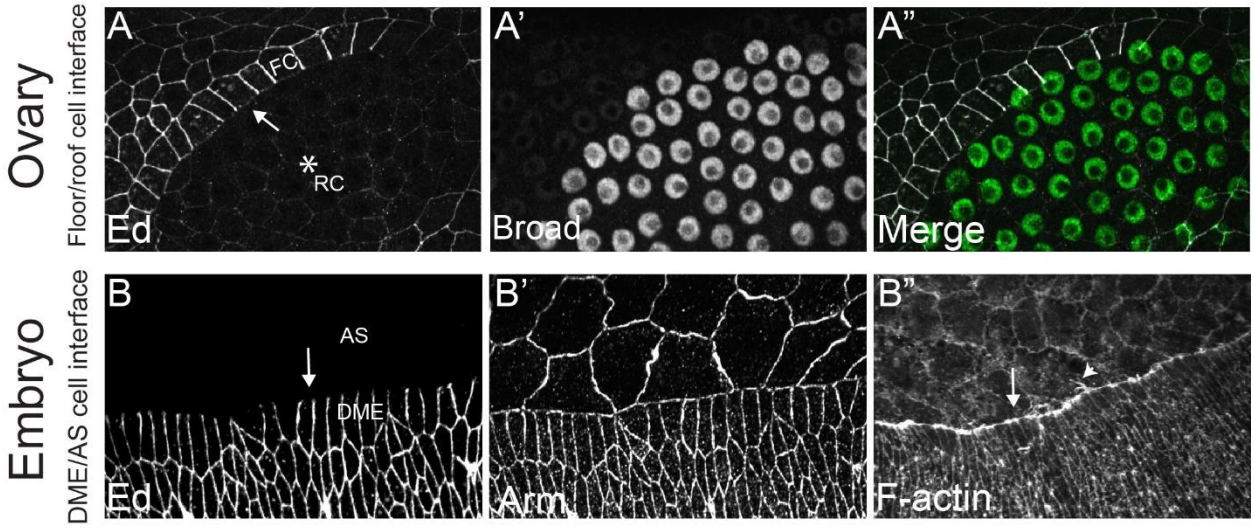
Ovary
Floor/roof cell interface
A
FC
RC
Ed
A'
Broad
A"
Merge
Embryo
DME/AS cell interface
B
AS
DME
Ed
B'
Arm
B"
F-actin

Figure 1.3. Ectopic Ed/no Ed interfaces display a smooth contour

(A – A') Mosaic follicular epithelium bearing an ed^{F72} homozygous mutant clone stained for Ed and F-actin. (B – D) Diagrams of the different interfaces are indicated by the arrow, arrowhead, and asterisk (A, A'). (B) Via homophilic binding *in trans*, Ed is stably localized at Ed/Ed interfaces (arrow), which do not display an enrichment in F-actin. (C) Absence of Ed from the Ed/no Ed interface (arrowhead) generates a planar polarized Ed in the wild-type cell, which coincides with the enrichment of F-actin at the Ed/no Ed interface. (D) Loss of Ed from both cells (no Ed/no Ed interface, asterisk) is not accompanied by an enrichment in F-actin.

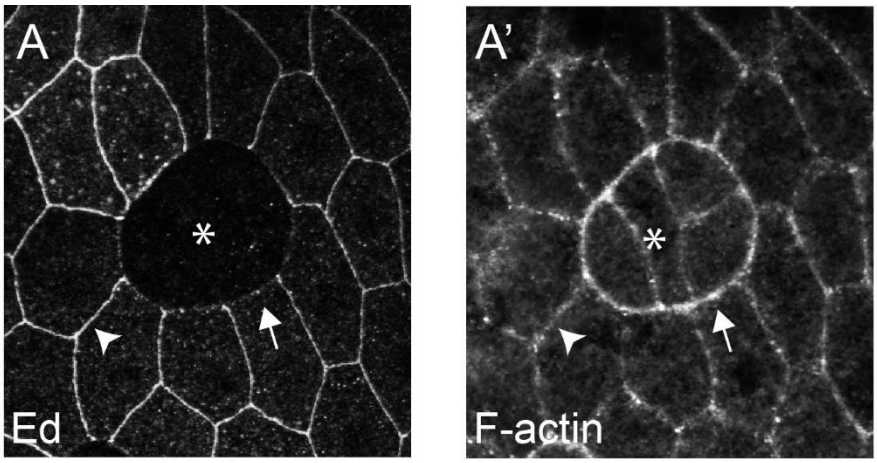
A
Ed
A'
F-actin

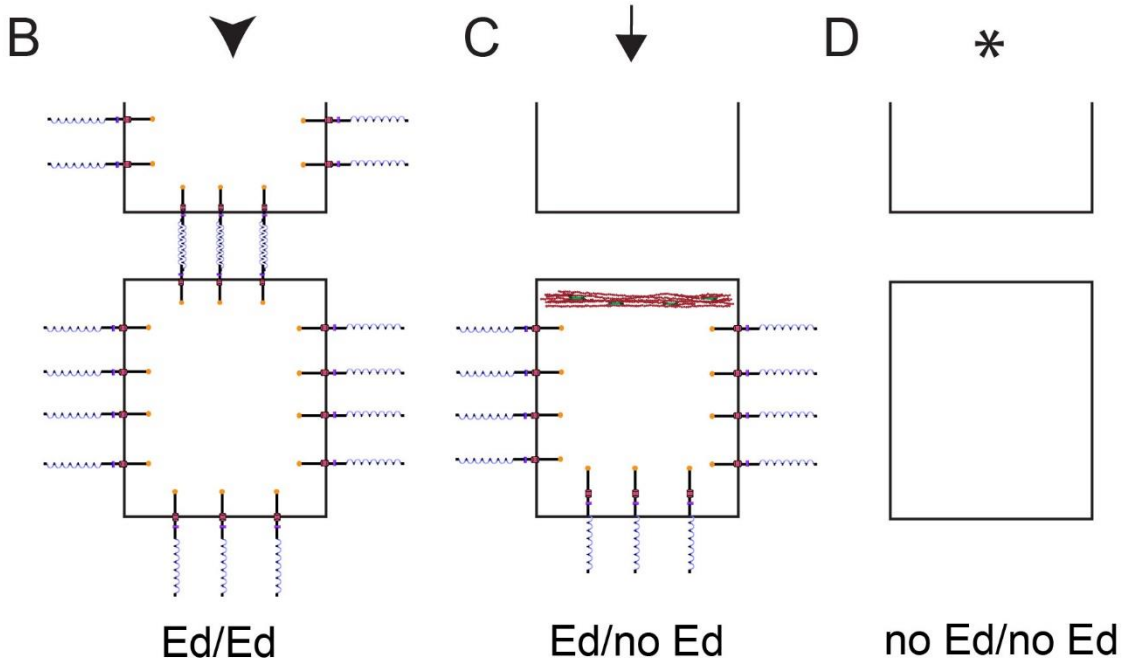
B
C
D
Ed/Ed
Ed/no Ed
no Ed/no Ed

Figure 1.4. Comparative analysis of the intracellular domain of Ed between different species.

(A) Sequence alignment of the intracellular domain of Ed from different *Drosophila* species indicating a high degree of similarity. (B) Sequence alignment of the intracellular domain of Ed from *D. melanogaster* and predicted Ed protein from two mosquito species, *A. gambi* and *A. aegypti*. The asterisks below indicate the conserved amino acids between the sequences. (C) Sequence alignment of the intracellular domain of Ed from *D. melanogaster* and the predicted Ed homologue, IGCM-1, in *C. elegans*. The asterisks bellow indicate the conserved amino acids between the two sequences.

A

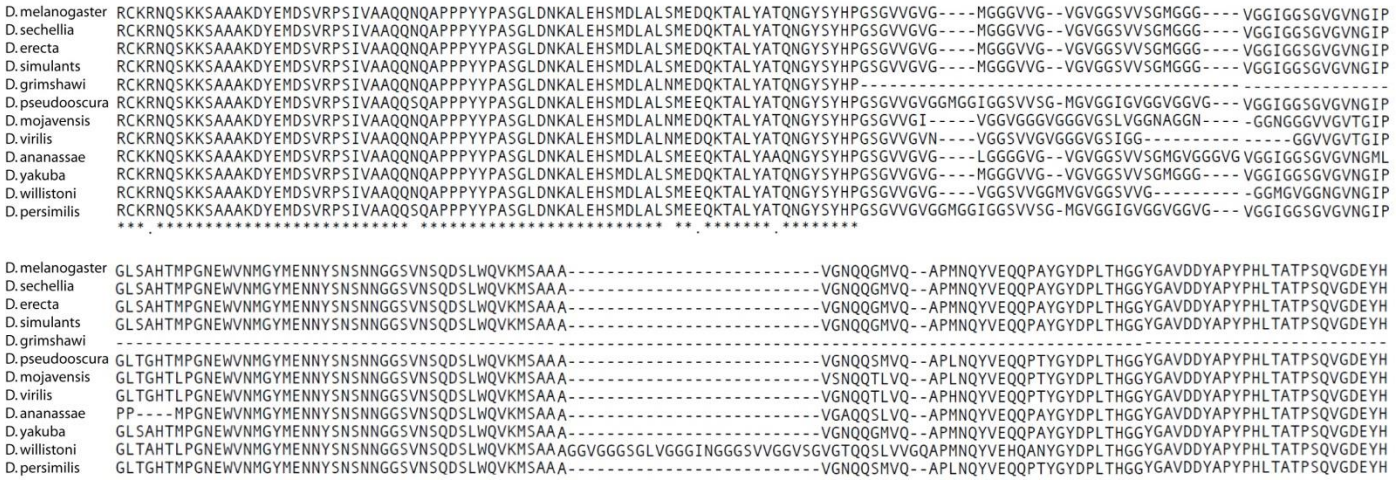
D. melanogaster
D. sechellia
D. erecta
D. simulants
D. grimshawi
D. pseudooscura
D. mojavensis
D. virilis
D. ananassae
D. yakuba
D. willistoni
D. persimilis

B


A. gambi
A. aegypti
D. melanogaster

C

D. melanogaster
C. elegans

Chapter 2: Identification of Ed effectors via tandem-tagged affinity purification (TAP) coupled with mass spectrometry analysis

2.1 Introduction

While the effect of Echinoid (Ed) on the rearrangement of the actin cytoskeleton and actin contractility at the tissue border is well established (Chang et al., 2011; Laplante and Nilson, 2011), the mechanism by which Ed exerts this effect remains to be elucidated. Several Ed interacting proteins have been previously reported (Bai et al., 2001; Chandra et al., 2003; Islam et al., 2003; Lin et al., 2007; Wei et al., 2005), however none of them seem fulfill all the requirements necessary for this particular function of Ed.

One protein that physically interacts with Ed is Canoe (Cno). Cno ia a homologue of mammalian Afadin, contains an actin-binding domain, and localizes at the adherens junctions (Mandai et al., 1997; Matsuo et al., 1999; Miyamoto et al., 1995). Cno coimmunoprecipitates with Ed from embryo lysates and in *in-vitro* binding assay (Wei et al., 2005). Because of similarities in protein structure, Ed is thought to be a homologue of mammalian Nectin, as both proteins contain an extracellular region with Ig-like domains, a single transmembrane region, and a cytoplasmic region with a four amino acid long conserved motif (Lin et al., 2007; Takai et al., 2008; Takai and Nakanishi, 2003; Wei et al., 2005). The association of Ed and Cno has been proposed to behave as the Nectin-Afadin complex, where Cno, by binding to the PDZ-binding motif of Ed, links Ed to the actin cytoskeleton (Wei et al., 2005). However, it is not clear whether this interaction can explain the Ed/no Ed interface phenotype. The PDZ-binding motif of Ed has been shown to be dispensable for making the cable (Laplante and Nilson, 2011; this work) suggesting that, although we cannot exclude the possibility that Cno may interact with Ed

independently of the PDZ-binding motif *in vivo,* Cno might not be the Ed effector for cable formation.

The relationship between Cno and Ed appears to be tissue specific. In mosaic wing imaginal discs bearing *ed* mutant clones, Cno localization is disrupted. At the clone border and in the $ed^{-/-}$ cells, Cno is not stabilized at the cell cortex but rather it is found in cytoplasmic puncta, suggesting that Cno localization is dependent on Ed (Wei et al., 2005). However, because the effect on Cno is not restricted to the border of the clone, it alone cannot explain the localized Ed-dependent formation of the actomyosin cable. In addition, in mosaic follicular epithelia bearing *ed* mutant clones, Cno localizes normally at the cell cortex in all $ed^{-/-}$ cells as well as at the border of the clone (C.L. and L.N., personal communication). Also, Cno localization is not disrupted in the absence of Ed in the aminoserosa cells (AS) or at the leading edge of the DME cells in wild-type embryos, in the epidermis or AS of $ed^{M/Z}$ embryos (Laplante, 2008; Sawyer et al., 2009). These results indicate that Cno localization is not dependent on Ed in all tissues.

Another Ed-interacting protein identified in a pull-down assay is the unconventional myosin VI motor protein Jaguar (Jar) (Lin et al., 2007; Wells et al., 1999). Ed binds directly to Jar via its intracellular domain *in vitro*. Because functional Jar is a dimer *in vivo* and loss of *jar* leads to dorsal closure defects, it was proposed that direct interaction with Ed might regulate dimerization of Jar *in vivo* (Lin et al., 2007; Millo et al., 2004). This dimerization of Jar then contributes to changes in cell morphology and actomyosin cable formation during dorsal closure (Lin et al., 2007). Such a model is confusing because in the course of dorsal closure, Jar becomes enriched at the leading edge of the DME cells, but Ed is absent at that face of the DME

cells(Laplante and Nilson, 2011; Lin et al., 2007). Therefore, it is not clear how the direct association with Jar can explain the mechanism by which Ed is affecting actin polarization.

Ed was also shown to physically interact with the Hippo-binding partner Salvador (Sav). Ed coimmunoprecipitates with Sav from transfected S2 cell lysates (Yue et al., 2012). The interaction between Ed and Sav was shown to be important in regulating the activity of the Hippo pathway. Loss of Ed leads to elevated levels of the transcription factor Yorkie (Yki), which in turn upregulates expression of Hippo pathway target genes resulting in tissue overgrowth (Yue et al., 2012). The interaction between Ed and Sav does not appear to be important for rearranging the cytoskeleton at an Ed/ no Ed interface.

The above results suggest that other as yet unidentified Ed interactors might be involved in regulating actomyosin cable formation. To understand the mechanism by which Ed directs the formation of the actin cable, we wanted to identify other proteins that interact with Ed. We used the tandem affinity purification (TAP) method to isolate Ed-interacting proteins, followed by mass spectrometry analysis to identify the isolated proteins. First developed in yeast (Rigaut et al., 1999), the TAP method has been successfully utilized in other organisms such as mammals, zebrafish, flies, plants, as well as in cell lines (Nakatani and Ogryzko, 2003; Rohila et al., 2004; Tiefenbach et al., 2010; Westermarck, 2002; Yang et al., 2006). This technique involves the addition of two or more affinity tags arranged in tandem (also referred to collectively as a TAP tag) to a protein of interest, either at the C- or N-terminus of the protein of interest to allow for sequential purification of the tagged protein. The original TAP tag was composed of a fusion cassette encoding Protein A (ProtA), a TEV cleavage site, and Calmodulin binding peptide (CBP) (Rigaut et al., 1999). In the following years, other tags with various combinations have been used. One great benefit of the addition of affinity tags is that it increases the versatility of

the TAP method in that it is generic enough to be applied to a diverse number of proteins, which can then be purified by a generalized protocol (Puig et al., 2001).

A particular advantage of the TAP method is that it allows for the isolation of protein complexes in close to physiological conditions, because the tagged protein is expressed inside the cell. There, the stably expressed exogenous protein, like its endogenous counterpart, is able to interact with other proteins. In simpler terms, the tagged protein acts as a bait for isolating other proteins that interact with it in a complex. Another approach for using a tagged protein for affinity purification is to immobilize it onto a column and then incubate it with cellular extract to allow interaction with proteins contained in the extract. However, a disadvantage of this method is that all protein interactions occur outside of a cell, which could result in the loss of the native conformation and post-translational modifications of the immobilized protein and its interacting partners present in the cellular lysate. And therefore, the TAP technique is the preferred method for isolating interacting proteins.

To isolate the intramolecular interaction partners, the tagged protein is introduced into the host system. The protein complexes are then extracted from the cell via affinity purification of the tags. The protein complexes are eluted and undergo a second affinity purification step to eliminate possible contaminating proteins. Both affinity purification steps are performed under mild conditions in order to preserve the native conformation of the protein complex. It has been previously demonstrated that this sequential purification allows for a higher purity of the protein sample, which in turn facilitates the identification of the isolated proteins (Puig et al., 2001; Rigaut et al., 1999).

Here we describe our preliminary results of using a TAP-tagged version of Ed as the bait protein to isolate Ed-interacting proteins. First, we generated a tagged version of Ed by adding a

3XFLAG, Strep, 6XHis (FSH) tag to the C-terminus of the protein, which we named Ed-FL-FSH. After generating stable transgenic lines, we determined that the addition of the tag did not compromise the localization and function of Ed. Sequential purification of Ed-FL-FSH using the FLAG and His tags was then performed three separate times, and a single purification with just the FLAG tag was performed once. Mass spectrometry analysis of the four purification trials revealed several putative interacting proteins.

2.2 Materials and Methods

2.2.1 Transgene generation

To generate the UAS-Ed-FL-FSH transgene, Ed cDNA from RE 66591 (DHSB) and FSH sequence from the pLT vector (Tiefenbach et al., 2010) were used. First, a BglII restriction site was added at the 5' of the Ed primers. The Ed PCR product, containing the entire coding sequence of the protein and the two exogenous BglII sites, was digested and cloned into the BglII site in the pUASt vector (pUASt-Ed-FL). Next, the FSH sequence was amplified with primers containing a unique restriction sites (NotI in the forward primer and XbaI in the reverse primer). The resulting PCR product was run on a 12% PAGE gel in TBE buffer (90mM Tris, 90mM boric acid, 2mM EDTA), purified using the "crush and soak" method (Sambrook and Russell, 2006), and cloned into pUASt-Ed-FL, resulting in pUASt-Ed-FL-FSH. Next, the Ed-FL-FSH sequence from pUASt-Ed-FL-FSH was amplified by PCR, cloned into pENTR vector (Invitrogen) and recombined into pUASg.attB destination vector (Bischof et al., 2007). The resulting plasmid was injected by standard procedures into embryos carrying the 86Fb landing site to generate stable transgenic lines.

Primers used
Ed amplification

B_forward: 5’ CGGAAGATCTCGTGTGTGCGAACAACAACTCAGC 3’
B_reverse: 5’ AGGAAGATCTGACAATAATCTCGCGTATGAC 3’

FSH amplification:

N_Forward: 5’ ATAAGAATGCGGCCGCGACTACAAGGACCAT 3’
X_Reverse: 5’ CTAGTCTAGACTGTGATGGTGATG 3’

EdFSH amplification:

Ed_Forward: 5’ CACCCGTGTGTGCGAACAACAACTC 3’
FSH_Reverse: 5’ CTAGTCTAGACTGTGATGGTGATG 3’

2.2.2 Drosophila genetics

To generate positively marked MARCM clones, *y w hsFlp; tub-GAL80 FRT 40A; tub-GAL4/TM6B* flies were crossed to ed^{F72} *FRT 40A* flies bearing *UAS-Ed-FL-FSH*. The resulting progeny were incubated at pupal stage at 37°C for 1 hour on three or four consecutive days. Female progeny were dissected 7-8 days after the first of these heat shocks. For ectopic expression of the transgene in embryos, flies bearing *UAS-Ed-FL-FSH* were crossed to *C381-GAL4* (Bloomington Drosophila Stock Center, BL 3734 (Manseau et al., 1997) or *daughterless-GAL4* (*da-GAL4*, BL 5460(Wodarz et al., 1995). The resulting progeny were collected at the embryo stage.

2.2.3 Immunohistochemistry

Before immunostaining, embryos were collected for 12-14hrs at room temperature to enrich for dorsal closure stages. Embryos were removed from the apple juice plate with a paint brush and distilled water, were placed in a wire-mesh collection basket, and were dechorionated

in 50% bleach for 2 min and rinsed with water. Embryos were fixed by hot methanol fixation (Müller and Wieschaus, 1996). Briefly, 10ml of boiling Triton X-100 salt solution (TSS; 70 mM NaCl and 0.03% Triton X-100) was added to the dechorionated embryos in a glass scintillation vial. The sample was swirled for 15s. 10ml ice-cold TSS was then added to the embryos followed by incubation on ice for 20 min. The TSS was removed and replaced with 10ml methanol (ACP) and 10ml heptane (Fischer Chemical). The vial was shaken vigorously by hand for 1 min. Only embryos that sank to the bottom of the vial after this step were collected for immunostaining. The heptane was then removed, and the embryos were rinsed with methanol and stored at −20°C for at least 2 days before staining. Prior to immunostaining, embryos were washed three time for 20 min in PBS + 0.1% Tween-20 (PBST), and blocked for 30 min in PBST + 1% BSA (Invitrogen) at room temperature on a nutator.

Ovary dissections were performed as described in Chapter 3. Immunostainings of ovaries and embryos was performed as described in Chapter 3.

Antibodies used were anti-DE-Cad DCAD2 supernatant (rat; 1:100; Developmental Studies Hybridoma Bank [DSHB]), anti-Ed (rabbit; 1:1,000, Laplante and Nilson 2011), anti-FLAG (mouse, 1:1000, Sigma), (TRITC)-phalloidin (Sigma-Aldrich; diluted 1:200 in PBST + 1% BSA).

2.2.4 Microscopy

Fixed samples were mounted in SlowFade Gold Antifade (Invitrogen). All the images were acquired with a LSM510 Meta confocal microscope (Carl Zeiss, Inc. McGill Cell Imaging and Analysis Network facility) at room temperature with a Plan Apochromat 63× 1.4 NA differential interference contrast oil. The images were analyzed using the imaging software

ImageJ 1.46r (NIH). Apart from minor linear adjustments to brightness and contrast, no image manipulations were performed.

2.2.5 Large-scale embryo collections

To collect large amounts of embryos, two population cages were each filled with 15 bottles worth of age-synchronized young fly adults. One cage contained only *daughterless-GAL4* (*da-GAL4*, BL 5460) flies, while the other had *da-GAL4* males and *UAS-Ed-FL-FSH* females. The cages were kept in an incubator at 25°C and 70% average relative humidity in a 12hr light-dark cycle.

Each population cage had a beaker filled with water inverted onto folded paper towels as a water source. During the first 24hr, five Styrofoam trays filled with corn meal based media were placed in each cage as a food source. In subsequent days, for easier embryo collections, 8 Petri dishes containing apple juice media with a thin band of yeast paste in the middle were placed in the cages, and changed three times per day, twice every six hours and once after twelve hours. The deposited embryos were aged to enrich for dorsal closure stages.

Embryos were removed from the apple juice plate with a paintbrush and distilled water, transferred in a homemade collection bottle with a nylon-mesh at the bottom, and washed several times with distilled water to remove all the yeast paste. Embryos were then dechorionated in 50% bleach for 2 min and rinsed with abundant amounts of distilled water, quickly dried and transferred with a spatula into a centrifuge tube, frozen in liquid nitrogen, and stored at -80°C.

2.2.6 Affinity purification

Purifications were performed at 4°C. Frozen embryos were homogenized in lysis buffer (50mM Tris pH 7.5, 125 mM NaCl, 15mM McCl, 1mM EDTA, 5% glycerol, 0.4% NP-40, 0.1% Tween-20, and 1 tablet of complete EDTA-free poteinase inhibitors (Roche)) in a dounce homogenizer with a tight pestle at a ratio of 5 ml of lysis buffer/g of embryo until complete lysis was obtained. The extract was transferred into centrifuge tubes and centrifuged at 10 000 rpm for 10 min at 4°C. After centrifugation, the supernatant was transferred into clean centrifuge tubes (Fischer Scientific) and the pellet was discarded. The protein concentration in the supernatant was measured by Bradford assay (Biorad). 15 mg of total protein was used in the subsequent steps. To reduce the amount of proteins that bind non-specifically to the agarose beads, the supernatant was transferred to Eppendorf tubes and was incubated with a prewashed agarose-bead slurry (4% Agarose Beads, ABT) for 1 hour. In the meantime, 20 µl anti-FLAG affinity gel per Eppendorf tube (Sigma) was equilibrated with lysis buffer. The supernatant from the agarose-bead slurry (the agarose flow through) was transferred into the anti-FLAG slurry and incubated for 2 hr. After incubation, the tubes were spun for 2 min in a microfuge and the supernatant was removed. The beads were washed 3 times for 10 min in lysis buffer. To elute the proteins, the beads were incubated in 300 µg/ml 3X FLAG peptide (Sigma) in lysis buffer for 1 hr. The eluate was then transferred to Eppendorf tubes containing 20 µl of Ni-NTA agarose beads (Qiagen) for His purification, and incubated for 2 hr. The tubes were spun for 2 min and the supernatant was removed. The beads were washed 3 times for 10 min in lysis buffer. To elute the proteins, 20 µl of 2X Laemmli sample buffer was added to the beads, and boiled for 3 min. The samples were then centrifuged at 10 000 rpm for 2 min at 4°C. The supernatant was loaded onto a 7.5% SDS-PAGE gel and was run until all the proteins entered the gel in one thick band.

The band was excised and sent for mass spectrometry analysis (IRIC Proteomic Facility, Montreal, QC, Canada).

2.2.7 Western blotting

For whole embryo protein extracts, embryos were placed in Eppendorf tubes and crushed in extraction buffer A (50 mM Tris pH 7.5, 150 mM NaCl, 1 mM EDTA, 1 mM EGTA, 0,1% Triton-X-100, and 1 tablet of EDTA-free protein inhibitors (Roche)) using a motor pestle at a 2:1 ratio. The sample was spun at 15,000 rpm for 15 min at 4°C. The supernatant was transferred into a clean Eppendorf tube. 2X Laemmli sample buffer was added to each sample, which was then boiled for 3 mins prior to being run on a 7.5% SDS-PAGE gel for 1 hr and 30 mins at 100V.

The protein samples collected at different steps during the affinity purification were run on a 7.5% SDS-PAGE gel for 1 hr and 30 min at 100V. All the protein samples were transferred from the SDS gel onto a nitrocellulose membrane (Hybond-C Extra, Amersham Biosciences) at 100V for 2 hr. After the transfer, the membrane was rinsed twice with distilled water and once with PBST, blocked for 30 min in PBST + 5% milk powder (PBST-milk, Bioshop) at room temperature, and incubated with the primary antibody diluted in 5 ml PBST-milk overnight at 4°C on a nutator. The membrane was washed 3 times for 10mins in PBST and incubated with the secondary antibody diluted in 10-15 ml PBST-milk for 30 min at room temperature. Afterwards, the membrane was washed 3 times for 10 min in PBST and developed using the Western Lightning ECL solutions (Perkin Elmer).

Primary antibody used was anti-Ed (rabbit; 1:1,000, Laplante and Nilson 2011), anti-FLAG (mouse 1:5000, Sigma). Secondary antibodies used were all ECL^{TM} horseradish peroxidase-linked whole antibodies (1:5000, Amersham Biosciences).

2.3 Results

2.3.1 Overview of the TAP method and construction of tagged Ed

To understand the mechanism by which Ed influences the organization of the actin cytoskeleton, we set out to isolate and identify Ed interacting proteins. For this, we used the tandem tag affinity purification (TAP) method coupled with mass spectrometry. The TAP method relies on affinity purification of a tagged protein being used as bait to isolate other proteins, which form a complex and interact with the bait protein (Puig et al., 2001; Rigaut et al., 1999). The bait protein often contains two or three affinity tags to allow for sequential rounds of purification employing the different tags. Among the possible tag combinations available for TAP, we decided to use a triple tag containing a 3XFLAG peptide, a Strep tag, and 6X His tag (FSH), which has been previously shown to provide higher protein yields than the original Protein A and Calmodulin binding peptide (CBP) tag (Tiefenbach et al., 2010). This combination of affinity tags is 36 amino acids long with a molecular weight of 4.36 kDa.

To isolate Ed protein complexes using the TAP technique, we generated a transgenic version of Ed full-length (FL) protein containing the FSH tag, Ed-FL-FSH (Figure 2.1 A). We decided to add the FSH triple tag to the C-terminal end of Ed because the addition of the tag at the N-terminus would disrupt the transport to the plasma membrane of the newly synthesized Ed. The translation product of the *ed* mRNA contains an N-terminal signal sequence which directs the localization of the newly synthesized protein, but ultimately gets cleaved and is not part of the final protein. If the tag were added to the N-terminal end of Ed, it would get cleaved together with the signal sequence, or it could interfere with the signal sequence and therefore with the proper membrane localization of the tagged protein. The addition of the FSH triple tag was limited to the C-terminal end of Ed.

One possible concern that arises from the presence of the FSH tag at the C-terminal end of Ed is its proximity to the PDZ-binding motif, which is located at the C-terminal end of Ed (Figure 2.1 A), and has been shown to mediate interaction with two other proteins, Baz and Cno (Wei et al., 2005). It has been shown that this motif is dispensable for Ed-mediated formation of the actomyosin cable, although we cannot exclude the possibility that the addition of the tag at this position could compromise the ability of Ed to interact with other proteins (This thesis Chapter 3, Figure 3.2; Laplante and Nilson, 2011).

A simplified overview of the TAP technique used to purify Ed protein complexes is shown in Figure 2.1 B. For the first purification step, embryo lysates containing the triple tagged bait protein (Figure 2.1 B, green-square) are incubated with anti-FLAG antibody coated beads for FLAG purification. After several washes, the retained protein complexes are removed from the anti-FLAG coated beads by competitive binding with a 3XFLAG peptide. The eluted protein complexes are then incubated with nickel charged agarose beads (Ni-NTA beads, Figure 2.1 B) for further purification with the 6X His tag. The protein complexes are then eluted from the beads by boiling.

2.3.1 Verification of construct functionality

An intrinsic concern with any tagging method is the possibility that the added tag may affect the tertiary structure and function of a protein. To test whether the addition of the FSH triple tag has an adverse effect on Ed expression and localization, we ectopically expressed Ed-FL-FSH in the AS, an embryonic tissue where endogenous Ed is not present during dorsal closure (Laplante and Nilson, 2011; Lin et al., 2007), under the control of tissue specific GAL4 driver, *C381*-GAL4. Immunostaining with an anti-Ed antiserum revealed that Ed-FL-FSH was

ectopically expressed at comparable levels to the endogenous protein, and exhibited a membrane localization indistinguishable from endogenous Ed (Figure 2.2 A, A'), indicating that the addition of the tag did not adversely affect protein expression and localization. Furthermore, Ed-FL-FSH was detected by the anti-FLAG antibody (Figure 2.2 B'), suggesting that the added tag is not hidden inside the protein's tertiary structure but is exposed at the surface, hence allowing for immunoaffinity purification of the 3XFLAG tag.

To determine whether the C-terminal FSH tag disrupts Ed function, we asked whether interfaces between cells lacking Ed and those expressing Ed-FL-FSH are smooth. For this, we generated MARCM *ed*$^{-/-}$ clones expressing Ed-FL-FSH in the follicular epithelium. One peculiar feature of the MARCM system is the formation of transgenic mosaicism within the *ed*$^{-/-}$ clone, where apparently random groups of *ed*$^{-/-}$ cells do not express the transgene, thus generating ectopic Ed interfaces (Laplante and Nilson, 2011). Analysis of such clones showed that interfaces between *ed* mutant cells lacking Ed and *ed* mutant cells expressing transgenic Ed-FL-FSH (Ed-FL-FSH/no Ed interface) are smooth (47/47 interfaces, Figure 2.2 C, C' arrowhead), similar to endogenous Ed/no Ed interfaces (Figure 2.2 C, C' arrow). These results indicate that the addition of the FSH tag does not interfere with Ed function and suggest that Ed-FL-FSH retains endogenous Ed function in this assay.

As we wanted to isolate and identify proteins interacting with Ed in the context of a smooth border characterized by the formation of an actomyosin cable, two requirements needed to be fulfilled. The first requirement was to find a tissue where an Ed-dependent actomyosin cable forms endogenously. For this reason, we used embryos undergoing dorsal closure where an endogenous actomyosin cable forms in the dorsal most epidermal (DME) cells abutting the AS cells (Jacinto et al., 2002b; Kiehart et al., 2000; Martin and Parkhurst, 2004). An advantage of

using embryos is the relative ease of collecting large amounts of tissue enriched for a specific developmental stage that would yield adequate amounts of proteins for large scale purifications. The second requirement was to induce the expression of the transgenic protein only in the epidermal tissue and not the aminoserosa in order to resemble the endogenous Ed expression pattern (Laplante and Nilson, 2011). However, our analysis of several GAL4-driver lines failed to identify a line that expressed GAL4 uniformly and exclusively in all epidermal cells (data not shown). To overcome this technical difficulty, we used a GAL4-driver line, *daughterless*-GAL4, which induces ubiquitous expression in the embryonic tissue, including the epidermis, in order to maximize the number of cells expressing the transgene. Previous reports have successfully utilized this driver in similar experiments (Lin et al., 2007).

Under the control of the *da*-GAL4 driver, UAS-Ed-FL-FSH was expressed at high levels in the epidermis (Figure 2.2 B'). In the epidermal cells, the ectopically expressed protein localized to the membrane and was also detected in intracellular puncta (Figure 2.2 B'). On the other hand, UAS-Ed-FL-FSH showed a punctate localization in the AS. Despite the high expression level of ectopic protein, embryos were able to complete embryogenesis (data not shown).

Lastly, to test whether Ed-FL-FSH was of the expected molecular weight, we used whole embryo extracts for immunoblotting analysis. As expected, Ed-FL-FSH was present in the supernatant (S) and debris (D) samples from embryos bearing the transgene and the *da*-GAL4 driver, but absent in samples from embryos expressing the driver alone (Figure 2.2 D, panel 1 and 2). To confirm that samples from the negative control embryos contained protein sample, we immunoblotted with the anti-Ed antibody. This antibody would recognize the ectopic tagged protein, Ed-FL-FSH, as well as endogenous Ed, which is present in both protein samples. As

predicted, endogenous Ed was present in the embryos expressing the *da*-GAL4 driver alone (Figure 2.2 D, panel 4). Interestingly, endogenous Ed was present only in the pellet sample (Figure 2.2 D, panel 4, P) and not in the supernatant, indicating that the buffer used was not extracting the protein from the embryonic tissues efficiently and therefore would not be suitable to use in the affinity purifications.

These preliminary tests have established that addition of the FSH triple tag at the C-terminus of Ed does not negatively affect the protein localization or function. We determined that Ed-FL-FSH was expressed and localized to the membrane, was of the expected molecular size, and was able to induce smooth boundary formation at an Ed-FL-FSH/no Ed interface.

2.3.2 Isolation of protein complexes and preliminary mass spectrometry data

After we successfully generated a functional FSH-tagged Ed transgenic line and determined that this tag did not disrupt the function or localization of the protein, we carried out Ed-protein complex purifications from whole embryo extracts. Briefly, embryo extracts containing Ed-FL-FSH were affinity purified with anti-FLAG antibody coated beads. The Ed-FL-FSH protein purified with the FLAG epitope tag. The protein complexes were eluted (FLAG eluate) and then subjected to a second purification step utilizing the His affinity tag (See Materials and Methods for further details). To increase the probability of isolating relevant Ed interacting proteins, embryo collections were timed appropriately to enrich for embryos undergoing dorsal closure, a developmental stage where an endogenous Ed-dependent actomyosin cable forms (Laplante and Nilson, 2006, 2011; Lin et al., 2007).

Immunoblot analysis of embryo extracts (Figure 2.3 A, lane 1 and 3) showed that, as expected, the tagged protein was present in the *da*-GAL4 driven UAS-Ed-FL-FSH sample (lane

3, Input), but absent from the negative control sample (*da*-GAL4 without transgenic Ed, lane 1, Da-Input). To monitor the efficiency of protein recovery in each fraction, samples from each step of the purification process were examined by immunoblotting (Figure 2.3). We saw that not all Ed-FL-FSH proteins present in the "Input" sample bound to the anti-FLAG antibody coated beads, as some of the protein was detected in the "Flow-Through" sample (Figure 2.3, lane 4). Also, although most of the Ed-FL-FSH protein was removed from the anti-FLAG antibody coated beads during the final step of FLAG purification via competitive binding with the 3XFLAG peptide, the efficiency of this removal was not one hundred percent as some protein did remain on the beads (Figure 2.3, lane 5). In the first step of the His purification, most of the protein sample bound to the Ni-NTA beads, as almost no Ed-FL-FSH was detected in the "Flow-Through" fraction (Figure 2.3, lane 7). The final FLAG-His eluate (Figure 2.3, lane 8, Eluate) was analyzed by mass spectrometry.

Many proteins were identified by mass spectrometry analysis. Proteins that were present in both the Ed-FL-FSH-containing sample and the negative control sample were deemed to represent non-specific contaminants and were therefore excluded from further analysis (Figure 2.3 C). Other proteins excluded from further considerations were those that were present only in the Ed-FL-FSH sample but seemed less likely to mediate this function of Ed. Such proteins were part of mRNA binding, chaperone binding, and protein translation group of proteins. Although we cannot rule out that these proteins are important, we would prioritize other targets. The isolation of proteins that represent abundant cellular proteins is not surprising given that Ed-FL-FSH is expressed at high levels under the control of a heterologous promoter.

From four different purification trials combined with mass spectrometry data analysis, we generated a short list of other putative interactors with potentially interesting predicted functions

(Figure 2.3, B). In our list we also included annotated genes whose function has not been previously studied. Although we would not immediately focus on further pursuing these genes, as the reagents are sparse and their function is unknown, they could become useful in the future. All proteins are listed by the number of times they were recovered from the purification trials.

One protein identified by our analysis was Friend-of-Echinoid (Fred). A paralogue of Ed, Fred has a high degree of similarity to Ed in the extracellular domain sequence, but a low degree in the intracellular domain (Chandra et al., 2003). Although its function is not well-characterized, Fred has been shown to interact with Ed in the wing imaginal disc (Chang et al., 2011). Ed and Fred also act in concert during ommatidial rotation in the eye imaginal disc and in the specification of sensory organ precursors in the wing imaginal disc (Chandra et al., 2003; Fetting et al., 2009). Further, *fred* and *ed* show similar mRNA expression pattern in the embryo, where both transcripts are absent from the AS during dorsal closure (Chandra et al., 2003). Given the known association between Ed and Fred, the recovery of Fred via tandem purification of Ed-FL-FSH validates the TAP technique.

The previously reported Ed interacting protein Jar was also isolated by TAP and identified by mass spectrometry (Lin et al., 2007). However, Jar was found to be present in the negative control sample of two different purification trials (Figure 2.3 B, gray line). Because of this discrepancy, it is unclear whether the interaction between Ed and Jar is valid.

Another protein isolated by this method is the serine-threonine kinase Par-1. The function of Par-1 has been extensively studied. During oocyte development in *Drosophila*, Par-1 reorganizes the microtubule network that is necessary for proper axis determination (Shulman et al., 2000). In *C. elegans*, the interplay between Par-1 and Par-3 (Bazooka in *Drosophila*) leads to their asymmetric and complementary localization in the oocyte, which then determines the axis

for the first cell division (Etemad-Moghadam et al., 1995). It is not immediately obvious how Par-1 would participate in Ed-mediated actomyosin cable because of the difference in localization between Par-1 and Ed. Par-1 localizes to the basolateral membrane whereas Ed localizes to the apical membrane at the level of the adherens junctions (Laplante and Nilson, 2006; Lin et al., 2007; Shulman et al., 2000; Vaccari et al., 2005). However, basolaterally localized Par-1 has been shown to interact with apically localized Baz (Benton and Johnston, 2003). Therefore, the isolation of Par-1 as a putative Ed interacting protein raises the possibility that Par-1 engages in another interaction with an apically localized protein to regulate the rearrangement of the actin cytoskeleton.

The unconventional myosin, Myosin V (Myo V, Didum in *Drosophila*) was identified as an Ed interactor in our mass spectrometry analysis. MyoV is one of the earliest identified unconventional myosins, which functions in the trafficking of intracellular cargo by binding to F-actin filaments (Johnston et al., 1991; Mercer et al., 1991; Wei et al., 2013; Woolner and Bement, 2009). It is possible that it functions in a similar way with Ed, where MyoV transports Ed-containing intracellular vesicles inside the cell. The interaction with MyoV could happen when Ed is trafficked from the ER to the Golgi apparatus, as MyoV has been shown to regulate this kind of vesicular trafficking in neuronal cells (Tabb et al., 1998), or trafficked in post-Golgi secretory vesicles, as MyoV have been shown to function in the rhabdomeres in *Drosophila* (Li et al., 2007; Pocha et al., 2011; Satoh et al., 2005). An alternative hypothesis is that MyoV could regulate the recycling of Ed from the plasma membrane, as it has been shown that MyoV regulates Rab11 containing vesicles (Hales et al., 2002; Lapierre et al., 2001).

2.4 Discussion

In our effort to understand how Ed affects the organization of the actin cytoskeleton, we used the TAP technique coupled with mass spectrometry to isolate and identify Ed interacting proteins. Here we have shown that we were able to isolate Ed interacting complexes from whole embryos with sufficient yields for the subsequent identification step.

Our preliminary mass spectrometry results identified many proteins. In our analysis of these new candidates, we excluded all proteins that were present in both the Ed-FL-FSH and negative control sample. Further, we also excluded proteins that, although were present only in the Ed-FL-FSH sample, did not appear to be an obvious choice to mediate the function of Ed that regulates the formation of an actomyosin cable at an Ed/no Ed smooth interface.

2.4.1 A previously known Ed interacting protein, Fred, is identified by TAP

Although several putative new Ed interacting proteins were identified in our analysis of the mass spectrometry data, it is arguable that not all these interacting proteins are involved with the polarization of the actin cytoskeleton at an Ed-expression interface. But at least two candidates have emerged that are worth pursuing further.

One of these proteins is Fred. The identification of Fred is encouraging because it has previously been shown to interact with Ed (Chandra et al., 2003; Fetting et al., 2009), thus demonstrating the efficacy of the TAP. Ed and Fred engage in a heterophillic interaction *in trans* via their extracellular domains. However, Ed preferentially engages in homophillic interactions (Chandra et al., 2003; Chang et al., 2011; Özkan et al., 2013).

Fred has been previously described as a paralogue of Ed, and the two proteins share a very high degree of similarity in their extracellular domains, but their intracellular domains are different (Chandra et al., 2003). It is unknown whether Fred is involved in any aspect of the Ed-

mediated formation of the actomyosin cable. Several lines of evidence indicate that Fred does not share a similar function with Ed in the regulation of the actomyosin network. In the embryo during dorsal closure, *fred* mRNA displays a similar expression pattern as *ed* mRNA, where the mRNA is present in the epidermis but absent from the AS (Chandra et al., 2003; Supplemental Figure 4.1). This result would suggest that, like Ed, Fred protein exhibits a similar expression profile as its mRNA. We predict that this differential expression of Fred generates a planar polarized distribution of Fred in the DME cells (Figure 2.4 A, left) as Fred engages in homophilic binding and therefore it cannot become stabilized at the LE due to the absence of Fred in the neighboring AS cell. Thus, in a wild-type embryo, both Ed and Fred exhibit a planar polarized distribution in the DME cell and an actomyosin cable is visible at the LE. Removal of Ed from the DME cells, in the case of $ed^{M/Z}$ mutant embryos, does abolish the formation of the actomyosin cable at the LE of the DME cells (Laplante and Nilson, 2006, 2011). We predict that the localization of Fred in these embryos remains unchanged (Figure 2.4 A, right). Thus, the localized rearrangement of the actin cytoskeleton is dependent on the presence of Ed and not Fred. In the absence of Ed, Fred alone does not appear to affect actomyosin cable formation. Therefore, for these reasons, we conclude that the planar polarized distribution of Fred alone does not contribute to the formation of an actomyosin cable.

Although we predict that Fred alone cannot induce the formation of an actomyosin cable in the absence of Ed, it remains possible that Fred is an effector of Ed. A simple model would predict that Ed binds to and activates Fred, which in turn regulates the formation of the cable (figure 2.4 D). To test this model, it would be informative to determine the spatial distribution of Fred in DME cells containing a uniformly distributed Ed. Because Ed is a homophilic binding protein, ectopically expressing Ed in the AS retains Ed at the LE thus generates a uniform

distribution of Ed in the DME cells (Ed-LE embryos). An actomyosin cable is not observed in Ed-LE embryos (Laplante and Nilson, 2011). If Fred exhibits a planar polarized distribution in the DME cells of Ed-LE embryos (Figure 2.4 B, left), then Fred can be excluded as an Ed effector for this particular function of Ed. However, it is also possible that Fred heterophillically interacts *in trans* with Ed, which is present in the neighboring AS cell, becomes stabilized at the LE, and assumes a uniform distribution in the DME cells (Figure 2.4 B, right). This outcome would not eliminate Fred as a plausible Ed effector, because possibly, the absence of the actomyosin cable in Ed-LE embryos could be a result of the uniform distribution of Ed, which in turn abolishes the polarized distribution of Fred by generating a uniformly distributed Fred in the DME cells.

Localization studies can lead to a hypothesis in which Fred functions as an Ed effector in regulating the rearrangement of the actin cytoskeleton at an Ed/no Ed interface, but a key test for this hypothesis would be to remove Fred from such interfaces and observe whether the actomyosin cable formation is abolished. For this test, we would generate mosaic follicular epithelia containing Ed/no Ed interfaces that also lack Fred (Figure 2.4 C) and assess whether these interfaces display a smooth or jagged phenotype. One caveat of this experiment is the fact that the expression pattern of Fred in the follicular epithelium is unknown. Because expression of Fred mimics the expression of Ed in other tissues, i.e. eye and wing imaginal discs, and the embryo (Chandra et al., 2003; Fetting et al., 2009), we predict that Fred is expressed in the follicular epithelium. If, in the absence of Fred, the Ed/ no Ed interfaces are smooth, it would indicate that Fred is not a necessary Ed effector for regulating the actomyosin cable formation. On the other hand, if Fred is necessary for the formation of the actomyosin cable at an Ed/no Ed

interface, then removal of Fred would suppress the actin phenotype and lead to jagged Ed/no Ed interface.

Mechanistically, it is not easy to speculate how the interaction between Ed and Fred might regulate the cytoskeleton, as not much is known about the function of Fred. Furthermore, the intracellular domain of Fred, like that of Ed, does not have any readily identifiable structural or functional motifs (Chandra et al., 2003). Because Ed and Fred share several similarities, these proposed experiments would determine whether they also share functional similarities.

2.4.2 Par-1 is an exciting possible Ed interacting protein

Another Ed interactor identified by TAP that is an attractive Ed effector candidate in regulating the formation of the actomyosin cable is the serine/threonine kinase Par-1. Although Par-1 was identified by TAP as a putative interactor, the interaction between Ed and Par-1 would need to be further validated by an independent method. Coimmunoprecipitation from tissue extracts is often employed as the method of choice to validate interaction between two proteins *in vivo*. As antibodies for both proteins, Ed and Par-1 (Benton and Johnston, 2003; Laplante and Nilson, 2006), are available, determining whether this interaction also occurs in wild-type embryos should be straightforward.

As the asymmetric distribution of Ed is essential for the formation of the actomyosin cable during dorsal closure (Laplante and Nilson, 2011), we predict that an Ed effector might well be planar polarized in the DME cells. Therefore, if Par-1 is an effector of Ed, we would predict Par-1 assumes a visible biased distribution in the DME cells during dorsal closure. To test our prediction, we would use immunohistochemistry to look at the localization of Par-1 in the embryo in the DME cells just prior and during dorsal closure. Two possible outcomes are

that Par-1 displays either a biased or a uniform distribution. The first scenario can be further divided into two possibilities. First, Par-1 exhibits a planar polarized distribution similar to Ed, where the protein is reduced from the leading edge (LE) of the DME cells (Figure 2.5 A, left). Such an observation would be consistent with a model in which binding of Ed to Par-1 is important for the localization of Par-1, because the removal of Ed from one side of the cell might cause the removal of Par-1 from that side of the cell. Alternatively, we might find that Par-1 is enriched at the LE of the DME cells, displaying a polarized distribution that is complementary to that of Ed (Figure 2.5 A, right). From such an observation we would predict that the binding of Ed to Par-1 might inhibit the localization of Par-1. Therefore, based on this prediction, we would expect that in the absence of Ed, Par-1 is able to be localized and stabilized at the LE.

If the bias in localization of Par-1 in the DME cells is indeed dependent on the distribution of Ed, we would predict that Par-1 assumes a uniform localization in these cells when Ed is also uniformly distributed (Figure 2.5 B). To achieve a uniform distribution of Ed in the DME cells, we would either remove Ed from those cells by generating $ed^{M/Z}$ mutant embryos, or ectopically express Ed in the aminoserosa to provide a binding partner and stabilize Ed in the LE of the DME cells (Ed-LE embryos (Laplante and Nilson, 2011). We would then use immunohistochemistry to visualize the distribution of Par-1 in these cells. In both cases, we expect to see an apparently uniform distribution of Par-1 (Figure 2.5 B, green circle).

Alternatively, Par-1 might display an apparently uniform localization in the DME cells during dorsal closure. However, a lack of an obvious planar polarized localization would not rule out a possible functional asymmetry. For example, Ed binding to Par-1 could either compromise the activity of Par-1, in which case Par-1 would be more active in the absence of Ed at the leading edge, or activate Par-1, in which case Par-1would be more active in the other three sides

of the DME cell. To date, it is unclear how Ed could affect the activity of Par-1 because the intracellular domain of Ed does not have any easily recognizable or functional motifs, such a kinase domain. However, what is important to determine is whether Ed does indeed affect the function of Par-1 by altering its activity, either increasing or decreasing it, at the leading edge of the DME cells.

A model in which Par-1 is an Ed effector would predict that no actomyosin cable forms at an Ed/no Ed interface in the absence of Par-1. To test this model, we would remove Par-1 from Ed/no Ed interfaces either by generating *par-1*$^{-/-}$ mutant clones or inducing *par-1* RNAi expression in the follicle cells and assess whether the Ed/no Ed interface exhibits a smooth or jagged border (Figure 2.5 C). If, in the absence of Par-1, the Ed/no Ed interfaces are smooth, it would indicate that Par-1 is not the necessary Ed effector for regulating the actomyosin cable formation. On the contrary, if Par-1 is necessary for the formation of the actomyosin cable at an Ed/no Ed interface, then removal of Par-1 would lead to jagged Ed/no Ed interface.

We envision two plausible mechanisms by which the asymmetric activity of Par-1 mediates the Ed-dependent formation of the actomyosin cable at the leading edge. The first mechanism is more direct. The serine-threonine kinase Par-1 was recently reported to regulate the activity of myosin-II during border cell migration (Majumder et al., 2012). In this process, Par-1 directly binds to myosin phosphatase and phosphorylates it at its inactivation site. As a result, the phosphatase cannot dephosophorylate and thus inactivate the regulatory subunit of myosin light chain (MLC). Interestingly, the myosin-binding subunit of myosin phosphatase was one of the proteins identified in our analysis (Figure 2.3 B). We can speculate that a similar mechanism occurs during dorsal closure, where by binding to Par-1, Ed compromises the functional activity of Par-1. At the leading edge, where Ed is absent, Par-1 is able to directly

bind to the phosphatase, inhibit its activity, and promote actomyosin contractility (Figure 2.5D, Model A).

An alternative and equally probable mechanism by which Par-1 might regulate the rearrangement of the cytoskeleton is less direct. A role of Par-1 in *Drosophila* and mammalian cells has been shown to be regulating the microtubule network. In mammalian cells the Par-1 homologues, microtubule affinity regulating kinases (MARKs), increase the microtubule dynamics by phosphorylating microtubule-associated proteins (MAPs) leading to their detachment from the microtubules (Drewes et al., 1997; Ebneth et al., 1999). On the contrary, in *Drosophila*, Par-1 promotes microtubule organization and stability in different tissues (Cox et al., 2001; Doerflinger et al., 2003; Vaccari et al., 2005). Although the exact mechanism is not clear, in the follicular epithelium, removal of Par-1 leads to the formation of more microtubules that are less stable in nature (Doerflinger et al., 2003), supporting a requirement for the kinase for the stability of the microtubule network in these cells.

Interestingly, a role for microtubules has been described for the process of dorsal closure (Jankovics and Brunner, 2006). Prior to dorsal closure, microtubules appear to be distributed irregularly inside the DME cells; however, at the onset of dorsal closure, they appear to align along the dorsal-ventral (D/V) axis and reorganize into highly dynamic apical bundles (Jankovics and Brunner, 2006; Kaltschmidt et al., 2002). This transient reorganization allows the microtubules to contribute to the cell protrusions that form during the zippering stage in dorsal closure (Jankovics and Brunner, 2006).

Collectively these data suggest a hypothesis in which Par-1 in the DME cells regulates the transient reorganization of the microtubule network in an Ed-dependent manner. However, immunostaining of the microtubules with α-tubulin did not show an obvious defect in the

organization of the microtubule network in the DME cells of *ed*$^{M/Z}$ embryos (Laplante and Nilson, 2011). Alternatively, Par-1 could regulate the dynamics of the microtubules, which in turn regulate the formation and stability of the lamellipodia and filopodia during the zippering stage (Jankovics and Brunner, 2006). Consistent with these data, the number of lamellipodia and filopodia is greatly reduced in *ed*$^{M/Z}$ embryos at this developmental stage (Laplante, 2008). These two different possibilities dictate a role for Par-1 either at the onset of dorsal closure by organizing the microtubules or at a later stage, during zippering, by regulating the protrusions (Figure 2.5 D, Model B). At the moment, we cannot distinguish between these two alternatives.

2.4.3 Two reported Ed interacting proteins were not identified by TAP

Surprisingly, the mass spectrometry results did not reveal two previously reported Ed interactors, Cno and Baz (Wei et al., 2005). In a candidate gene approach, both Cno and Baz were shown to coimmunoprecipitate with Ed from wild-type embryo lysates, and GST-pull down and yeast two-hybrid assays demonstrated that these interactions were dependent on the PDZ-binding motif of Ed (Wei et al., 2005). It is possible that these proteins were not recovered in our TAP experiments because this interaction was obscured by the addition of the FSH tag in close proximity to the PDZ-binding motif. However, it is also possible that the interaction between Cno, Baz and Ed is of a transient nature. This interaction could be weak or happening in a short period of time during a specific developmental event. In either case, such interaction could be difficult to reveal using the current TAP technique because the first step of TAP is carried out under native conditions and therefore increases occurrence of protein degradation and thus complex disassembly (Tagwerker et al., 2006). The current TAP technique is more suited to isolate strongly interacting proteins.

One possible alternative approach to identify weak and transiently interacting proteins is to chemically cross-link protein complexes *in vivo* prior to purification. Cross-linking stabilizes protein interactions via the formation of covalent bonds, and the TAP technique coupled with *in vivo* cross-linking has been successfully used previously in yeast (Guerrero et al., 2006; Tagwerker et al., 2006). These studies use a new tandem affinity tag consisting of 6XHis tag and biotin (HB) tag. This tag allowed for the purification of protein complexes under fully denaturing conditions after *in vivo* cross-linking, and it was compatible with the stringent purification conditions necessary to reduce non-specific binding of contaminant proteins.

Another drawback of the current TAP technique is the long period of time that is needed for the tandem purification, which increases the possibility of protein degradation, and thereby the disassembly of the complex. It is plausible that some Ed interacting proteins were lost during the long purification steps. One possible approach to circumvent this problem would be to purify Ed protein complexes using only one purification step instead of two. It has been previously shown that one-step purification with the Strep tag allowed for the recovery of the tagged protein with the same degree of purity as the dual-affinity purification with the original TAP tag (Protein A – TEV – CBP tag) in plant tissue (Witte et al., 2004). It is unclear whether this result is also true for *Drosophila* proteins isolated with the FSH triple tag, as comparison of parallel purifications of a tagged protein with the one-step Strep purification and the FSH triple tag has not been previously reported. In addition, Rigaut *et al*. showed that one-step purification of a tagged yeast protein with either CBP or ProtA had a higher level of contaminating proteins than the same yeast protein sequentially purified with both tags. Furthermore, it is the general consensus that sequential purification yields highly improved sample purity (Puig et al., 2001; Rohila et al., 2004; Westermarck, 2002; Yang et al., 2006).

In addition, the TAP method relies on the exogenous tagged protein being preferentially expressed at the same level and pattern as its endogenous counterpart. In the case of Ed-FL-FSH, we were not able to find a suitable way to induce its expression to reproduce that of endogenous Ed in the embryo, which is expressed only in the epidermis and not the AS. We ubiquitously expressed Ed-FL-FSH in both tissues. The ectopic expression of Ed-FL-FSH in the AS could result in false-positive interactions that would not normally occur because endogenous Ed is not present in that tissue during dorsal closure. Therefore, in the future, it would be advantageous to express the tagged protein in the embryonic epidermis only. Although in our previous analysis we did not find a suitable GAL4-driver line to ubiquitously express Ed-FL-FSH in the epidermis (data not shown), in future experiments a combination of two GAL4-driver lines, *engrailed*-GAL4 and *wingless*-GAL4, each of which drive transgene expression in a subset of epidermal cells could be used (Brand and Perrimon, 1993).

2.5 Conclusion

Although our groundwork into identifying Ed interacting partners has yielded results, further work is needed to verify the results. Of all the proteins identified, Par-1 is a likely candidate to investigate further. Par-1 is a well-studied protein and many reagents, such as antibodies and mutant fly lines, are available.

In addition to TAP coupled mass spectrometry analysis, we also took a candidate gene approach to identify an Ed-interactor that mediated Ed-dependent actomyosin cable formation. The candidate protein we studied is Bazooka (Baz). That data is presented in Chapter 3.

Figure 2.1. Overview of the strategy used for purification of Ed protein complexes.

(A) Schematic representation of transgenic Ed with a C-terminal FLAG-Strep-His (FSH) triple tag. (B) General overview of the tandem affinity purification of protein complexes. Green rectangle represents the tagged protein of interest in a complex with two other interacting proteins (orange and pink ovals). Contaminant proteins © bind non-specifically to the beads.

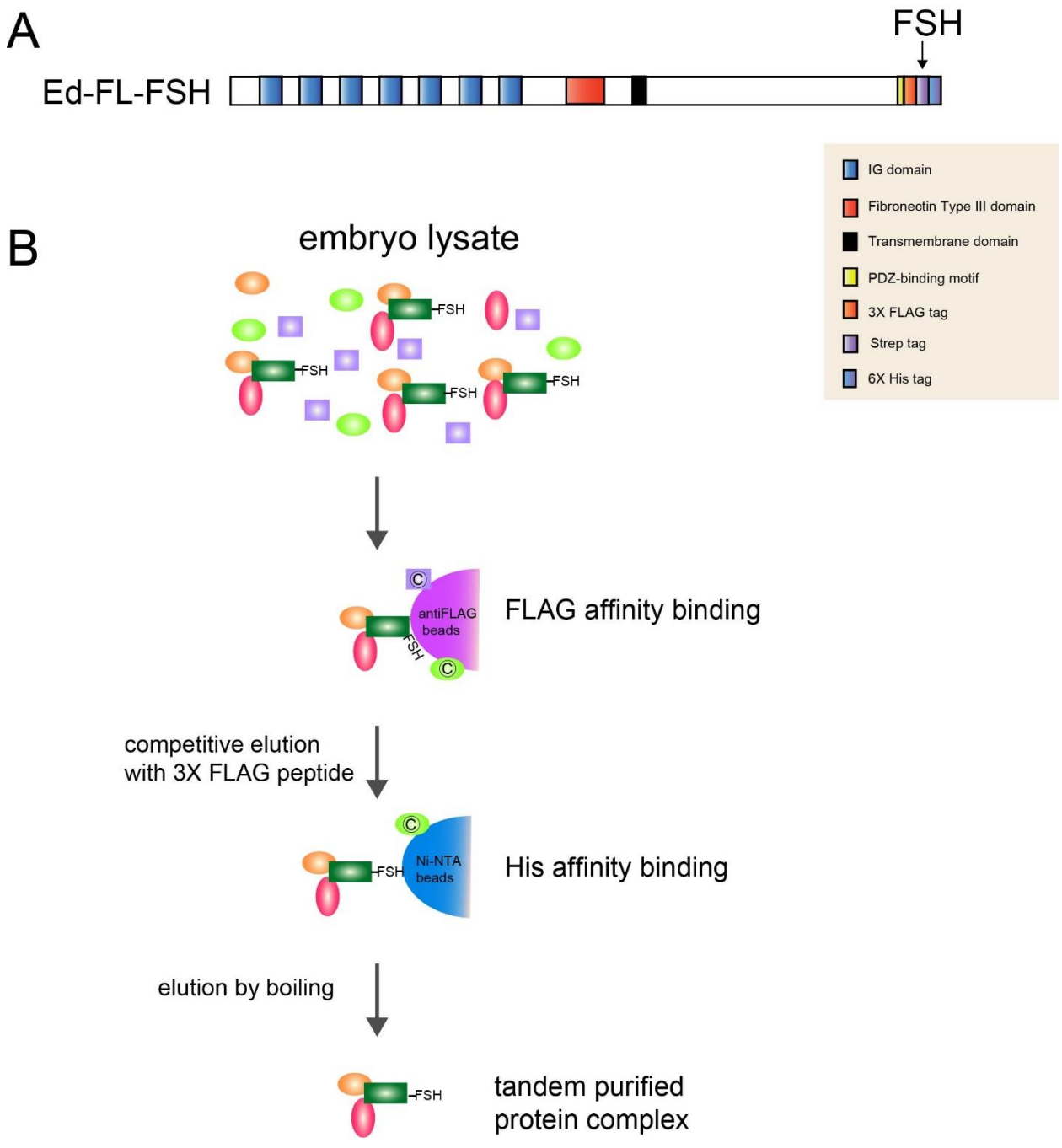
A
FSH
Ed-FL-FSH
IG domain
Fibronectin Type III domain
Transmembrane domain
PDZ-binding motif
3X FLAG tag
Strep tag
6X His tag
B
embryo lysate
FSH
FSH
FSH
FSH
antiFLAG beads
FSH
FLAG affinity binding
competitive elution with 3X FLAG peptide
Ni-NTA beads
FSH
His affinity binding
elution by boiling
FSH
tandem purified protein complex

Figure 2.2. The C-terminal triple tag does not affect the membrane localization or function of Ed.

(A- B') Dorsal closure stage embryos expressing UAS-Ed-FL-FSH in the aminoserosa under the control of the *C381*-GAL4 driver (A – A') and stained for Ed and FLAG, or in all tissues under the control of *daughterless*-GAL4 driver (B – B') and stained for Arm and FLAG. (C – C') Mosaic follicular epithelium with MARCM clone homozygous for ed^{F72} expressing Ed-FL-FSH stained for Ed and F-actin (C – C'). Arrowheads indicate the smooth interfaces between *ed* mutant cells and *ed* mutant cells expressing Ed-FL-FSH (47/47 clones). Arrows indicate the smooth interface between wild-type cells and *ed* mutant cells. AS: aminoserosa; EPI: epidermis. (D) Immunoblots of whole embryo extracts of Ed-FL-FSH expressing embryos (1, 3) and *daughterless*-GAL4 expressing embryos (2, 4) blotted for FLAG (IB: FLAG, 1, 2) or Ed (IB: Ed, 3, 4). S: supernatant; D: debris.

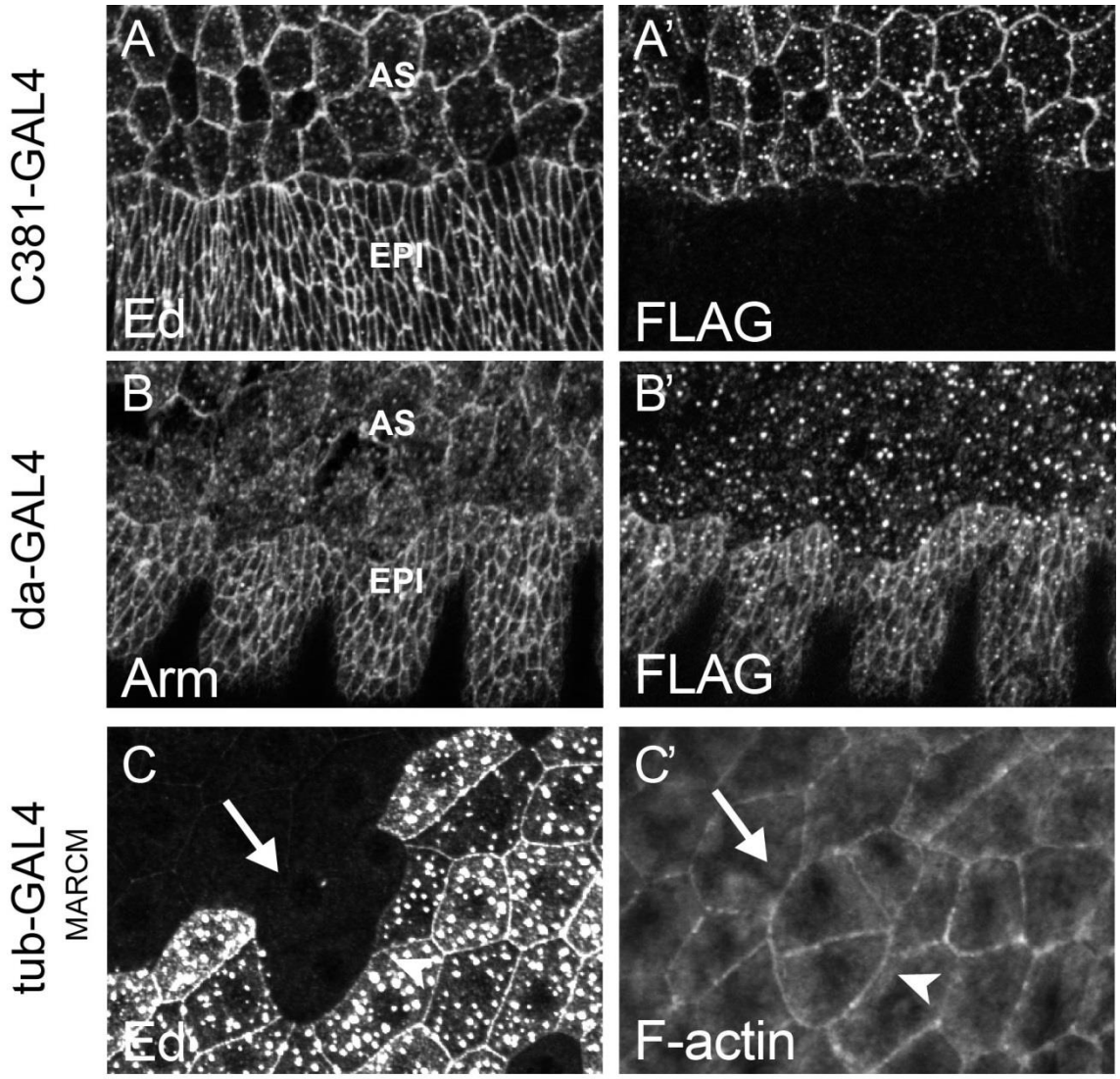
C381-GAL4
da-GAL4
tub-GAL4
MARCM
A
AS
EPI
Ed
A'
FLAG
B
AS
EPI
Arm
B'
FLAG
C
Ed
C'
F-actin

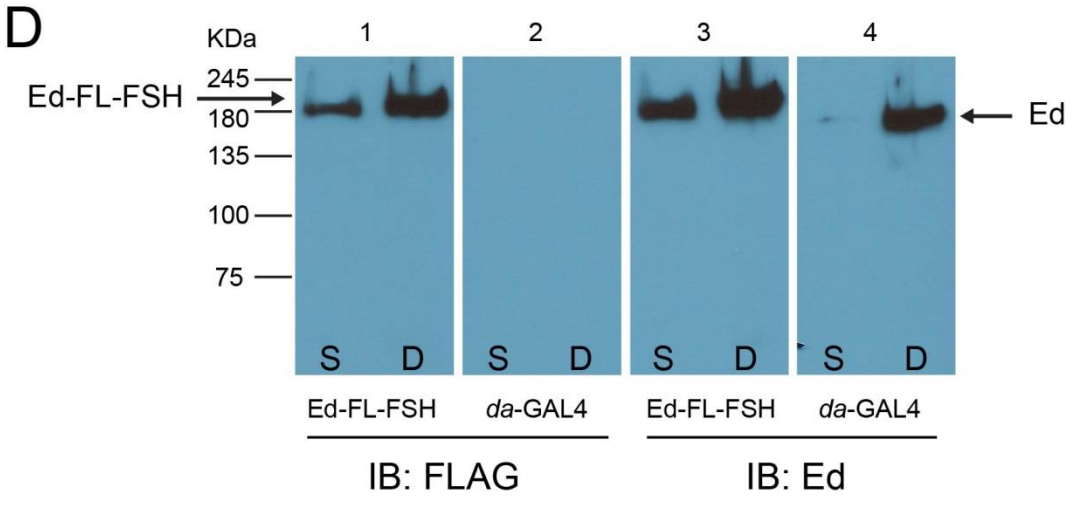
D
KDa
1
2
3
4
Ed-FL-FSH
245
180
135
100
75
Ed
S
D
Ed-FL-FSH
da-GAL4
Ed-FL-FSH
da-GAL4
IB: FLAG
IB: Ed

Figure 2.3. Preliminary TAP/mass spectrometry results identify several potential Ed interacting proteins.

(A) Immunoblot of fractions from steps of the protein purification process blotted for Ed. The arrow indicates intact Ed-FL-FSH protein. The numbers at the bottom label the lanes on the blot. Samples from the negative control embryo lysates (DA, da-GAL4 embryos) are shown in lanes 1 and 2. Samples from the Ed-FL-FSH expressing embryos are in lanes 3 – 8. "Input" refers to the initial embryo lysate used for purification, where as "Flow-Through" refers to the supernatant after the lysate is incubated with the beads. (B) Summary of selected potential Ed-interacting proteins identified via mass spectrometry. Flag-His refers to sequential purification with both tags, whereas Flag refers to purification with the FLAG tag only. Ed-sample is the sample containing the tagged protein, whereas Da-sample is the negative control sample without the tagged protein. The numbers in each column show the number of peptides recovered for that protein. Highlighted in orange are proteins identified in three or four purification trials, in beige are protein identified in two purification trials, and white those identified only in one purification trial. Jar is highlighted in grey because even though it was identified in three purification trial, it was present in the negative control sample as well. (C) Summary of the number of protein isolate by TAP and identified by mass spectrometry. Common proteins refers to the number of proteins that were identical in both samples.

A

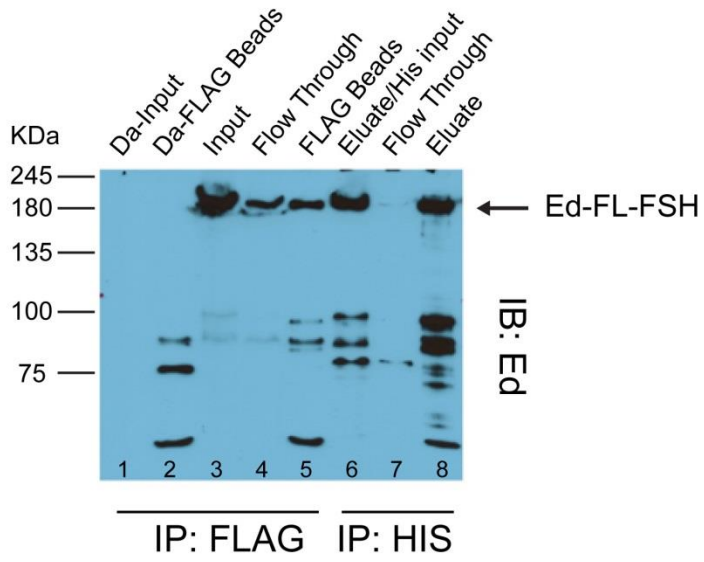

B

Purification	Flag-His		Flag-His		Flag-His		Flag	
Gene name	Ed-Sample	Da-sample	Ed-Sample	Da-sample	Ed-Sample	Da-sample	Ed-Sample	Da-sample
CG31774 - Fred	6	1	5	-	1	-	9	-
CG8201 -PAR1	2	-	5	-	-	-	8	-
CG9155 - Myosin61F	6	-	14	3	-	-	12	-
CG2146 - Didum (Myosin V)	7	-	23	-	10	1	-	-
CG1539/RE70606 (tropomodulin)	13	-	8	-	14	-	-	-
CG16009 -myosin heavy chain like	11	-	-	-	10	-	-	-
CG 12008 - Karst (b-heavy spectrin)	-	-	15	-	9	-	-	-
RE67887 -CG33521	1	-	5	-	-	-	-	-
RE02061 -Contactin	-	-	-	-	1	-	9	-
CG31195	-	-	-	-	2	-	22	-
CG5695 - Jaguar (Myosin VI)	55	73	64	-	-	-	50	66
CG9263	-	-	50	-	-	-	-	-
CG10984	-	-	27	-	-	-	-	-
RE 36860 - Quail	-	-	8	-	-	-	-	-
CG33481 -Zormin	-	-	5	-	-	-	-	-
CG16757 -Spinophilin	-	-	-	-	-	-	4	-
Myosin binding subunit of myosin phosphatase	-	-	-	5	-	-	31	-
CG31012 - Cindr	-	-	-	-	-	-	38	-
CG1634 -Neuroglian	-	-	-	-	-	-	5	-

C

	Flag-His			Flag-His			Flag-His			Flag		
	Common Prot.	Total Prot.	Percentage	Common Prot.	Total Prot.	Percentage	Common Prot.	Total Prot.	Percentage	Common Prot.	Total Prot.	Percentage
Ed-Sample	129	223	58	115	222	52	84	108	78	132	586	23
DA-Sample	129	224	58	115	224	52	84	216	34	132	472	28

Figure 2.4. Fred is putative Ed effector for actomyosin cable formation

(A – B) Diagrams illustrating the distribution of Ed (purple rectangle) and Fred (orange rectangle) in a dorsal-most epidermal (DME) cell and its neighboring aminoserosa (AS) cell. (C) Diagram of two follicle cells mutant for *fred*. One of the cells does not express Ed (top), whereas the other one displays a planar polarized distribution of Ed (bottom). (D) Hypothetical model of Ed regulating the activity of Fred, which in turn leads to the formation of an actomyosin cable.

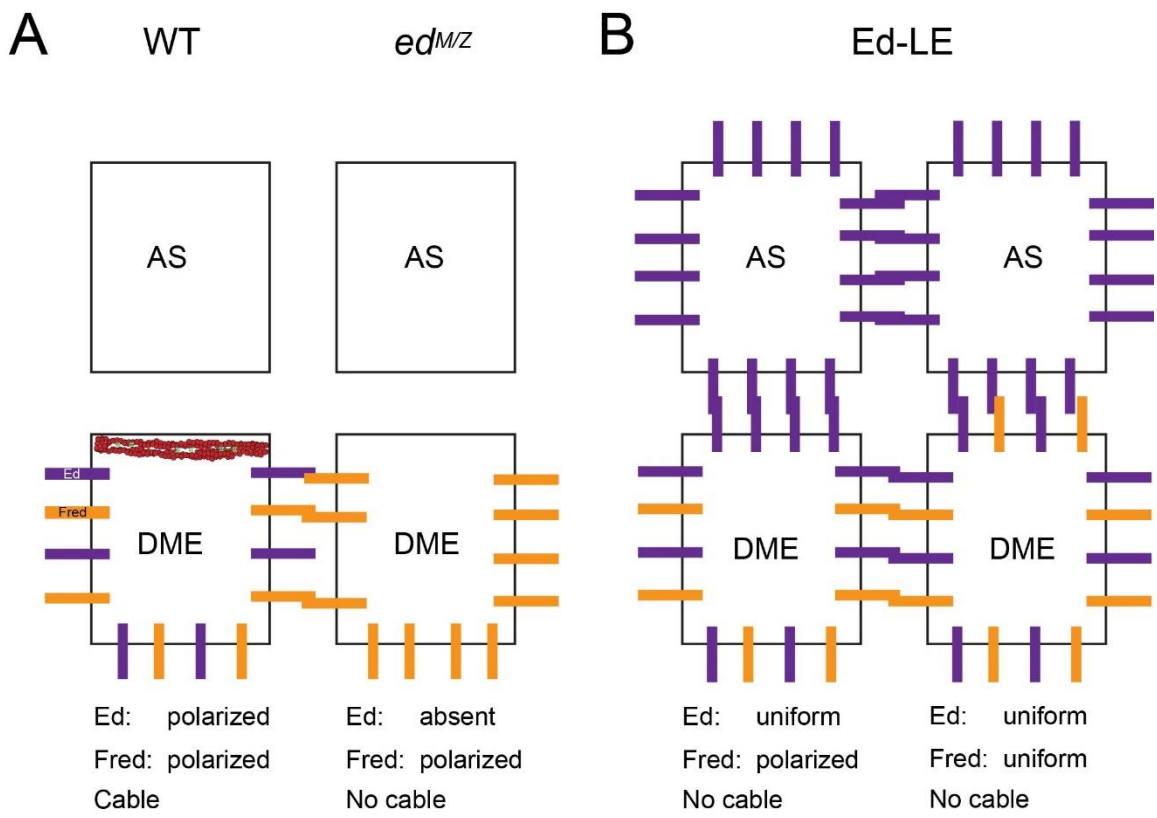
A
WT
ed M/Z
AS
AS
Ed
Fred
DME
DME
Ed: polarized
Fred: polarized
Cable
Ed: absent
Fred: polarized
No cable
B
Ed-LE
AS
AS
DME
DME
Ed: uniform
Fred: polarized
No cable
Ed: uniform
Fred: uniform
No cable

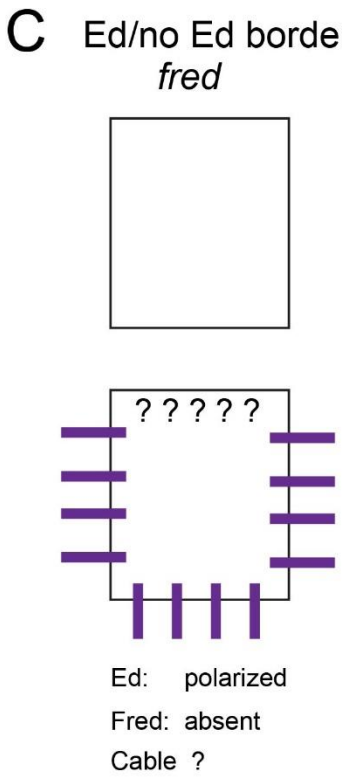
C
Ed/no Ed border
fred
? ? ? ? ?
Ed: polarized
Fred: absent
Cable ?

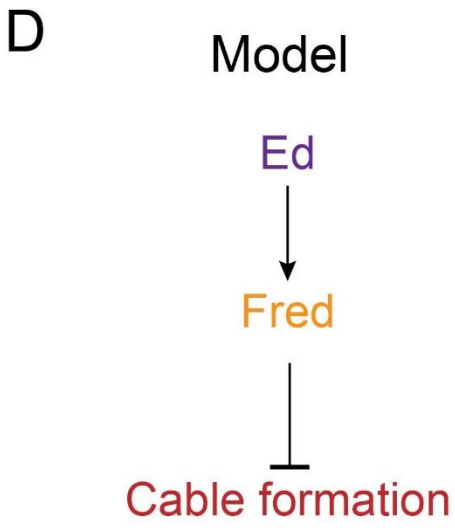
D
Model
Ed
Fred
Cable formation

Figure 2.5. Par-1 is a putative Ed interacting protein that might regulate the actomyosin cable formation.

(A – B) Diagrams illustrating the distribution of Ed (purple rectangle) and Par-1 (green circle) in a dorsal-most epidermal (DME) cell and its neighboring aminoserosa (AS) cell. (C) Diagram of two follicle cells mutant for *par-1*. One of the cells does not express Ed (top), whereas the other one displays a planar polarized distribution of Ed (bottom). (D) Hypothetical models of Ed regulating the activity of Par-1, which in turn contributes to the formation of an actomyosin cable.

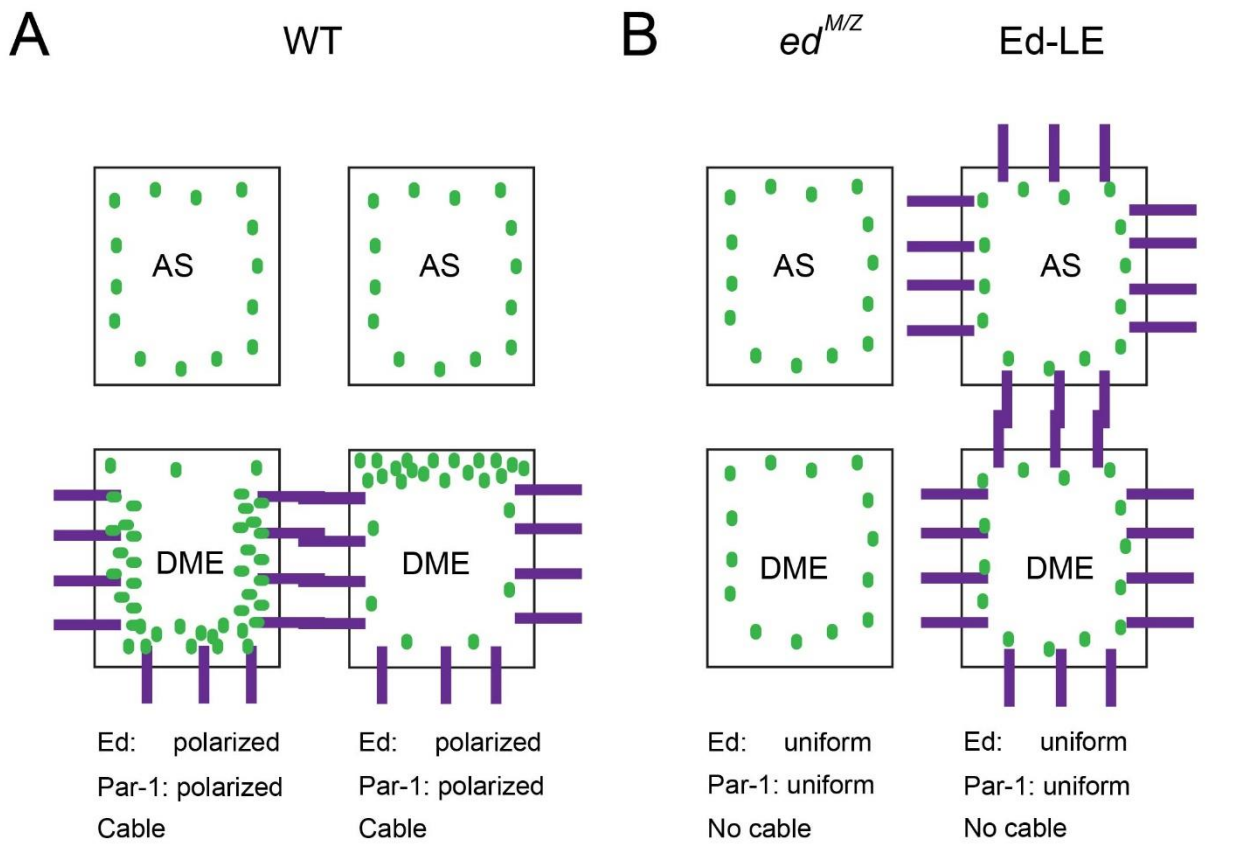
A
WT
AS
AS
DME
DME
Ed: polarized
Par-1: polarized
Cable
Ed: polarized
Par-1: polarized
Cable
B
ed M/Z
Ed-LE
AS
AS
DME
DME
Ed: uniform
Par-1: uniform
No cable
Ed: uniform
Par-1: uniform
No cable

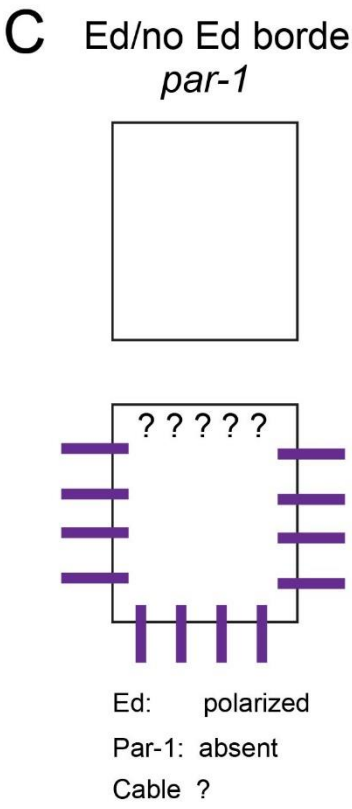
C
Ed/no Ed border
par-1
? ? ? ? ?
Ed: polarized
Par-1: absent
Cable ?

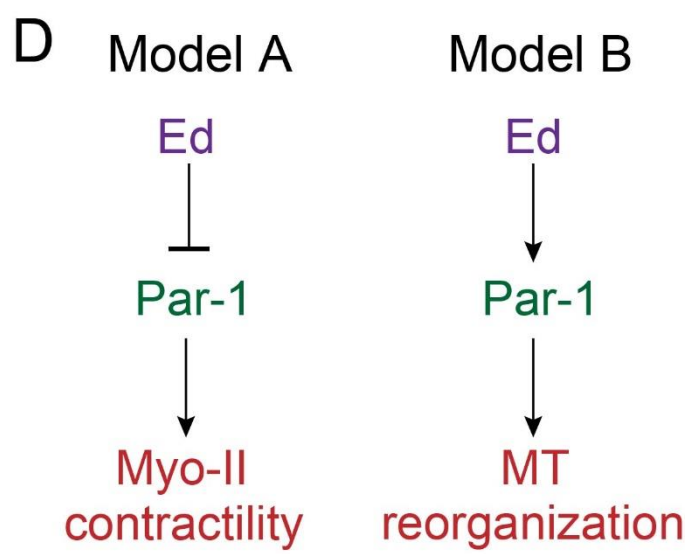
D
Model A
Ed
Par-1
Myo-II
contractility
Model B
Ed
Par-1
MT
reorganization

Chapter 3: The intracellular domain of the homophilic protein Echinoid regulates localized actomyosin contractility via Bazooka/Par-3.

3.1 Introduction

Epithelial morphogenesis is triggered by cell shape changes which are driven by subcellular localized actin dynamics (Lecuit and Lenne, 2007; Pilot and Lecuit, 2005; Zallen, 2007). Deciphering the signals that provide the spatial information for regulating the actin cytoskeleton is important in understanding the remodeling of epithelial tissues.

The homophilic binding protein Echinoid (Ed) has been proposed to provide the necessary spatial information for localized actin contractility (Laplante and Nilson, 2006, 2011; Lin et al., 2007). Ed localizes to the level of adherens junctions and engages in homophilic binding via its extracellular domain (Laplante and Nilson, 2006; Wei et al., 2005). The effect of Ed on the actin cytoskeleton is exerted when Ed becomes differentially expressed between two neighboring cells; when an Ed-expressing cell is in contact with an Ed-non expressing cell (Ed/no Ed interface), the interface between the two cells displays a smooth contour and a contractile actomyosin cable necessary for proper morphogenesis (Chang et al., 2011; Laplante and Nilson, 2006, 2011; Lin et al., 2007; Wei et al., 2005). The intracellular domain of Ed is required for this effect on the actin cytoskeleton and changes in cell shape (Chang et al., 2011; Laplante and Nilson, 2011; Lin et al., 2007).

To understand the mechanism by which Ed regulates the formation of an actomyosin cable, we focused on the intracellular domain of Ed. We examined the role of this domain by generating and testing two protein chimeras that contained the Ed intracellular domain sequence. As this domain of Ed does not have any easily recognizable motifs, except a PDZ-binding motif

at its C-terminus (Wei et al., 2005), we performed a deletion analysis to identify functional domains within the intracellular sequence that might mediate the Ed/no Ed interface phenotype.

In an alternative method, we undertook a candidate gene approach for elucidating the mechanism by which Ed regulates the localized actomyosin contractility. We investigated the function of the polarity protein Bazooka/Par-3 (Baz) as a candidate downstream Ed effector. During the process of germband extension, planar polarized distribution of Baz drives a reciprocal enriched localization of myosin-II, which in turn is necessary for proper junctional remodeling (Bertet et al., 2004; Simoes Sde et al., 2010). Baz also displays a functional reciprocal localization to myosin-II in the follicular epithelium in the floor cells during appendage morphogenesis in the eggchamber (Osterfield et al., 2013). Interestingly, Ed appears to be polarized in these cells and its asymmetric localization is necessary for proper morphogenesis of the appendages (Laplante and Nilson, 2006). Another example where the polarized distribution of Ed directly influences the polarized distribution of Baz is in the dorsal most epidermal (DME) cells during dorsal closure (Laplante and Nilson, 2011). In these cells, both Ed and Baz exhibit a reciprocal localization to the contractile actomyosin cable present at the leading edge (LE), where the DME cells abut and the AS cells (Jacinto et al., 2002b; Kiehart et al., 2000; Laplante and Nilson, 2011; Pickering et al., 2013). Furthermore, manipulating the distribution of Ed in the DME cells leads to an altered Baz distribution in these cells (Laplante and Nilson, 2011), suggesting that Ed might behaving as a cue for directing the localization of Baz, which in turn drives actomyosin network remodeling at an Ed/no Ed interface.

Here we provide evidence that the intracellular domain of Ed is necessary to drive formation of the actomyosin cable at an Ed/no Ed interface. We also show that the polarized distribution of intracellular domain is sufficient for this function of Ed, and that a sequence

within this domain is necessary for this function of Ed. We provide further evidence that Baz/Par-3 is an Ed effector for this function of Ed. We propose that Ed indirectly regulates the polarized distribution of Baz/Par-3 at ectopic Ed/ no Ed interface, which in turn is necessary for the formation of the contractile actomyosin cable at these interfaces.

3.2 Materials and Methods

3.2.1 Immunohistochemistry

Flies were placed at room temperature in vials with fresh food sprinkled with dry yeast for around 24 hours. Ovaries were dissected in 1xPBS and fixed at room temperature for 20 minutes in 4% formaldehyde (EM grade, methanol free; Polyscience, Inc.) in PBS/1% NP-40 saturated with heptane (Fisher Chemical). After fixation, ovaries were rinsed three times with PBS + 0.1% Tween-20 (PBST), washed three times for 10 minutes in PBST at room temperature, blocked for 30 minutes to 1 hour in PBST + 1% BSA, then incubated overnight at 4°C in PBST + 1% BSA with the primary antibody. Ovaries were then rinsed three times with PBST + 1% BSA, washed three times for 20 minutes each at room temperature in PBST + 1% BSA, and then overnight at 4°C in PBST + 1% BSA with the appropriate secondary antibody. For F-actin staining, samples were incubated with (TRITC)-phalloidin (Sigma-Aldrich; diluted 1:200 in PBST + 1% BSA). Ovaries were then washed three times for 20 minutes at room temperature in PBST, and then incubated in SlowFade Gold Antifade (Invitrogen) mounting media and cured overnight. When mounting the samples, stage 14 egg chambers were manually removed to optimize imaging.

Antibodies used in this study were anti-Armadillo (N2 7A1, mouse; 1:100; Developmental Studies Hybridoma Bank (DSHB)), anti-Ed (rat; 1:1,000;(Laplante and Nilson,

2011), anti-Ed (rabbit; 1:1,000; (Laplante, 2008)) anti-DE-Cad (DCAD2, rat 1:100; DHSB), anti-Nrg (1B7, mouse 1:400; M. Hortsch), anti-Baz (rabbit 1:1000; (Wodarz et al., 1999)). All secondary antibodies (Invitrogen) were highly cross-adsorbed Alexa Fluor–conjugated anti-IgG, preblocked against fixed embryos, and used at a final concentration of 1:1,000.

3.2.2 Drosophila genetics

Negatively marked homozygous ed^{F72} loss-of-function clones were generated by Flp/FRT – mediated mitotic recombination as previously described (Laplante and Nilson, 2006). Briefly, *y w hsFlp;* ed^{F72} *FRT 40A/NM FRT 40A* females were incubated at 37°C for 1 hour on three consecutive days beginning at the pupae stage to induce Flp expression. Females were dissected on day 6-8 after the first heat shock.

Negatively marked baz^{815-8} loss-of-function clones (McKim et al., 1996), gift of A. Wodarz) were induced in baz^{815-8}*FRT 19A/ubi GFP FRT19A; hs Flp/CyO* females by incubation at 37°C for 1 hour on three consecutive days beginning at the pupae stage to induce Flp expression. Females were dissected on day 6 after the first heat shock.

For positively marked MARCM clones, *y w hsFlp; tub-GAL80 FRT 40A; tub-GAL4/TM6B* flies (gift of D. Hipfner) were crossed to ed^{F72} *FRT 40A* flies bearing *UAS-Ed-FL-GFP, UAS-Ed*Δ*C, UAS-NRG-*Ed^{intra}*, UAS-Ed-257, UAS-Ed-187, UAS-Ed-82GFP,* or ed^{F72} *FRT 40A, UAS-Ed-FL; UAS-bazRNAi* (Bloomington Drosophila Stock Center, BL 31523). ed^{F72} *FRT 40A* flies bearing *UAS-DECad-*Ed^{intra} were crossed to *y w hsFlp; tub-GAL80 FRT 40A; Vm-GAL4/TM6B* flies (Vm-GAL4,(Peters et al., 2013). The resulting progeny were incubated at pupal stage at 37°C for 1 hour on three or four consecutive days. Female progeny were dissected 7-8 days after the first heat shock.

3.2.3 Generation of transgenes

Ed transgenes were generated by PCR amplification from cDNAs RE66591 (Ed), PCR products were inserted into the pENTR vector (Invitrogen). The resulting clones were recombined into a destination vector pUASg.attB (Bischof et al., 2007) or pTWG (for Ed-82-GFP; DGRC).

Forward primer for all Ed constructs:

5’ CACCCGTGTGTGCGAACAACAACTCAGC 3’

Reverse primers used:

Ed-257 5’ CTATGGTGAATCTAAATGCTGATCGACTCGCTT 3’

Ed-187 5’ CTAGGCGGGCTGCTGTTCCACATACTGATT 3’

Ed-82GFP 5’ACTTCCCGGATGATAGCTATAT 3’

Nrg-Ed^{intra} was generated by adding two ectopic restriction enzyme sites into the 3’ end of the Nrg extracellular domain sequence from the GH03573 cDNA clone (DGRC), the resulting PCR amplification product was then cloned into a pENTR-SD vector (Life Technologies). Ectopic restriction sites were added to the 5’ and 3’ end of the Ed sequence by PCR. The PCR amplicon was then digested with the corresponding restriction enzymes and ligated into the pENTR-Nrg vector. The ligation product was recombined into the pUASg.attB destination vector (Bischof et al., 2007).

Nrg Forward: 5’ CACCCCAAATCGTATTTACTG 3’

Nrg-BamHI Reveres: 5’ ATCGGTGATGGATCCGGCCACCATTATTGGTCCCT 3’

Nrg-XbaI Reverse: 5’ AATCTAGAATCGGTGATGGATCCGGCCACCATT 3’

Ed-BamHI Forward: 5’ TTTGGATCCATCACCGATCCCAGGGTCACA 3’

Ed-XbaI Reverse: 5’ CCTCTAGACTAGACAATAATCTCGCGTAT 3’

To generate the DE-Cad-Ed^{intra} transgene, the extracellular and the transmembrane domains of DE-Cad were amplified by PCR from the cDNA clone RE56318 (DGRC) and a restriction enzyme sites were designed into the primers and added to the 5’ and 3’ end of the PCR product, which was subsequently cloned into the pUAST vector (DGRC). The intracellular domain of Ed was amplified by PCR and inserted into the pUAST-DE-Cad clone. The resulting chimeric sequence, DE-Cad-Ed^{intra} , was then amplified by PCR and cloned into pENTR vector (Invitrogen) and recombined into the pUASg.attB destination vector(Bischof et al., 2007).
DE-Cad-EcoR1 Forward: 5’ CAGATCGGATTCATGTCCACCAGTGTCCAG 3’
DE-Cad-XbaI Reverse: 5’ CAGATCTCTAGACACCACCACTGCCAACAG 3’
Ed-XbaI Forward: 5’ GCGATCTCTAGATGCAAGCGCAATCAATCG 3’
Ed-XbaI Reverse: 5’ GCGATCTCTAGAGACTAGACAATAATCTCGCG 3’
DE-Cad in TOPO Forward: 5’ CACCATGTCCACCAGTGTCCAG 3’
Ed in TOPO Reverse: 5’ CTAGACAATAATCTCGCG 3’

3.2.4 Microscopy

Fixed samples were mounted in SlowFade Gold Antifade (Invitrogen). All the images were acquired with a LSM510 Meta confocal microscope (Carl Zeiss, Inc. McGill Cell Imaging and Analysis Network facility) at room temperature with a Plan Apochromat 63× 1.4 NA differential interference contrast oil. The images were analyzed using the imaging software ImageJ 1.46r (NIH). Apart from minor linear adjustments to brightness and contrast, no image manipulations were performed.

3.2.5 Post-acquisition analysis

To quantify Baz and DE-Cad fluorescence levels, maximum intensity projections of confocal z-stacks were generated using ImageJ 1.46r (NIH). Mean fluorescence intensities of Ed/Ed interfaces, Ed/no Ed interfaces, and no Ed/no Ed interfaces were measured following manual traces of a 5 pixel wide line. Each image had a scale of 7.002 pixels/μm. To quantify the background fluorescence intensity for each image, a 5 pixel wide line was drawn manually at a random position inside a cell, excluding the cell interfaces. For each image, at least three measurements were made for each category. The average of the mean intensity values was then calculated and the average background intensity subtracted, resulting in one value for each interface per image. In each image, the value of Ed/Ed interface was considered to represent the wild-type mean intensity value for Baz/DE-Cad. To correct for differences between images, mean intensity values for each category were normalized to the wild-type mean intensity value for each image. The values were exported to an excel spreadsheet and plotted in a graph. Error bars indicate the standard error of the mean.

3.3 Results

3.3.1 Ed smooth border phenotype requires the intracellular domain

ed^{F72} homozygous mutant follicle cell clones exhibit a smooth border, which is composed of individual smooth interfaces between *ed* mutant cells and the adjacent wild-type Ed-expressing cells (Figure 3.1. A, A", arrow). These smooth interfaces are characterized by an enrichment of F-actin (Figure 3.1. A', arrow) and the phosphorylated form of myosin regulatory light chain (pMRLC) (data not shown), suggesting that a contractile actomyosin cable forms at these interfaces and accounts for their smooth contour (Chang et al., 2011; Laplante and Nilson,

2006, 2011; Lin et al., 2007). A closer examination of an Ed/no Ed interface shows that endogenous Ed is largely undetected at the interface, implying that, in addition to being absent from the *ed* mutant cell, it is also locally absent from the wild-type cell at that interface (Figure 3.1. A, arrow). This observation suggests that Ed is stabilized at the membrane by homophilic interaction *in trans* with Ed in the neighboring cell (Chang et al., 2011; Laplante and Nilson, 2006, 2011), and thus shows that lack of a binding partner at Ed/no Ed interfaces results in a planar polarized distribution of Ed at that cell interface (Figure 3.1. A, arrow). These data indicate that loss of Ed alone is not solely responsible for the smooth border phenotype at an Ed/ no Ed interface, since no Ed/no Ed interfaces display an apparently normal jagged contour (Figure 3.1. A', asterisk). Therefore, as previously proposed, this asymmetric distribution of Ed within the wild-type cell is required for the cell shape changes occurring at an Ed/no Ed border (Laplante and Nilson, 2011).

One prediction of this hypothesis is that intracellular domain of Ed mediates the effect on the actomyosin cable and the smooth border formation. To test this prediction, we wanted to create ectopic Ed/no Ed interfaces where we could manipulate the form of Ed that is present in the Ed-expressing cells, thus allowing us to ask whether the intracellular domain is required for this function of Ed. To generate such interfaces, we made use of the mosaic analysis with a repressible cell marker (MARCM) system to induce follicle cell clones that are mutant for *ed* and also express transgenic Ed under the control of a GAL4/UAS expression system (Figure 3.2.; Laplante and Nilson, 2011). This system thus allowed us to replace endogenous Ed with a transgenic form of Ed. Although the MARCM system predicts that all *ed* mutant cells will express the Ed transgene, we found instead that transgene expression in such clones is mosaic (transgenic mosaics). In other words, although all the *ed* mutant cells contain GAL4 and

therefore should express the UAS-Ed transgene, apparently random groups of those mutant cells do not (Figure 3.2. C, middle). Although the reason for this mosaic expression of the transgene is unclear, these groups of cells are easily identifiable because they lack Ed staining. Importantly, the presence of such cells generates interfaces between $ed^{-/-}$ cells expressing and not expressing the transgene, creating transgenic Ed/no Ed interfaces within the clone and allowing us to analyze the ability of different Ed transgenes to direct the formation of a smooth border at such interfaces.

Analysis of such clones has shown that, as predicted, interfaces between *ed* mutant cells lacking Ed and *ed* mutant cells expressing transgenic full-length Ed(Ed-FL/no Ed interfaces) are smooth (Laplante and Nilson, 2011). This phenotype is similar to Ed/ no Ed interfaces in *ed* loss-of-function clones (Figure 3.1 A – A', arrow), thus validating this system. In contrast, interfaces between cells lacking Ed and cells expressing transgenic Ed lacking the intracellular domain, EdΔC-GFP, are not smooth but jagged, indicating that the intracellular domain of Ed is necessary for the smooth interface phenotype (57/57 interfaces, Figure 3.1 C – C", arrowhead/ (Laplante and Nilson, 2011). To control for an effect of the C-terminal GFP tag on Ed function, we made and tested an Ed full-length (Ed-FL) transgene with a GFP tag at its C-terminus (Ed-FL-GFP). Similar to endogenous Ed or Ed-FL/ no Ed interfaces, Ed-FL-GFP/no Ed interfaces are smooth (32/32 interfaces, Figure 3.1 B –B", arrowhead), despite the overexpression the transgene, suggesting that the addition of a GFP tag at the C-terminus of Ed does not interfere with smooth border formation. Taken together, these data are consistent with previously published observations (Laplante and Nilson, 2011) and indicate that the intracellular domain of Ed in the Ed-expressing cell is required for smooth border formation.

3.3.2 Asymmetric distribution of Ed intracellular domain is necessary and sufficient for smooth border formation

To test whether the intracellular domain of Ed is also sufficient for smooth border formation, we used the MARCM system described above (Figure 3.2) to generate transgenic mosaics that create ectopic Ed/no Ed interfaces where the Ed-expressing cell bears only the intracellular domain of Ed. As a preliminary approach, we expressed a transgene encoding a truncated form of Ed containing only the transmembrane and intracellular domains (Ed^{TMC} , (Yue et al., 2012) in *ed* mutant cells, but found that this form of Ed did not localize to the cell surface (data not shown). This result is perhaps not surprising given that Ed requires homophilic interactions *in trans* to be stably localized at the plasma membrane (Chang et al., 2011; Laplante and Nilson, 2011). Although this observation is contradictory to a previous report, which showed the same truncated form of Ed localizing to the plasma membrane in S2 cells, this localization discrepancy could be due to the fact that the ectopic protein was expressed in different types of cells (Yue et al., 2012).

As an alternative approach to stably localize this truncated form of Ed at the membrane, we fused the Ed transmembrane and intracellular domains to an ectopic extracellular domain. Specifically, we replaced the extracellular domain of Ed with that of Neuroglian (Nrg), a homophilic binding septate junction protein that localizes to the basolateral membrane (Figure 3.3 B', arrow; Wei et al., 2004), generating an Nrg – Ed^{intra} chimeric protein. When we ectopically expressed the Nrg-Ed^{intra} chimeric protein in the follicle cells, we saw that it localized to the membrane, indicating that providing an ectopic extracellular domain to this truncated form of Ed was sufficient to stabilize it at the plasma membrane (Figure 3.3 A, B). Interestingly, Nrg-Ed^{intra} localized not only to the basolateral membrane, similarly to endogenous Nrg, but also to

the apical membrane (Figure 3.3 B – B", arrowhead). The apical localization of the Nrg-Ed^{intra} chimeric protein could be due to either the high expression levels of the transgene or the presence of the intracellular domain of Ed.

To test whether the intracellular domain of Ed alone is sufficient for smooth border formation, we then used the MARCM system to generate interfaces between *ed* mutant cells expressing and lacking the Nrg-Ed^{intra} (Figure 3.3 A"', arrowhead). We found that in these *ed* transgenic mosaic epithelia, Nrg – Ed^{intra}/no Ed interfaces exhibited a smooth contour (65/65 clones, Figure. 3.3 A – A", arrowhead). This phenotype was similar to endogenous Ed/no Ed interfaces (Figure. 3.3 A – A"', arrow), indicating that the Ed intracellular domain alone is sufficient for smooth border formation.

Our model on how Ed regulates the actomyosin network would predict that the intracellular domain sequence of Ed is not only required but also asymmetrically distributed within the Ed-expressing cell. Since Nrg-Ed^{intra} is localized apically and basolaterally and endogenous Nrg is localized only basally, we predicted that this apicobasal difference in localization results in an apically planar polarized Ed intracellular domain in the Ed-expressing cell at a Nrg-Ed^{intra}/no Ed interface. Basolaterally, endogenous Nrg in the cell that lacks Ed provides a binding partner for the basolaterally localized Nrg-Ed^{intra} protein in the Ed-expressing cell (Figure 3.3 D, arrow). However, apically, endogenous Nrg is not present and is therefore not available to stabilize Nrg-Ed^{intra} at Nrg-Ed^{intra}/no Ed interfaces (Figure 3.3 D, arrowhead). The intracellular domain of Ed thus becomes asymmetrically distributed at the apical side of the cell and this inferred localization is consistent with the model where the polarized distribution of Ed leads to the smooth contour phenotype of the Ed/no Ed interface (Laplante and Nilson, 2011).

One prediction of this model would be that uniform distribution of just the intracellular domain of Ed would be sufficient to block the formation of a smooth border at an Ed/no Ed interface. To generate a uniformly distributed Ed intracellular domain, we made an Ed transgene where we substituted the extracellular domain of Ed for the homophilic binding adherens junction molecule DE-cadherin (DE-Cad) (Niewiadomska et al., 1999; Tepass et al., 1996), creating a DE-Cad-Ed^{intra} chimeric protein. We reasoned that because of the homophilic binding property of DE-Cad, ectopically expressed DE-Cad-Ed^{intra} chimeric protein would get stabilized at the apical domain by interacting *in trans* with the apically localized DE-Cad in the neighboring cell, thus resulting in a uniformly distributed Ed intracellular domain, even though the neighboring cell lacks Ed, which in turn would allow us to assess our prediction.

To test our reasoning, we used the MARCM system to generate interfaces between *ed* mutant cells expressing and lacking the DE-Cad-Ed^{intra} chimeric protein (Figure 3.3 C”’, arrowhead). We observed that in *ed* transgenic mosaic epithelia, DE-Cad-Ed^{intra} appeared to be uniformly distributed (Figure. 3.3. C’, arrowhead). In addition, contrary to the smooth interface between an *ed* mutant and a wild-type cell with endogenous Ed (Figure 3.3 C – C”’, arrow), the interfaces between a no Ed cell and a DE-Cad-Ed^{intra}-expressing cell were not smooth (13/13 clones, Figure. 3.3. C”, C”’, arrowhead). Our interpretation of these data is that DE-Cad-Ed^{intra} becomes stabilized at the clonal interface by the homophilic interaction with DE-Cad in the neighboring cell leading to a uniformly distributed Ed intracellular domain (Figure 3.3. E, right). These data thus indicate that the polarized distribution of the intracellular domain is required and sufficient for smooth border formation.

Given the importance of the Ed intracellular domain in smooth border formation, we set out to identify a functional domain in this region that mediates this phenotype. We systematically

deleted regions of the intracellular domain, including the PDZ-binding motif at its C-terminus (Wei et al., 2005), which seems to be dispensable for the smooth border phenotype (Supplemental Fig. 3.2 A – A"; Laplante and Nilson, 2011). To choose where to make molecular lesions in the intracellular domain of Ed, we compared the sequence of this domain between different *Drosophila* species as well as two mosquito species and identified conserved regions within this domain (Figure 1.4 B). We then generated a series of transgenes missing one or more of these regions (Supplemental Fig. 3.1), and tested their functionality in generating smooth transgenic Ed/no Ed borders.

The deletion mapping analysis of the Ed intracellular domain revealed two regions within the Ed intracellular domain that mediate smooth border formation: one region between amino acids 1134 and 1205, and another between amino acids 1206 and1328 (Supplemental Fig. 3.1; Functional Domain 1B and 2). Expression of a transgene lacking both intracellular regions (Ed-82-GFP) led to a jagged contour of Ed-82-GFP/no Ed interfaces (Supplemental Fig. 3.1; 0/110 smooth borders), suggesting that this missing domain between amino acids 1134 and 1328 is required for this function of Ed in this assay. However, expression of a transgene lacking the only the second functional domain (Ed 187) led to smooth interfaces between Ed 187/no Ed cells (Supplemental Fig 3.1; Ed187, 174/174 smooth borders). On the contrary only 1/3 of interfaces between EdΔ1134-1205/no Ed cells displayed a smooth contour (Supplemental Fig 3.1; EdΔ1134-1205 12/37 smooth borders, 25/37 jagged borders). These results suggest that the region of the intracellular domain of Ed absent from the Ed 187 transgene, from amino acids 1206 and 1328, imparts some auxiliary function in directing the formation of a smooth border at a differential Ed-expression interface.

Taken together, our data indicate that Ed directs smooth border formation at an Ed/no Ed interface via its planar polarized intracellular domain. This domain is both necessary and sufficient for this function of Ed. Within this domain, we identified two functional regions that mediate this function of Ed.

3.3.3 The intracellular domain of Ed disrupts Bazooka localization at an Ed/no Ed interface

To understand how the Ed intracellular domain directs localized actomyosin contractility at an Ed/ no Ed interface, we took a candidate gene approach. For several reasons we investigated the polarity protein Bazooka/Par-3 (Baz) as a possible Ed effector. Baz has been reported to physically interact with Ed via the PDZ-binding motif (Wei et al., 2005). Ed and Baz display a similar asymmetric distribution in the DME cells during the process of dorsal closure and in the floor cells of the dorsal appendage primordial in the follicular epithelium, which is reciprocal to the enrichment of myosin-II in the same cells (A. Noçka, unpublished observationa; Laplante and Nilson, 2006; Osterfield et al., 2013).

To test whether the localization of Baz is also affected by the distribution of Ed at ectopic Ed/no Ed interfaces, which would be generated within the same type of cells, we generated homozygous $ed^{-/-}$ mutant clones in the follicular epithelium and looked at the distribution of Baz in these mosaic epithelia. We found that Baz localization was affected at Ed/no Ed clone borders, where Baz appeared to be absent in the majority (90/109 clones, Figure 3.4 A, arrowhead) of the borders but sometimes its localization appeared continuous (19/109 clones; Figure 3.4 A', arrowhead). This variance in Baz localization was independent of the position or size of the clone, or the stage of the eggchamber. Interestingly, we observed that the localization of Baz

appeared unchanged at *ed*$^{-/-}$ mutant cell (no Ed/no Ed) interfaces (Figure 3.4 A, A', arrows) suggesting that loss of Ed alone is not responsible for this altered distribution of Baz.

A closer examination of the distribution of Baz at an Ed/no Ed interface revealed that the disruption of Baz localization within the same clone was not uniform. Therefore, we decided to characterize the disruption of Baz localization at an individual Ed/no Ed interface based on the Ed-expressing cell and found that it could be classified into three categories, where Baz was absent (28%), disrupted (54%), or continuous (18%; nr. interfaces = 538, in 61 clones; Figure 3.4, B – B", arrowheads). To determine whether the amount of Baz at the "continuous" interfaces was unaffected or rather decreased, we quantified the mean fluorescence intensity of Baz immunoreactivity at such Ed/no Ed interfaces and compared it to that of wild-type Ed/Ed interfaces and *ed*$^{-/-}$ mutant no Ed/no Ed interfaces. Our analysis revealed that indeed the Baz immunoreactivity was significantly decreased at the "continuous" Ed/no Ed interfaces (Figure 3.4, B"'), indicating that the amount of Baz at these interfaces is lower.

A model where Baz acts as an Ed effector in mediating the contractile Ed/no Ed interfaces would predict that the distribution of Baz would be affected at all Ed/no Ed interfaces that display a smooth contour despite the form of Ed present in the Ed-expressing cell, but remain unaffected in Ed/no Ed interfaces with a jagged contour. To test this prediction, we used the MARCM system to generate Ed/no Ed interfaces where the Ed-expressing cell contains an Ed transgene (Supplemental Fig. 3.1) and analyzed the distribution of Baz at such interfaces. To control for differences in genetic background, we generated Ed/no Ed interfaces using the MARCM system to generate *ed* mutant clones that do not express an Ed transgene (L.O.F. 2) and found that the degree of disruption of Baz in such interfaces was similar to that in *ed*$^{-/-}$ loss-of-function clones not generated via the MARCM system (Figure 3.4, C. L.O.F.2, L.O.F.1 nr of

interfaces = 575, in 72 clones). As predicted, Baz localization appeared disrupted at smooth Ed/no Ed interfaces (Ed-FL, Ed-FL-GFP, EdΔP, Ed 187/no Ed interface, Figure 3.4, C), but not disrupted at jagged Ed/no Ed interfaces (EdΔC, Ed-82GFP/no Ed) where it was indistinguishable from Baz localization at the other interfaces (Figure 3.4, C). Such observations are also consistent with a hypothesis that Baz might be an Ed effector for this function of Ed.

3.3.4 Adherens junctions are disrupted at an Ed/no Ed interface

Differential expression of Ed disrupts Baz localization only at the border between cells expressing or lacking Ed, although the degree of the disruption of the localization of Baz is not uniform at all Ed/no Ed interfaces. One hypothesis for the altered distribution is that Baz is an Ed effector for this function of Ed. An alternative hypothesis is that the disruption Baz localization at Ed/no Ed interface is simply a consequence and not the cause for the accumulation of the actomyosin network at such interfaces. For example, as the tension generated by the contractile force of an actomyosin cable has been shown to disrupt adherens junctions (AJ) (Bertet et al., 2004; Sahai and Marshall, 2002), and Baz localizes to the AJs by binding to the PDZ-domain of either Arm or Ed (Wei et al., 2005), it is possible that the altered distribution of Baz at an Ed expression interface results from the disruption of AJs.

To distinguish between these two possibilities, we looked whether the AJs become destabilized at an Ed/no Ed interface by examining the distribution of DE-Cad at such interfaces. DE-cad localization at the Ed/no Ed interfaces was altered (Figure 3.5) and can be further classified into the same three categories where DE-cad was either absent (13%), disrupted (44%) or continuous (43%; Figure 3.5, A – A", arrows). Next, we quantified the levels of DE-Cad immunoreactivity for the Ed/no Ed interfaces that displayed a "continuous" distribution and

found it to be only slightly decreased compared to the Ed/Ed or no Ed/no Ed interfaces (total number of interfaces = 92, in 13 clones; Figure 3.5, A"').

A model where the altered distribution of Baz is a consequence of the altered distribution of the AJs would predict that they would display the same degree of disruption. Our observations are not consistent with this prediction, although we cannot rule out that there is a disruption of AJs that is not detectable via immunohistochemistry. However, our data suggest that the AJs seem to be destabilized at an Ed/no Ed interface, Baz localization is affected to a greater degree at similar interfaces, suggesting that the localization of AJs and Baz might be altered independently.

3.3.5 Loss of Baz does not disrupt junctional stability or the integrity of the follicular epithelium

To further investigate the hypothesis that Baz acts as an Ed effector in regulating the actomyosin cytoskeleton, we reasoned that generating an Ed/no Ed interface in cells that lack Baz should suppress the smooth border phenotype. However, since Baz has been previously proposed to maintain the identity of the apical domain of the follicle cells and their organization (Abdelilah-Seyfried et al., 2003; Benton and Johnston, 2003; Morais-de-Sa et al., 2010), we first wanted to see whether loss of Baz would cause loss of integrity in this tissue.

We generated mosaic epithelia with *baz*$^{-/-}$ loss-of-function clones and looked at the localization of DE-Cad, Arm, and Ed as markers of the apical membrane. We observed that the localization of DE-Cad, Arm, and Ed in the *baz*$^{-/-}$ mutant cell was indistinguishable from that in the neighboring wild-type cell (50/50 clones; Figure 3.6, A – B"', arrowhead, arrow), suggesting that the apical identity of *baz*$^{-/-}$ mutant cells is not compromised. Looking at the organization of the follicular epithelium bearing *baz*$^{-/-}$ loss-of-function clones, we found that the interfaces

between *baz*$^{-/-}$ mutant cells were mainly jagged (53/57 clones, Figure 3. 6, C" – E"', arrowhead), however, in a few instances, some *baz*$^{-/-}$ mutant cells appeared smaller than their neighboring cells and round suggesting that they were being extruded from the epithelium (4/57 clones, Figure 3. 6, F' – F"', arrowhead). Interfaces between *baz*$^{-/-}$ cells and the wild-type cells (Baz/no Baz interface) appeared jagged (18/57 clones, Figure 3. 6, C", C"', arrow), round (18/57 clones, Figure 3. 6, E", E"', arrow), or a combination of jagged and round (17/57 clones, mixed Figure 3. 6, D", D"', arrow). These phenotypes were independent of the size of the clone, or the stage of the egg chamber. It is worth noting that the round shape of the Baz/no Baz interface is different than the smooth contour of an Ed/no Ed interface. The *baz*$^{-/-}$ mutant cells individually exhibit a round contour (Figure 3.6 D", E", arrow) giving the clone border a scalloped shape, rather than the characteristic smooth contour of the *ed*$^{-/-}$ clones, suggesting that the cell shape changes at the Baz/no Baz interface appear to be driven by the *baz*$^{-/-}$ mutant cells as opposed to the wild-type cell at an Ed/no Ed interface.

The reason for the discrepancy in the severity of the *baz*$^{-/-}$ mutant clones phenotype between our observations and the previously reported ones is not clear. One explanation could be the use of different *baz* alleles between the studies. The *baz* allele used in this study, although reported as a strong loss-of-function rather than a null allele, contains an early nonsense mutation in the coding region of Baz which would produce a truncated protein that is most likely completely nonfunctional (Krahn et al., 2010). Consistent with this report, Baz immunoreactivity in *baz*$^{-/-}$ mutant cells was not detected (Figure 3.6, D'). An alternative explanation for the variance in the observed phenotypes could be a difference in the genetic background. We cannot rule out the possibility that, in addition to the mutant allele, there might have been a suppressor mutation in the flies we used, or an enhancer mutation in the flies used in the other studies.

3.3.6 Baz suppresses the smooth border phenotype at an Ed/no Ed interface

Because the *baz*$^{-/-}$ mutant phenotype did not appear to critically affect the integrity of the follicular epithelium, we could then address the question whether loss of Baz suppresses the smooth border of the Ed/no Ed interface. We used the MARCM system to generate interfaces between *ed* mutant cells expressing or lacking Ed-FL transgene. In addition, to remove Baz expression in all the cells within the clone, the *ed* mutant cells also expressed a Baz^{RNAi} transgene, which was more uniformly expressed within the clone as detected by the lack of immunostaining with an anti-Baz antibody (data not shown).

As previously reported, in the presence of Baz, interfaces between Ed-FL expressing cells and no Ed cells exhibit a smooth contour (Figure 3.7 A – A", arrow). Baz localization appears disrupted at these Ed/no Ed interfaces. Interestingly, in the absence of Baz, the same Ed-FL/no Ed interfaces no longer exhibit their characteristic smooth contour, but instead they appear jagged (53/53 interfaces; Figure 3.7 B – B", arrow), indicating that loss of Baz suppresses the smooth border phenotype.

These results are consistent with our hypothesis that Baz functions downstream of Ed to regulate the formation of the actomyosin cable at the Ed/no Ed interfaces. Our observations support a model where a planar polarized distribution of Ed in the Ed-expressing cell directs the asymmetric distribution of Baz in that same cell, which in turn generates a localized actomyosin contractility (Figure 3.7, C; Laplante and Nilson, 2011).

3.4 Discussion

3.4.1 The polarized distribution of the intracellular domain of Ed is required for the assembly of the actomyosin cable at the Ed/no Ed interface

Our data demonstrate that Ed exerts its effect on the actin cytoskeleton via its intracellular domain. Unlike the smooth interfaces between wild-type cells expressing endogenous Ed and *ed*$^{-/-}$ mutant cells, the interfaces between cells expressing a form of Ed lacking the intracellular domain (EdΔC) and *ed*$^{-/-}$ mutant cells are jagged. Further, to exert its effect on the actomyosin network, the intracellular domain of Ed needs to assume an asymmetric distribution within the Ed-expressing cell.

Since homophilic binding of the extracellular domain stabilizes Ed at the cell surface, it determines the localization of the intracellular domain. It could be speculated that the extracellular domain of Ed, via its homophilic binding property, functions in sensing the extracellular environment and in turn provides spatial information via the intracellular domain about the surroundings, whether the neighboring cell expresses or lacks Ed, to the inside of the cell.

3.4.2 Asymmetric distribution of Ed directs polarized localization of Baz/Par-3

Baz assumes a polarized distribution in the follicular epithelium in the Ed-expressing cell at ectopic and endogenous Ed/no Ed interfaces (this work; Osterfield et al., 2013). Baz distribution is also polarized in the embryo in DME cells during dorsal closure, and this distribution is dependent on the localization of Ed (Laplante and Nilson, 2011; Pickering et al., 2013). However, the molecular mechanism by which Ed affects the localization of Baz at such interfaces in unclear. One possibility is that the direct physical binding of Ed and Baz via their PDZ-domains (Wei et al., 2005) results in the exclusion of Baz from the face of the cells that

lacks Ed, so that the polarized distribution of Baz in the Ed-expressing cell would match that of Ed. Such a direct binding model would predict that Baz localization should also be disrupted in cells lacking Ed. Contrary to this prediction, in the absence of Ed, Baz localization appears unaffected in the AS cells during dorsal closure that lack Ed expression (David et al., 2013; Laplante and Nilson, 2011). In addition, Baz localization did not appear disrupted in the $ed^{-/-}$ mutant cells (no Ed/no Ed interfaces) in the follicular epithelium. Furthermore, a direct binding model cannot explain our observations that Baz localization is affect at EdΔP/no Ed interfaces and assumes a polarized distribution in the EdΔP expressing cell (Figure 3.4, C). Therefore, we propose instead an indirect interaction model, where loss of Ed from one side of the cell results in a polarized Ed distribution in that cell, which in turn initiates intracellular changes that ultimately alter the distribution of Baz.

A plausible candidate for mediating the relationship between Ed and Baz is Rho-kinase. In the Ed-expressing cell, the polarized distribution of intracellular domain of Ed, influences the reciprocal enrichment of Rho-kinase, which in turn directs the asymmetric localization of Baz in that cell. A role for Rho-kinase in displacing and reorganizing the localization of Baz has been characterized in the process of germband extension (Simoes Sde et al., 2010) and for the maintenance of proper segment boundaries in late embryogenesis (Bulgakova et al., 2013). Baz has been shown to be a substrate for Rho-kinase in mammalian cells (Nakayama et al., 2008) and *Drosophila* embryos where phosphorylation of Baz causes its displacement from the cell cortex (Morais-de-Sa et al., 2010). Interestingly, an asymmetric and complementary localization of Rho-kinase and Baz has been described to occur in the DME cells during dorsal closure, where their respective distributions are dependent on the polarized distribution of Ed (R. Rote, unpublished data, (Laplante and Nilson, 2011; Pickering et al., 2013), suggesting that a function

of Rho-kinase might be to alter the distribution of Baz in these cells. Such a model would predict that in the absence of phosphorylation by Rho-kinase, Baz would remain present at an Ed/no Ed interface and thus display a uniform distribution in the Ed-expressing cell, despite the polarized distribution of Ed. One way to test this prediction would be to inhibit Rho-kinase activity either by injecting dorsal closure stage embryos with a Rho-kinase inhibitor, or alternatively by generating Rho-kinase mutant embryos solely expressing a kinase-dead Rho-kinase transgene and assess whether the loss of kinase activity causes the redistribution of Baz in the DME cells during dorsal closure. If Rho-kinase is responsible for mediating the asymmetric distribution of Baz, then inhibiting the activity of Rho-kinase should lead to a uniform distribution of Baz in these cells.

It is unclear how Ed could influence the polarized localization of Rho-kinase, because the intracellular domain of Ed does not have any obvious functional motifs. One hypothesis is that Ed might direct Rho-kinase localization indirectly, rather than via direct physical interaction. Consistent with this hypothesis, the Rho-kinase upstream activator, RhoGTPase and its activating GEF, RhoGEF2, both appear to be enriched at the leading edge, and this enrichment is dependent on the polarized localization of Ed (Azevedo et al., 2011; Laplante and Nilson, 2011), thus suggesting that Ed might function upstream of RhoGEF2 to regulate the polarized distribution of these proteins. Therefore, the asymmetric and complementary distributions of Baz and the regulators of actomyosin contractility within the Ed-expressing cell appear to be dependent on the asymmetric localization of the intracellular domain of Ed.

The disruption of Baz at the Ed/no Ed interface indicates that Baz localization is also altered in the $ed^{-/-}$ mutant cell at the interface. Therefore, Baz assumed a polarized distribution in the $ed^{-/-}$ mutant cells as well as in the wild-type cell. It is unclear what would cause this change

in the distribution of Baz in the neighboring *ed*$^{-/-}$ cell. One hypothesis is that, similarly to Ed, loss of Baz from one side of the interface would somehow lead to loss of Baz in the adjacent cell; however, in the *baz*$^{-/-}$ loss-of-function clones, we noticed that localization of Baz in the wild-type cell adjacent to the *baz*$^{-/-}$ mutant cell appeared unchanged (Figure 6, D').

An alternative hypothesis is that the tension generated by the contractile force of the actomyosin cable in the wild-type cell induces the disruption of Baz localization in the neighboring *ed*$^{-/-}$ mutant cell. One way to test this hypothesis would be to remove or greatly reduce the tension at an Ed/no Ed interface and determine whether localization of Baz at the interface of the no Ed cell abutting the Ed-expressing cell becomes restored. In non-muscle cells, the contractile force of the actomyosin cable is generated by the non-muscle myosin II (myosin II) motor protein, which is activated when MRLC gets phosphorylated by Rho-kinase (Matsumura, 2005; Shutova et al., 2012). One approach to test whether the contractile force is responsible for loss of Baz in the *ed*$^{-/-}$ cell would be to inhibit the phosphorylation of MRLC by expressing a MRLC phosphovariant that mimics a non-phosphorylatable form of MRLC (Kasza et al., 2014) and generating Ed/no Ed interfaces. If tension is responsible for the disruption of Baz localization in *ed*$^{-/-}$ mutant cell then, reducing tension should restore Baz at that face of the cell. On the contrary, if the contractile force of the actomyosin cable does not disrupt the localization of Baz in *ed*$^{-/-}$ mutant cell, then reducing tension would not affect the distribution of Baz.

3.4.3 The polarized distribution of Baz regulates actomyosin cable assembly at an Ed/no Ed interface

Our observation that the absence of Baz suppresses the smooth phenotype of Ed/no Ed interfaces implies that Baz is an Ed effector for this function of Ed. However, it is also conceivable that loss of Baz somehow changes the properties of the tissue such that the epithelial cells lose their identity and do not regulate their actomyosin network. A role for Baz in establishing the identity of the apical domain in epithelial cells during early embryonic development has been described (Harris and Peifer, 2004; McGill et al., 2009). In the absence of Baz, follicle cells have been reported to lose their cuboidal morphology, fail to assemble their AJ, as visualized by DE-cad and Arm immunostainings, and the epithelium displays a multilayering phenotype, although visually not as severe as in *dlg* or *lgl* mutant clones (Abdelilah-Seyfried et al., 2003; Benton and Johnston, 2003; Morais-de-Sa et al., 2010). These observations would be consistent with the hypothesis that the suppression of the smooth border at an Ed/no Ed interface in the follicular epithelium in the absence of Baz results from changes in the properties of these cells. However, in our analysis of *baz* mutant clones in the follicular epithelium, we noticed that AJ components were localized properly in such cells, we did not observe a multilayering phenotype, and the overall organization of the follicular epithelium seemed mostly unchanged. Thus, our observations suggested that these cells, in the absence of Baz, did not lose their identity and therefore allowed us to identify Baz as an Ed effector for smooth border formation.

It is not known how the polarized distribution of Baz directs the polarization of the actomyosin network. It is possible that Baz regulates actin remodeling at Ed/no Ed interfaces. Baz has been proposed to regulate F-actin in post-synaptic muscles in the neuromuscular juntions (NMJ) in *Drosophila* by interacting with aPKC and the phosphoinositide lipid phosphatase PTEN (Ramachandran et al., 2009). Interestingly, the interaction the

phosphoinositide lipids has been shown to be necessary for the proper membrane localization of Baz (Krahn et al., 2010), and the phosphoinositide lipids have been shown to regulate actin dynamics by interacting with actin binding proteins (van Rheenen and Jalink, 2002). Therefore, it is possible that at Ed/no Ed interfaces, the polarized distribution of Baz influences the composition of the membrane phosopholipids, which in turn remodel the actin cytoskeleton. Consistent with this hypothesis, Baz via its interaction with PTEN, has been shown to regulate the actin cytoskeleton dynamics in the DME cells during dorsal closure (Pickering et al., 2013). However, this polarized PIP3 distribution only affected the formation of the localized protrusions at the LE but not the formation of the actomyosin cable (Pickering et al., 2013).

Alternatively, it is possible that Baz influences the localized enrichment of myosin II. Indeed, such a function for Baz has been proposed to occur in rosette formation in the epidermis during germband extension in the embryo, where changing the distribution of Baz also affected the polarized enrichment of myosin II (Simoes Sde et al., 2010). A reciprocal localization between a planar polarized Baz and an asymmetric enrichment of myosin II has also been described in the floor cells during appendage morphogenesis in the egg chamber (Osterfield et al., 2013), in the DME cells during dorsal closure (Laplante and Nilson, 2011), at an ectopic wound edge (Pickering et al., 2013), at the D/V boundary in the wing-disk (Major and Irvine, 2006), and during cell rearrangement in the parasegment in late embryogenesis (Simone and DiNardo, 2010). These numerous examples of the complementary distribution between Baz and myosin II suggest that Baz might exert an inhibitory effect on myosin II enrichment and thus contractility. However, it is unclear how Baz directly affects the distribution of myosin II, which ultimately leads to increased asymmetric contractility in a cell.

3.5 Conclusion

Our work has elucidated the molecular mechanism by which the planar polarized distribution of the cell adhesion protein Ed causes changes in the subcellular composition of a cell. Loss of Ed from the interface of the Ed-expressing cell where it abuts an Ed-non-expressing cell appears to be the earliest event that triggers the subsequent subcellular changes that ultimately lead to the localized actomyosin contractility.

Figure 3.1. The intracellular domain of Ed is necessary for the smooth border formation at an Ed/no Ed interface.

Mosaic follicular epithelia with an *ed* loss of function clone (A – A") and *ed* MARCM clones (B – C"), stained for Ed and F-actin (A – B") and for GFP and Bazooka (Baz) (C, C'). The diagrams in A", B", and C" illustrate the corresponding genotypes that generate interfaces between wild-type cells expressing endogenous Ed and *ed* mutant cells (Ed/no Ed interface) (A", arrow), and between *ed* mutant cells that either express or lack expression of transgenic Ed (Ed-Full-GFP/no Ed and EdΔC-GFP/no Ed, B", C", arrowhead). Note that Ed/no Ed and Ed-Full-GFP/ no Ed interfaces are smooth (A – B", arrow, arrowhead), whereas EdΔC-GFP/no Ed interfaces are jagged (C-C", arrowhead).

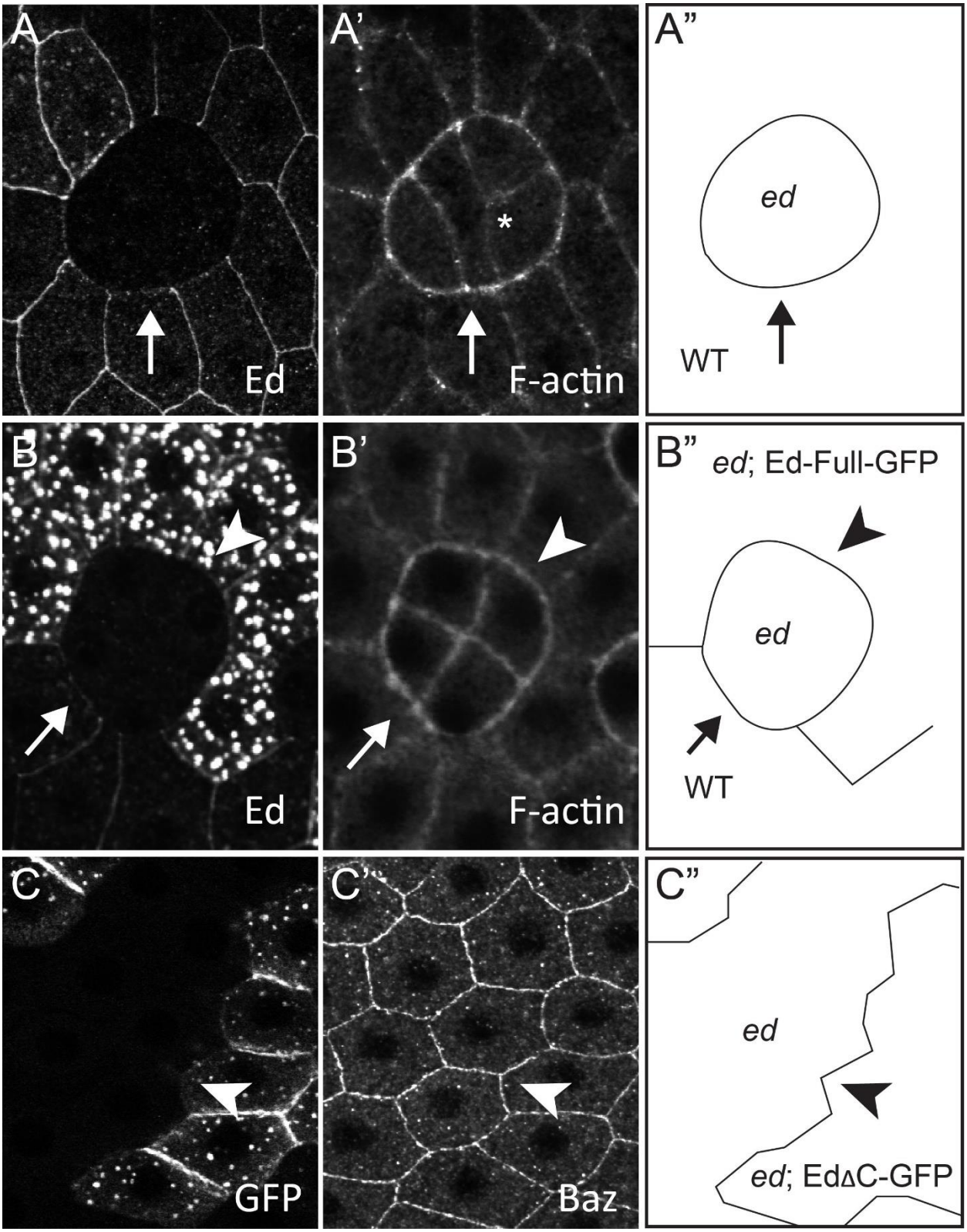
A
Ed
A'
F-actin
A"
ed
WT
B
Ed
B'
F-actin
B"
ed; Ed-Full-GFP
ed
WT
C
GFP
C'
Baz
C"
ed
ed; EdΔC-GFP

Figure 3.2. Schematic representation of the MARCM system for *ed* clones expressing transgenic Ed.

The MARCM system relies on inducible FRT-mediated mitotic recombination to generate clones of homozygous mutant cells that lack the GAL4 repressor GAL80 and thus express a GAL4-dependent UAS-transgene. (A) In the experiments described here, the parent cell contains an *ed* mutation on a chromosome bearing a proximal FRT site; the homologous chromosome is wild-type for *ed* and bears the same FRT site as well as transgene encoding the GAL4 repressor, GAL80 (pink rectangle). The parent cell also has a transgene encoding the transcription activator GAL4 (orange rectangle), a UAS- Ed transgene (green/ yellow), and a flipase transgene (not shown) on the other chromosome arms. (B) After DNA replication, site-specific mitotic recombination at FRT sites, followed by appropriate segregation during mitosis, results in two daughter cells that are either homozygous for GAL80 or homozygous for the mutation. (C) In the cell lacking GAL80, the GAL4 is able to induce the expression of the UAS-transgene (left), while the wild-type cell has the GAL4 repressor GAL80, which does not allow GAL4-dependent UAS-transgene expression (right). Unexpectedly, on occasion some homozygous mutant cells that lack GAL80 but do not express the UAS-transgene (middle); the reason is unclear, but these cells can be unambiguously identified by their lack of anti-Ed immunoreactivity.

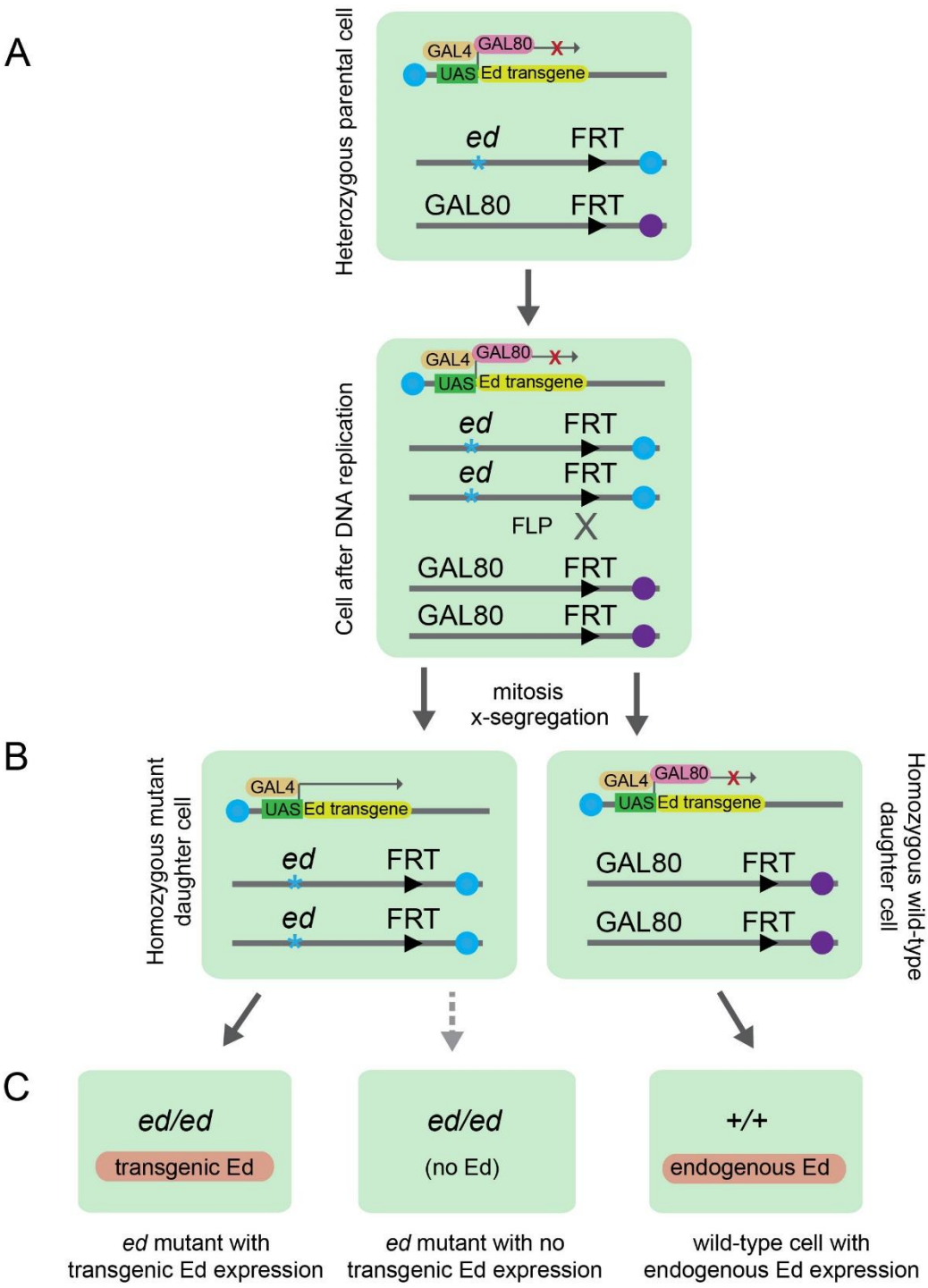
A
Heterozygous parental cell
GAL4
GAL80
UAS
Ed transgene
ed
FRT
GAL80
FRT
Cell after DNA replication
FLP
mitosis
x-segregation
B
Homozygous mutant daughter cell
Homozygous wild-type daughter cell
C
ed/ed
transgenic Ed
ed/ed
(no Ed)
+/+
endogenous Ed
ed mutant with transgenic Ed expression
ed mutant with no transgenic Ed expression
wild-type cell with endogenous Ed expression

Figure 3.3. Planar polarized distribution of the intracellular domain of Ed is necessary for smooth border formation at an Ed/no Ed interface.

(A – C") Mosaic follicular epithelia with *ed* MARCM clones expressing Nrg-Ed^{intra} transgene (A –B") or and DE-Cad-Ed^{intra} (C – C"), stained to visualize Ed (A, B, C), Nrg (A', B'), F-actin (A", C"), and DE-Cad (C'). The diagrams (right) illustrate the corresponding genotypes that generate the smooth interfaces between wild-type endogenous Ed/no Ed (arrow, A – A"', C – C"'), the smooth interface between Nrg-Ed^{intra}/ no Ed (arrowhead, A – A"'), and the jagged interface between DECad-Ed^{intra}/ no Ed (arrowhead, C – C"'). (D) Schematic representation in 3D of two *ed* mutant cells where one is expressing Nrg-Ed^{intra} transgene (purple-gray, left and the other is not (right). For simplicity, endogenous Nrg (purple) is only shown in one cell (right). (E) Schematic representation of an apical surface view of Ed/no Ed interfaces, where the Ed-expressing cell bears planar polarized Ed-FL (left), asymmetrically distributed Ed intracellular domain (Nrg-Ed^{intra}, middle) or uniformly distributed Ed intracellular domain (DE-Cad-Ed^{intra}, right). Note that all cells express endogenous DE-Cad, but for simplicity it is only shown in the *ed* mutant cell at the right.

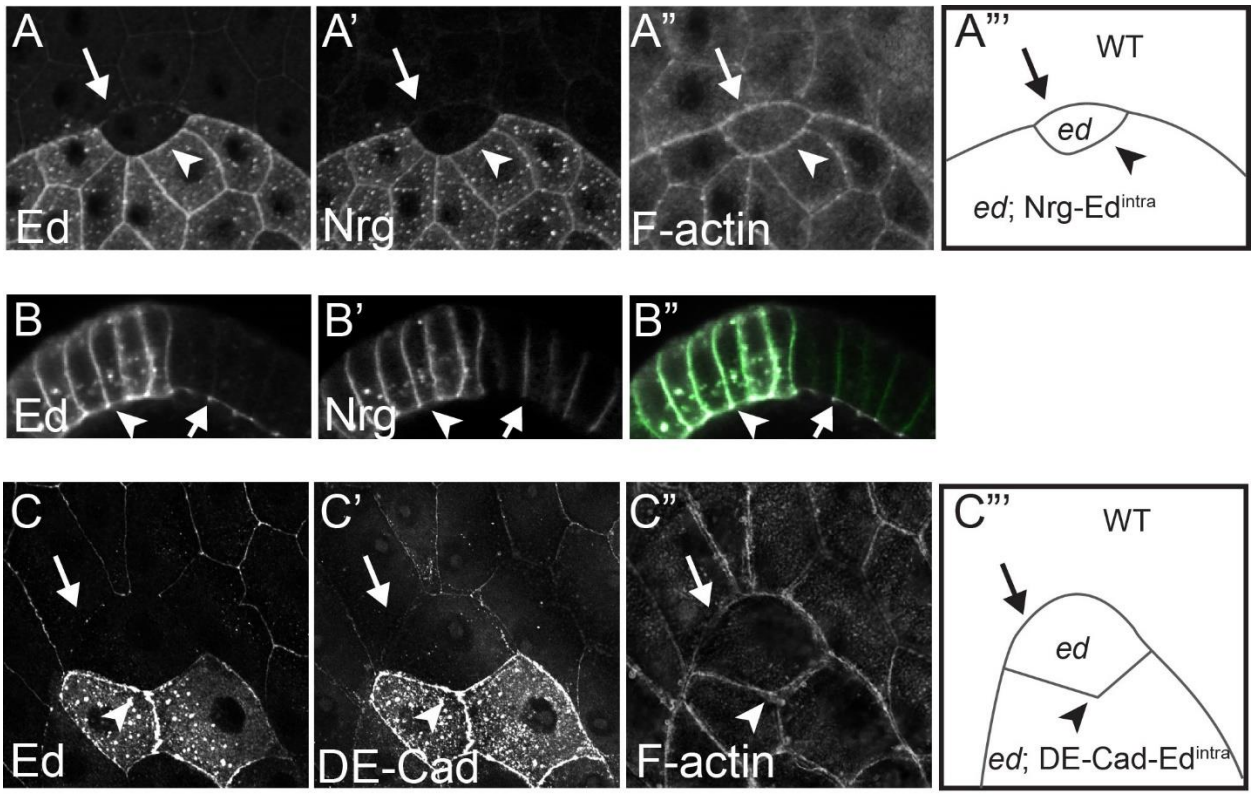
A
Ed
A'
Nrg
A''
F-actin
A'''
WT
ed
ed; Nrg-Ed^intra
B
Ed
B'
Nrg
B''
C
Ed
C'
DE-Cad
C''
F-actin
C'''
WT
ed
ed; DE-Cad-Ed^intra

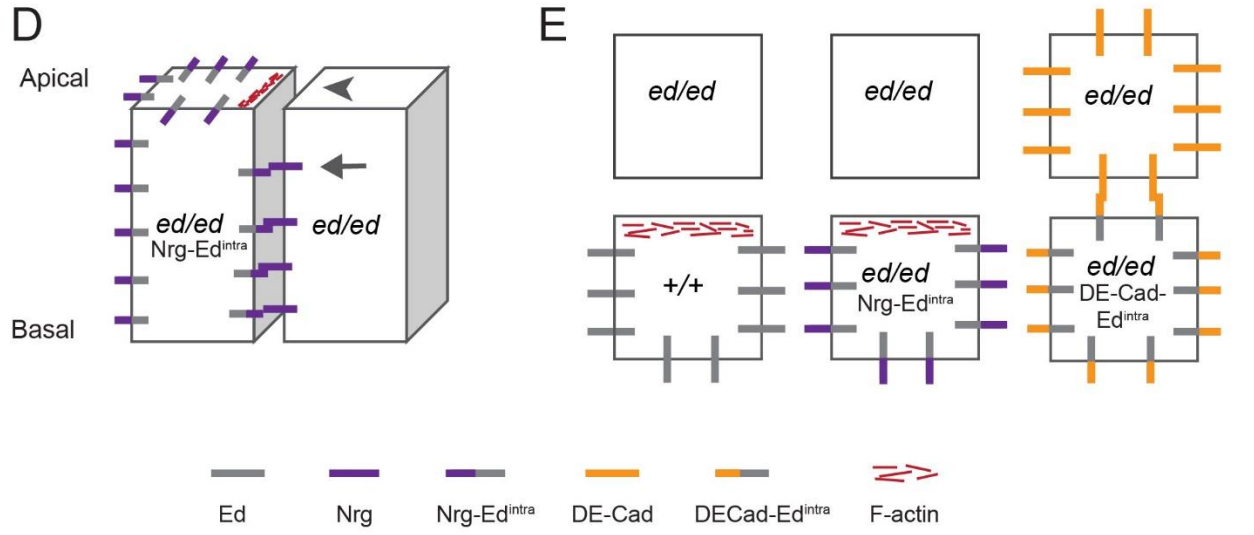
D
Apical
Basal
ed/ed
Nrg-Ed^intra
ed/ed
E
ed/ed
ed/ed
ed/ed
+/+
ed/ed
Nrg-Ed^intra
ed/ed
DE-Cad-
Ed^intra
Ed
Nrg
Nrg-Ed^intra
DE-Cad
DECad-Ed^intra
F-actin

Figure 3.4. Baz localization is disrupted at an Ed/no Ed interface

(A – B”) Mosaic follicular epithelia with an *ed* loss of function clone stained for Baz Arrowheads indicate Baz localization at an Ed/ no Ed border. (B”’) Normalized Baz intensity levels at Ed/ no Ed interfaces where Baz localization appears “continuous”, as shown in B”. Error bars indicate the standard error of the mean. (C) Percentage of individual interfaces exhibiting the indicated category of Baz disruption at Ed/ no Ed individual cell interfaces, where the Ed expressing cell has either endogenous Ed (L.O.F 1, L.O.F 2; *ed* loss-of-function clones) or transgenic Ed (FL, FL-GFP, ΔP, 187, 82-GFP, or ΔC; MARCM clones).

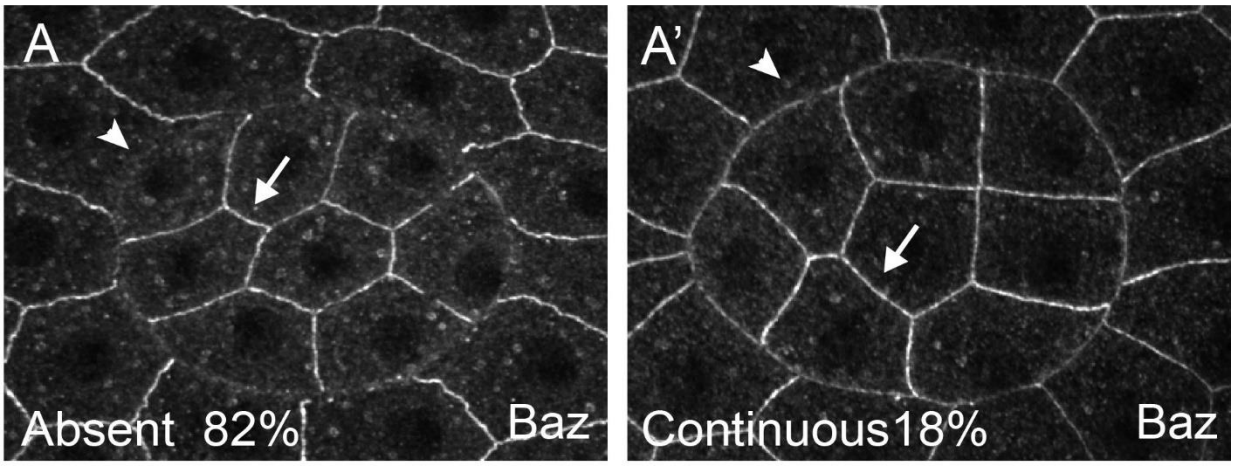
A
Absent 82%
Baz
A'
Continuous18%
Baz

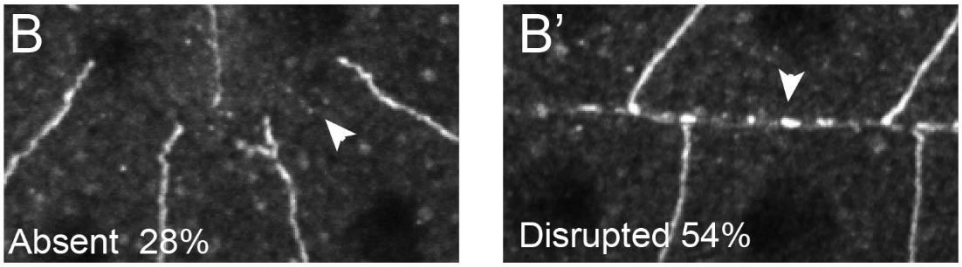
B
Absent 28%
B'
Disrupted 54%

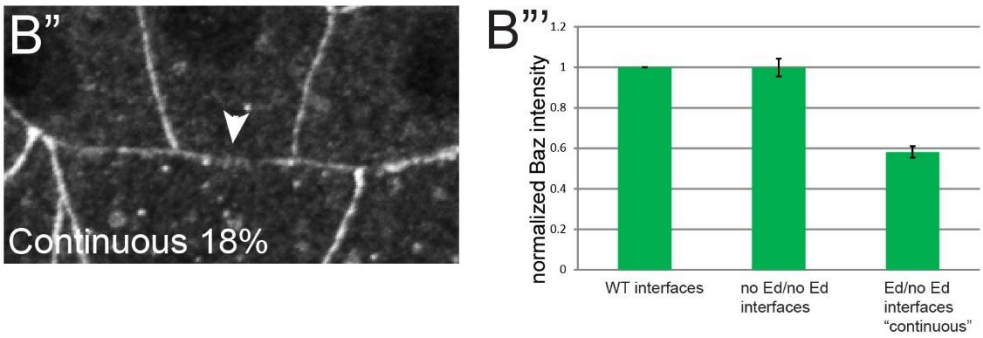
B"
Continuous 18%
B'''
normalized Baz intensity
1.2
1
0.8
0.6
0.4
0.2
0
WT interfaces
no Ed/no Ed interfaces
Ed/no Ed interfaces "continuous"

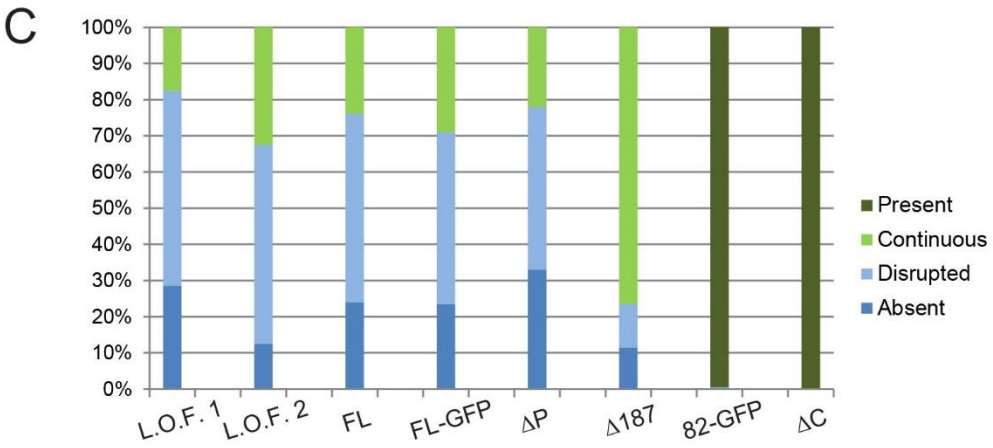
C
100%
90%
80%
70%
60%
50%
40%
30%
20%
10%
0%
L.O.F. 1
L.O.F. 2
FL
FL-GFP
ΔP
Δ187
82-GFP
ΔC
Present
Continuous
Disrupted
Absent

Figure 3.5. Adherens junctions appear disrupted at an Ed/no Ed interface.

(A – A") Mosaic follicular epithelia with an *ed* loss of function clone stained for DE-cad. Arrowheads indicate DE-cad localization at an Ed/ no Ed border. (A"') Normalized DE-cad intensity levels at Ed/ no Ed interfaces where DE-cad localization appears "continuous". Error bars indicate the standard error of the mean.

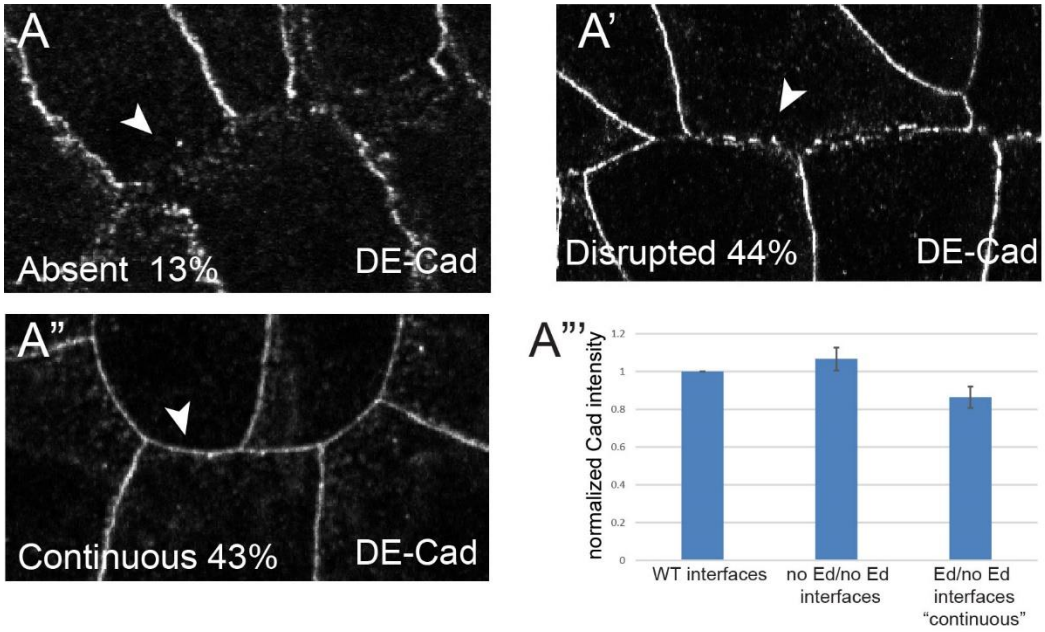
A
Absent 13%
DE-Cad
A'
Disrupted 44%
DE-Cad
A''
Continuous 43%
DE-Cad
A'''
normalized Cad intensity
1.2
1
0.8
0.6
0.4
0.2
0
WT interfaces
no Ed/no Ed interfaces
Ed/no Ed interfaces "continuous"

Figure 3.6. Loss of Baz does not disrupt adherens junctions in the follicular epithelium.

(A – F”’) Mosaic follicular epithelia with a *baz*$^{-/-}$ loss of function clone stained for GFP (A – F), DE-Cad (A’), Ed (A” – F”), Arm (B’, F’), and Baz (C’ – E’). Arrows indicate wild-type cells, and arrowheads indicated *baz*$^{-/-}$ cells. (C’ – E”’) Interfaces between wild-type cells and *baz*$^{-/-}$ cells display a jagged contour (C – C”’, 18/57 clones, arrow), a mixed contour (jagged and round, D – D”’, 17/57 clones, arrow), a round contour (E – E”’, 31/50 clones, arrow). Arrowheads indicate the jagged interfaces between *baz*$^{-/-}$ cells. (F – F”’) Some *baz*$^{-/-}$ cells have a small round contour.

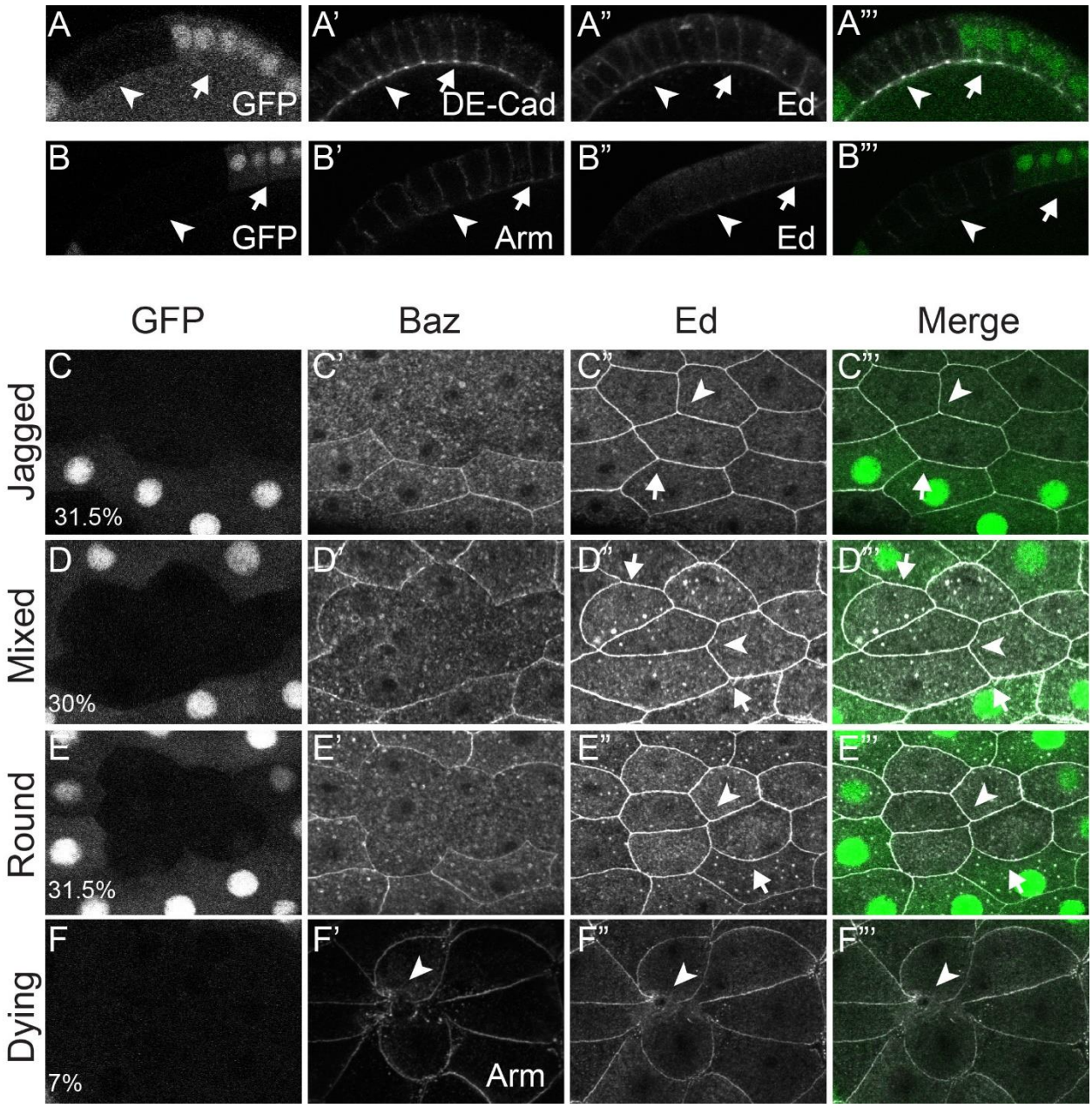
A
GFP
A'
DE-Cad
A"
Ed
A"'
B
GFP
B'
Arm
B"
Ed
B"'
GFP
Baz
Ed
Merge
Jagged
C
31.5%
C'
C"
C"'
Mixed
D
30%
D'
D"
D"'
Round
E
31.5%
E'
E"
E"'
Dying
F
7%
F'
Arm
F"
F"'

Figure 3.7. Loss of Baz abolishes smooth border formation at an Ed/no Ed interface.

Mosaic follicular epithelia with MARCM clones homozygous for ed^{F72} expressing Ed-FL (A – B') and baz^{RNAi} (B – B') stained to visualize Ed (A, B) and Baz (B, B'). Diagrams (right) indicate the different cell genotypes within the mosaic epithelia, and the outlines show the border between cells expressing and lacking Ed. (C) At an Ed/no Ed interface, Baz assumes a polarized distribution in the Ed-expressing cell, which coincides with the formation of a smooth border at that interface (left); however, in the absence of Baz, an Ed/no Ed interface is not smooth (right).

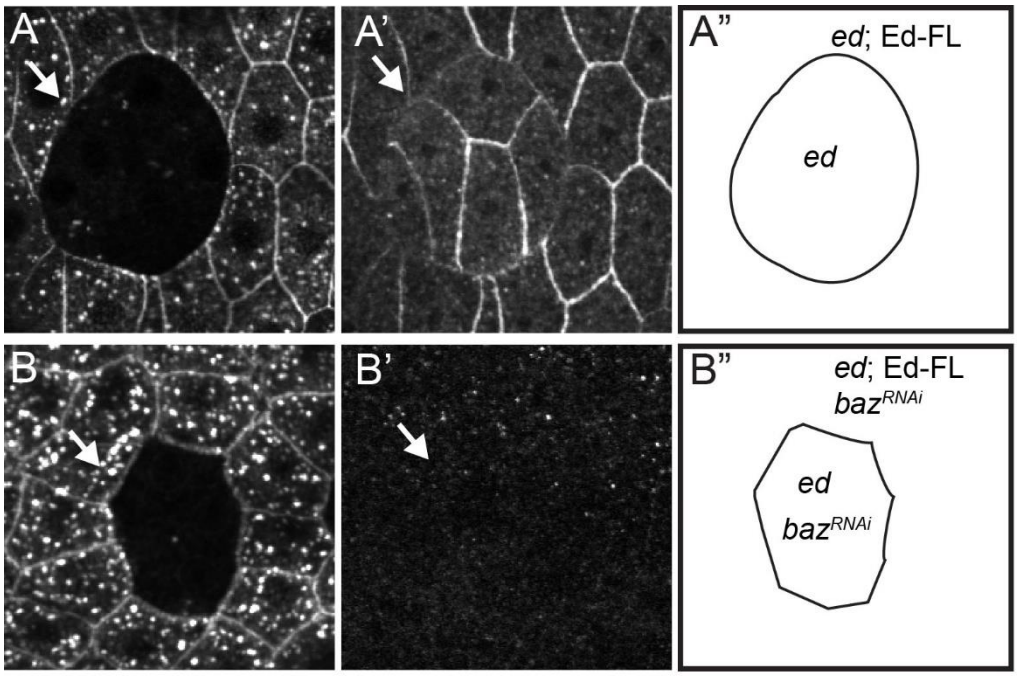
A
A'
A"
ed; Ed-FL
ed
B
B'
B"
ed; Ed-FL
baz^RNAi
ed
baz^RNAi

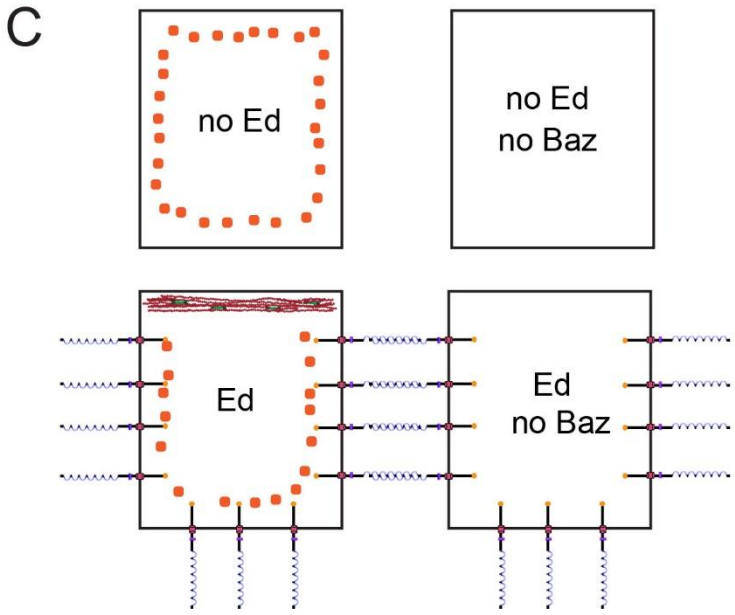
C
no Ed
no Ed
no Baz
Ed
Ed
no Baz

Supplemental Figure 3.1. Structure-function analysis of Ed

Schematic representation of Ed deletion transgenes tested to identify the intracellular domain region of the protein necessary for smooth border formation. The Ed/no Ed border phenotype is divided into two categories, smooth and jagged. Numbers correspond to the clones counted. The dotted lines indicate the border of each functional domain.

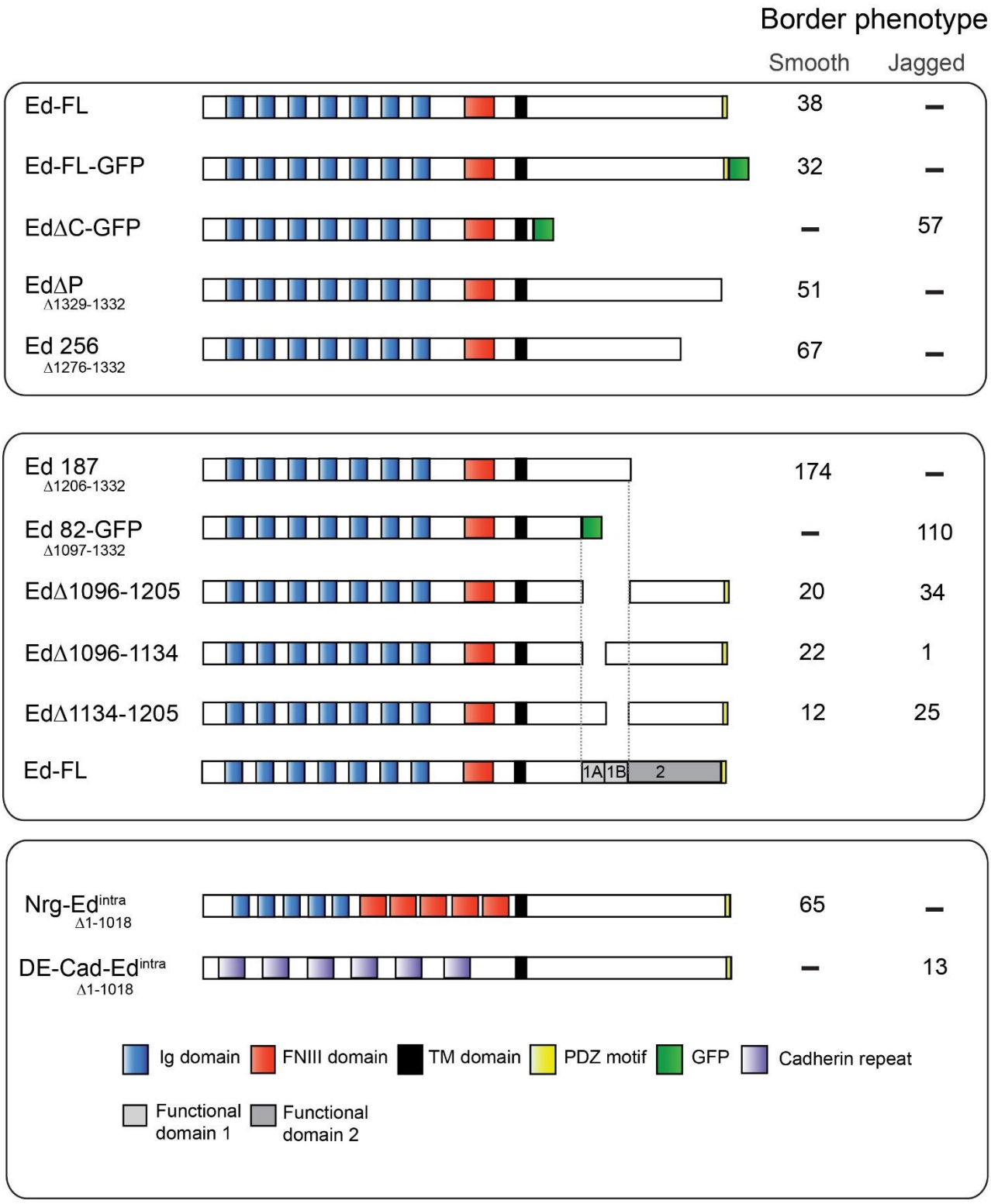
Border phenotype
Smooth
Jagged
Ed-FL
38
–
Ed-FL-GFP
32
–
EdΔC-GFP
–
57
EdΔP
Δ1329-1332
51
–
Ed 256
Δ1276-1332
67
–
Ed 187
Δ1206-1332
174
–
Ed 82-GFP
Δ1097-1332
–
110
EdΔ1096-1205
20
34
EdΔ1096-1134
22
1
EdΔ1134-1205
12
25
Ed-FL
1A
1B
2
Nrg-Ed intra
Δ1-1018
65
–
DE-Cad-Ed intra
Δ1-1018
–
13
Ig domain
FNIII domain
TM domain
PDZ motif
GFP
Cadherin repeat
Functional domain 1
Functional domain 2

Supplemental Figure 3.2. Ed intracellular domain sequence between amino acids 1097-1205 is required for the smooth border phenotype.

Mosaic follicular epithelia with MARCM clones homozygous for ed^{F72} expressing Ed deletion transgenes stained for Ed (A, B, C', D'), F-actin (A', B', C", D"), and GFP (C, D). Diagrams on the right indicate the cell genotypes and the outlines show the border between cells expressing and lacking Ed. Arrowheads indicate the interfaces between *ed* mutant cells and *ed* mutant cells expressing a transgene, which display a smooth contour (A, EdΔP, 51/51 clones, and B, Ed187, 184/184 clones) or jagged contour (C, Ed-82-GFP, 110/110 clones). (D') arrow indicates endogenous Ed that is retained at the wild-type cell interface by interacting homophilically with Ed-81-GFP that is expressed in the neighboring cell but not recognized by the anti-Ed antiserum.

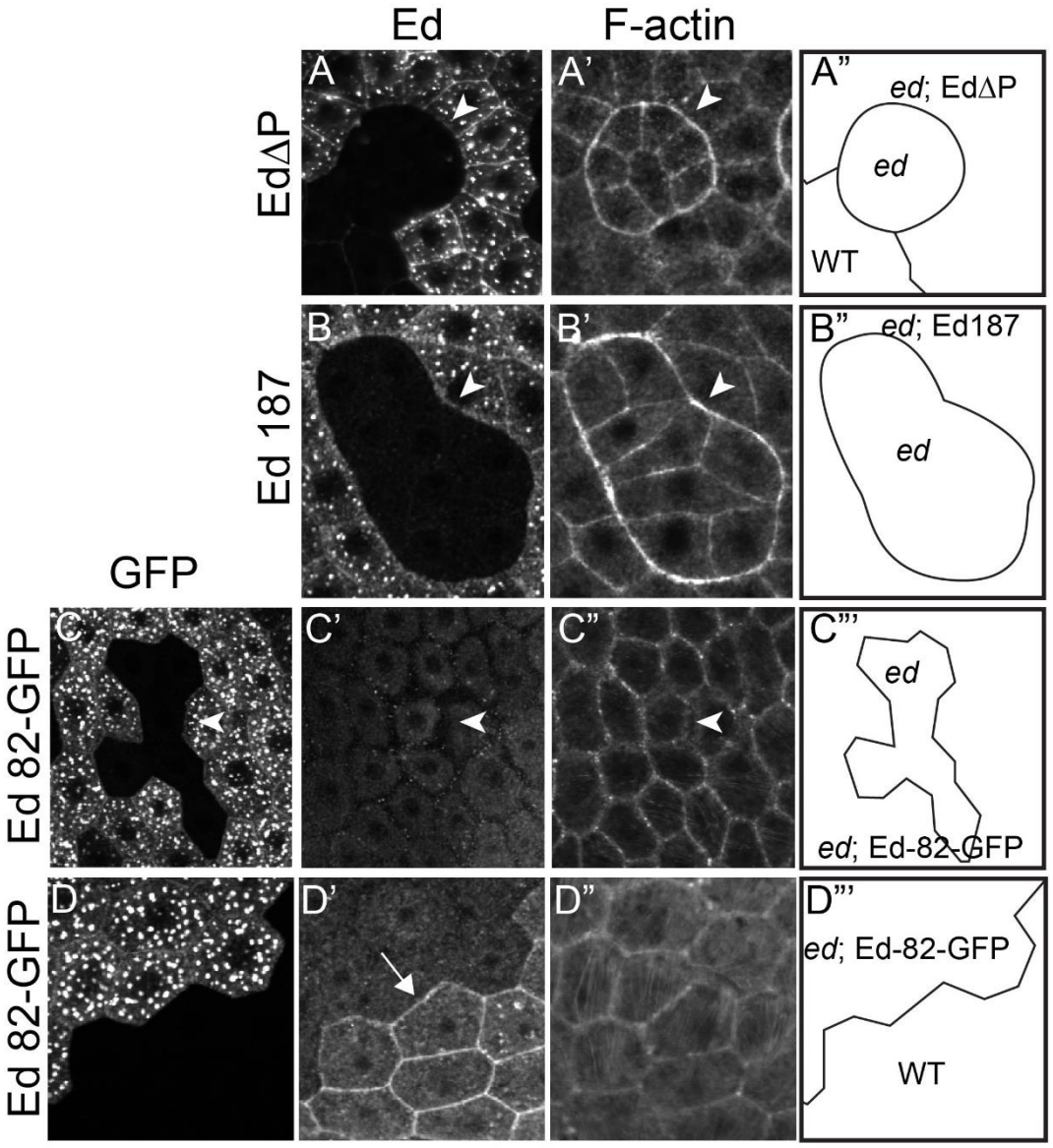
Ed
F-actin
EdΔP
Ed 187
GFP
Ed 82-GFP
Ed 82-GFP
A
A'
A"
ed; EdΔP
ed
WT
B
B'
B"
ed; Ed187
ed
C
C'
C"
C"'
ed
ed; Ed-82-GFP
D
D'
D"
D"'
ed; Ed-82-GFP
WT

Chapter 4: Investigation of the mechanisms that regulate the expression pattern of Ed during development.

4.1 Introduction

In the study of Ed, we have mainly focused on the downstream effects of Ed in regulating the actomyosin network by identifying and investigating candidate effectors and by analyzing the intracellular domain of Ed. The planar polarization of the actomyosin cytoskeleton occurs when Ed becomes differentially expressed between two cells, thus generating smooth Ed/no Ed interfaces (Laplante and Nilson, 2006, 2011; Lin et al., 2007; Wei et al., 2005). During development, endogenous differential Ed-expression borders are generated in the embryo and in the follicular epithelium in the egg chamber (Laplante and Nilson, 2006, 2011; Lin et al., 2007). These endogenous borders between Ed-expressing cells and Ed-lacking cells, are characterized by a smooth interface and the formation of an actomyosin cable (Laplante and Nilson, 2006, 2011; Lin et al., 2007). In both systems, during dorsal closure and appendage formation, these endogenous Ed/no Ed interfaces are functionally relevant because disruption of this differential expression in Ed, either by removing Ed from the Ed-expressing cell or expressing Ed in the Ed-lacking cell, results in aberrant morphogenesis (Laplante and Nilson, 2006, 2011). Despite the importance of the differential Ed-expression borders for proper morphogenesis, the mechanisms that generate this differential Ed expression remain unknown.

Regulation of protein expression within a cell occurs at multiple levels including the synthesis of the protein and its stability. The synthesis of the protein comprises the transcription and the translation of the mRNA and each of these processes are strictly regulated. Transcription of an mRNA is influenced by many factors, including the general chromatin structure of the

DNA, the assembly of the initiation complex, and the presence and activity of activator and repressor proteins (Freeman, 2000). On the other hand, translation of the mRNA is largely regulated at the translation initiation step (Preiss and W. Hentze, 2003; Sonenberg and Dever, 2003). Once the protein is synthesized, the stability of the protein is regulated by post-translational modifications that either increase the stability of the protein or target the protein for degradation (Prabakaran et al., 2012).

Here, we investigate the upstream mechanisms that regulate Ed expression in the ovary and in the embryo. We found that in the embryo regulation of Ed expression occurs at the level of transcription, as the disappearance of Ed protein coincides with the disappearance of *ed* mRNA. On the contrary, in the ovary, the disappearance of the protein occurs even when the mRNA is present, suggesting that the regulation of Ed in this tissue is more complex.

4.2 Materials and Methods

4.2.1 Drosophila genetics

Negatively marked homozygous ed^{F72} loss-of-function clones were generated by Flp/FRT – mediated mitotic recombination as previously described (Laplante and Nilson, 2006). Briefly, *y w* $hsFl^{122}p$; ed^{F72} *FRT 40A/NM FRT 40A* females were incubated at 37°C for 1 hour on three consecutive days beginning at the pupal stage to induce Flippase expression. Females were dissected on day 6-8 after the first heat shock.

For positively marked Flp-out clones, *y w; AyGal4, UAS-GFP/CyO* flies were crossed to *y w* $hsFlp^{122}$;ed^{F72}*FRT 40A, UAS-Ed-FL/SM6 flies* or *y w* $hsFlp^{122}$*; UAS-EdΔC-GFP*. The resulting adult progeny were heat-shocked at 37°C for 2 minutes and dissected 5 days after the heat-shock.

For positively marked MARCM clones, *y w hsFlp; tub-GAL80 FRT 40A; tub-GAL4/TM6B* flies were crossed to *ed*^{F72} *FRT 40A* flies bearing UAS-Ed-82GFP. The resulting progeny were heat-shocked at pupal stage at 37°C for 1 hour on three or four consecutive days. Female progeny were dissected 7-8 days later.

Ectopic expression of Ed in midoogenesis was in induced in flies bearing *vitelline membrane*-GAL4 (Vm-GAL4,(Peters et al., 2013) and UAS-Ed-FL and UAS-GFP or UAS-EdΔC-GFP.

4.2.2 Immunohistochemistry

Ovary dissections and embryo collection and fixation were performed as described in Chapters 2 and 3. Immunostainings of ovaries and embryos was performed as described in Chapter 2.

Antibodies used were anti-Ed (rabbit; 1:1,000, (Laplante and Nilson, 2011), anti-BR-C core hybridoma supernatant 25E9.D7 (1:200, Developmental Studies Hybridoma Bank), TRITC-phalloidin (Sigma-Aldrich; diluted 1:200 in PBST + 1% BSA).

All secondary antibodies (Molecular Probes) were highly cross-adsorbed Alexa Fluor–conjugated anti-IgG, preblocked against fixed embryos, and used at a final concentration of 1:1,000.

4.2.3 RNA in situ hybridization

RNA *in situ* hybridization for embryos and ovaries was performed as previously described with digoxinenin-labeled RNA probes (Lehmann and Tautz, 1994). For the probe, Ed cDNA RE66591 was amplified by PCR using primers containing the T3 and T7 RNA polymerase binding sites. The resulting PCR product was used as a template for *in vitro*

transcription with the DIG RNA labelling kit (Roche Applied Science) to generate full-length antisense and sense mRNA probes.

PCR amplification primers used:

T3 primer:
5’ AATTAACCCTCACTAAAGGGAGAGCCCGAGGAAAATCTCTACGAAG 3’

T7 primer:
5’ TAATACGACTCACTATAGGGAGAGCGAGTTCAAACCATTGTCATCC 3’

4.2.4 Microscopy

Fixed samples were mounted in SlowFade Gold Antifade (Invitrogen). All the images were acquired with a LSM510 Meta confocal microscope (Carl Zeiss, Inc.; McGill Cell Imaging and Analysis Network facility) at room temperature with a Plan Neofluar 40 x 1.3 NA and Plan Apochromat 63 x 1.4 NA differential interference contrast oil objectives. The images were analyzed using the LSM image browser (Carl Zeiss, Inc.) imaging software. Adjustments to brightness and contrast were applied to the whole image.

For whole-mount *in situ* hybridization, samples were embedded in Permount (Fisher Scientific). Images were obtained on a steromicroscope (MZ16-FA; Leica) using a Plan Apochromat 2.0 x objective with a digital camera (Qicam). Images were analyzed using OpenLab software (Improvision).

4.3 Results

4.3.1 Ed expression pattern is temporally and spatially dynamic during oogenesis and embryogenesis.

In the follicular epithelium, Ed displays a dynamic expression pattern (Laplante and Nilson, 2006). Immunostaining of wild-type eggchambers with anti-Ed antibody revealed that Ed

is readily detectable and is present uniformly in all cells of the epithelium during early stages of oogenesis (Figure 4.1 A). Close examination of individual follicle cells showed that Ed localizes at the apical side and, consistent with previous reports, its distribution is similar to that of the adherens junction protein DE-cad (Figure 4.1 A, inset; Laplante and Nilson, 2006; Wei et al., 2005). Ed protein levels decrease during midoogenesis, starting by stage 9 (Figure 4.1 B) and reaching their lowest point at stage 10A and 10B (Figure 4.1 C, D). Ed expression levels increase in later stages of oogenesis in almost all main body follicular cells (Figure 4.1 E, F). Interestingly, at stage 11, the protein levels remain low in two groups of cells which correspond to the roof cells of the dorsal appendage primordia (Figure 4.1 E, arrowhead).

Our observations that Ed levels are low but detectable in midoogenesis differ somewhat from previously published work, which showed that there was no detectable Ed in those stages of oogenesis as well as in the roof cells at stage 11 (Laplante and Nilson, 2006). To confirm that the low level of signal detected in stages 9 and 10 and in the roof cells of the dorsal appendages was specific to Ed and not background from the antibody, we generated mosaic follicular epithelia bearing $ed^{-/-}$ cells. Such mosaic epithelia would allow side-by-side comparison of cells expressing endogenous Ed or lacking Ed. In these mosaic tissues, $ed^{-/-}$ cells lack detectable Ed (Figure 4.1 A-F, arrows), indicating that the immunoreactivity detected by the antibody in the neighbouring wild-type cells is specific. Although the source of the discrepancy between our observations and the previously publish data remains unknown, one possible explanation could be the use of a more sensitive anti-Ed antibody in this study. However, most importantly, despite the difference between our observations (Figure 4.1) and the previously reported ones (Laplante, 2008) on the presence or absence of detectable Ed in midoogenesis, the low level of Ed is present in stages 10A and 10B, is not enough to induce a smooth boundary at an Ed/no Ed

interface (data not shown). This result is consistent with the previous report (Laplante and Nilson, 2006).

The decrease in Ed levels in midoogenesis is accompanied by a change in its subcellular distribution (Figure 4.2). At earlier stages and stage 9, Ed is detected apically in what appears as a continuous line at the level of the adherens junctions (Figure 4.2 A", arrow, data not shown). As the protein levels decrease, Ed expression profile, although mostly a continuous line, appears more punctate (Figure 4.2 B", arrow), culminating in an expression pattern that has the appearance of distinct puncta around the cell when Ed is at its lowest levels of expression (Figure 4.2 C", D", arrow). Ultimately, as the protein levels start to increase, the continuous uniform apical expression of Ed is restored (Figure 4.2 E", arrow).

The dynamic expression pattern of Ed in the follicle cells is reminiscent of the changes in the expression pattern of Ed in the embryo (Laplante and Nilson, 2011; Wei et al., 2005). From embryonic stage 5 to stage 10, Ed is expressed in all tissues (Supplemental Figure 4.1 A, B) (Laplante, 2008). However, Ed expression starts to decrease in the AS by the onset of germband retraction (stage 12) and later on Ed is not detected in this tissue (Supplemental Figure 4.1 C, D, asterisk).

Our data demonstrate that Ed displays a temporally and spatially dynamic expression profile during oogenesis and embryogenesis; yet, there is one noticeable difference in Ed expression pattern between these two developmental stages. In the embryo, Ed is not detected in the AS by late stage 12 and its expression does not return in this tissue for the remainder of the embryogenesis; however, in the ovary, Ed expression is not completely lost but rather greatly downregulated in the follicular epithelium during midoogenesis, and Ed expression levels are restored in most of the main body follicle cells from stage 11 until the end of oogenesis. The

difference in the expression pattern of Ed between the embryo and the ovary suggests that protein expression might be regulated differently in the two tissues. This difference is not surprising as the dynamics of Ed expression are different in the two tissues.

4.3.2 ed mRNA is present in the follicle cells during midoogenesis but absent from the amnioserosa in late embryogenesis.

The dynamic expression pattern of Ed during development is intriguing with regards to the regulation of the protein. We hypothesized that the dynamic expression of Ed is a reflection of changes in the *ed* mRNA expression pattern, suggesting that Ed expression is regulated at the level of transcription. Based on this hypothesis, we would predict that *ed* mRNA, similarly to Ed protein, displays the same temporal and spatial dynamic expression pattern in the embryo and in the ovary. To test this prediction, we performed *in situ* hybridization (ISH) experiments (Lehmann and Tautz, 1994) to visualize *ed* mRNA expression.

In the embryo, *ed* mRNA expression displayed the same pattern as Ed protein (Supplemental Figure 4.1, E – H). The mRNA was expressed in all tissues in early stages of embryogenesis (Supplemental Figure 4.1 E). By stage 12, when Ed levels start to decline, *ed* mRNA was not detected in the AS (Supplemental Figure 4.1 C, G, arrow). Similarly to Ed protein, the mRNA was not detected in the AS during dorsal closure (Supplemental Figure 4.1 D, H, arrow; data not shown). These results showed that the disappearance of Ed protein in the AS coincided with the absence of the mRNA from this tissue, consistent with the hypothesis that loss of Ed from the AS is due to the loss of *ed* mRNA from this tissue. This would support our prediction that Ed expression in the AS is regulated at the transcriptional level.

We hypothesized that, similarly to the embryo, the dynamic changes in the expression levels of Ed in the follicular epithelium result from a negative regulation at the level of transcription. To test our hypothesis, we looked at the *ed* mRNA expression pattern. In the eggchamber, unlike the protein expression, the mRNA is present at very high levels in the germ cells (Figure 4.3 asterisk). Furthermore, *ed* mRNA is expressed during all stages of oogenesis in the follicular cells including the stages where Ed protein levels are strongly reduced (Figure 4.3 A – D arrows, data not shown). This observation is contrary to *ed* mRNA expression pattern in the embryo. In the ovary, the transiently decreased levels of Ed in midoogenesis do not coincide with the disappearance of the mRNA, suggesting that during midoogenesis Ed expression is presumably regulated post-transcriptionally.

4.3.3 Regulation of Ed expression happens at two different levels in the follicular epithelium during midoogenesis

The observation that *ed* mRNA is present even during stages when Ed protein levels are decreased suggested that the decreased levels of Ed are a consequence of a negative post-transcriptional regulation occurring during midoogenesis. However, because non-isotopic ISH is generally not considered a quantitative method (Jonker et al., 1997; Lee et al., 2008; Stylianopoulou et al., 2012), we cannot rule out the possibility that there is a biologically relevant decrease in *ed* mRNA at these stages that would suggest a negative regulation at the level of transcription. Due to this particular limitation of the technique, it is possible that the amount of *ed* mRNA present in stages 9 and 10 is less than in the other stages and also that the mRNA signal detected via ISH could be mRNA persisting from earlier stages. This in turn would suggest an additional contribution of a negative transcriptional regulation.

As a complementary approach, we asked whether driving *ed* expression with a heterologous promoter would lead to detectable Ed in the follicle cells. A model where the downregulation of Ed in midoogenesis results from a negative transcriptional regulation would predict that placing *ed* under a heterologous promoter should bypass any negative regulation at the transcriptional level, and result in the expression of Ed during midoogenesis at similar levels to those in early oogenesis. To test this prediction, we used the Flp-out technique (Golic and Lindquist, 1989; Pignoni and Zipursky, 1997; Struhl and Basler, 1993) to generate positively marked follicle cell clones expressing a transgenic form of Ed that contained the coding sequence of the protein placed under a UAS promoter (Ed-FL) (Laplante and Nilson, 2011), and examined the expression of Ed-FL in such clones.

Generation of follicle cell clones by the Flp-out technique combines the Flp-FRT and the Gal4-UAS systems (Brand and Perrimon, 1993; Golic and Lindquist, 1989; Struhl and Basler, 1993). The central component of this technique is the Flp-out cassette (Figure 4.4A, top left), which consists of a ubiquitously expressed *actin5c* promoter, a transcription termination sequence flanked by two unidirectional FRT sites, as well as a GAL4 transgene. To generate Flp-out clones, a fly containing the Flp-out cassette is crossed with a fly containing the heat-inducible Flp and the UAS-transgene (UAS-Ed). The resulting progeny will contain all the components necessary to make the clones (Figure 4.4, Progeny). Under normal temperature conditions, induction of GAL4 by the *actin* promoter is kept silenced by the intervening transcriptional termination sequence. As a result, GAL4 cannot drive expression of the UAS transgene. However, a transient heat-shock treatment induces the expression of Flp, which in turn mediates recombination at the two FRT sites, resulting in the excision of the transcription termination sequence (Figure 4.4A, orange rectangle). This recombination process juxtaposes the

actin promoter to the GAL4 transgene and leads to the ubiquitous expression of GAL4 in the cells that underwent the Flp-mediated recombination event. GAL4 then induces the expression of the UAS-Ed transgene in these cells (Figure 4.4A, green rectangle, bottom right). Once this genetic alteration has occurred, the ubiquitously expressed GAL4 will induce expression of the UAS-transgene indefinitely.

Analysis of such clones revealed that ectopically induced Ed-FL was expressed in both stages of midoogenesis and at higher levels compared to its endogenous counterpart (Figure 4.5, A', B'). This outcome, where placing Ed under a heterologous promoter restored the expression levels of Ed, suggested that during these midoogenesis stages, the low levels of Ed are a consequence of a negative regulatory mechanism occurring at the level of transcription.

In addition to the high expression levels, we also noticed that most of the ectopic Ed-FL protein localized to the cytoplasm in distinct puncta without a distinct membrane localization, especially during stage 10 (Figure 4.5, A', B', arrow), but in later stages, Ed-FL displayed a membrane localization (Figure 4.5, C' arrow). These observations led us to hypothesize that there might be a secondary mechanism occurring at the post-transcriptional level, which is needed for proper localization of Ed at these midoogenesis stages. Given that Ed is transmembrane protein, we hypothesized that it utilizes its intracellular domain to direct its proper localization at the membrane. Based on this hypothesis, we predicted that a negative post-transcriptional regulatory mechanism in midoogenesis would act on the intracellular domain of Ed. To test our prediction, we generated Flp-out clones that induced the expression of a transgenic form of Ed lacking most of the intracellular domain (EdΔC) and examined its expression in the follicular epithelium. To detect its expression, transgenic EdΔC bears a C-terminal GFP epitope tag (Laplante and Nilson, 2011).

Similar to Ed-FL, transgenic EdΔC was expressed in the follicle cells in midoogenesis; however, unlike Ed-FL, EdΔC was mostly localized at the membrane (Figure 4.5, D', E', F'), suggesting that the intracellular domain of Ed imparts information that is necessary for the proper localization of the protein, and the removal of the cytoplasmic domain alleviates the inhibitory signal that prevents Ed-FL from proper localization at the membrane. Therefore, since proper localization of Ed in midoogenesis appears to depend on information present in the intracellular domain of Ed, it supports the presence of a post-transcriptional regulatory mechanism.

Collectively, our Flp-out clonal data suggest that the low Ed expression levels in midoogenesis are orchestrated by two negative regulation mechanisms: one mechanism operating at the transcriptional level, which prevents the synthesis of *ed* mRNA, and the other mechanism operating at the post-transcriptional level, which prevents any Ed protein from localizing at the membrane.

However, we noted that one particularly important limitation of the Flp-out technique. As Flp-out clones could occur at any stage during oogenesis (Figure 4.4, B), this technique does not allow for a precise temporal control of transgene expression. Once the Flp-out cassette has been removed, GAL4 continuously drives the expression of the transgene. Therefore the presence of Ed-FL at high levels in the follicle cells at stage 9 and 10 might not reflect the synthesis of Ed at these stages, but rather the persistence of transgenic Ed synthesized at high levels in earlier stages. As the induction of Flp-out clones is not temporally restricted, this technique might not allow us to address whether in midoogenesis transcription of *ed* mRNA is negatively regulated.

4.3.4 Expression of Ed in midoogenesis is regulated post-trascriptionally and requires its intracellular domain.

To further investigate the hypothesis that the low levels of Ed expression in midoogenesis are a consequence of a negative regulation occurring at the transcriptional level, we wanted to express an Ed transgene exclusively at stage 9 and stage 10 of oogenesis, but not during the earlier stages. It was imperative to avoid any transgenic contribution from earlier stages of oogenesis, as to not confound the interpretation of the data.

One possible way to express transgenic Ed in stages 9 and 10 of ooggenesis is to induce its expression via a GAL4 driver that displays a temporally restricted expression pattern. *Vitelline membrane* 26Aa-GAL4 (Vm-GAL4) was previously described to display a temporally dynamic expression pattern in the follicular epithelium (Peters et al., 2013). To define the timing of expression of this particular GAL4 driver more precisely, we induced the expression of EdΔC transgene under the control of Vm-GAL4 in the follicle cells. We chose EdΔC because this transgene is not recognized by the anti-Ed antibody but contains a GFP tag and therefore it was possible to distinguish between follicle cells that express transgenic Ed and those that express endogenous Ed only.

Analysis of follicular epithelia expressing EdΔC under the control of Vm-GAL4 driver revealed that this particular GAL4 driver displays not only a temporally restricted but also spatially dynamic expression pattern in the follicular epithelium. At early stages of oogenesis, endogenous Ed was present in the follicle cells, while no GFP signal from EdΔC was detected in these cells (Figure 4.6 A, A'), suggesting that Vm-GAL4 was not inducing transgene expression at these early stages. At early stage 9, the GFP signal was noticeable in a few cells and by late stage 9 and onward the number of GFP positive follicle cells increased (Figure 4.6 B' – F'), indicating that Vm-GAL4 driver starts to induce expression of the transgene in midoogenesis. Furthermore, we noticed that EdΔC was not expressed in all follicle cells (Figure 4.6 B' – F')

and thus generated a mosaic follicular epithelium where some cells expressed the transgene and some did not. Such a stochastic expression of EdΔC suggested that Vm-GAL4 expression was also not uniform in the follicular epithelium. Therefore, this spatially dynamic expression pattern of the driver would allow side-by-side comparison of cells that express or not the transgene.

We took advantage of the temporally and spatially dynamic expression pattern of Vm-GAL4 driver (Peters et al., 2013) to induce expression of Ed-FL in the follicular epithelium. Given the mosaic expression of the GAL4 driver, we incorporated a UAS-GFP transgene as a cell marker to distinguish between cells expressing or lacking Ed-FL expression.

At stages 9 and 10, Vm-GAL4 driven Ed-FL was expressed and localized to the apical side of the follicle cells (Figure 4.7 A – C, arrowhead). The expression levels of Ed-FL in each of these stages were comparable to those of endogenous Ed in the neighboring cell (Figure 4.7 A – C, arrowhead, arrow). Interestingly, similar to endogenous Ed, the levels of Ed-FL appeared to decrease from stage 9 to stage 10B (Figure 4.7 A – C, arrow, arrowhead). These observations are not consistent with a model which predicts that the reduced levels of Ed in midoogenesis result from only a negative transcriptional regulation, because Ed-FL was not expressed at high levels in stage 9 and 10.

An alternative hypothesis is that the levels of Ed in midoogenesis are regulated at the post-transcriptional level, which is consistent with the observation that *ed* mRNA is present in midoogenesis (Figure 4.3). To test this hypothesis, we looked at the expression and localization of EdΔC induced under the control of Vm-GAL4 driver. At stage 10, EdΔC was expressed in the follicle cells (Figure 4.7, D', E', arrowhead). EdΔC was localized apically and unlike endogenous Ed or transgenic Ed-FL, it was localized basolaterally as well, suggesting that the intracellular domain of Ed is necessary for proper localization of the protein. Furthermore, we

noticed no apparent decrease in the expression levels of EdΔC from stage 10A to stage 10B. This observation indicates that the decrease in Ed-FL expression levels from stage 9 to stage 10B cannot be accounted for solely by the strength of the GAL4 driver.

Taken together, all these observations of the expression of Ed-FL and EdΔC during midoogenesis are consistent with a model in which the expression levels of Ed in midoogenesis are regulated at the post-transcriptional level, which require the intracellular domain of Ed.

4.4 Discussion

While the effects of the differential expression of Ed on the actomyosin cytoskeleton are well described (Chang et al., 2011; Laplante and Nilson, 2006, 2011; Lin et al., 2007; Wei et al., 2005), the mechanisms that regulate Ed expression during development remain unknown. Here, we have presented preliminary findings in the regulation of Ed expression in two developmental stages. In the embryo, regulation of Ed expression appears to be regulated at the transcriptional level. More work on the regulation of Ed expression during embryogenesis is presented elsewhere (Rakic, 2013). On the other hand, in the ovary, our data indicate that regulation of Ed expression appears to be more complex.

4.4.1 Downregulation of Ed expression in midoogenesis is orchestrated by a change in the protein turnover

The low expression levels of Ed in midoogenesis imply that there is a change in the rate of either the synthesis of Ed, the transcription or translation of the mRNA, or the removal of the protein. Our preliminary data on protein synthesis, the *ed* mRNA expression profile and ectopic expression of transgenic Ed under a heterologous promoter, suggest that Ed does get synthesized in the follicle cells in midoogenesis. Also, our preliminary results of the apparently low levels of

the ectopically expressed Ed-FL suggest that Ed is degraded in midoogenesis, while the seemingly unchanged expression levels of EdΔC imply a requirement of the Ed intracellular domain for this process.

The simplest interpretation of our observations of the *ed* mRNA expression pattern in midoogenesis is that negative regulation of transcription might not be the process limiting Ed expression. However, it is unclear whether the detected mRNA is *ed* mRNA persisting from earlier stages or whether it is newly transcribed mRNA. A model where this detected mRNA derives solely from *ed* mRNA persisting from earlier stages would predict that the mRNA levels would be lower in midoogenesis than at earlier stages. As non-isotopic ISH is not sensitive enough to allow for quantitative analysis (Jonker et al., 1997), another modified version of non-isotopic ISH technique that permit quantitative analysis (Lee et al., 2008; Stylianopoulou et al., 2012) could be used to compare the relative abundance of *ed* mRNA. Alternatively, qtRT-PCR could be used to measure the amount of *ed* mRNA in stage 9 and stage 10 and compare it to the amount of *ed* mRNA in stage 7, for early oogenesis, and stage 12, for late oogenesis. However, such a comparison of *ed* mRNA levels would require precise separation of eggchambers of the same stage, which would not be straightforward to achieve. Furthermore, we predict that any subtle change in the *ed* mRNA levels in the follicle cells would be obscured by the high levels of *ed* mRNA present in the germ cells.

The observation that ectopic expression of a transgenic version of Ed resulted in the production of the protein in midoogenesis suggests that protein synthesis was not impaired. However, the transgenic version of Ed derives from a cDNA and does not contain introns present in the endogenous *ed* gene. Therefore, the pre-mRNA processing of the transgenic form of Ed would not be the same as that of endogenous Ed, specifically because there is no intron-splicing

event. Pre-mRNA splicing is an important step in the processing of the mRNA because not only it removes introns but also deposits the exon junction complex (EJC) at the splice junctions, which remain with the mRNA until it is translated (Kim et al., 2001; Le Hir and Andersen, 2008; Lejeune et al., 2002). The observations that EJC does not bind intronless mRNAs and it can sometimes negatively affect the translation efficiency of the mRNA (Dreyfuss et al., 2002; Isken et al., 2008) suggest that transgenic *ed* mRNA might not be undergoing the same translational regulation as the endogenous *ed* mRNA.

To determine whether translation of endogenous *ed* mRNA occurs in midoogenesis, one approach would be to remove all Ed present in the cell and analyze whether *de novo* protein synthesis occurs in that same cell. Although commonly used to visualize the dynamics of a protein within a given cell, the fluorescence recovery after photobleaching (FRAP) technique has been successfully employed to determine protein synthesis *in vivo*, even for low abundance and membrane-localized proteins (Kourtis and Tavernarakis, 2009; Reits and Neefjes, 2001). To test whether Ed protein synthesis occurs in midoogenesis using FRAP, follicle cells should exclusively express a fluorescently tagged version of Ed. A YFP-tagged version of endogenous Ed under the control of the endogenous promoter is expressed in the follicle cells (A.Noçka, unpublished observation). In cultured eggchambers of either stage 9 or stage 10, the fluorescence of YFP within an entire follicle cell would be illuminated using a strong excitation laser to photobleach any existing Ed protein from the cell. Recovery of YFP-fluorescence within that same follicle cell would be indicative of newly synthesized Ed-YFP protein. Based on our observations that some endogenous Ed is still present in midoogenesis and that expression of transgenic Ed under the control of a heterologous promoter does occur, we predict that YFP-fluorescence recovery would occur in the photobleached cells, suggesting that translation of Ed

is not negatively regulated in midoogenesis. However, it is important to note that even though the FRAP data would allow us to determine if *de novo* protein synthesis occurs, it would be impossible to discern whether the new protein results from the translation of the already existing mRNA of newly transcribed mRNA, or whether the rate of translation is slower at these stages.

Although the FRAP experiment is conceptually straightforward, the technical aspect is rather complicated. Culturing midoogenesis stage egg chambers for live-imaging analysis is difficult, especially for processes that require a long amount of time, because the sample degenerates quickly and morphological movements that take place *in vivo* become arrested; however, studies in the migration of the border cell cluster have made possible culturing of stage 9 egg chambers for up to six hours (Prasad et al., 2007). Therefore the FRAP analysis on Ed protein synthesis is confined within the six hour time frame. In addition, it remains to be tested whether this protocol works for stage 10 egg chambers, which lasts about ten hours (Spradling, 1993). Another important component that the FRAP analysis relies on is the expression of the Ed-YFP fusion protein. Expression of Ed-YFP resembles that of endogenous Ed in early and late stage egg chambers (A. Noçka and Rahul Rote, unpublished observations); however, expression of this fusion protein in midoogenesis to date is unknown, but could be determined simply by looking at fixed egg chambers expressing Ed-YFP. Because endogenous Ed expression was detected by immunostaining, we predict that Ed-YFP expression will also be detected in the follicle cells in midoogenesis.

Our observations of the low levels of expression of Ed-FL under the control of a UAS-promoter driven by Vm-GAL4 are consistent with a model where the low detectable levels of endogenous Ed in midoogenesis result from a post-trancriptional regulation that affects the removal of the protein. This model is further supported by the observations that ectopic

expression of transgenic EdΔC under the same conditions resulted in high levels of expression that did not appear to decrease from stage 9 to stage 10 of oogenesis. Because Ed is a transmembrane protein, it is not surprising that its removal from the membrane depends on its intracellular domain. Indeed, in our functional analysis of transgenic Ed deletion constructs (Chapter 3, Supplemental Figure 3.1), we noticed that one transgene, EdΔ77, displayed high membrane accumulation (data not shown), suggesting that this form of Ed was more stable and was not being removed from the membrane. Consistent with this interpretation, ectopically expressed EdΔ77 under the control of Vm-GAL4 driver localized to the membrane in a pattern similar to that of EdΔC (data not shown).

A closer examination of the amino acid sequence absent from EdΔ77 revealed the presence of a conserved motif, a PY motif, which serves as a recognition site for C2-WW-HECT-type E3 ubiquitin ligases (Bernassola et al., 2008; Huibregtse et al., 1995; Rotin and Kumar, 2009), raising the hypothesis that the levels of Ed in midoogenesis are regulated via a post-translational ubiquitinatin-tag modification of the protein. One approach to test this hypothesis would be to generate mosaic follicular cell clones mutant for a candidate HECT E3-ligase and examine whether the levels of Ed change in the mutant cells compared to the wild-type neighbors. As the hepatocyte growth factor-regulated tyrosine kinase substrate (Hrs) is a known HECT E3 ligase expressed in the follicular epithelium (Jékely and Rørth, 2003; Lloyd et al., 2002), we tested whether it also regulated the levels of Ed in midoogenesis by generating *hrs* $^{-/-}$ mutant follicle cell clones, but found that Ed levels did not appear to be different in the *hrs* $^{-/-}$ mutant cells compared to the wild-type neighboring cells (data not shown), consistent with the role of Hrs regulating the levels of signaling receptors but not adhesion molecules (Jékely and Rørth, 2003). An alternative approach to test our hypothesis would be to generate a transgenic

form of Ed lacking the PPXP conserved motif and induce and examine its expression in midoogenesis. Consistent with our hypothesis, we would predict that the Ed transgene lacking the PY-motif would display a similar localization pattern as EdΔC and EdΔ77. As ubiquitylation occurs on lysine residues and the intracellular domain of Ed contains ten lysine residues, six of which are located within the region deleted in EdΔ77, a simple prediction would be that removing either one, if only one is required, or all of the lysine residue should abolish the reduced levels of Ed seen in the follicle cells in midoogenesis. An indirect approach to test this prediction would be to generate transgenic forms of Ed where either one or all of the lysine residues are substituted to alanine residues and assess their induced expression in midoogenesis. The observation that a transgenic form of Ed lacking one or more lysine residues is expressed at higher levels than endogenous Ed and similar to EdΔ77 or EdΔC would support the hypothesis that the low levels of Ed are mediated by ubiquitylation.

Although ubiquitylation often is associated with proteasome-mediated protein degradation, ubiquitin-tagging also functions as a signal for entry into the endocytic pathway (Bernassola et al., 2008; Hicke, 2001; Mukhopadhyay and Riezman, 2007; Pickart, 2001). It is possible that ubiquitylation of the intracellular domain of Ed triggers the recycling of Ed out of the plasma membrane. Our observations of the localization pattern of Ed in the follicle cells at early stages of oogenesis show that Ed is not only localized at the membrane but also in distinct foci in the cytoplasm of these cells (data not shown), which could possibly represent Ed within endocytic vesicles. It remains to be determined whether the rate of the removal of Ed from the membrane increases just prior to the midoogenesis stages or if it remains the same as in the earlier stages. It is easy to speculate that the rate of endocytosis of Ed increases prior to

midoogenesis and coincides with the follicle cells undergoing a Notch-dependent switch from mitotically dividing to endoreplicating cells (Deng et al., 2001; Shcherbata et al., 2004).

Taken together our data suggest that the regulation of Ed expression in midoogenesis that results in the low levels of Ed appears to be a complex process. Further investigation is needed to elucidate the possible mechanisms that downregulate the levels of Ed in the follicle cells.

4.4.2 Downregulation of Ed in the ovary coincides with morphological changes occurring in midoogenesis.

What stands out from comparing the expression pattern of Ed at stage 8 with stage 11 of oogenesis is that Ed protein levels appear to be downregulated in two patches corresponding to the floor cells of the dorsal appendages. Based on this comparison, a simple prediction of the expression pattern of Ed would be that Ed is present at high levels in all follicle cells throughout midoogenesis and that Ed becomes downregulated in the floor cells at the onset of the dorsal appendage morphogenesis. However, our observations on the expression profile of Ed in oogenesis are not consistent with this prediction. Instead, we observed that in midoogenesis Ed expression is barely detectable in the follicle cells and homozygous mutant $ed^{-/-}$ clones do not display the characteristic smooth boundary phenotype in these cells (Laplante and Nilson, 2006).

The expression pattern of Ed in oogenesis can clearly be divided into three distinct phases, where Ed is highly expressed in early oogenesis, Ed expression is downregulated in midoogenesis, but its expression levels increase in late oogenesis. It is not clear why Ed expression undergoes this transition phase in midoogenesis where the levels of Ed are greatly downregulated. Presumably, such a dynamic expression might be reflective of the global changes occurring in the eggchamber at that time in development. Midoogenesis is characterized

by the multiple morphogenetic changes occurring in the follicle cells described as posterior follicle cell migration, squamous cell flattening and the formation of the stretch cells, columnarization of the main body follicle cells and border cell migration (Horne-Badovinac and Bilder, 2005; Kolahi et al., 2009; Spradling, 1993). Given that Ed is generally described as an adherens junction cell adhesion molecule (CAM) (Chang et al., 2011), it is possible that the downregulation of Ed in midoogenesis modulates the connections between cells, for example, to allow for the cell shape changes occurring during this time period. However, the adherens junctions (AJs), visualized by DE-cad immunostaining, do not appear to be lost or downregulated in main body follicle cells during these stages (Niewiadomska et al., 1999), although some Notch-dependent AJs disassembly does occur during the cuboidal-to-squamous cell shape change during the formation of the stretch cells (Grammont, 2007).

The characterization of Ed as a CAM might not be fully correct as Ed does not seem to function in adhesion *per se* because cells lacking Ed do not lose contact with their neighbors and are not extruded from the epithelium (Laplante and Nilson, 2006; Wei et al., 2005). If Ed were functioning as an adhesion molecule to regulate junctional remodeling to achieve the cell shape changes, then a simple prediction would be that overexpression of Ed in stages 9 and 10 of midoogenesis should negatively impact the cell shape changes. However, our data show that ectopic expression of EdΔC or EdΔ77 (Figure 4.5, data not shown), which display strong membrane localization, do not appear to influence cell shape changes, suggesting that Ed might not function as an adhesion protein. Nonetheless, we cannot rule out the possibility that the intracellular domain sequence lacking in these two Ed transgenes is necessary for the function of Ed in adhesion as pertains to cell shape changes.

An alternative possibility is that Ed could be functioning as a cell surface signaling receptor in midoogenesis, for example Ed utilizes its extracellular domain to sense the extracellular environment and convey the information to the inside of the cell via its intracellular domain. As such, the downregulation of Ed allows the follicle cells to enter into a new developmental phase. For example, Ed function could be similar to that of the septate junction protein, Fascilin III (Fas III), which becomes downregulated in the main body follicle cells in midoogenesis (Ruohola et al., 1991), and this Fringe-dependent downregulation of Fas III is considered a marker for cell differentiation, rather than loss of adhesion (Grammont and Irvine, 2001). However, follicle cells overexpressing either Ed-FL or EdΔC under the control of *actin*-GAL4 or *Vm*-GAL4 did not appear different in shape or size than their neighboring wild-type cells, suggesting that Ed is likely not acting as a permissive factor in these cells.

Lastly, it is possible that the downregulation of Ed expression is a consequence of the multiple changes occurring in midoogenesis rather than a cause for a specific morphological or signaling event. It remains to be elucidated the reason why Ed becomes downregulated in midoogenesis. It seems as if the follicular epithelium is getting ready for a new developmental phase and erasing the pattern set at earlier stages in preparation for the patterning event that will take place during subsequent stages.

Figure 4.1. Ed displays a temporally dynamic expression pattern during oogenesis.

(A – F) Mosaic follicular epithelia with ed^{F72} loss of function clones stained for Ed in cross-sectional view (A – D) and top view (E, F). The dotted lines indicate the border between WT and *ed* mutant cells, and the arrows point to the *ed* mutant cells. (A) Inset represents a close-up view of Ed apical localization indicated by the arrowhead. (E) Arrowheads indicate Ed apical localization the roof cells of the dorsal appendages.

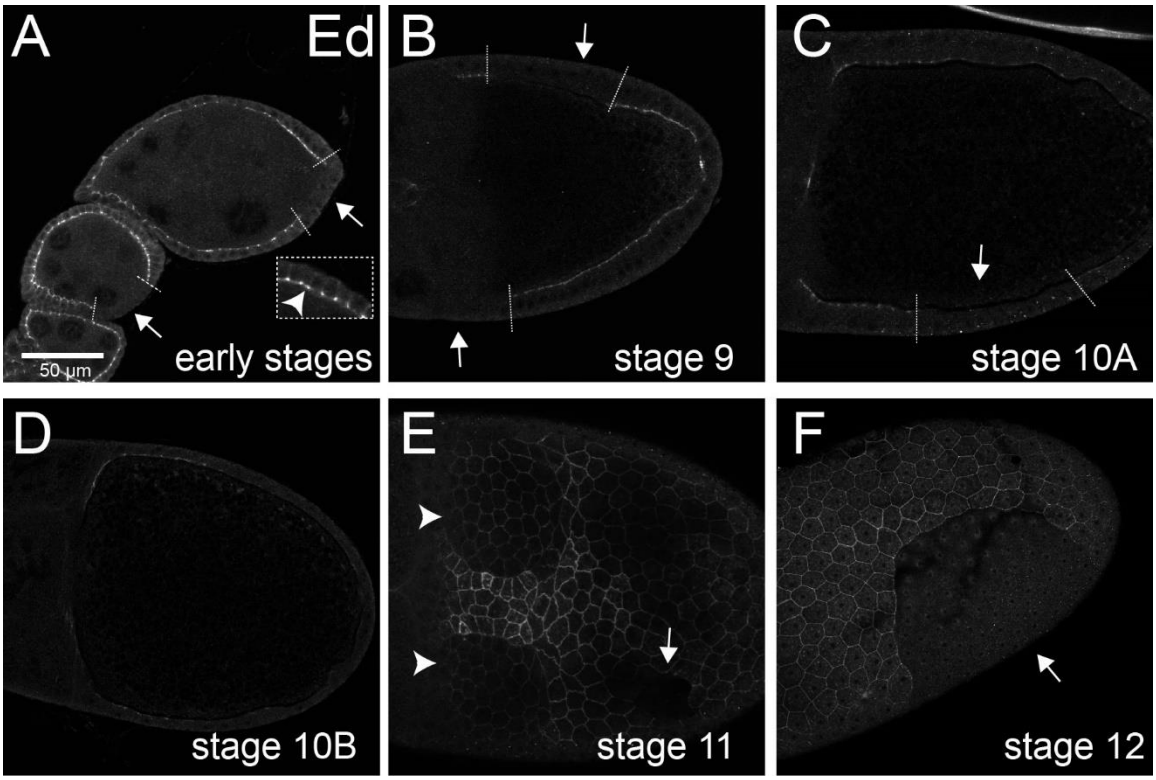
A
Ed
50 µm
early stages
B
stage 9
C
stage 10A
D
stage 10B
E
stage 11
F
stage 12

Figure 4.2. The downregulated levels of Ed in midoogenesis are accompanied by a change in the distribution of the protein.

(A – E”) Wild-type egg chambers stained for Broad (A – E) and Ed (A’ – E”). Broad staining is used as a marker to distinguish the different stages of oogenesis. (A” – E”) A close-up view of Ed localization in the follicular epithelium. Arrows indicate Ed distribution.

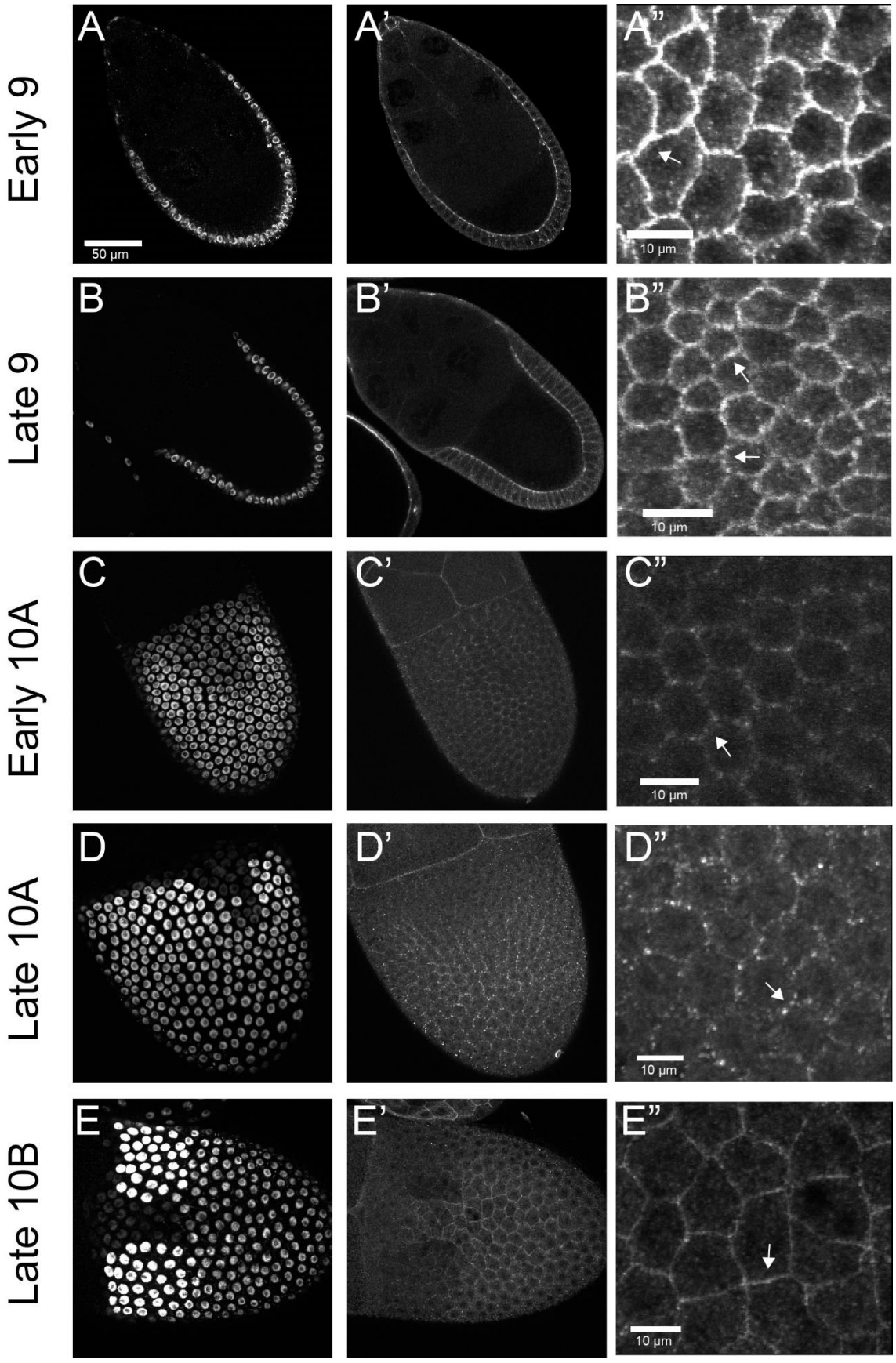
Early 9
Late 9
Early 10A
Late 10A
Late 10B
A
A'
A''
B
B'
B''
C
C'
C''
D
D'
D''
E
E'
E''
50 µm
10 µm

Figure 4.3. *ed* mRNA is expressed in the germline and the follicular epithelium during midoogenesis.

(A – D) Whole-mount *in situ* hybridization showing the spatial distribution of *ed* mRNA in wild-type egg chambers. Arrows indicate *ed* mRNA signal in the follicular cells.

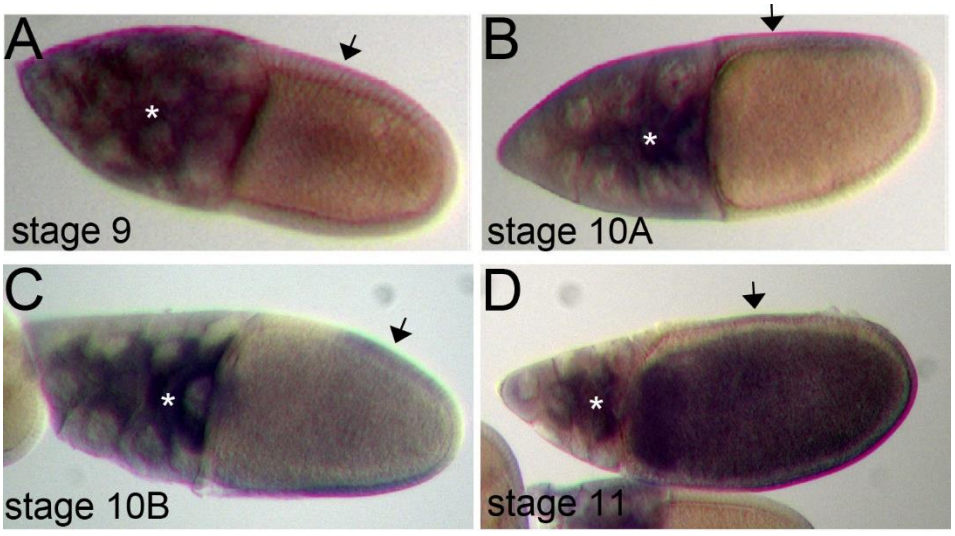
A
stage 9
B
stage 10A
C
stage 10B
D
stage 11

Figure 4.4. Schematic representation of the Flp-out system inducing expression of transgenic Ed in the follicular epithelium.

The Flp-out system relies on the excision of Flp-out cassette, which alleviates the inhibition of GAL4-induced transgene expression. (A) In the experiments described here, the parent flies contain either the Flp-out cassette (left) or the UAS-Ed transgene and a flippase transgene (right) and their progeny contains both components (Progeny). A transient heat-shock pulse will induce Flipasse activity, which in turn would mediate recombination between the two FRT sites present in the Flp-out cassette, resulting in the removal of the transcription termination signal (orange rectangle, right) and thus GAL4 would induce expression of the transgene (Flp-mediated recombination, green rectangle, bottom right). If no Flp-mediated recombination occurred, then GAL4 would not be expressed to induce expression of transgenic Ed (No recombination, green rectangle, bottom left). (B) Schematic representation of an ovariole containing pre-mitotic (green) or post-mitotic (purple) Flp-out clones.

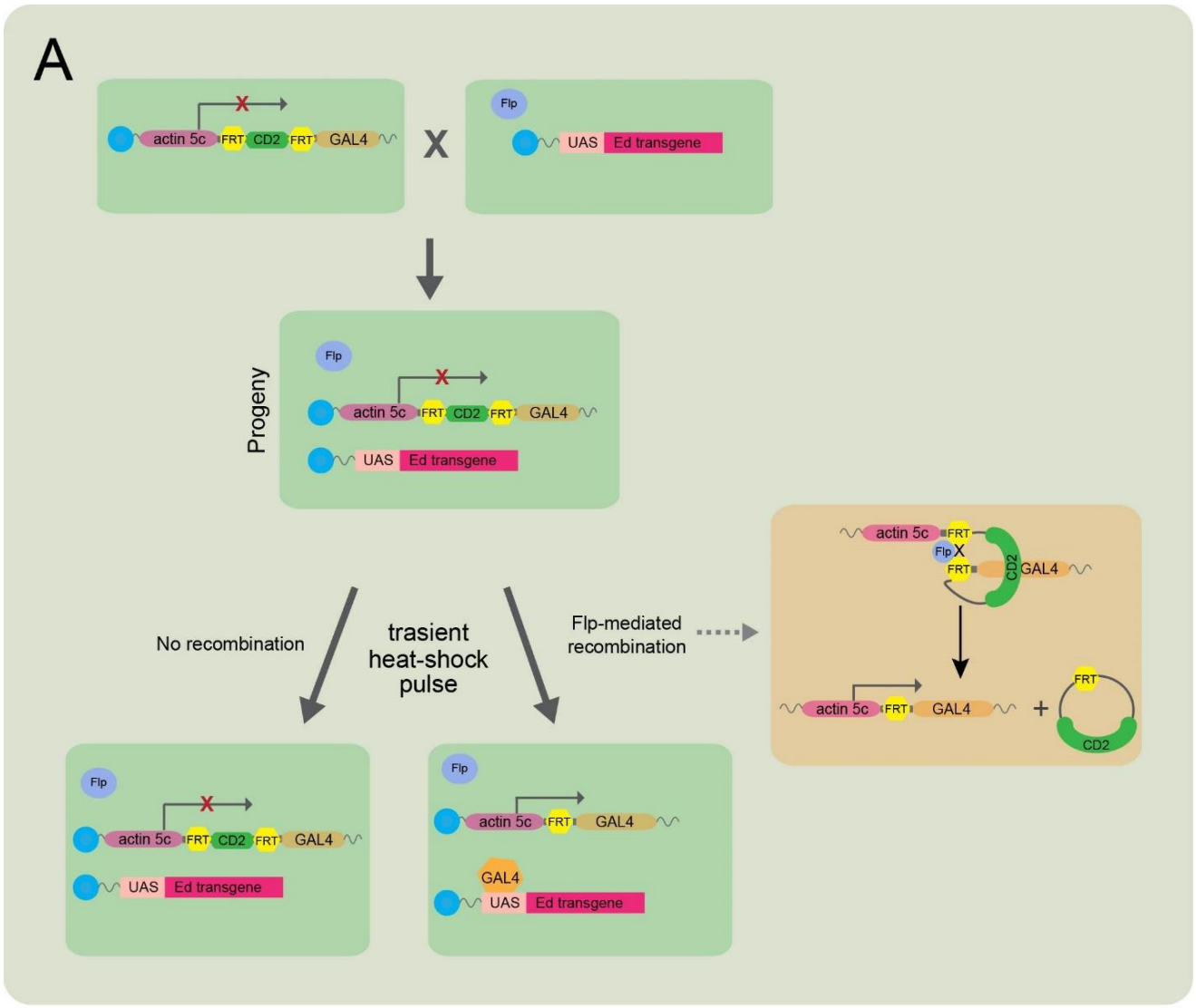
A
actin 5c
FRT
CD2
FRT
GAL4
X
Flp
UAS
Ed transgene
Progeny
No recombination
trasient
heat-shock
pulse
Flp-mediated
recombination
GAL4
B
clone
induction
mitotic
clones
post-mitotic
clone
germarium
stage 6
last round
of mitosis
stage 8
stage 9
stage 10
stage 12

Figure 4.5. Ed expression in midoogenesis is regulated at two levels.

(A – F') Mosaic follicular epithelia with Flp-out clones expressing transgenic Ed-FL (A – C') or EdΔC (D – F') stained for Ed (A'- C', E, F), *lacZ* (A, D), or GFP (B, C, D' – F'). Arrows indicate transgenic Ed localization. (D', F') GFP indicates EdΔC localization. Inset shows a magnified view of the cells.

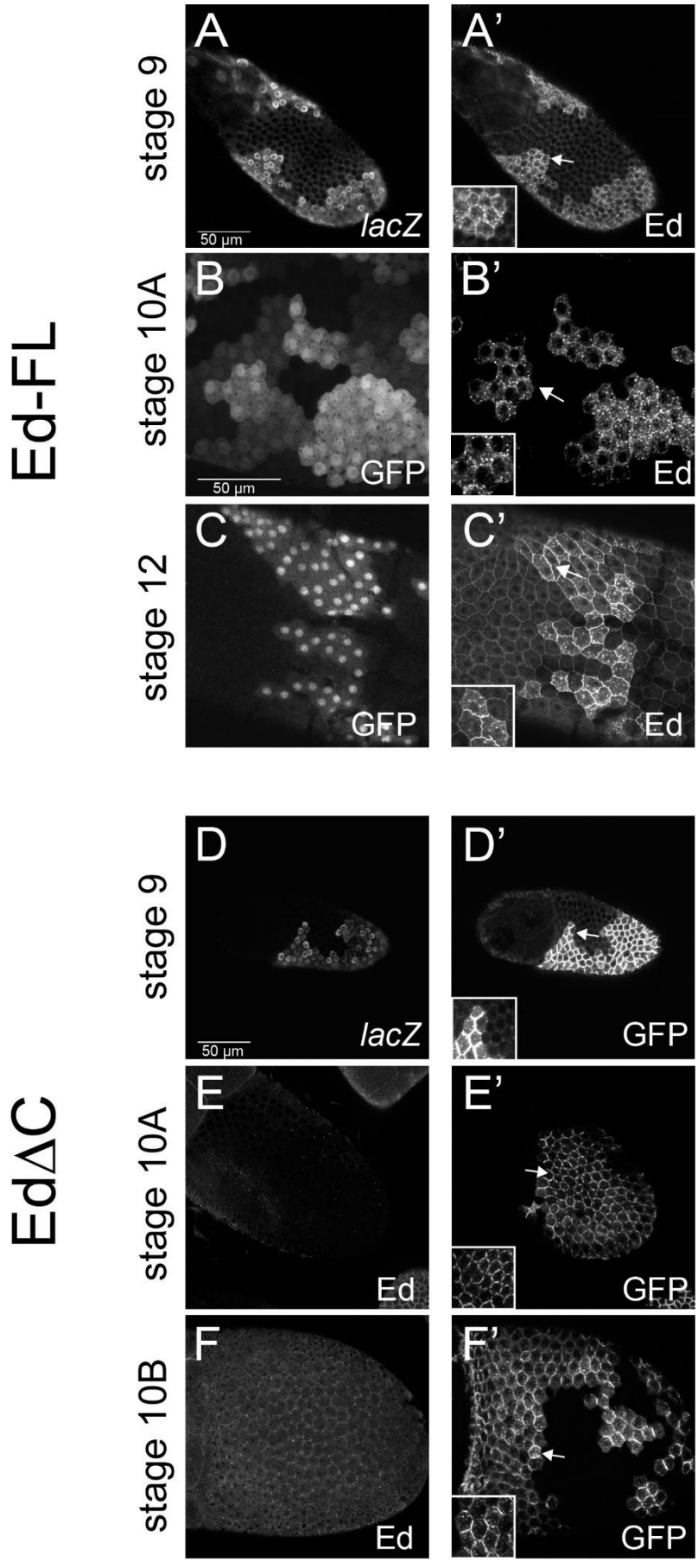
Ed-FL
EdΔC
stage 9
stage 10A
stage 12
stage 10B
A
A'
B
B'
C
C'
D
D'
E
E'
F
F'
lacZ
GFP
Ed
50 µm

Figure 4.6. *vitelline membrane*-GAL4 drivers induces expression of a transgene from midoogenesis and onwards in a spatially dynamic pattern.

(A – F") Wild-type egg chambers stained for Ed (A – F), GFP (A' – F'), and Broad (B" – F"). The expression profile of GFP indicated the expression pattern of UAS-EdΔC-GFP induced by the *vitelline membrane*-GAL4 driver (VM-GAL4). Broad staining is used as a marker to distinguish between the different stages of oogenesis.

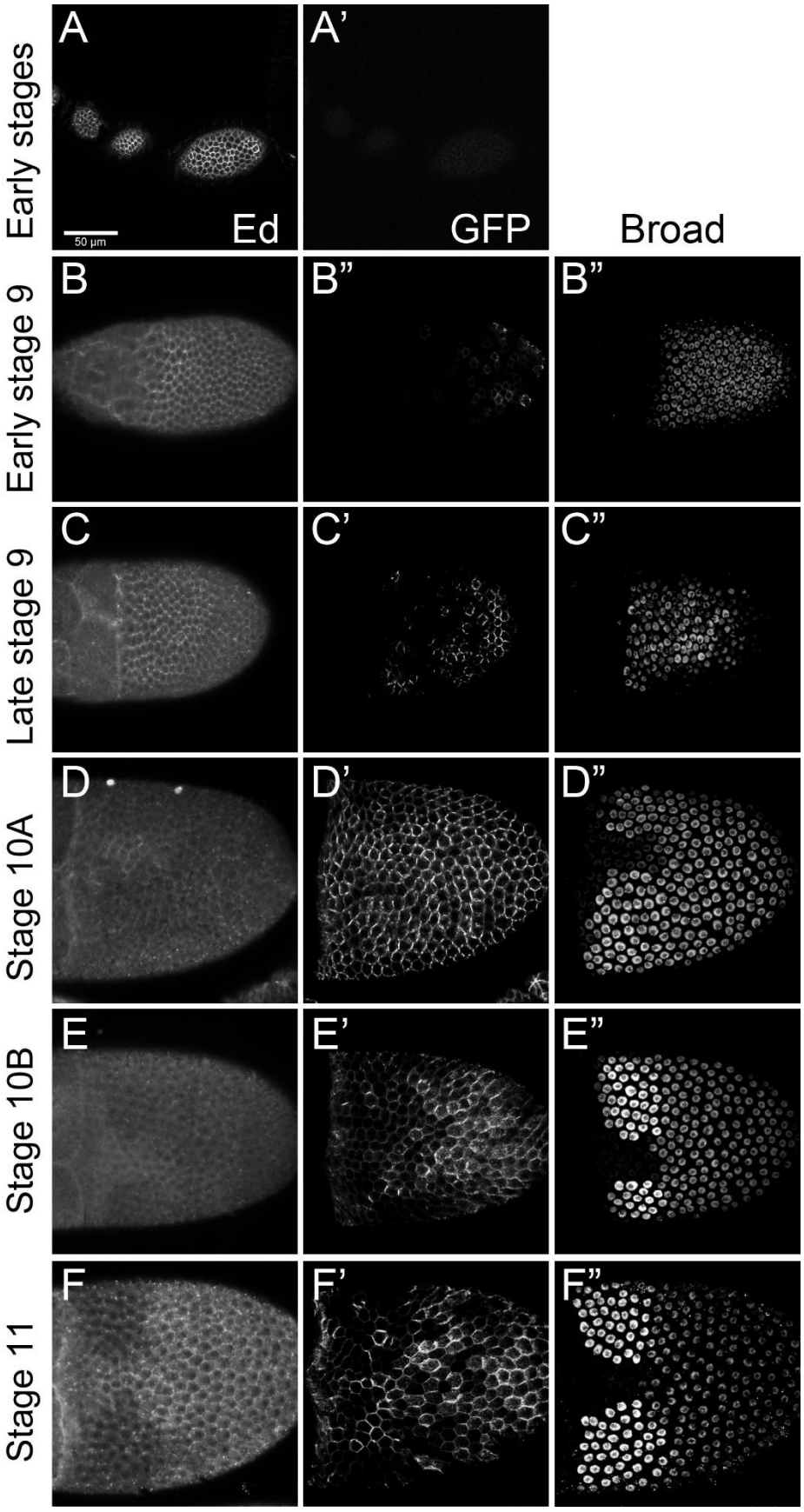
Early stages
A
Ed
50 µm
A'
GFP
Broad
Early stage 9
B
B"
B"
Late stage 9
C
C'
C"
Stage 10A
D
D'
D"
Stage 10B
E
E'
E"
Stage 11
F
F'
F"

Figure 4.7. Expression of Ed in midoogenesis is regulated post-transcriptionally and requires the intramk.cellular domain.

(A – E”) Mosaic follicular epithelia expressing transgenic Ed-FL and UAS-GFP (A – C”) or EdΔC (D – E”) stained for Ed (A – E) or GFP (A’ – E’). Arrows indicate endogenous Ed localization, whereas arrowheads indicated transgenic Ed localization. (D’, E’) GFP indicates EdΔC localization.

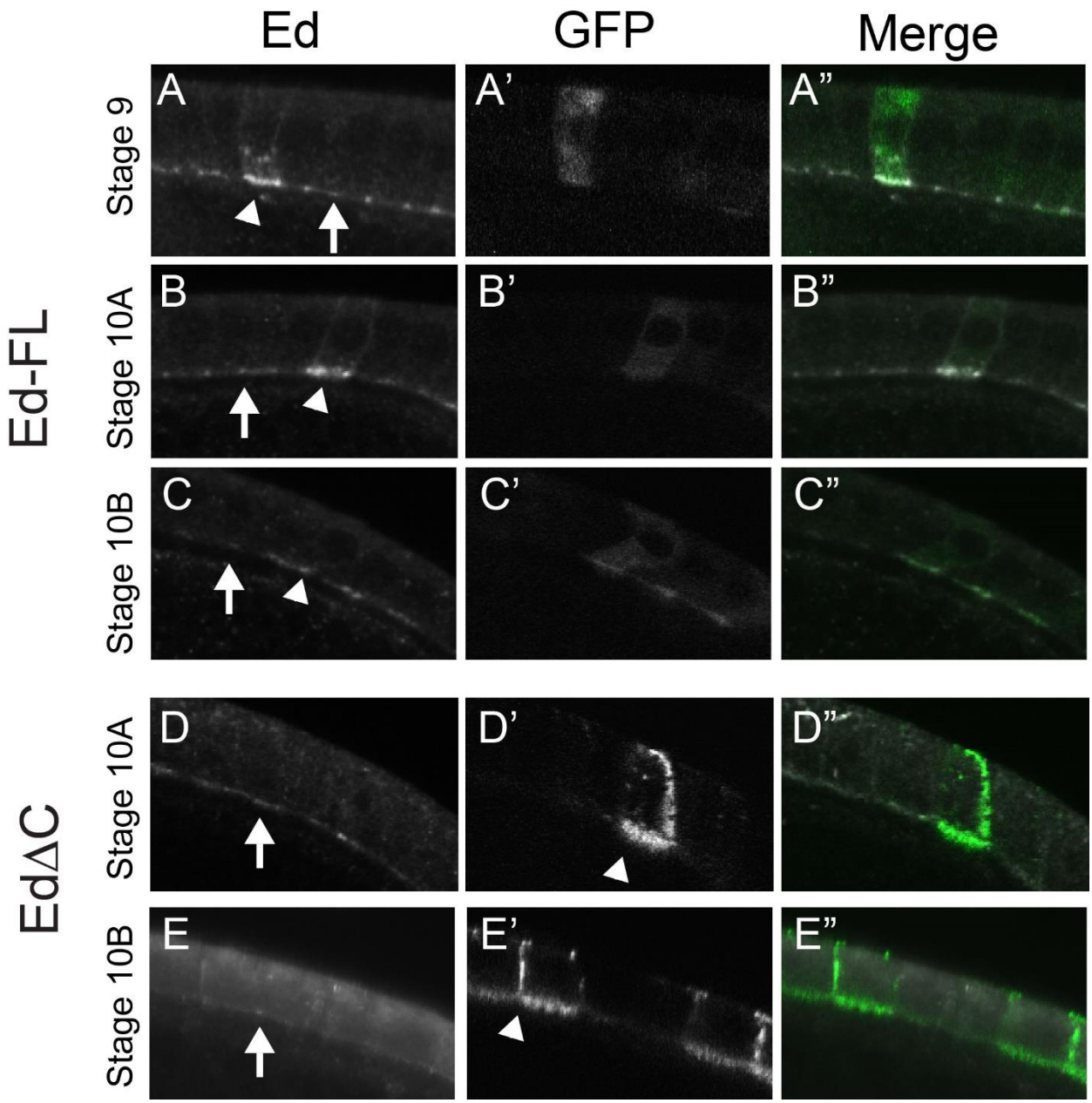
Ed
GFP
Merge
Ed-FL
EdΔC
Stage 9
Stage 10A
Stage 10B
Stage 10A
Stage 10B
A
A'
A"
B
B'
B"
C
C'
C"
D
D'
D"
E
E'
E"

Supplemental Figure 4.1. The temporal and spatial dynamic expression pattern of Ed in embryogenesis is regulated at the transcriptional level.

(A – D) Wild-type embryos of different stages stained for Ed. The asterisk indicates the amnioserosa tissue, where no Ed is detected. (E – F) Whole-mount in situ hybridization of wild-type embryos of different stages showing the distribution of *ed* mRNA. Arrows indicated the amnioserosa tissue, where *ed* mRNA is not detected.

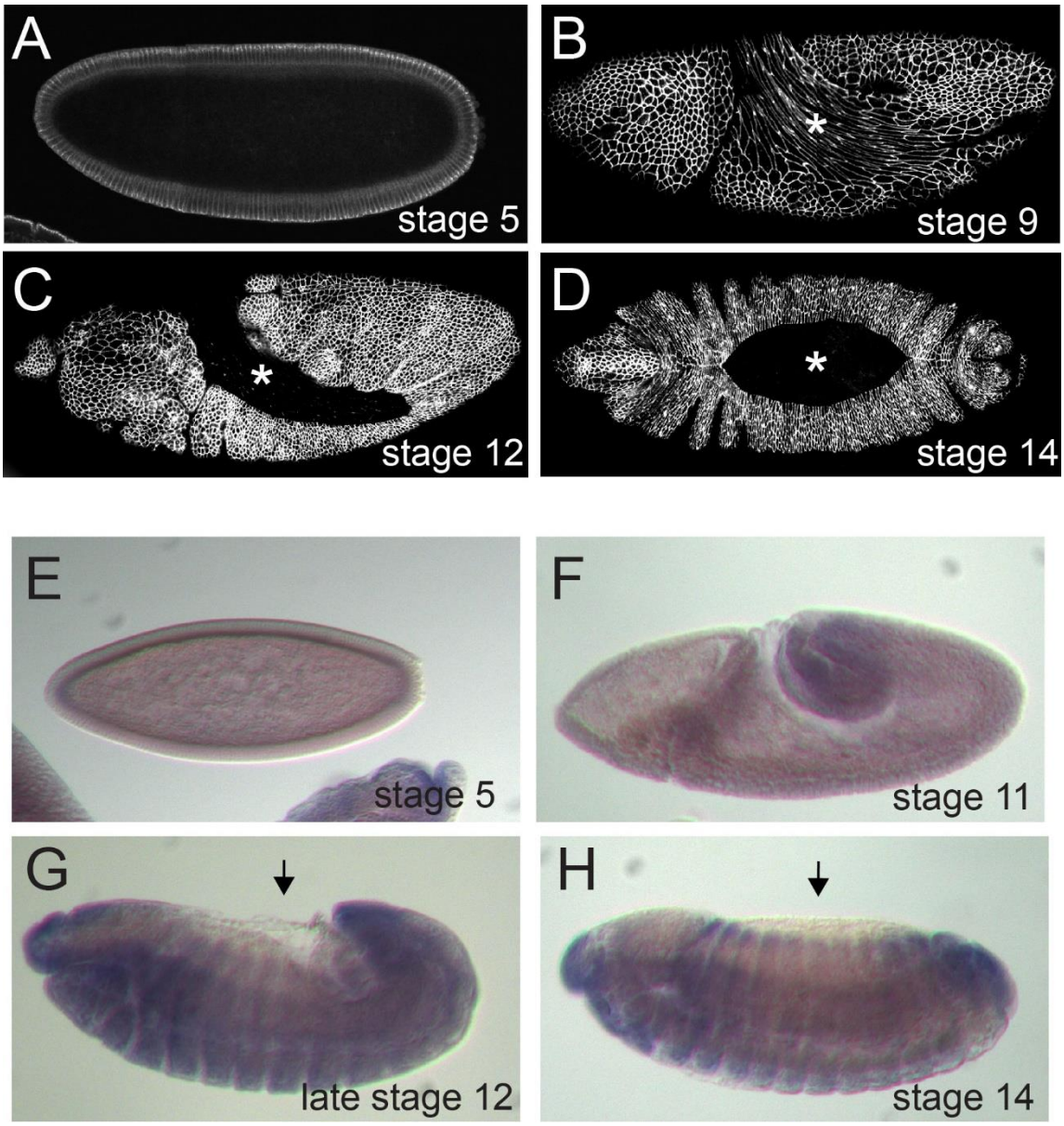
A
stage 5
B
stage 9
C
stage 12
D
stage 14
E
stage 5
F
stage 11
G
late stage 12
H
stage 14

Chapter 5: Discussion

5.1 Differential expression of Ed triggers actomyosin cable formation

During development, the contractile activity of the actomyosin network generates a tensile force that contributes to tissue morphogenesis (Lecuit and Lenne, 2007; Paluch and Heisenberg, 2009). In *Drosophila*, the cell adhesion molecule Ed mediates the spatial reorganization of the actomyosin network, where a difference in Ed expression between two neighboring cells is sufficient to induce localized actomyosin contractility at their interface (Ed/no Ed interface) (Chang et al., 2011; Laplante and Nilson, 2006, 2011; Lin et al., 2007; Wei et al., 2005). This difference in Ed expression occurs in two distinct morphogenetic events. During embryonic dorsal closure, loss of Ed expression from the AS generates an Ed/no Ed interface between this tissue and the DME cells in the lateral epidermis (Laplante and Nilson, 2011; Lin et al., 2007). This interface is associated with the formation of a contractile actomyosin cable between the two cells (Laplante and Nilson, 2011; Lin et al., 2007). Similarly, an Ed/no Ed interface occurs between two groups of neighboring cells of the dorsal appendage primordia in the follicular epithelium during appendage morphogenesis (Laplante and Nilson, 2006). The juxtaposition of the floor cells that express Ed and the roof cells that lack Ed generates an Ed/no Ed interface that coincides with and induces actomyosin cable formation (Laplante and Nilson, 2006). In addition, ectopically generated Ed/no Ed interfaces, between mitotically induced *ed* homozygous mutant clones and their neighboring wild-type cells, also exhibit a contractile actomyosin cable (Chang et al., 2011; Laplante and Nilson, 2006; Wei et al., 2005). Loss of the Ed/no Ed interface, as a consequence of manipulating Ed expression in these tissues, results in the disruption of the localized actomyosin cable formation and subsequent defects morphogenesis in both processes (Laplante and Nilson, 2006, 2011; Lin et al., 2007).

Therefore, it was proposed that Ed functions as a positional cue that dictates the spatial distribution of the actomyosin network and its contractile activity during these morphogenetic events; however, the molecular mechanism on how Ed exerts this function is just beginning to be uncovered.

Besides the actomyosin cable, another phenotype associated with the Ed/no Ed interfaces is the absence of Ed from the membrane of the Ed-expressing cell where it abuts the cell lacking Ed (Chang et al., 2011; Laplante and Nilson, 2006, 2011; Lin et al., 2007; Wei et al., 2005). This observation is perhaps not surprising as stabilization of Ed at the membrane depends on its homophilic binding *in trans*, implying that the distribution of Ed within the Ed-expressing cell is influenced and regulated by whether the neighboring cell expresses or lacks Ed (Laplante and Nilson, 2011). Thus, the homophilic binding of Ed mediates cell-cell recognition as well as the distribution of Ed within the Ed-expressing cell.

As a result, loss of Ed from one cell results in a planar polarized distribution of Ed in the neighboring Ed-expressing cell. Genetic manipulation experiments that change the distribution of Ed within the Ed-expressing cell have demonstrated that the planar polarized localization of Ed is necessary and sufficient to drive actomyosin cable formation at an Ed/no Ed interface (Chang et al., 2011; Laplante and Nilson, 2011). My data support this finding (Figure 3.3). Thus the working model (the planar polarized model) on Ed function proposes that the planar distribution of Ed within the Ed-expressing cell leads to the localized enrichment of the actomyosin network at the Ed/no Ed interface (Laplante and Nilson, 2011).

An alternative and mechanistically simpler model that could account for how Ed directs the spatial distribution of the actomyosin network at the Ed/no Ed interfaces is the "negative regulator" model (Rakic, 2013). Based on this model, Ed functions as an inhibitory signal for

actomyosin cable formation, and thus absence of Ed from the Ed/no Ed interfaces relieves this inhibition and allows the enrichment of the actomyosin network. Contrary to the " planar polarized" which predicts that the asymmetric distribution of Ed within a cell directs cable formation, the "negative regulator" model would predict that the loss of Ed rather than its distribution directs cable formation at an Ed/no Ed interface. Distinguishing between these two models is thus essential to uncover the molecular mechanism and the downstream effectors that mediate this function of Ed.

5.2 Planar polarized model vs. negative regulator model

The phenotypes associated with Ed/no Ed interfaces are consistent with a model where the asymmetric distribution of Ed in the Ed-expressing cell influences the spatial reorganization of the actomyosin network. This is termed the "planar polarized" model, based on which Ed acts as a positive and instructive signal to direct the polarized actomyosin localization (Figure 5.1 A, A'). However, these same phenotypes present at these Ed/no Ed interfaces could also be explained by an alternative model, where the absence of Ed triggers the enrichment of actin and myosin at these interfaces. This is the "negative regulator" model, which characterizes Ed as a negative and inhibitory signal for the formation of the actomyosin cable (Figure 5.1 B, B'). Although both of these models could explain the various phenotypes of the Ed/no Ed interfaces, they differ significantly on the mechanism by which Ed functions. Therefore discerning between these two seemingly opposite models is important to determine how Ed influences the reorganization of the actomyosin network. In an effort to increase support for one model over the other, in this section I will discuss how each model can account for the phenotypes associated with loss of Ed at the Ed/no Ed interface as well as within cells.

The most obvious phenotype associated with the Ed/no Ed interfaces, endogenous or ectopic, is the localized enrichment of actin and its motor protein myosin II at such interfaces. Both models are consistent with and predict this phenotype, but for different reasons. The "planar polarized" model implies that the molecular changes that culminate with the localized enrichment of the actomyosin network at the Ed/no Ed interfaces occur solely in the Ed-expressing cell and not in the cells lacking Ed (Figure 5.1 A'). On the contrary, the "negative regulator" model predicts that actomyosin accumulation would occur at all interfaces that void of Ed (Figure 5.1 B'), including the interfaces between cells lacking Ed expression (no Ed/no Ed interfaces), for instance interfaces between the AS cells during dorsal closure, the roof cells of the appendage primordia, as well as *ed* mutant cells in the follicular epithelium. Interestingly, all these different types of cells do exhibit higher levels of actomyosin (See sections 1.4.3/4; Rakic, 2013). It is possible that the increase in actomyosin levels in roof and the AS cells can be accounted by the various signals that pattern these two groups of cells. A simple experiment to test whether the higher levels of F-actin in the AS cells during dorsal closure are due to the absence of Ed would be to reintroduce Ed expression in these cells and determine whether F-actin levels decrease. One approach would be to use *paired*-GAL4 driver to induce the expression of Ed-FL transgene in a stripe manner in the AS generating alternating rows of cells expressing and lacking Ed and measure and compare F-actin intensity levels between the AS cells with and without Ed. A similar experiment is not possible for the roof cells due to lack of GAL4 drivers that selectively induce transgene expression in these cells. In *ed* mutant follicle cells, the observed increase of F-actin and myosin levels (Rakic, 2013; Rahul Rote, personal communication) can only be explained by the absence of Ed in these cells, suggesting that Ed might act as a negative regulator of actomyosin accumulation. Comparative quantitative analysis

of F-actin levels between *ed* mutant cell interfaces (no Ed/no Ed interfaces) and Ed/no Ed interfaces in homozygous *ed* mutant follicle cells clones demonstrated that Ed/no Ed interfaces exhibit higher levels of F-actin (Rakic, 2013; Rahul Rote, personal communication). These observations suggest that Ed/no Ed interfaces are characteristically different than no Ed/no Ed interfaces and that the higher levels of F-actin at Ed/no Ed interfaces cannot be accounted for simply by the absence of Ed. Therefore, it is possible that Ed functions as both a negative regulator and as an instructive signal to direct the localized enrichment of the actomyosin network.

However, a dual function of Ed in regulating actomyosin enrichment would be inconsistent with several observations. Manipulating the distribution of Ed by rending it uniform around the cell or by removing Ed completely disrupts actomyosin cable formation in the DME cells during dorsal closure (Laplante and Nilson, 2011). Given that both these scenarios have the same phenotype and that DME cells lacking Ed, in $ed^{M/Z}$ mutant embryos, do not display higher levels of F-actin all around indicates that the asymmetric distribution of Ed is necessary for the spatially localized actomyosin cable in these cells. In addition, upstream regulators of the actomyosin network, RhoGEF2 and Dia, are both enriched only at the Ed/no Ed interface in the DME cells during dorsal closure and thus display a spatially localized distribution within these cells (Laplante and Nilson, 2011). Changing the distribution of Ed in the DME cells disrupts the localized enrichment of RhoGEF2 and Dia, suggesting that the asymmetric distribution of Ed is required for the polarized distribution of the upstream molecular signals that regulate the organization and activity of the actomyosin network (Laplante and Nilson, 2011). It is not known whether RhoGEF2 and Dia, or other upstream regulators of actomyosin activity, display a

polarized enrichment at endogenous Ed/no Ed interfaces in the floor cells or in the ectopic ones generated in *ed* mutant follicle cell clones.

Another feature associated with *ed* mutant follicle cell clones that supports the "planar polarized" model is the difference in the apical circumference of the *ed* mutant cells between large and small clones. In small and medium size clones, *ed* mutant cells appear to be constricted in their apical side compared to their basal side, but this apical constriction fades in larger size *ed* clones (Chang et al., 2011; Rakic, 2013). These observations suggest that the apparent apical constriction of *ed* mutant cells in small and medium size clones in presumably due to the contractile activity of the actomyosin network at the border.

Lastly, our finding that Baz appears to be the downstream Ed effector that mediates actomyosin cable formation provides strong support for the "planar polarized" model for Ed function. Similarly to Ed, Baz assumes a planar polarized distribution in the Ed-expressing cell at endogenous and ectopic Ed/no Ed interfaces (Figure 3.4; Laplante and Nilson, 2011; Osterfield et al., 2013; Pickering et al., 2013). However, Baz localization does not appear disrupted at cells lacking Ed, including *ed* mutant cells in the follicular epithelium and wing disc (Figure 3.4; Wei et al., 2005), the roof cells, (A. Noçka, unpublished observations; Osterfield et al., 2013), as well as the AS cells (David et al., 2010; Laplante and Nilson, 2011; Pickering et al., 2013), indicating that the change in the distribution of this Ed effector occurs only in the cell where Ed assumes an asymmetric localization. Therefore, the planar distribution of Ed, not absence of Ed, alters the distribution of Baz in the Ed-expressing cell. Given that uniform loss of Baz abolishes the smooth contour phenotype of the Ed/no Ed interfaces (Figure 3.7 B, B'), we propose that the planar polarized distribution of Ed directs the asymmetric distribution of Baz, which in turn

dictates the spatial reorganization of the actomyosin network in the Ed-expressing cell at the Ed/no Ed interface, consistent with the "planar polarized" model of Ed function.

Collectively, our data show that the asymmetric distribution of Ed is important to influence the remodeling of the actomyosin network, consistent with the "planar polarized" model (Laplante and Nilson, 2011); however the molecular mechanism by which Ed affects the actomyosin cytoskeleton is unclear. It is possible that a planar polarized Ed in a cell somehow induces intracellular changes that affect the spatial distribution and activity of the actomyosin network. An alternative hypothesis is that the endocytic pathway signaling responsible for clearing Ed from the interface where it does not encounter a homophilic binding partner could concomitantly remove Baz from the same interface and affect upstream regulator of the actomyosin network. Indeed, consistent with this hypothesis, during dorsal closure in the DME cell, Baz and Ed appear to colocalize in foci (puncta) as they are being cleared from the leading edge (Laplante and Nilson, 2011). It would be interesting to see whether disruption of signaling in the endocytic pathway affects the distribution of Ed and ultimately the reorganization of the cytoskeleton. However, such experiments might not be straightforward to interpret as the endocytic pathway is involved in the recycling of many different proteins and abrogating it might cause alternative defects in the cell.

In summary, most of our observations with respect to the general mechanism how Ed influences the actomyosin network favor the "planar polarized" model. However, the fact that *ed* mutant cells in the follicular epithelium also show increased F-actin intensity contradict this model of Ed function, and instead favor the "negative regulator" model. It is unclear whether other *ed* mutant cells, such as in the wing disc, also show higher F-actin accumulation than the Ed-expressing cells. Careful measurements of F-actin levels as well as other components of the

actomyosin network, such as pMLC levels using various reagents in cell that lack Ed expression might provide further insights on the mechanism of Ed function. Ultimately, all of these data will provide a better understanding on the molecular signals downstream of Ed.

5.3 Endogenous and ectopic Ed/no Ed interfaces are not alike

Our study of Ed and its role in regulating the distribution of the actomyosin network during development has been greatly facilitated by the fact that ectopically generated Ed/no Ed interfaces in the follicular epithelium appear almost identical to the endogenous Ed/no Ed interfaces. All Ed/no Ed interfaces exhibit a smooth contour, are enriched in F-actin and myosin, and either lack Baz or its localization is greatly affected (Figure 3.1, 3.4; Laplante and Nilson, 2006, 2011). Ectopically generated Ed/no Ed interfaces provide a great system for studying the functions of Ed because such interfaces occur in the same type of cells in the follicular epithelium, where the only difference between the cells is whether they express or lack Ed. In addition, carrying out the necessary genetic manipulation experiments is relatively simple in the follicular epithelium, which in turn allows us to better investigate the function of Ed.

Despite of the many similarities endogenous and ectopic Ed/no Ed interfaces differ in one respect. AJ components appear intact in the endogenous Ed/no Ed interfaces in the DME cells and the floor cells (A.N. unpublished observations; Gorfinkiel and Arias, 2007; Osterfield et al., 2013). However, AJ components appear destabilized at ectopic Ed/no Ed interfaces in the follicular epithelium and wing imaginal disc since DE-cad localization is affected at different degrees (Figure 3.5; Laplante and Nilson, 2006; Wei et al., 2005). These observations suggest that endogenous and ectopic Ed/no Ed interfaces, although they share many similarities, are not identical.

The reason for this difference between endogenous and ectopic Ed/no Ed interfaces is not known. As contractility has been shown to negatively affect the stability of AJs (Sahai and Marshall, 2002), one possibility is that the tension generated by the contractile activity of the actomyosin cable is greater in the ectopic than the endogenous Ed/no Ed interfaces. An alternative possibility is that other signaling pathways regulate the stability AJs at endogenous Ed/no Ed interfaces, given that these occur during morphogenetic events, which depend on the coordinated movements between different cells mediated by cell-cell contacts.

Taken together, these observations suggest that not all Ed/no Ed interfaces manifest the same phenotypes. Yet, despite this difference in the stability of the AJs, ectopic Ed/no Ed interfaces are in many aspects similar to endogenous Ed/no Ed interfaces. For our purposes, these interfaces provide a great system, which can be genetically manipulated with ease, and serve as another, more simple system to study the function of Ed.

5.4 Ed provides a general mechanism how homophilic interactions regulate localized actomyosin contractility during morphogenesis

During development, morphogenesis of epithelial tissues is often driven by changes in cell shape (Lecuit and Lenne, 2007). In the different examples described in this thesis, cell shape changes arise as a consequence of the contractile activity of the actomyosin network, which induces a tensile force that directly contributes to alter the morphology of individual cells (Lecuit and Lenne, 2007; Paluch and Heisenberg, 2009). Further, spatially localized contractility of the actomyosin network within a cell is associated with tissue rearrangement and movement (Bertet et al., 2004; Blankenship et al., 2006; Jacinto et al., 2002a; Kiehart et al., 2000), indicating that upstream signals confer positional information at the subcellular level to direct localized actomyosin enrichment.

The homophilic binding protein Ed has emerged as a good candidate acting upstream to dictate the subcellular distribution of actomyosin enrichment during two developmental processes (Laplante and Nilson, 2006, 2011; Lin et al., 2007). In the DME cells during dorsal closure and in the floor cells during appendage morphogenesis, an asymmetrically distributed Ed directs the localized enrichment of a contractile actomyosin structure, which is necessary for proper morphogenesis. Although the specific molecular mechanism how Ed induces cytoskeletal changes remains largely unknown, during my Ph.D work, I identified Baz as a downstream effector that mediates this function of Ed. Thus, we propose that a planar polarized Ed directs the asymmetric distribution of Baz, which in turn remodels the distribution of the actomyosin network.

A role for Baz in directing localized actomyosin contractility has also been demonstrated during GBE in early embryogenesis, where Baz and myosin II show a highly complementary localization (Simoes Sde et al., 2010; Zallen and Wieschaus, 2004). This relationship between Baz and myosin II is reminiscent of the complementary localization in the DME and floor cells (Laplante and Nilson, 2011; Osterfield et al., 2013; Pickering et al., 2013). However, in the epidermal cells during GBE, Ed does not display a clear asymmetric distribution, but rather appears to be uniformly localized around the cell (Laplante, 2008), suggesting that during this process Ed might not be the upstream signal responsible for generating the reciprocal planar polarized localization between Baz and myosin II.

Asymmetric distribution of Ed also appears to be dispensable in generating localized contractility of the actomyosin network during the invagination of the presumptive salivary glands (Roper, 2012). During this process, the salivary gland placode, composed of specified epidermal cells (Myat and Andrew, 2002), is encircled by a contractile actomyosin cable, which

provides a driving force for tissue bending (Roper, 2012). This actomyosin cable surrounding the placode is reminiscent of the cable assembled in the floor cells that encircles the roof cells during appendage morphogenesis, and both cables ultimately contribute to tube formation (Osterfield et al., 2013; Roper, 2012). Similarly to differences in Ed expression that occur in the dorsal appendage primordia, actomyosin cable assembly at the border of the placode is induced by differential expression levels of Crumbs (Crb), a homophilic binding transmembrane protein and central component of the apical complex (Bulgakova and Knust, 2009; Roper, 2012). Crb is expressed at high levels within the placode cells, but at lower level in the outside epidermal cells (Myat and Andrew, 2002; Roper, 2012). Given that Crb, similar to Ed, is stabilized at the membrane by homophilically interacting *in trans*, this difference in Crb levels between the two different cell populations, the placode and the neighboring epidermal cells, is translated into an asymmetrically distributed Crb in the placode cells at the border (Roper, 2012). Downregulation of Crb from the placode/epidermal cell interface is accompanied by the subsequent enrichment of myosin II and F-actin at that interface, which is necessary for the cell shape changes that induce invagination of the placode (Roper, 2012). Thus, during this process, Crb provides the spatial cue to direct the localized actomyosin contractility. The functional similarities between Crb and Ed provides another example of how differences in protein expression become translated into cytoskeletal remodeling.

Given that Ed does not appear to have a direct or functional homologue in other species, other than in *Drosophila* or mosquitos, the existence of other upstream signals that mediate localized organization of the actomyosin cytoskeleton is not surprising. However, the principle that homophilic interactions direct the spatial organization of upstream positional cues which in

turn contribute to the subcellular localization of actomyosin contractility might provide a general mechanism for promoting epithelial morphogenesis.

Figure 5.1. Alternative models for Ed function in regulating the distribution of actomyosin contractility in epithelial cells.

(A – B) Diagrams representing mosaic follicular epithelia bearing an *ed* mutant clone. ed^{+} cells represent wild-type cells expressing Ed, while the ed^{-} cells indicate *ed* mutant cells lacking Ed expression. The red line indicates enrichment of actomyosin network at cell interfaces. (A) Based on the "planar polarized" model for Ed function, actomyosin assembly and contractile activity occur specifically at Ed/no Ed interfaces. (A') Consistent with this model, the planar polarized distribution of Ed in the ed^{+} cell directs actomyosin enrichment in that cell. (B) According to the "negative regulator" model for Ed function, actomyosin assembly and contractile activity occur at Ed/no Ed interfaces as well as no Ed/no Ed interfaces. (B') Consistent with this model, all cell interfaces that lack Ed should display an enrichment in actomyosin.

A’ Polarized distribution model

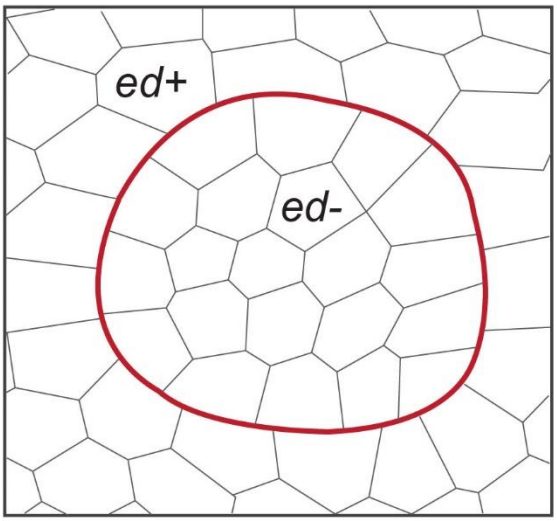

B Negative regulator model

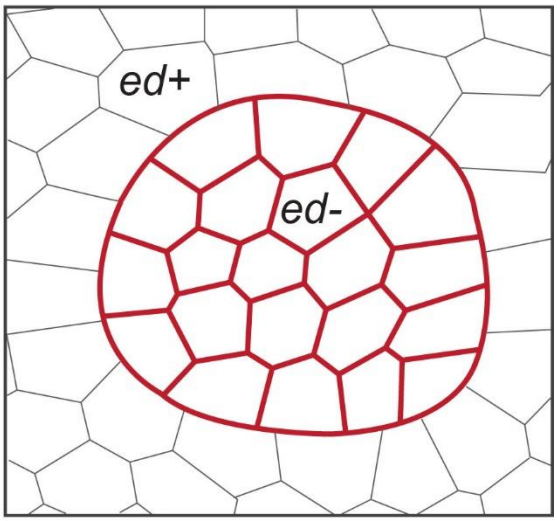

A’

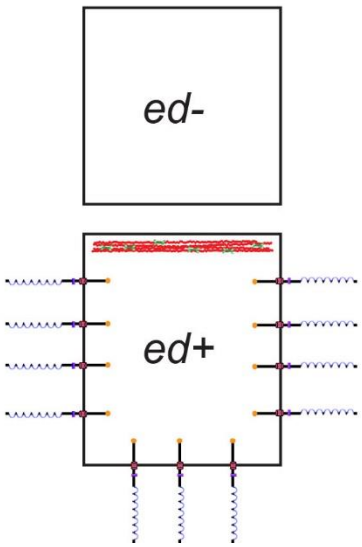

B’

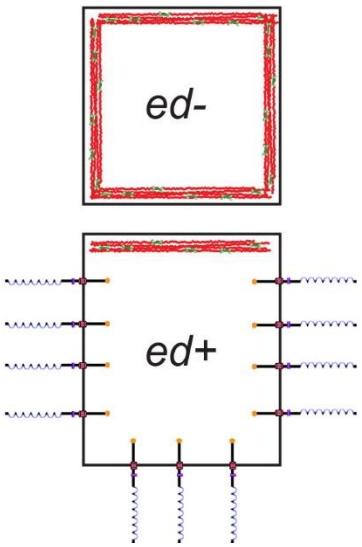

References

Abdelilah-Seyfried, S., Cox, D.N., and Jan, Y.N. (2003). Bazooka is a permissive factor for the invasive behavior of discs large tumor cells in Drosophila ovarian follicular epithelia. Development *130*, 1927-1935.

Ahmed, A., Chandra, S., Magarinos, M., and Vaessin, H. (2003). Echinoid mutants exhibit neurogenic phenotypes and show synergistic interactions with the Notch signaling pathway. Development *130*, 6295-6304.

Amano, M., Ito, M., Kimura, K., Fukata, Y., Chihara, K., Nakano, T., Matsuura, Y., and Kaibuchi, K. (1996). Phosphorylation and activation of myosin by Rho-associated kinase (Rho-kinase). The Journal of biological chemistry *271*, 20246-20249.

Asakura, S., Kasai, M., and Oosawa, F. (1960). The effect of temperature on the equilibrium state of actin solutions. Journal of Polymer Science *44*, 35-49.

Azevedo, D., Antunes, M., Prag, S., Ma, X., Hacker, U., Brodland, G.W., Hutson, M.S., Solon, J., and Jacinto, A. (2011). DRhoGEF2 Regulates Cellular Tension and Cell Pulsations in the Amnioserosa during Drosophila Dorsal Closure. PLoS ONE *6*, e23964.

Bai, J., Chiu, W., Wang, J., Tzeng, T., Perrimon, N., and Hsu, J. (2001). The cell adhesion molecule Echinoid defines a new pathway that antagonizes the Drosophila EGF receptor signaling pathway. Development *128*, 591-601.

Bamburg, J.R. (1999). PROTEINS OF THE ADF/COFILIN FAMILY: Essential Regulators of Actin Dynamics. Annual Review of Cell and Developmental Biology *15*, 185-230.

Bamburg, J.R., McGough, A., and Ono, S. (1999). Putting a new twist on actin: ADF/cofilins modulate actin dynamics. Trends in Cell Biology *9*, 364-370.

Barrett, K., Leptin, M., and Settleman, J. (1997). The Rho GTPase and a putative RhoGEF mediate a signaling pathway for the cell shape changes in Drosophila gastrulation. Cell *91*, 905-915.

Benton, R., and Johnston, D.S. (2003). Drosophila PAR-1 and 14-3-3 Inhibit Bazooka/PAR-3 to Establish Complementary Cortical Domains in Polarized Cells. Cell *115*, 691-704.

Bernards, A. (2003). GAPs galore! A survey of putative Ras superfamily GTPase activating proteins in man and Drosophila. Biochim Biophys Acta *1603*, 47-82.

Bernassola, F., Karin, M., Ciechanover, A., and Melino, G. (2008). The HECT Family of E3 Ubiquitin Ligases: Multiple Players in Cancer Development. Cancer Cell *14*, 10-21.

Bertet, C., Sulak, L., and Lecuit, T. (2004). Myosin-dependent junction remodelling controls planar cell intercalation and axis elongation. Nature *429*, 667-671.

Bilder, D., and Perrimon, N. (2000). Localization of apical epithelial determinants by the basolateral PDZ protein Scribble. Nature *403*, 676-680.

Bischof, J., Maeda, R.K., Hediger, M., Karch, F., and Basler, K. (2007). An optimized transgenesis system for Drosophila using germ-line-specific φC31 integrases. Proceedings of the National Academy of Sciences *104*, 3312-3317.

Blanchard, G.B., Murugesu, S., Adams, R.J., Martinez-Arias, A., and Gorfinkiel, N. (2010). Cytoskeletal dynamics and supracellular organisation of cell shape fluctuations during dorsal closure. Development *137*, 2743-2752.

Blanchoin, L., Amann, K.J., Higgs, H.N., Marchand, J.B., Kaiser, D.A., and Pollard, T.D. (2000). Direct observation of dendritic actin filament networks nucleated by Arp2/3 complex and WASP/Scar proteins. Nature *404*, 1007-1011.

Blanchoin, L., and Pollard, T.D. (2002). Hydrolysis of ATP by polymerized actin depends on the bound divalent cation but not profilin. Biochemistry *41*, 597-602.

Blankenship, J.T., Backovic, S.T., Sanny, J.S., Weitz, O., and Zallen, J.A. (2006). Multicellular rosette formation links planar cell polarity to tissue morphogenesis. Dev Cell *11*, 459-470.

Brand, A.H., and Perrimon, N. (1993). Targeted gene expression as a means of altering cell fates and generating dominant phenotypes. Development *118*, 401-415.

Buchsbaum, R.J. (2007). Rho activation at a glance. Journal of Cell Science *120*, 1149-1152.
Bulgakova, N.A., Grigoriev, I., Yap, A.S., Akhmanova, A., and Brown, N.H. (2013). Dynamic microtubules produce an asymmetric E-cadherin–Bazooka complex to maintain segment boundaries. The Journal of Cell Biology *201*, 887-901.

Bulgakova, N.A., and Knust, E. (2009). The Crumbs complex: from epithelial-cell polarity to retinal degeneration. Journal of Cell Science *122*, 2587-2596.

Carlier, M.-F., Laurent, V., Santolini, J., Melki, R., Didry, D., Xia, G.-X., Hong, Y., Chua, N.-H., and Pantaloni, D. (1997). Actin Depolymerizing Factor (ADF/Cofilin) Enhances the Rate of Filament Turnover: Implication in Actin-based Motility. The Journal of Cell Biology *136*, 1307-1322.

Carlier, M.F., and Pantaloni, D. (1986). Direct evidence for ADP-Pi-F-actin as the major intermediate in ATP-actin polymerization. Rate of dissociation of Pi from actin filaments. Biochemistry *25*, 7789-7792.

Carlier, M.F., Pantaloni, D., Evans, J.A., Lambooy, P.K., Korn, E.D., and Webb, M.R. (1988). The hydrolysis of ATP that accompanies actin polymerization is essentially irreversible. FEBS Letters *235*, 211-214.

Carlsson, L., Nyström, L.E., Sundkvist, I., Markey, F., and Lindberg, U. (1977). Actin polymerizability is influenced by profilin, a low molecular weight protein in non-muscle cells. Journal of Molecular Biology *115*, 465-483.

Chandra, S., Ahmed, A., and Vaessin, H. (2003). The Drosophila IgC2 domain protein Friend-of-Echinoid, a paralogue of Echinoid, limits the number of sensory organ precursors in the wing disc and interacts with the Notch signaling pathway. Developmental Biology *256*, 302-316.

Chang, L.-H., Chen, P., Lien, M.-T., Ho, Y.-H., Lin, C.-M., Pan, Y.-T., Wei, S.-Y., and Hsu, J.-C. (2011). Differential adhesion and actomyosin cable collaborate to drive Echinoid-mediated cell sorting. Development *138*, 3803-3812.

Cheney, R.E., and Mooseker, M.S. (1992). Unconventional myosins. Current opinion in cell biology *4*, 27-35.

Cherfils, J., and Chardin, P. (1999). GEFs: structural basis for their activation of small GTP-binding proteins. Trends in Biochemical Sciences *24*, 306-311.

Chuang, T.H., Xu, X., Knaus, U.G., Hart, M.J., and Bokoch, G.M. (1993). GDP dissociation inhibitor prevents intrinsic and GTPase activating protein-stimulated GTP hydrolysis by the Rac GTP-binding protein. Journal of Biological Chemistry *268*, 775-778.

Cohen, L.H., Pieterman, E., van Leeuwen, R.E.W., Overhand, M., Burm, B.E.A., van der Marel, G.A., and van Boom, J.H. (2000). Inhibitors of prenylation of Ras and other G-proteins and their application as therapeutics. Biochemical Pharmacology *60*, 1061-1068.

Cooke, R., and Murdoch, L. (1973). Interaction of actin with analogs of adenosine triphosphate. Biochemistry *12*, 3927-3932.

Cooper, J., Walker, S., and Pollard, T. (1983). Pyrene actin: documentation of the validity of a sensitive assay for actin polymerization. J Muscle Res Cell Motil *4*, 253-262.

Cox, D.N., Lu, B., Sun, T.-Q., Williams, L.T., and Jan, Y.N. (2001). Drosophila par-1 is required for oocyte differentiation and microtubule organization. Current Biology *11*, 75-87.

Craig, R., Smith, R., and Kendrick-Jones, J. (1983). Light-chain phosphorylation controls the conformation of vertebrate non-muscle and smooth muscle myosin molecules. Nature *302*, 436-439.

Cross, R.A., Cross, K.E., and Sobieszek, A. (1986). ATP-linked monomer-polymer equilibrium of smooth muscle myosin: the free folded monomer traps ADP.Pi. Embo j *5*, 2637-2641.

David, D.J.V., Tishkina, A., and Harris, T.J.C. (2010). The PAR complex regulates pulsed actomyosin contractions during amnioserosa apical constriction in Drosophila. Development *137*, 1645-1655.

David, D.J.V., Wang, Q., Feng, J.J., and Harris, T.J.C. (2013). Bazooka inhibits aPKC to limit antagonism of actomyosin networks during amnioserosa apical constriction. Development *140*, 4719-4729.

Dawes-Hoang, R.E., Parmar, K.M., Christiansen, A.E., Phelps, C.B., Brand, A.H., and Wieschaus, E.F. (2005). folded gastrulation, cell shape change and the control of myosin localization. Development *132*, 4165-4178.

De La Cruz, E.M., Mandinova, A., Steinmetz, M.O., Stoffler, D., Aebi, U., and Pollard, T.D. (2000). Polymerization and structure of nucleotide-free actin filaments. Journal of Molecular Biology *295*, 517-526.

Deng, W.-M., Althauser, C., and Ruohola-Baker, H. (2001). Notch-Delta signaling induces a transition from mitotic cell cycle to endocycle in Drosophila follicle cells. Development *128*, 4737-4746.

Desai, R., Sarpal, R., Ishiyama, N., Pellikka, M., Ikura, M., and Tepass, U. (2013). Monomeric alpha-catenin links cadherin to the actin cytoskeleton. Nat Cell Biol *15*, 261-273.

Doerflinger, H., Benton, R., Shulman, J.M., and Johnston, D.S. (2003). The role of PAR-1 in regulating the polarised microtubule cytoskeleton in the Drosophila follicular epithelium. Development *130*, 3965-3975.

Dorman, J.B., James, K.E., Fraser, S.E., Kiehart, D.P., and Berg, C.A. (2004). bullwinkle is required for epithelial morphogenesis during Drosophila oogenesis. Developmental Biology *267*, 320-341.

Drees, F., Pokutta, S., Yamada, S., Nelson, W.J., and Weis, W.I. α-Catenin Is a Molecular Switch that Binds E-Cadherin-β-Catenin and Regulates Actin-Filament Assembly. Cell *123*, 903-915.

Drewes, G., Ebneth, A., Preuss, U., Mandelkow, E.-M., and Mandelkow, E. (1997). MARK, a Novel Family of Protein Kinases That Phosphorylate Microtubule-Associated Proteins and Trigger Microtubule Disruption. Cell *89*, 297-308.

Dreyfuss, G., Kim, V.N., and Kataoka, N. (2002). Messenger-RNA-binding proteins and the messages they carry. Nature Reviews Molecular Cell Biology *3*, 195-205.

Ebneth, A., Drewes, G., Mandelkow, E.M., and Mandelkow, E. (1999). Phosphorylation of MAP2c and MAP4 by MARK kinases leads to the destabilization of microtubules in cells. Cell Motility and the Cytoskeleton *44*, 209-224.

Eden, S., Rohatgi, R., Podtelejnikov, A.V., Mann, M., and Kirschner, M.W. (2002). Mechanism of regulation of WAVE1-induced actin nucleation by Rac1 and Nck. Nature *418*, 790-793.

Edwards, K.A., Chang, X.J., and Kiehart, D.P. (1995). Essential light chain of Drosophila nonmuscle myosin II. J Muscle Res Cell Motil *16*, 491-498.

Escudero, L.M., Wei, S.Y., Chiu, W.H., Modolell, J., and Hsu, J.C. (2003). Echinoid synergizes with the Notch signaling pathway in Drosophila mesothorax bristle patterning. Development *130*, 6305-6316.

Etemad-Moghadam, B., Guo, S., and Kemphues, K.J. (1995). Asymmetrically distributed PAR-3 protein contributes to cell polarity and spindle alignment in early C. elegans embryos. Cell *83*, 743-752.

Etienne-Manneville, S., and Hall, A. (2002). Rho GTPases in cell biology. Nature *420*, 629-635.

Fernandez-Gonzalez, R., Simoes Sde, M., Roper, J.C., Eaton, S., and Zallen, J.A. (2009). Myosin II dynamics are regulated by tension in intercalating cells. Dev Cell *17*, 736-743.

Fetting, J.L., Spencer, S.A., and Wolff, T. (2009). The cell adhesion molecules Echinoid and Friend of Echinoid coordinate cell adhesion and cell signaling to regulate the fidelity of ommatidial rotation in the Drosophila eye. Development *136*, 3323-3333.

Fox, D.T., and Peifer, M. (2007). Abelson kinase (Abl) and RhoGEF2 regulate actin organization during cell constriction in Drosophila. Development *134*, 567-578.

Franke, J.D., Montague, R.A., and Kiehart, D.P. (2005). Nonmuscle Myosin II Generates Forces that Transmit Tension and Drive Contraction in Multiple Tissues during Dorsal Closure. Current Biology *15*, 2208-2221.

Freeman, W.H. (2000). Molecular Mechanisms of Eukaryotic Transcriptional Control, 4th Edition edn (New York).

Fujisawa, K., Fujita, A., Ishizaki, T., Saito, Y., and Narumiya, S. (1996). Identification of the Rho-binding domain of p160ROCK, a Rho-associated coiled-coil containing protein kinase. The Journal of biological chemistry *271*, 23022-23028.

Fujiwara, I., Takahashi, S., Tadakuma, H., Funatsu, T., and Ishiwata, S.i. (2002). Microscopic analysis of polymerization dynamics with individual actin filaments. Nat Cell Biol *4*, 666-673.

Fujiwara, I., Vavylonis, D., and Pollard, T.D. (2007). Polymerization kinetics of ADP- and ADP-P(i)-actin determined by fluorescence microscopy. Proceedings of the National Academy of Sciences of the United States of America *104*, 8827-8832.

Gates, J., and Peifer, M. Can 1000 Reviews Be Wrong? Actin, α-Catenin, and Adherens Junctions. Cell *123*, 769-772.

Goldschmidt-Clermont, P.J., Machesky, L.M., Doberstein, S.K., and Pollard, T.D. (1991). Mechanism of the interaction of human platelet profilin with actin. J Cell Biol *113*, 1081-1089.

Golic, K.G., and Lindquist, S. (1989). The FLP recombinase of yeast catalyzes site-specific recombination in the drosophila genome. Cell *59*, 499-509.

Goode, B.L., and Eck, M.J. (2007). Mechanism and Function of Formins in the Control of Actin Assembly. Annual Review of Biochemistry *76*, 593-627.

Gorfinkiel, N., and Arias, A.M. (2007). Requirements for adherens junction components in the interaction between epithelial tissues during dorsal closure in Drosophila. Journal of Cell Science *120*, 3289-3298.

Gorfinkiel, N., Blanchard, G.B., Adams, R.J., and Martinez Arias, A. (2009). Mechanical control of global cell behaviour during dorsal closure in Drosophila. Development *136*, 1889-1898.

Grammont, M. (2007). Adherens junction remodeling by the Notch pathway in Drosophila melanogaster oogenesis. The Journal of Cell Biology *177*, 139-150.

Grammont, M., and Irvine, K.D. (2001). fringe and Notch specify polar cell fate during Drosophila oogenesis. Development *128*, 2243-2253.

Guerrero, C., Tagwerker, C., Kaiser, P., and Huang, L. (2006). An Integrated Mass Spectrometry-based Proteomic Approach: Quantitative Analysis of Tandem Affinity-purified in vivo Cross-linked Protein Complexes (qtax) to Decipher the 26 s Proteasome-interacting Network. Molecular & Cellular Proteomics *5*, 366-378.

Hales, C.M., Vaerman, J.-P., and Goldenring, J.R. (2002). Rab11 Family Interacting Protein 2 Associates with Myosin Vb and Regulates Plasma Membrane Recycling. Journal of Biological Chemistry *277*, 50415-50421.

Hall, A. (1998). Rho GTPases and the Actin Cytoskeleton. Science *279*, 509-514.

Harden, N., Ricos, M., Ong, Y.M., Chia, W., and Lim, L. (1999). Participation of small GTPases in dorsal closure of the Drosophila embryo: distinct roles for Rho subfamily proteins in epithelial morphogenesis. Journal of Cell Science *112*, 273-284.

Harris, T.J., and Tepass, U. (2010). Adherens junctions: from molecules to morphogenesis. Nat Rev Mol Cell Biol *11*, 502-514.

Harris, T.J.C., and Peifer, M. (2004). Adherens junction-dependent and -independent steps in the establishment of epithelial cell polarity in Drosophila. The Journal of Cell Biology *167*, 135-147.

Hart, M., Maru, Y., Leonard, D., Witte, O., Evans, T., and Cerione, R. (1992). A GDP dissociation inhibitor that serves as a GTPase inhibitor for the Ras-like protein CDC42Hs. Science *258*, 812-815.

Hart, M.J., Eva, A., Zangrilli, D., Aaronson, S.A., Evans, T., Cerione, R.A., and Zheng, Y. (1994). Cellular transformation and guanine nucleotide exchange activity are catalyzed by a common domain on the dbl oncogene product. The Journal of biological chemistry *269*, 62-65.

Hartenstein, V., and Posakony, J.W. (1990). A dual function of the Notch gene in Drosophila sensillum development. Dev Biol *142*, 13-30.

Heitzler, P., and Simpson, P. (1991). The choice of cell fate in the epidermis of Drosophila. Cell *64*, 1083-1092.

Hicke, L. (2001). Protein regulation by monoubiquitin. Nat Rev Mol Cell Biol *2*, 195-201.

Hildebrand, J.D. (2005). Shroom regulates epithelial cell shape via the apical positioning of an actomyosin network. J Cell Sci *118*, 5191-5203.

Homem, C.C.F., and Peifer, M. (2008). Diaphanous regulates myosin and adherens junctions to control cell contractility and protrusive behavior during morphogenesis. Development *135*, 1005-1018.

Hong, J.-W., Hendrix, D.A., Papatsenko, D., and Levine, M.S. (2008). How the Dorsal gradient works: Insights from postgenome technologies. Proceedings of the National Academy of Sciences *105*, 20072-20076.

Hori, Y., Kikuchi, A., Isomura, M., Katayama, M., Miura, Y., Fujioka, H., Kaibuchi, K., and Takai, Y. (1991). Post-translational modifications of the C-terminal region of the rho protein are important for its interaction with membranes and the stimulatory and inhibitory GDP/GTP exchange proteins. Oncogene *6*, 515-522.

Horne-Badovinac, S., and Bilder, D. (2005). Mass transit: Epithelial morphogenesis in the Drosophila egg chamber. Developmental Dynamics *232*, 559-574.

Houdusse, A., Kalabokis, V.N., Himmel, D., Szent-Gyorgyi, A.G., and Cohen, C. (1999). Atomic structure of scallop myosin subfragment S1 complexed with MgADP: a novel conformation of the myosin head. Cell *97*, 459-470.

Huibregtse, J.M., Scheffner, M., Beaudenon, S., and Howley, P.M. (1995). A family of proteins structurally and functionally related to the E6-AP ubiquitin-protein ligase. Proceedings of the National Academy of Sciences *92*, 2563-2567.

Irvine, K.D., and Wieschaus, E. (1994). Cell intercalation during Drosophila germband extension and its regulation by pair-rule segmentation genes. Development *120*, 827-841.

Isken, O., Kim, Y.K., Hosoda, N., Mayeur, G.L., Hershey, J.W., and Maquat, L.E. (2008). Upf1 phosphorylation triggers translational repression during nonsense-mediated mRNA decay. Cell *133*, 314-327.

Islam, R., Wei, S.-Y., Chiu, W.-H., Hortsch, M., and Hsu, J.-C. (2003). Neuroglian activates Echinoid to antagonize the Drosophila EGF receptor signaling pathway. Development *130*, 2051-2059.

Jacinto, A., Wood, W., Balayo, T., Turmaine, M., Martinez-Arias, A., and Martin, P. (2000). Dynamic actin-based epithelial adhesion and cell matching during Drosophila dorsal closure. Current biology : CB *10*, 1420-1426.

Jacinto, A., Wood, W., Woolner, S., Hiley, C., Turner, L., Wilson, C., Martinez-Arias, A., and Martin, P. (2002a). Dynamic analysis of actin cable function during Drosophila dorsal closure. Current biology : CB *12*, 1245-1250.

Jacinto, A., Woolner, S., and Martin, P. (2002b). Dynamic Analysis of Dorsal Closure in Drosophila: From Genetics to Cell Biology. Developmental Cell *3*, 9-19.

Jankovics, F., and Brunner, D. (2006). Transiently Reorganized Microtubules Are Essential for Zippering during Dorsal Closure in Drosophila melanogaster. Developmental Cell *11*, 375-385.

Jékely, G., and Rørth, P. (2003). Hrs mediates downregulation of multiple signalling receptors in Drosophila, Vol 4.

Jiang, J., and Levine, M. (1993). Binding affinities and cooperative interactions with bHLH activators delimit threshold responses to the dorsal gradient morphogen. Cell *72*, 741-752.

Johnston, G.C., Prendergast, J.A., and Singer, R.A. (1991). The Saccharomyces cerevisiae MYO2 gene encodes an essential myosin for vectorial transport of vesicles. The Journal of Cell Biology *113*, 539-551.

Jonker, A., Boer, P.A.J.d., Hoff, M.J.B.v.d., Lamers, W.H., and Moorman, A.F.M. (1997). Towards Quantitative In Situ Hybridization. Journal of Histochemistry & Cytochemistry *45*, 413-423.

Jung, H.S., Komatsu, S., Ikebe, M., and Craig, R. (2008). Head-head and head-tail interaction: a general mechanism for switching off myosin II activity in cells. Mol Biol Cell *19*, 3234-3242.

Kabsch, W., Mannherz, H.G., and Suck, D. (1985). Three-dimensional structure of the complex of actin and DNase I at 4.5 A resolution. Embo j *4*, 2113-2118.

Kabsch, W., Mannherz, H.G., Suck, D., Pai, E.F., and Holmes, K.C. (1990). Atomic structure of the actin:DNase I complex. Nature *347*, 37-44.

Kaltschmidt, J.A., Lawrence, N., Morel, V., Balayo, T., Fernandez, B.G., Pelissier, A., Jacinto, A., and Martinez Arias, A. (2002). Planar polarity and actin dynamics in the epidermis of Drosophila. Nat Cell Biol *4*, 937-944.

Kam, Z., Minden, J.S., Agard, D.A., Sedat, J.W., and Leptin, M. (1991). Drosophila gastrulation: analysis of cell shape changes in living embryos by three-dimensional fluorescence microscopy. Development *112*, 365-370.

Kasza, K.E., Farrell, D.L., and Zallen, J.A. (2014). Spatiotemporal control of epithelial remodeling by regulated myosin phosphorylation. Proceedings of the National Academy of Sciences *111*, 11732-11737.

Kiehart, D.P., Galbraith, C.G., Edwards, K.A., Rickoll, W.L., and Montague, R.A. (2000). Multiple Forces Contribute to Cell Sheet Morphogenesis for Dorsal Closure in Drosophila. The Journal of Cell Biology *149*, 471-490.

Kim, V.N., Yong, J., Kataoka, N., Abel, L., Diem, M.D., and Dreyfuss, G. (2001). The Y14 protein communicates to the cytoplasm the position of exon-exon junctions. EMBO Journal *20*, 2062-2068.

Kimura, K., Ito, M., Amano, M., Chihara, K., Fukata, Y., Nakafuku, M., Yamamori, B., Feng, J., Nakano, T., Okawa, K., *et al.* (1996). Regulation of myosin phosphatase by Rho and Rho-associated kinase (Rho-kinase). Science *273*, 245-248.

Klebes, A., and Knust, E. (2000). A conserved motif in Crumbs is required for E-cadherin localisation and zonula adherens formation in Drosophila. Current biology : CB *10*, 76-85.

Knox, A.L., and Brown, N.H. (2002). Rap1 GTPase regulation of adherens junction positioning and cell adhesion. Science *295*, 1285-1288.

Kohno, H., Tanaka, K., Mino, A., Umikawa, M., Imamura, H., Fujiwara, T., Fujita, Y., Hotta, K., Qadota, H., Watanabe, T., *et al.* (1996). Bni1p implicated in cytoskeletal control is a putative target of Rho1p small GTP binding protein in Saccharomyces cerevisiae. The EMBO Journal *15*, 6060-6068.

Kolahi, K.S., White, P.F., Shreter, D.M., Classen, A.K., Bilder, D., and Mofrad, M.R.K. (2009). Quantitative analysis of epithelial morphogenesis in Drosophila oogenesis: New insights based on morphometric analysis and mechanical modeling. Developmental Biology *331*, 129-139.

Kölsch, V., Seher, T., Fernandez-Ballester, G.J., Serrano, L., and Leptin, M. (2007). Control of Drosophila Gastrulation by Apical Localization of Adherens Junctions and RhoGEF2. Science *315*, 384-386.

Kourtis, N., and Tavernarakis, N. (2009). Cell-specific monitoring of protein synthesis in vivo. PLoS ONE *4*, e4547.

Kovar, D.R., Harris, E.S., Mahaffy, R., Higgs, H.N., and Pollard, T.D. (2006). Control of the assembly of ATP- and ADP-actin by formins and profilin. Cell *124*, 423-435.

Krahn, M.P., Klopfenstein, D.R., Fischer, N., and Wodarz, A. (2010). Membrane Targeting of Bazooka/PAR-3 Is Mediated by Direct Binding to Phosphoinositide Lipids. Current Biology *20*, 636-642.

Labouesse, M. (2011). Forces and tension in development. Preface. Current topics in developmental biology *95*, xi-xvi.

Lapierre, L.A., Kumar, R., Hales, C.M., Navarre, J., Bhartur, S.G., Burnette, J.O., Provance, D.W., Mercer, J.A., Bähler, M., and Goldenring, J.R. (2001). Myosin Vb Is Associated with Plasma Membrane Recycling Systems. Molecular Biology of the Cell *12*, 1843-1857.

Laplante, C. (2008). Tension at the leading edge: differential expression of the cell-adhesion molecule Echinoid regulates morphogenesis in Drosophila. In Biology Department (McGill University).

Laplante, C., and Nilson, L.A. (2006). Differential expression of the adhesion molecule Echinoid drives epithelial morphogenesis in Drosophila. Development *133*, 3255-3264.

Laplante, C., and Nilson, L.A. (2011). Asymmetric distribution of Echinoid defines the epidermal leading edge during Drosophila dorsal closure. The Journal of Cell Biology *192*, 335-348.

Lappalainen, P., and Drubin, D.G. (1997). Cofilin promotes rapid actin filament turnover in vivo. Nature *388*, 78-82.

Le Hir, H., and Andersen, G.R. (2008). Structural insights into the exon junction complex. Current Opinion in Structural Biology *18*, 112-119.

Lecuit, T., and Lenne, P.-F. (2007). Cell surface mechanics and the control of cell shape, tissue patterns and morphogenesis. Nat Rev Mol Cell Biol *8*, 633-644.

Lee, C.-K., Sunkin, S., Kuan, C., Thompson, C., Pathak, S., Ng, L., Lau, C., Fischer, S., Mortrud, M., Slaughterbeck, C., *et al.* (2008). Quantitative methods for genome-scale analysis of in situ hybridization and correlation with microarray data. Genome Biology *9*, R23.
Lehmann, R., and Tautz, D. (1994). In situ hybridization to RNA. Methods in cell biology *44*, 575-598.

Lejeune, F., Ishigaki, Y., Li, X., and Maquat, L.E. (2002). The exon junction complex is detected on CBP80-bound but not eIF4E-bound mRNA in mammalian cells: Dynamics of mRNP remodeling. EMBO Journal *21*, 3536-3545.

Leptin, M. (1999). Gastrulation in Drosophila: the logic and the cellular mechanisms. The EMBO Journal *18*, 3187-3192.

Leptin, M., and Grunewald, B. (1990). Cell shape changes during gastrulation in Drosophila. Development *110*, 73-84.

Leung, T., Chen, X.Q., Manser, E., and Lim, L. (1996). The p160 RhoA-binding kinase ROK alpha is a member of a kinase family and is involved in the reorganization of the cytoskeleton. Molecular and cellular biology *16*, 5313-5327.

Leung, T., Manser, E., Tan, L., and Lim, L. (1995). A Novel Serine/Threonine Kinase Binding the Ras-related RhoA GTPase Which Translocates the Kinase to Peripheral Membranes. Journal of Biological Chemistry *270*, 29051-29054.

Li, B.X., Satoh, A.K., and Ready, D.F. (2007). Myosin V, Rab11, and dRip11 direct apical secretion and cellular morphogenesis in developing Drosophila photoreceptors. The Journal of Cell Biology *177*, 659-669.

Lin, H.-P., Chen, H.-M., Wei, S.-Y., Chen, L.-Y., Chang, L.-H., Sun, Y.-J., Huang, S.-Y., and Hsu, J.-C. (2007). Cell adhesion molecule Echinoid associates with unconventional myosin VI/Jaguar motor to regulate cell morphology during dorsal closure in Drosophila. Developmental Biology *311*, 423-433.

Liu, R., Linardopoulou, E.V., Osborn, G.E., and Parkhurst, S.M. (2010). Formins in Development: Orchestrating Body Plan Origami. Biochimica et biophysica acta *1803*, 207-225.

Lloyd, T.E., Atkinson, R., Wu, M.N., Zhou, Y., Pennetta, G., and Bellen, H.J. (2002). Hrs Regulates Endosome Membrane Invagination and Tyrosine Kinase Receptor Signaling in Drosophila. Cell *108*, 261-269.

Machesky, L.M., Mullins, R.D., Higgs, H.N., Kaiser, D.A., Blanchoin, L., May, R.C., Hall, M.E., and Pollard, T.D. (1999). Scar, a WASp-related protein, activates nucleation of actin filaments by the Arp2/3 complex. Proc Natl Acad Sci U S A *96*, 3739-3744.

Magie, C.R., Meyer, M.R., Gorsuch, M.S., and Parkhurst, S.M. (1999). Mutations in the Rho1 small GTPase disrupt morphogenesis and segmentation during early Drosophila development. Development *126*, 5353-5364.

Major, R.J., and Irvine, K.D. (2006). Localization and requirement for Myosin II at the dorsal-ventral compartment boundary of the Drosophila wing. Developmental Dynamics *235*, 3051-3058.

Majumder, P., Aranjuez, G., Amick, J., and McDonald, Jocelyn A. (2012). Par-1 Controls Myosin-II Activity through Myosin Phosphatase to Regulate Border Cell Migration. Current Biology *22*, 363-372.

Mandai, K., Nakanishi, H., Satoh, A., Obaishi, H., Wada, M., Nishioka, H., Itoh, M., Mizoguchi, A., Aoki, T., Fujimoto, T., *et al.* (1997). Afadin: A Novel Actin Filament–binding Protein with One PDZ Domain Localized at Cadherin-based Cell-to-Cell Adherens Junction. The Journal of Cell Biology *139*, 517-528.

Manseau, L., Baradaran, A., Brower, D., Budhu, A., Elefant, F., Phan, H., Philp, A.V., Yang, M., Glover, D., Kaiser, K., *et al.* (1997). GAL4 enhancer traps expressed in the embryo, larval brain, imaginal discs, and ovary of Drosophila. Developmental dynamics : an official publication of the American Association of Anatomists *209*, 310-322.

Martin, A.C., Gelbart, M., Fernandez-Gonzalez, R., Kaschube, M., and Wieschaus, E.F. (2010). Integration of contractile forces during tissue invagination. J Cell Biol *188*, 735-749.

Martin, A.C., Kaschube, M., and Wieschaus, E.F. (2009). Pulsed contractions of an actin-myosin network drive apical constriction. Nature *457*, 495-499.

Martin, P., and Parkhurst, S.M. (2004). Parallels between tissue repair and embryo morphogenesis. Development *131*, 3021-3034.

Matsumura, F. (2005). Regulation of myosin II during cytokinesis in higher eukaryotes. Trends Cell Biol *15*, 371-377.

Matsuo, T., Takahashi, K., Suzuki, E., and Yamamoto, D. (1999). The Canoe protein is necessary in adherens junctions for development of ommatidial architecture in the Drosophila compound eye. Cell Tissue Res *298*, 397-404.

Mattila, P.K., and Lappalainen, P. (2008). Filopodia: molecular architecture and cellular functions. Nat Rev Mol Cell Biol *9*, 446-454.

McGill, M.A., McKinley, R.F.A., and Harris, T.J.C. (2009). Independent cadherin–catenin and Bazooka clusters interact to assemble adherens junctions. The Journal of Cell Biology *185*, 787-796.

McGough, A., Pope, B., Chiu, W., and Weeds, A. (1997). Cofilin changes the twist of F-actin: Implications for actin filament dynamics and cellular function. Journal of Cell Biology *138*, 771-781.

McKim, K.S., Dahmus, J.B., and Hawley, R.S. (1996). Cloning of the Drosophila melanogaster meiotic recombination gene mei- 218: A genetic and molecular analysis of interval 15E. Genetics *144*, 215-228.

Mercer, J.A., Seperack, P.K., Strobel, M.C., Copeland, N.G., and Jenkins, N.A. (1991). Novel myosin heavy chain encoded by murine dilute coat colour locus. Nature *349*, 709-713.

Michaelson, D., Silletti, J., Murphy, G., D'Eustachio, P., Rush, M., and Philips, M.R. (2001). Differential localization of Rho GTPases in live cells: regulation by hypervariable regions and RhoGDI binding. J Cell Biol *152*, 111-126.

Miki, H., Suetsugu, S., and Takenawa, T. (1998). WAVE, a novel WASP-family protein involved in actin reorganization induced by Rac. Embo j *17*, 6932-6941.

Millard, T.H., and Martin, P. (2008). Dynamic analysis of filopodial interactions during the zippering phase of Drosophila dorsal closure. Development *135*, 621-626.

Millo, H., Leaper, K., Lazou, V., and Bownes, M. (2004). Myosin VI plays a role in cell–cell adhesion during epithelial morphogenesis. Mechanisms of Development *121*, 1335-1351.

Miyamoto, H., Nihonmatsu, I., Kondo, S., Ueda, R., Togashi, S., Hirata, K., Ikegami, Y., and Yamamoto, D. (1995). canoe encodes a novel protein containing a GLGF/DHR motif and functions with Notch and scabrous in common developmental pathways in Drosophila. Genes & Development *9*, 612-625.

Mondal, M.S., Wang, Z., Seeds, A.M., and Rando, R.R. (2000). The specific binding of small molecule isoprenoids to rhoGDP dissociation inhibitor (rhoGDI). Biochemistry *39*, 406-412.
Moore, P.B., Huxley, H.E., and DeRosier, D.J. (1970). Three-dimensional reconstruction of F-actin, thin filaments and decorated thin filaments. J Mol Biol *50*, 279-295.

Morais-de-Sa, E., Mirouse, V., and St Johnston, D. (2010). aPKC phosphorylation of Bazooka defines the apical/lateral border in Drosophila epithelial cells. Cell *141*, 509-523.

Mukhopadhyay, D., and Riezman, H. (2007). Proteasome-Independent Functions of Ubiquitin in Endocytosis and Signaling. Science *315*, 201-205.

Muller, H.A. (2000). Genetic control of epithelial cell polarity: lessons from Drosophila. Developmental dynamics : an official publication of the American Association of Anatomists *218*, 52-67.

Müller, H.A., and Wieschaus, E. (1996). armadillo, bazooka, and stardust are critical for early stages in formation of the zonula adherens and maintenance of the polarized blastoderm epithelium in Drosophila. The Journal of Cell Biology *134*, 149-163.

Mullins, R.D., Heuser, J.A., and Pollard, T.D. (1998). The interaction of Arp2/3 complex with actin: nucleation, high affinity pointed end capping, and formation of branching networks of filaments. Proc Natl Acad Sci U S A *95*, 6181-6186.

Murakami, K., Yasunaga, T., Noguchi, T.Q.P., Gomibuchi, Y., Ngo, K.X., Uyeda, T.Q.P., and Wakabayashi, T. (2010). Structural Basis for Actin Assembly, Activation of ATP Hydrolysis, and Delayed Phosphate Release. Cell *143*, 275-287.

Myat, M.M., and Andrew, D.J. (2002). Epithelial Tube Morphology Is Determined by the Polarized Growth and Delivery of Apical Membrane. Cell *111*, 879-891.

Nakatani, Y., and Ogryzko, V. (2003). Immunoaffinity Purification of Mammalian Protein Complexes. In Methods in Enzymology, A. Sankar, and G. Susan, eds. (Academic Press), pp. 430-444.

Nakayama, M., Goto, T.M., Sugimoto, M., Nishimura, T., Shinagawa, T., Ohno, S., Amano, M., and Kaibuchi, K. (2008). Rho-Kinase Phosphorylates PAR-3 and Disrupts PAR Complex Formation. Developmental Cell *14*, 205-215.

Nakayama, S., Moncrief, N.D., and Kretsinger, R.H. (1992). Evolution of EF-hand calcium-modulated proteins. II. Domains of several subfamilies have diverse evolutionary histories. Journal of molecular evolution *34*, 416-448.

Niewiadomska, P., Godt, D., and Tepass, U. (1999). DE-Cadherin Is Required for Intercellular Motility during Drosophila Oogenesis. The Journal of Cell Biology *144*, 533-547.

Nikolaidou, K.K., and Barrett, K. (2004). A Rho GTPase signaling pathway is used reiteratively in epithelial folding and potentially selects the outcome of Rho activation. Current biology : CB *14*, 1822-1826.

Nilson, L.A., and Schupbach, T. (1999). EGF receptor signaling in Drosophila oogenesis. Current topics in developmental biology *44*, 203-243.

Nobes, C.D., and Hall, A. (1995). Rho, rac, and cdc42 GTPases regulate the assembly of multimolecular focal complexes associated with actin stress fibers, lamellipodia, and filopodia. Cell *81*, 53-62.

Oda, T., Iwasa, M., Aihara, T., Maeda, Y., and Narita, A. (2009). The nature of the globular- to fibrous-actin transition. Nature *457*, 441-445.

Olofsson, B. (1999). Rho guanine dissociation inhibitors: pivotal molecules in cellular signalling. Cellular signalling *11*, 545-554.

Osterfield, M., Du, X., Schupbach, T., Wieschaus, E., and Shvartsman, S.Y. (2013). Three-dimensional epithelial morphogenesis in the developing Drosophila egg. Dev Cell *24*, 400-410.

Otomo, T., Otomo, C., Tomchick, D.R., Machius, M., and Rosen, M.K. (2005). Structural basis of Rho GTPase-mediated activation of the formin mDia1. Molecular cell *18*, 273-281.

Özkan, E., Carrillo, Robert A., Eastman, Catharine L., Weiszmann, R., Waghray, D., Johnson, Karl G., Zinn, K., Celniker, Susan E., and Garcia, K.C. (2013). An Extracellular Interactome of Immunoglobulin and LRR Proteins Reveals Receptor-Ligand Networks. Cell *154*, 228-239.

Paluch, E., and Heisenberg, C.-P. (2009). Biology and Physics of Cell Shape Changes in Development. Current Biology *19*, R790-R799.

Pardee, J.D., and Spudich, J.A. (1982). Mechanism of K+-induced actin assembly. The Journal of Cell Biology *93*, 648-654.

Parks, A.L., and Muskavitch, M.A. (1993). Delta Function Is Required for Bristle Organ Determination and Morphogenesis in Drosophila. Developmental Biology *157*, 484-496.

Parks, S., and Wieschaus, E. (1991). The Drosophila gastrulation gene concertina encodes a G alpha-like protein. Cell *64*, 447-458.

Peters, N.C., Thayer, N.H., Kerr, S.A., Tompa, M., and Berg, C.A. (2013). Following the 'tracks': Tramtrack69 regulates epithelial tube expansion in the Drosophila ovary through Paxillin, Dynamin, and the homeobox protein Mirror. Developmental Biology *378*, 154-169.

Pickart, C.M. (2001). MECHANISMS UNDERLYING UBIQUITINATION. Annual Review of Biochemistry *70*, 503-533.

Pickering, K., Alves-Silva, J., Goberdhan, D., and Millard, T.H. (2013). Par3/Bazooka and phosphoinositides regulate actin protrusion formation during Drosophila dorsal closure and wound healing. Development *140*, 800-809.

Pignoni, F., and Zipursky, S.L. (1997). Induction of Drosophila eye development by decapentaplegic. Development *124*, 271-278.

Pilot, F., and Lecuit, T. (2005). Compartmentalized morphogenesis in epithelia: From cell to tissue shape. Developmental Dynamics *232*, 685-694.

Pocha, S.M., Shevchenko, A., and Knust, E. (2011). Crumbs regulates rhodopsin transport by interacting with and stabilizing myosin V. The Journal of Cell Biology *195*, 827-838.

Pollard, T.D. (1983). Measurement of rate constants for actin filament elongation in solution. Analytical biochemistry *134*, 406-412.

Pollard, T.D. (1986). Rate constants for the reactions of ATP- and ADP-actin with the ends of actin filaments. J Cell Biol *103*, 2747-2754.

Pollard, T.D. (2007). Regulation of actin filament assembly by Arp2/3 complex and formins. Annual review of biophysics and biomolecular structure *36*, 451-477.

Pollard, T.D., and Borisy, G.G. (2003). Cellular Motility Driven by Assembly and Disassembly of Actin Filaments. Cell *112*, 453-465.

Pollard, T.D., and Cooper, J.A. (2009). Actin, a Central Player in Cell Shape and Movement. Science *326*, 1208-1212.

Pollard, T.D., and Weeds, A.G. (1984). The rate constant for ATP hydrolysis by polymerized actin. FEBS Letters *170*, 94-98.

Prabakaran, S., Lippens, G., Steen, H., and Gunawardena, J. (2012). Post-translational modification: nature's escape from genetic imprisonment and the basis for dynamic information encoding. Wiley Interdisciplinary Reviews: Systems Biology and Medicine *4*, 565-583.

Prasad, M., Jang, A.C.C., Starz-Gaiano, M., Melani, M., and Montell, D.J. (2007). A protocol for culturing Drosophila melanogaster stage 9 egg chambers for live imaging. Nat Protocols *2*, 2467-2473.

Preiss, T., and W. Hentze, M. (2003). Starting the protein synthesis machine: eukaryotic translation initiation. BioEssays *25*, 1201-1211.

Pruyne, D., Evangelista, M., Yang, C., Bi, E., Zigmond, S., Bretscher, A., and Boone, C. (2002). Role of formins in actin assembly: nucleation and barbed-end association. Science *297*, 612-615.

Puig, O., Caspary, F., Rigaut, G., Rutz, B., Bouveret, E., Bragado-Nilsson, E., Wilm, M., and Séraphin, B. (2001). The Tandem Affinity Purification (TAP) Method: A General Procedure of Protein Complex Purification. Methods *24*, 218-229.

Quintin, S., Gally, C., and Labouesse, M. (2008). Epithelial morphogenesis in embryos: asymmetries, motors and brakes. Trends in genetics : TIG *24*, 221-230.

Rakic, D. (2013). Regulation of expression of the cell adhesion molecule Echinoid and its effects on the actin cytoskeleton during Drosophila melanogaster development. In Department of Biology (Montreal, Quebec, Canada: McGill University).

Ramachandran, P., Barria, R., Ashley, J., and Budnik, V. (2009). A critical step for postsynaptic F-actin organization: Regulation of Baz/Par-3 localization by aPKC and PTEN. Developmental Neurobiology *69*, 583-602.

Rauzi, M., Lenne, P.-F., and Lecuit, T. (2010). Planar polarized actomyosin contractile flows control epithelial junction remodelling. Nature *468*, 1110-1114.

Rauzi, M., and Lenne, P.F. (2011). Cortical forces in cell shape changes and tissue morphogenesis. Current topics in developmental biology *95*, 93-144.

Rauzi, M., Verant, P., Lecuit, T., and Lenne, P.F. (2008). Nature and anisotropy of cortical forces orienting Drosophila tissue morphogenesis. Nat Cell Biol *10*, 1401-1410.

Rawlins, E.L., Lovegrove, B., and Jarman, A.P. (2003a). Echinoid facilitates Notch pathway signalling during Drosophila neurogenesis through functional interaction with Delta. Development *130*, 6475-6484.

Rawlins, E.L., White, N.M., and Jarman, A.P. (2003b). Echinoid limits R8 photoreceptor specification by inhibiting inappropriate EGF receptor signalling within R8 equivalence groups. Development *130*, 3715-3724.

Rayment, I., Rypniewski, W.R., Schmidt-Base, K., Smith, R., Tomchick, D.R., Benning, M.M., Winkelmann, D.A., Wesenberg, G., and Holden, H.M. (1993). Three-dimensional structure of myosin subfragment-1: a molecular motor. Science *261*, 50-58.

Rebecchi, M.J., and Scarlata, S. (1998). PLECKSTRIN HOMOLOGY DOMAINS: A Common Fold with Diverse Functions. Annual review of biophysics and biomolecular structure *27*, 503-528.

Reits, E.A.J., and Neefjes, J.J. (2001). From fixed to FRAP: measuring protein mobility and activity in living cells. Nat Cell Biol *3*, E145-E147.

Riento, K., and Ridley, A.J. (2003). Rocks: multifunctional kinases in cell behaviour. Nat Rev Mol Cell Biol *4*, 446-456.

Rigaut, G., Shevchenko, A., Rutz, B., Wilm, M., Mann, M., and Seraphin, B. (1999). A generic protein purification method for protein complex characterization and proteome exploration. Nat Biotech *17*, 1030-1032.

Rohatgi, R., Ma, L., Miki, H., Lopez, M., Kirchhausen, T., Takenawa, T., and Kirschner, M.W. (1999). The Interaction between N-WASP and the Arp2/3 Complex Links Cdc42-Dependent Signals to Actin Assembly. Cell *97*, 221-231.

Rohila, J.S., Chen, M., Cerny, R., and Fromm, M.E. (2004). Improved tandem affinity purification tag and methods for isolation of protein heterocomplexes from plants. The Plant Journal *38*, 172-181.

Romero, S., Le Clainche, C., Didry, D., Egile, C., Pantaloni, D., and Carlier, M.F. (2004). Formin is a processive motor that requires profilin to accelerate actin assembly and associated ATP hydrolysis. Cell *119*, 419-429.

Roper, K. (2012). Anisotropy of Crumbs and aPKC drives myosin cable assembly during tube formation. Dev Cell *23*, 939-953.

Rose, R., Weyand, M., Lammers, M., Ishizaki, T., Ahmadian, M.R., and Wittinghofer, A. (2005). Structural and mechanistic insights into the interaction between Rho and mammalian Dia. Nature *435*, 513-518.

Rotin, D., and Kumar, S. (2009). Physiological functions of the HECT family of ubiquitin ligases. Nat Rev Mol Cell Biol *10*, 398-409.

Rould, M.A., Wan, Q., Joel, P.B., Lowey, S., and Trybus, K.M. (2006). Crystal structures of expressed non-polymerizable monomeric actin in the ADP and ATP states. The Journal of biological chemistry *281*, 31909-31919.

Ruohola, H., Bremer, K.A., Baker, D., Swedlow, J.R., Jan, L.Y., and Jan, Y.N. (1991). Role of neurogenic genes in establishment of follicle cell fate and oocyte polarity during oogenesis in Drosophila. Cell *66*, 433-449.

Sahai, E., and Marshall, C.J. (2002). ROCK and Dia have opposing effects on adherens junctions downstream of Rho. Nat Cell Biol *4*, 408-415.

Sambrook, J., and Russell, D.W. (2006). Isolation of DNA Fragments from Polyacrylamide Gels by the Crush and Soak Method. Cold Spring Harbor Protocols *2006*, pdb.prot2936.

Satoh, A.K., O'Tousa, J.E., Ozaki, K., and Ready, D.F. (2005). Rab11 mediates post-Golgi trafficking of rhodopsin to the photosensitive apical membrane of Drosophila photoreceptors. Development *132*, 1487-1497.

Sawyer, J.K., Harris, N.J., Slep, K.C., Gaul, U., and Peifer, M. (2009). The Drosophila afadin homologue Canoe regulates linkage of the actin cytoskeleton to adherens junctions during apical constriction. The Journal of Cell Biology *186*, 57-73.

Schmidt, A., and Hall, A. (2002). Guanine nucleotide exchange factors for Rho GTPases: turning on the switch. Genes & Development *16*, 1587-1609.

Sellers, J.R. (2000). Myosins: a diverse superfamily. Biochimica et Biophysica Acta (BBA) - Molecular Cell Research *1496*, 3-22.

Selve, N., and Wegner, A. (1986). Rate of treadmilling of actin filaments in vitro. J Mol Biol *187*, 627-631.

Shcherbata, H.R., Althauser, C., Findley, S.D., and Ruohola-Baker, H. (2004). The mitotic-to-endocycle switch in Drosophila follicle cells is executed by Notch-dependent regulation of G1/S, G2/M and M/G1 cell-cycle transitions. Development *131*, 3169-3181.

Shulman, J.M., Benton, R., and St Johnston, D. (2000). The Drosophila Homolog of C. elegans PAR-1 Organizes the Oocyte Cytoskeleton and Directs oskar mRNA Localization to the Posterior Pole. Cell *101*, 377-388.

Shutova, M., Yang, C., Vasiliev, J.M., and Svitkina, T. (2012). Functions of Nonmuscle Myosin II in Assembly of the Cellular Contractile System. PLoS ONE *7*, e40814.

Simoes Sde, M., Blankenship, J.T., Weitz, O., Farrell, D.L., Tamada, M., Fernandez-Gonzalez, R., and Zallen, J.A. (2010). Rho-kinase directs Bazooka/Par-3 planar polarity during Drosophila axis elongation. Dev Cell *19*, 377-388.

Simões, S.d.M., Mainieri, A., and Zallen, J.A. (2014). Rho GTPase and Shroom direct planar polarized actomyosin contractility during convergent extension. The Journal of Cell Biology *204*, 575-589.

Simone, R.P., and DiNardo, S. (2010). Actomyosin contractility and Discs large contribute to junctional conversion in guiding cell alignment within the Drosophila embryonic epithelium. Development *137*, 1385-1394.

Solon, J., Kaya-Çopur, A., Colombelli, J., and Brunner, D. (2009). Pulsed Forces Timed by a Ratchet-like Mechanism Drive Directed Tissue Movement during Dorsal Closure. Cell *137*, 1331-1342.

Sonenberg, N., and Dever, T.E. (2003). Eukaryotic translation initiation factors and regulators. Current Opinion in Structural Biology *13*, 56-63.

Southwick, F.S., and Young, C.L. (1990). The actin released from profilin - actin complexes is insufficient to account for the increase in F-actin in chemoattractant-stimulated polymorphonuclear leukocytes. Journal of Cell Biology *110*, 1965-1973.

Spencer, S.A., and Cagan, R.L. (2003). Echinoid is essential for regulation of Egfr signaling and R8 formation during Drosophila eye development. Development *130*, 3725-3733.

Spradling, A.C. (1993). Developmental genetics of oogenesis. In The Development of Drosophila melanogaster, M.B.a.A.M. Arias, ed. (Cold Spring Harbor Laboratory Press), pp. 1-70.

Struhl, G., and Basler, K. (1993). Organizing activity of wingless protein in Drosophila. Cell *72*, 527-540.

Stylianopoulou, E., Lykidis, D., Ypsilantis, P., Simopoulos, C., Skavdis, G., and Grigoriou, M. (2012). A Rapid and Highly Sensitive Method of Non Radioactive Colorimetric *In Situ* Hybridization for the Detection of mRNA on Tissue Sections. PLoS ONE *7*, e33898.

Sweeton, D., Parks, S., Costa, M., and Wieschaus, E. (1991). Gastrulation in Drosophila: the formation of the ventral furrow and posterior midgut invaginations. Development *112*, 775-789.

Symons, M., Derry, J.M.J., Karlak, B., Jiang, S., Lemahieu, V., McCormick, F., Francke, U., and Abo, A. (1996). Wiskott–Aldrich Syndrome Protein, a Novel Effector for the GTPase CDC42Hs, Is Implicated in Actin Polymerization. Cell *84*, 723-734.

Tabb, J.S., Molyneaux, B.J., Cohen, D.L., Kuznetsov, S.A., and Langford, G.M. (1998). Transport of ER vesicles on actin filaments in neurons by myosin V. Journal of Cell Science *111*, 3221-3234.

Tagwerker, C., Flick, K., Cui, M., Guerrero, C., Dou, Y., Auer, B., Baldi, P., Huang, L., and Kaiser, P. (2006). A Tandem Affinity Tag for Two-step Purification under Fully Denaturing Conditions: Application in Ubiquitin Profiling and Protein Complex Identification Combined with in vivoCross-Linking. Molecular & Cellular Proteomics *5*, 737-748.

Takai, Y., Ikeda, W., Ogita, H., and Rikitake, Y. (2008). The Immunoglobulin-Like Cell Adhesion Molecule Nectin and Its Associated Protein Afadin. Annual Review of Cell and Developmental Biology *24*, 309-342.

Takai, Y., and Nakanishi, H. (2003). Nectin and afadin: novel organizers of intercellular junctions. Journal of Cell Science *116*, 17-27.

Tepass, U., Gruszynski-DeFeo, E., Haag, T.A., Omatyar, L., Török, T., and Hartenstein, V. (1996). shotgun encodes Drosophila E-cadherin and is preferentially required during cell

rearrangement in the neurectoderm and other morphogenetically active epithelia. Genes & Development *10*, 672-685.

Tepass, U., Tanentzapf, G., Ward, R., and Fehon, R. (2001). Epithelial cell polarity and cell junctions in Drosophila. Annual review of genetics *35*, 747-784.

Tiefenbach, J., Moll, P.R., Nelson, M.R., Hu, C., Baev, L., Kislinger, T., and Krause, H.M. (2010). A Live Zebrafish-Based Screening System for Human Nuclear Receptor Ligand and Cofactor Discovery. PLoS ONE *5*, e9797.

Toyama, Y., Peralta, X.G., Wells, A.R., Kiehart, D.P., and Edwards, G.S. (2008). Apoptotic force and tissue dynamics during Drosophila embryogenesis. Science *321*, 1683-1686.

Troyanovsky, S. (2005). Cadherin dimers in cell–cell adhesion. European Journal of Cell Biology *84*, 225-233.

Ushakov, D.S. (2008). [Structure and function of the essential light chain of myosin]. Biofizika *53*, 950-955.

Vaccari, T., Rabouille, C., and Ephrussi, A. (2005). The Drosophila PAR-1 Spacer Domain Is Required for Lateral Membrane Association and for Polarization of Follicular Epithelial Cells. Current Biology *15*, 255-261.

Van Aelst, L., and Symons, M. (2002). Role of Rho family GTPases in epithelial morphogenesis. Genes & Development *16*, 1032-1054.

van Rheenen, J., and Jalink, K. (2002). Agonist-induced PIP2 Hydrolysis Inhibits Cortical Actin Dynamics: Regulation at a Global but not at a Micrometer Scale. Molecular Biology of the Cell *13*, 3257-3267.

Velasco, G., Armstrong, C., Morrice, N., Frame, S., and Cohen, P. (2002). Phosphorylation of the regulatory subunit of smooth muscle protein phosphatase 1M at Thr850 induces its dissociation from myosin. FEBS Lett *527*, 101-104.

Vicente-Manzanares, M., Ma, X., Adelstein, R.S., and Horwitz, A.R. (2009). Non-muscle myosin II takes centre stage in cell adhesion and migration. Nat Rev Mol Cell Biol *10*, 778-790.

Vogel, C., Teichmann, S.A., and Chothia, C. (2003). The immunoglobulin superfamily in Drosophila melanogaster and Caenorhabditis elegans and the evolution of complexity. Development *130*, 6317-6328.

Ward, E.J., and Berg, C.A. (2005). Juxtaposition between two cell types is necessary for dorsal appendage tube formation. Mech Dev *122*, 241-255.

Watanabe, N., and Mitchison, T.J. (2002). Single-molecule speckle analysis of actin filament turnover in lamellipodia. Science *295*, 1083-1086.

Weernink, P.A.O., Meletiadis, K., Hommeltenberg, S., Hinz, M., Ishihara, H., Schmidt, M., and Jakobs, K.H. (2004). Activation of Type I Phosphatidylinositol 4-Phosphate 5-Kinase Isoforms by the Rho GTPases, RhoA, Rac1, and Cdc42. Journal of Biological Chemistry *279*, 7840-7849.

Weernink, P.A.O., Schulte, P., Guo, Y., Wetzel, J., Amano, M., Kaibuchi, K., Haverland, S., Voß, M., Schmidt, M., Mayr, G.W., *et al.* (2000). Stimulation of Phosphatidylinositol-4-phosphate 5-Kinase by Rho-Kinase. Journal of Biological Chemistry *275*, 10168-10174.

Wegner, A. (1976). Head to tail polymerization of actin. Journal of Molecular Biology *108*, 139-150.

Wegner, A., and Isenberg, G. (1983). 12-fold difference between the critical monomer concentrations of the two ends of actin filaments in physiological salt conditions. Proceedings of the National Academy of Sciences of the United States of America *80*, 4922-4925.

Wei, J., Hortsch, M., and Goode, S. (2004). Neuroglian stabilizes epithelial structure during Drosophila oogenesis. Developmental Dynamics *230*, 800-808.

Wei, S.-Y., Escudero, L.M., Yu, F., Chang, L.-H., Chen, L.-Y., Ho, Y.-H., Lin, C.-M., Chou, C.-S., Chia, W., Modolell, J., *et al.* (2005). Echinoid Is a Component of Adherens Junctions That Cooperates with DE-Cadherin to Mediate Cell Adhesion. Developmental Cell *8*, 493-504.

Wei, Z., Liu, X., Yu, C., and Zhang, M. (2013). Structural basis of cargo recognitions for class V myosins. Proceedings of the National Academy of Sciences *110*, 11314-11319.

Wells, A.L., Lin, A.W., Chen, L.-Q., Safer, D., Cain, S.M., Hasson, T., Carragher, B.O., Milligan, R.A., and Sweeney, H.L. (1999). Myosin VI is an actin-based motor that moves backwards. Nature *401*, 505-508.

Westermarck, J.W.C.S.R.K.J.M.A.M.W.M.A.W.S.B.W.M.V.B.C.B.D. (2002). The DEXD/H-box RNA helicase RHII/Gu is a co-factor for c-Jun-activated transcription. The EMBO Journal *21*, 451-460.

Witte, C.-P., Noël, L., Gielbert, J., Parker, J., and Romeis, T. (2004). Rapid one-step protein purification from plant material using the eight-amino acid StrepII epitope. Plant Mol Biol *55*, 135-147.

Wodarz, A., Hinz, U., Engelbert, M., and Knust, E. (1995). Expression of crumbs confers apical character on plasma membrane domains of ectodermal epithelia of drosophila. Cell *82*, 67-76.

Wodarz, A., Ramrath, A., Kuchinke, U., and Knust, E. (1999). Bazooka provides an apical cue for Inscuteable localization in Drosophila neuroblasts. Nature *402*, 544-547.

Woodrum, D.T., Rich, S.A., and Pollard, T.D. (1975). Evidence for biased bidirectional polymerization of actin filaments using heavy meromyosin prepared by an improved method. The Journal of Cell Biology *67*, 231-237.

Woolner, S., and Bement, W.M. (2009). Unconventional myosins acting unconventionally. Trends in Cell Biology *19*, 245-252.

Xie, X., Harrison, D.H., Schlichting, I., Sweet, R.M., Kalabokis, V.N., Szent-Gyorgyi, A.G., and Cohen, C. (1994). Structure of the regulatory domain of scallop myosin at 2.8 A resolution. Nature *368*, 306-312.

Yamada, S., Pokutta, S., Drees, F., Weis, W.I., and Nelson, W.J. Deconstructing the Cadherin-Catenin-Actin Complex. Cell *123*, 889-901.

Yang, P., Sampson, H.M., and Krause, H.M. (2006). A modified tandem affinity purification strategy identifies cofactors of the Drosophila nuclear receptor dHNF4. PROTEOMICS *6*, 927-935.

Young, P.E., Richman, A.M., Ketchum, A.S., and Kiehart, D.P. (1993). Morphogenesis in Drosophila requires nonmuscle myosin heavy chain function. Genes & Development *7*, 29-41.

Yu, F.-X., and Guan, K.-L. (2013). The Hippo pathway: regulators and regulations. Genes & Development *27*, 355-371.

Yue, T., Tian, A., and Jiang, J. (2012). The Cell Adhesion Molecule Echinoid Functions as a Tumor Suppressor and Upstream Regulator of the Hippo Signaling Pathway. Developmental Cell *22*, 255-267.

Zallen, J., and Zallen, R. (2004). Cell-pattern disordering during convergent extension in Drosophila. Journal of Physics: Condensed Matter *16*, S5073.

Zallen, J.A. (2007). Planar polarity and tissue morphogenesis. Cell *129*, 1051-1063.

Zallen, J.A., and Wieschaus, E. (2004). Patterned gene expression directs bipolar planar polarity in Drosophila. Dev Cell *6*, 343-355.